Methods in Molecular Biology 761

Springer Protocols

Gaspar Banfalvi *Editor*

# Cell Cycle Synchronization

## Methods and Protocols

Humana Press

# METHODS IN MOLECULAR BIOLOGY™

*Series Editor*
**John M. Walker**
**School of Life Sciences**
**University of Hertfordshire**
**Hatfield, Hertfordshire, AL10 9AB, UK**

For other titles published in this series, go to
www.springer.com/series/7651

# Cell Cycle Synchronization

## Methods and Protocols

Edited by

**Gaspar Banfalvi**

*Department of Microbial Biotechnology and Cell Biology,*
*University of Debrecen, Debrecen, Hungary*

Humana Press

*Editor*
Gaspar Banfalvi
Department of Microbial
Biotechnology and Cell Biology
University of Debrecen
Debrecen 4010, Hungary
bgaspar@delfin.klte.hu

ISSN 1064-3745 e-ISSN 1940-6029
ISBN 978-1-61779-181-9 e-ISBN 978-1-61779-182-6
DOI 10.1007/978-1-61779-182-6
Springer New York Dordrecht Heidelberg London

Library of Congress Control Number: 2011931108



Printed on acid-free paper

Humana Press is part of Springer Science+Business Media (www.springer.com)

# Preface

## What Kind of Cells Can Be Synchronized?

To study how cells progress through the cell cycle, cell cultures have to be brought to the same phase. The unique feature of this book is exactly this: to prepare synchronized cells representing different stages of the cell cycle. The book also shows the latest techniques for the enhanced study of regulatory mechanisms to understand cell cycle events. The synchronization methods presented in the book are based principally on two major strategies. The "arrest-and-release" approach involves different chemical treatments to block cells at certain stages of the cell cycle. The physical strategy contains physical methods to collect cells belonging to subpopulations of the cell cycle. The collection of synchronized cells from asynchronous bacterial, plant, protozoan, yeast, fish, and mammalian cell cultures consisting of individual cells is described by professionals of their respective field. Additional chapters include synchronization of transfected and embryonic cells.

## Why Edit a Book on Synchronization?

This question can be easily answered by making a computer search typing in the words "cell synchronization." It turns out that there are many scientists who are desperately looking for synchronization protocols. Researchers are interested in synchronizing mammalian, plant, yeast, fungal, and even bacterial cells but do not know how to do it. Enthusiastic students often try synchronization without experience and then recognize that it does not work. In such cases, the easiest way is to ask someone known for his/her expertise to send a protocol. As some of the synchronizing techniques are tricky, brief instructions usually would not help either. Alternatively, one can trace research papers that contain descriptions without extensive practical details but describe only rarely how problems encountered could be solved. This book aims to address such deficiencies. But the most important feature of this book is to supply detailed protocols providing first the theoretical background of the procedure and then step-by-step instructions on how to implement synchronization. Chapters of the book are written for those competent scientists who would like to do, but are not familiar with, synchronization. They should be able to carry out successfully the technique at the first attempt by following closely the detailed practical instructions of the protocols.

## Major Sections of Chapters

Each protocol starts with an Abstract and consists of four major sections: Introduction, Materials, Methods, and Notes. Exceptions are only the first and last review chapters

that do not follow this format. The "Abstract" gives an overview of the synchronization technique(s). The "Introduction" contains a summary, a brief theoretical view of the procedure referring to the work of other authors, and outlines the major procedures of the protocol. The "Materials" section is the major part of the chapter listing the buffers, reagents, solutions, disposables, and equipments necessary to carry out the synchronization. Attention is called to special requirements such as storage conditions, stability, purity, toxicity of reagents, special treatment, or protection. The "Methods" section contains all relevant practical details and explains individual steps to be carried out normally by listing these steps in numerical order. The "Notes" section is the hallmark of the series of *Methods in Molecular Biology* as it is meant to indicate the sources of problems and how to identify and overcome them.

## Brief Content of Chapters

The introductory chapter overviews synchronization methods. Chapters of physical fractionations include centrifugal elutriation (**Chapter 2**), cytofluorometric purification of diploid and tetraploid cancer cells (**Chapter 3**) and large-scale mitotic cell synchronization (**Chapter 4**), as well as applying serum deprivation (**Chapter 5**). Chemical blockades imply inhibitors of DNA replication (**Chapters 6** and **7**), butyrate (**Chapter 8**), nocodazole to arrest cells at the $G_2/M$ border, and aphidicolin to synchronize cells at the $G_1/S$ border and to monitor progression through S phase by pulse-labeling individual cultures with [$^3$H]-thymidine (**Chapter 9**). Different ways have been used to synchronize HeLa cells in **Chapter 10**. The synchronization of unicellular organisms (*Bacillus subtilis*, yeast, protozoans) is described in **Chapters 11**, **12**, and **13**. The synchronization of mammalian and plant cells is studied in **Chapters 14** and **15**, respectively. A protocol for the synchronization for the purposes of nuclear transfer is given in **Chapter 16**. Hematopoietic stem cells improve the engraftment in transplantation (**Chapter 17**). Flow cytometry developments in clinical studies are described in **Chapter 18**. Finally cell cycle control is discussed (**Chapter 19**).

## Which Is the Best Synchronization Protocol?

It is neither the intention of this book to make a judgment as to which synchronizing procedure is the best or to set a "gold standard" against which other methods should be measured. Debates on synchronization methodologies can be found in opinion papers referred to in **Chapter 1** (14–18). A simple method for obtaining synchrony in all types of cells, that would last through several cycles and with minimal overall metabolic perturbations, does not exist. Thus scientists interested in synchronization after reading the chapters of interest can decide for themselves which technique would be appropriate for adaptation.

## The Potential Audience of This Book

First of all, those students and scientists who are looking for synchronization protocols will be interested. The main target audience includes

- libraries of universities and biological research institutions;
- researchers interested in general science, pharmacy, medicine and public health, computer science, and the life sciences;
- specialists and professionals in cell biology, genetics, molecular biology, biochemistry, and pharmacology;
- biologists, molecular biologists, biotechnologists, geneticists, immunologists, medical students, PhD students, and postdoctoral fellows who are expected to be the primary users of the synchronizing techniques and protocols;
- pharma companies and factories.

***Gaspar Banfalvi***

# Contents

# Contributors


EDIT ÁBRAHÁM • *Cellular Imaging Laboratory, Institute of Plant Biology, Biological Research Centre, Hungarian Academy of Sciences, Szeged, Hungary*

LESLEY ABRAHAM • *Department of Cell Biology and Biochemistry, Texas Tech University Health Sciences Center, Lubbock, TX, USA*

FERHAN AYAYDIN • *Cellular Imaging Laboratory, Biological Research Centre, Hungarian Academy of Sciences, Szeged, Hungary*

GASPAR BANFALVI • *Department of Microbial Biotechnology and Cell Biology, University of Debrecen, Debrecen, Hungary*

SALVATORE CARADONNA • *Department of Molecular Biology, University of Medicine and Dentistry, Stratford, NJ, USA*

MARIA CASTEDO • *INSERM, U848, Institut Gustave Roussy, Villejuif, France*

RICHARD C. CHOU • *Dartmouth School of Medicine, Lebanon, NH, USA*

ATTILA CSIKÁSZ-NAGY • *The Microsoft Research, University of Trento Centre for Computational and Systems Biology, Povo-Trento, Italy*

ZBIGNIEW DARZYNKIEWICZ • *Department of Pathology, Brander Cancer Research Institute, New York Medical College, Valhalla, NY, USA*

ALLA DOLNIKOV • *Sydney Cord & Marrow Transplant Facility, Faculty of Medicine, Sydney Children's Hospital, University of New South Wales, Sydney, NSW, Australia*

KALYAN DULLA • *Department of Molecular Diagnostics, Philips Research, Eindhoven, The Netherlands*

HUZEFA DUNGRAWALA • *Department of Cell Biology and Biochemistry, Texas Tech University Health Sciences Center, Lubbock, TX, USA*

JENNIFER A. FISCHER • *Department of Molecular Biology, University of Medicine and Dentistry, Stratford, NJ, USA*

LORENZO GALLUZZI • *INSERM, U848, Institut Gustave Roussy, Villejuif, France*

CAROLINE GUIGNANT • *Laboratoire d'Immunologie, Hopital E. Herriot, Hospices Civils de Lyon, Lyon Cedex 03, France*

H. DOROTA HALICKA • *Department of Pathology, New York Medical College, Brander Cancer Research Institute, Valhalla, NY, USA*

YUJI HIRAO • *National Agriculture and Food Research Organization (NARO), National Agricultural Research Center for Tohoku Region (NARCT), Morioka, Japan*

GÁBOR V. HORVÁTH • *Institute of Plant Biology, Biological Research Center, Hungarian Academy of Sciences, Szeged, Hungary*

TAKASHI IWAMATSU • *Aichi University of Education, Karia, Japan*

MOHAMED JÈMAÀ • *INSERM, U848, Institut Gustave Roussy, Villejuif, France*

KAP-HYOUN KO • *Sydney Cord & Marrow Transplant Facility, Graduate School of Biomedical Engineering, Sydney Children's Hospital, University of New South Wales, Kensington, NSW, Australia*

EDIT KOTOGÁNY • *Cellular Imaging Laboratory, Biological Research Centre, Hungarian Academy of Sciences, Szeged, Hungary*

GUIDO KROEMER • *INSERM, U848, Institut Gustave Roussy, Villejuif, France*

THOMAS J. LANGAN • *Department of Neurology, School of Medicine and Biomedical Sciences, Children's Hospital, State University of New York, Buffalo, NY, USA*
CONGJUN LI • *Bovine Functional Genomics Laboratory, Animal and Natural Resources Institute, ARS, USDA, Beltsville, MD, USA*
HOI TANG MA • *Division of Life Science, Hong Kong University of Science and Technology, Hong Kong, China*
ARKADI MANUKYAN • *Department of Cell Biology and Biochemistry, Texas Tech University Health Sciences Center, Lubbock, TX, USA*
DIDIER MÉTIVIER • *INSERM, U848, Institut Gustave Roussy, Villejuif, France*
GUILLAUME MONNERET • *Laboratoire d'Immunologie, Hopital E. Herriot, Hospices Civils de Lyon, Lyon Cedex 03, France*
ROBERT NORDON • *Graduate School of Biomedical Engineering, University of New South Wales, Kensington, NSW, Australia*
TRACEY A. O'BRIEN • *Sydney Cord & Marrow Transplant Facility, Centre for Children's Cancer & Blood Disorders, Sydney Children's Hospital, Sydney, Australia*
ALIDA PALMISANO • *Department of Biological Sciences, Virginia Polytechnic Institute & State University, VA*
MONIKA PODHORECKA • *Department of Hemato-Oncology and Bone Marrow Transplantation, Medical University, Lublin, Poland*
RANDY Y.C. POON • *Division of Life Science, Hong Kong University of Science and Technology, Hong Kong, China*
SANTIAGO RELLO-VARONA • *INSERM, U848, Institut Gustave Roussy, Villejuif, France*
BENJAMIN E. REUBINOFF • *Department of Obstetrics and Gynecology and the Hadassah Human Embryonic Stem Cell Research Center, the Goldyne Savad Institute of Gene Therapy, Hadassah University Hospital, Jerusalem, Israel*
ANNA SANTAMARIA • *Biozentrum, University of Basel, Basel, Switzerland*
BRANDT L. SCHNEIDER • *Department of Cell Biology and Biochemistry, Texas Tech University Health Sciences Center, Lubbock, TX, USA*
LAURA SENOVILLA • *INSERM, U848, Institut Gustave Roussy, Villejuif, France*
YOEL SHUFARO • *Department of Obstetrics and Gynecology and the Hadassah Human Embryonic Stem Cell Research Center, the Goldyne Savad Institute of Gene Therapy, Hadassah University Hospital, Jerusalem, Israel*
TAMAS SOMFAI • *National Agriculture and Food Research Organization (NARO), National Institute of Livestock and Grassland Science (NILGS), Ibaraki, Japan*
STAFFAN SVÄRD • *Department of Cell and Molecular Biology, Uppsala University, Uppsala, Sweden*
GEOFF SYMONDS • *Faculty of Medicine, University of New South Wales, Kensington, NSW, Australia*
KARIN TROELL • *National Veterinary Institute, S-751 89 Uppsala, Sweden*
FABIENNE VENET • *Laboratoire d'Immunologie, Hopital E. Herriot, Hospices Civils de Lyon, Lyon, France*
ILIO VITALE • *INSERM, U848, Institut Gustave Roussy, Villejuif, France*
JUDIT ZÁMBORSZKY • *Centre for Integrative Biology (CIBIO), University of Trento, via della Regole, Mattarello (TN), Italy*
HONG ZHAO • *Department of Pathology, New York Medical College, Brander Cancer Research Institute, Valhalla, NY, USA*

# Chapter 1

# Overview of Cell Synchronization

Gaspar Banfalvi

## Abstract

Widespread interest in cell synchronization is maintained by the studies of control mechanisms involved in cell cycle regulation. During the synchronization distinct subpopulations of cells are obtained representing different stages of the cell cycle. These subpopulations are then used to study regulatory mechanisms of the cycle at the level of macromolecular biosynthesis (DNA synthesis, gene expression, protein synthesis), protein phosphorylation, development of new drugs, etc. Although several synchronization methods have been described, it is of general interest that scientists get a compilation and an updated view of these synchronization techniques. This introductory chapter summarizes: (1) the basic concepts and principal criteria of cell cycle synchronizations, (2) the most frequently used synchronization methods, such as physical fractionation (flow cytometry, dielectrophoresis, cytofluorometric purification), chemical blockade, (3) synchronization of embryonic cells, (4) synchronization at low temperature, (5) comparison of cell synchrony techniques, (6) synchronization of unicellular organisms, and (7) the effect of synchronization on transfection.

**Key words:** Basic concepts of synchronization, criteria of synchronization, DNA staining, DNA analysis, *C*-value.

## 1. Introduction

The most famous research paper in biology was and has remained the description of the double helical structure of DNA (1). In 1953 there was another important paper published that established the model of the cell cycle as we know it today (2). The famous sentence of the reduplication of DNA recognized by Watson and Crick – "It has not escaped our notice that the specific pairing we have postulated immediately suggests a possible copying mechanism for the genetic material" – initiated studies on DNA replication. Howard and Pelc used $^{32}$P label and after the

G. Banfalvi (ed.), *Cell Cycle Synchronization*, Methods in Molecular Biology 761,
DOI 10.1007/978-1-61779-182-6_1, 

incorporation of the biological tracer in the root cells of *Vicia faba* (broad bean) they removed all of the non-DNA phosphorus-labeled compounds with hydrochloric acid at 60°C which allowed them to trace the cellular levels of DNA. Their autoradiographic analysis showed that DNA synthesis occurs only at one discrete period during the interphase between two mitoses. Microspectrometric methods confirmed that DNA replication is limited to a well-defined segment of the interphase preceded and succeeded by other periods where the DNA content was constant (3, 4). Better spatial resolution was obtained when the highly localized tritiated thymidine was introduced as a radioactive probe which increased the precision of autoradiographic procedures (5). The incorporation of tritiated thymidine was restricted specifically to DNA, not to RNA, and only one of the double strands was labeled. This result was consistent with semiconservative model proposed by Watson and Crick. The principle of semiconservative replication was then proved by the classical experiments of Meselson and Stahl in 1958 (6).

The importance of the experiments of Howard and Pelc is that they led to the recognition that the cell cycle consists of phases known as G1, S, G2, and M. Although the examination of the kinetics of cell proliferation with labeled compounds and autoradiography remained an important technique especially when the duration of the cell cycle phases matters, flow cytometry has become a more popular way to study the cell cycle. Laser scanning cytometry (LSC) technology of flow cytometry heritage is not limited to cell cycle analysis. LSC also allows to inspect and interrogate specific cells of defined genetic, biochemical, or morphological properties.

### *1.1. Basic Concepts of Cell Cycle Synchronization*

Synchronization of cell populations offers a unique strategy to study the molecular and structural events taking place as cells travel through the cell cycle. It allows the exact study of individual phases of the cell cycle, the regulatory mechanisms which determine cell cycle regulation at the level of gene expression and posttranscriptional protein modifications, and contributes to drug discovery. Before going into details first of all we define the basic concepts of cell cycle synchronization. In the process of synchronization, cells representing different stages of the cell cycle are selected and brought to the same phase. The cell cycle is composed of the replication of genetic materials (S phase) and the successive distribution of genetic materials as well as the other components of the cell onto two daughter cells (M phase). The progression of these two processes is intermitted by two gap phases (G1 and G2) and defined as the cell cycle (**Fig. 1.1**).

Originally the cell cycle was recognized in plant cells (7), but soon it turned out that the principal mechanism of the cell cycle is common in all eukaryotic organisms. The study of molecular

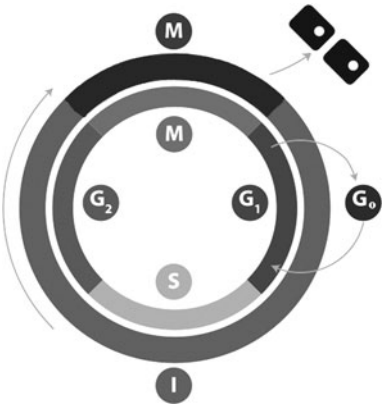


Fig. 1.1. Cell cycle phases of eukaryotic cells. Cells start to increase in size in Gap 1 (G1) phase. In the resting phase ($G_0$, Gap 0) cells have left the cycle and stopped dividing. DNA replication occurs during the synthetic (S) phase. During the Gap 2 (G2) between DNA synthesis and mitosis cells continue to grow. In mitosis (M) cell growth stops and the orderly division into two daughter cells takes place. Interphase (I) consists of three stages: G1, S, G2.

events of the cell cycle was taken over by animal and yeast cells (8) simply because there were no suitable cell synchronization systems in plant cells.

### 1.2. Principal Criteria and Shortcomings of Synchronization Methods

There are several principal criteria for synchronization that should be met: (a) both normal and tumor cells should be arrested at the same specific phase of the cell cycle, (b) synchronization must be noncytotoxic and reversible, (c) the metabolic block should be targeted to a specific reaction and must be reversible, (d) large quantities of synchronous cell populations should be obtained, (e) the synchronization must be medium independent, (f) synchrony should be maintained for more than one cell cycle to study biochemical processes taking place in cycling cells, (g) synchronized cells should exhibit uniform size, and (h) DNA content in the initial cell culture and during their growth should be the same. These criteria turned out to be quite stringent and resulted in heated debates that still exist among scientists. The major problem is that although many methods have been developed, none of them seems to be perfect for more reasons: (a) the proportion of synchronized cells is not sufficiently high, (b) manipulations during synchronization perturb cell physiology to an unacceptable extent, (c) most of the synchronizing methods are toxic and not applicable *in vivo*. For example, agents that prevent DNA synthesis (excess thymidine, hydroxyurea, aphidicolin) or inhibit the formation of mitotic spindles (nocodazole) not only arrest the cell cycle at certain points (9, 10), but may also kill important fractions of the cells due to their toxic effect (11). The low cost and simplicity of DNA replication inhibitors are contrasted by

their major disadvantage of inducing growth imbalance. Another example is nocodazole treatment. Cells subjected to this agent do not enter mitosis and cannot form metaphase spindles due to the inhibition of polymerization of microtubules. Moreover, when nocodazole was used as a whole-culture synchronization agent, it worked poorly on bovine kidney (MDBK) cells. After 0.5 ng/ml nocodazole treatment for 4 h there was no accumulation of M phase cells, rather a massive cell death (>80%) was induced (12). Other observations also demonstrated that populations of synchronized cells obtained by different drug treatments supposedly blocked at biochemically distinct cell cycle points were not apparent by cytometric measurement of DNA content. These results indicate that induced synchrony methods may differ with respect to their impact on cell cycle organization and from the pattern seen with nonperturbing cell selection methods (13). The intention of this book is neither to make strict distinctions nor to decide which method should be used. Debates on cell synchronization methodologies are found in opinion papers (14–18).

## 2. Methods of Cell Cycle Synchronization

The most widely used methods of cell cycle synchronization are based on two distinct strategies: physical fractionation and the chemical approach.

### *2.1. Physical Fractionation*

The separation of cells by physical means is based on cell density, cell size, antibody binding to cell surface epitopes, fluorescent emission of labeled cells, and light scatter analysis. The two most often used methods of biophysical fractionation are the centrifugal elutriation and fluorescent-activated cell sorting.

#### *2.1.1. Velocity Sedimentation*

Several techniques that separate cells take advantage of their differences in sedimentation velocity. These methods belong to three classes:

- Sedimentation at unit gravity (19–21),
- Density gradient centrifugation (22–25),
- Velocity sedimentation by counterstreaming centrifugation (27–33).

Major objections against the velocity sedimentation techniques are that they are relatively slow and the size of the nearby fractions may overlap substantially increasing the heterogeneity of the samples. Other major problems with the sedimentation at unit gravity and density gradient centrifugation are the reproducibility, owing to artifacts associated with sedimentation in swinging

bucket rotors (26). These two techniques are not used anymore, and therefore they will not be discussed.

### 2.1.2. Centrifugal Elutriation

The sedimentation velocity that is based on cell size is operative in the technique of centrifugal elutriation, also referred to as counterstreaming centrifugation (27–33). Lindahl was the first to describe the separation of cells by velocity sedimentation utilizing counterstreaming centrifugation. His method was later modified and renamed centrifugal elutriation. The Beckman elutriation system is an advanced centrifugation device that uses an increasing sedimentation rate to yield a better separation of cells in a specially designed centrifuge and a rotor containing the elutriation chamber. The advantages of centrifugal elutriation are as follows:

1. Differences in sedimentation velocity are exploited to isolate various types of cells from various inhomogeneous cell suspensions.
2. Different subpopulations representing different stages of the cell cycle of the same cell type can be separated.
3. The isolated cells or subpopulations of cells can be used in clinical experiments.
4. Centrifugal elutriation fullfills the principal criteria for synchronization.

Autoradiographic data indicated that fractions containing ≥97% Gl cells, >80% S cells, and 70–75% G2 cells could be routinely recovered with centrifugal elutriation (34). This distribution indicates that the resolution of the G1 and S phases belonging to the interphase could be increased while the heterogeneity of the G2 and M phases would not allow a higher resolution. In exponentially growing cultures ≥20% of the cells are in G1, about ≥60% in S phase, and only 16–18% in G2/M phase. This distribution makes it clear that in animal cells the resolution of the interphase G1 and S phases would be possible. As a result of the improved resolution of the centrifugal elutriation the two known replicative phases (early and late S phase) could be resolved to many subphases the number of which corresponded to the number of chromosomes (35, 36).

In the budding yeast G1 phase cells are unbudded and often smaller than one would expect from the cell cycle status. The budding profile serves as a basis of estimating cell synchrony. In the fission yeast there is no such distinctive feature that would allow the morphological determination of the cell cycle position. The cell cycle progression of the yeast cells is size dependent similarly to the cells of budding yeasts and higher eukaryotes (37).

With centrifugal elutriation, several different cell populations synchronized throughout the cell cycle could be rapidly obtained with a purity comparable to mitotic selection and cell sorting

(38). Centrifugal elutriation will be described in **Chapter 2**. **Chapter 12** compares the results from the elutriation protocols with other synchronization protocols.

*2.1.3. Flow Cytometry and Cell Sorting*

The original name of this technology was pulse cytophotometry, but flow cytometry became the most popular among others such as cytofluorometry, flow microfluorometry, and flow microfluorimetry. To understand this technique that uses a system for the measurement of individual cells obtained from cell suspension, the analogy with a conveyor belt is taken. Conveyor belts were originally used as rubber belts in factories (39), but they are also used in supermarkets, where they carry selected goods to the interrogation point. From there the cashier picks the goods individually and identifies them with a laser that reads the barcode. At the interrogation point the items can then be packed into shopping bags or similar items can be grouped and then packed in separate bags. A similar process takes place during flow cytometry without the separation of cells or combined with their separation named cell sorting (**Fig. 1.2**).

Flow cytometry is a technique that allows the counting and examination of small (0.2–150 μm) particles (chromosomes, nuclei, cells) suspended in a stream of fluid passed through an electronic detection apparatus. In cell biology, individual cells contained in a thin stream of fluid intercept the light source. These cells scatter light and fluorochrome dyes are excited. There are several fluorochrome dyes that can be used for DNA staining. For quantitative DNA analysis, cells are normally fixed in ethanol, followed by staining with DNA-binding dyes, such as

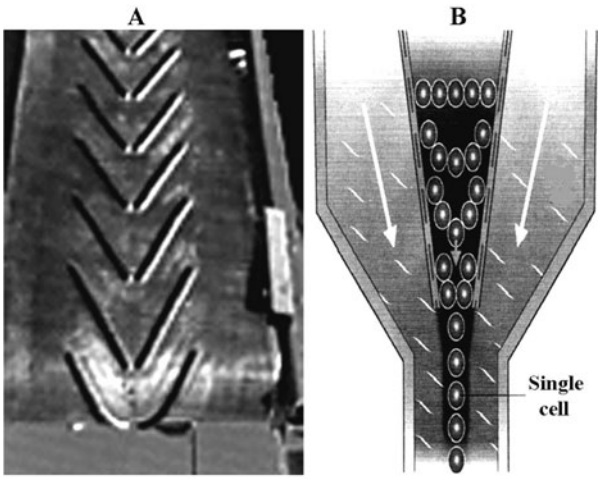


Fig. 1.2. Analogy between a conveyor belt and flow cytometry. (**a**) Industrial belt (38). (**b**) Hydrodynamic focusing during flow cytometry to produce a single stream of cells (39).

1. Propidium iodide (Phenatridinium compound)
2. Hoechst 33342 (Bisbenzimidazole)
3. DAPI (4′,6-diamidino-2-phenylindole)
4. 7-Aminoactinomycin D (Actinomycin)
5. Mithramycin (Chromomycinone)
6. DRAQ5 (Anthraquinone)
7. TO-PRO-3 (comprising a single cyanine dye and a cationic side chain, with only two positive charges).

Some of the dyes are used to quantitatively stain DNA and to separate live from dead cells in unfixed samples. Fluorochromes excited from a lower (300–650 nm) to a higher energy state emit this energy as a photon of light at various frequencies (450–700 nm) with spectral properties unique to different fluorochromes. Photomultipliers convert the light to electrical signals and cell data are collected. High-purity (100%) cell subpopulations can be identified and sorted when flow cytometry is combined with cell sorting.

Flow cytometers and analyzers are capable to collect multiparameter cytometry data but do not separate or purify cells. Sorting is an additional process requiring sophisticated electronic components not incorporated into most bench-top instruments. In flow cytometry and fluorescent-activated cell sorting (FACS analysis) the light beam (regularly laser) is directed to the stream of fluid containing the particles. Most often used light sources in flow cytometry are argon-, krypton-, helium–neon-, helium cadmium lasers, and mercury lamp. Detectors are focused to the interrogation point where the light beam (regularly laser beam) passes through the fluid stream. In forward scatter analysis (FSC), detectors are in line with the light beam, while in side scatter analysis (SSC) several detectors, among them fluorescent detectors, are directed perpendicularly to the beam. Forward and side scatter are used for the preliminary identification of cells. Forward scatter depends on the cell volume and cell size, while side scatter analysis is correlated with the inner complexity of the particle (i.e., shape of the cell or nucleus, amount and type of granules or roughness of cellular membranes). Forward and side scatter were used earlier to exclude debris and dead cells. Recently forward scatter has been adapted for the detection of apoptotic cell death.

Advantages and disadvantages of flow cytometry

1. Flow cytometry measures fluorescence per cell or particle and contrasts with spectrophotometry where the percent absorption and transmission at a certain wavelength is measured for a bulk volume. One of the fundamentals of flow cytometry is its ability to measure the properties of individual particles.

2. The sorting of particles based on their physical properties, to purify populations of interest.
3. The simultaneous physical and/or chemical analysis of thousands of particles per second.
4. Routinely used diagnostic tool in health disorders (especially cancers) and has many applications in both research and clinical practice.
5. Data of samples can be stored in computer as listmode and/or histogram files.
6. The disadvantage of cell sorting is that it exhibits limitations in sample size and time required for synchronization (40).

Listmode files contain the complete list of all events corresponding to all the parameters collected and written in the file. Listmode files contain raw cytometer data. Listmode describes flow cytometry values of the scatter and fluorescence parameters for each event, in the order it passed through the cytometer's interrogation point. Listmode files can be replayed by the computer and appropriate software. Different signals can be amplified and processed by an Analog to Digital Converter (ADC) allowing the events to be plotted on a graphical scale. These histogram files can be either single-parameter or two-parameter files. The single-parameter histograms have 1,024 channels and consist of graphs plotting the cell count on the *y*-axis and the measurement parameter (e.g., *C*-value) on *x*-axis (**Fig. 1.3**). When measuring fluorescence from a DNA-binding fluorochrome, we regard this to

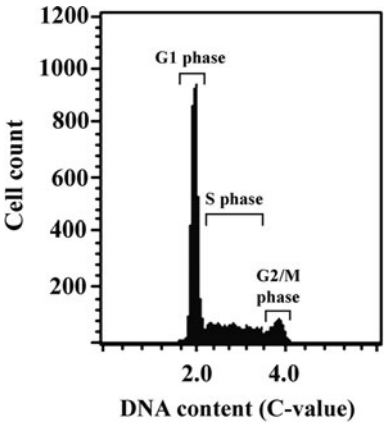


Fig. 1.3. Flow cytometry: single-parameter histogram. Flow cytometry measures the properties of individual particles. After injecting the sample solution into flow cytometer, the particles are randomly distributed in three-dimensional space. Upon hydrodynamic focusing, each particle passes through one or more beams of light. Single particles can be interrogated by the machine's detection system. Histograms can be given as density plots, contour diagrams, single parameter (see DNA profile, **Fig. 1.3**) or two-parameter (dual-color fluorescence) histogram (**Fig. 1.4**).

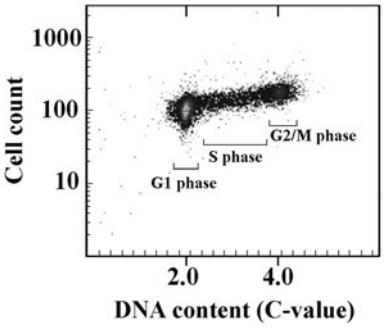


Fig. 1.4. Flow cytometry: two-parameter histogram. The graph displays two measurement parameters, one on the *y*-axis and one on the *x*-axis and the cell count as a density plot. Parameters may come from side scatter channel (SSC), forward scatter channel (FSC), or fluorescence.

be the same as the DNA content, expressed in *C*-value (*C*-value of 1 corresponds to haploid DNA content per cell). A graph of a two parameter histogram represents two parameters of measurements: the DNA content on the *x*-axis and the cell count height on the *y*-axis similar to a topographical map (**Fig. 1.4**).

DNA histograms yield the relative number of cells in G1/G0, S, and G2/M phases of the cell cycle. The percentage of cells being in each of these phases can be estimated. However, the static information of histograms does not provide information on how many cells are progressing through these phases and what percentage of cells is trapped in these phases.

*2.1.4. Cytofluorometric Purification of Cells*

A novel procedure for the purification of cells in distinct phases of the cell cycle was developed based on the stable transfection of cells with a chimeric protein made up of histone H2B and green fluorescent protein (GFP) (11). Cytofluorometric purification of cells by their size and their H2B-GFP-dependent fluorescence allowed the efficient separation of diploid and tetraploid cells in a fluorescence-activated cell sorter (FACS). DNA content analysis after staining with fluorochromes (propidium iodide, Hoechst 33342) serves as a basis for fluorescence-activated cell sorting (FACS) to obtain synchronous cell populations. A more detailed description and protocol for cytofluorometric purification will be given in **Chapter 3**.

*2.1.5. Microchip-Based Flow Cytometers*

Flow cytometry is carried out for various medical purposes including the counting of blood cells, detection of pathogenic microbes. However, the running of commercial flow cytometers is expensive and requires skilled operators. Microchip-based flow cytometers have been developed which require much lower volumes of reagents. These devices reduce substantially the cost of diagnosis especially when the chips are disposable. In microchip-based flow

cytometers, the detected and sort particles are focused hydrodynamically to pass them through a small detection region (41–46). Particles are pressed through the device under an external hydrostatic pressure gradient or under electro-osmotic flow by controlling the movement of the fluid.

*2.1.6. Dielectrophoresis*

This method uses laminar flow and electrokinetic forces for the efficient, noninvasive separation of living cells. The alternative current moves particles forward and backward from microelectrodes by periodically reversing the direction of the electric charge (47, 48). A dielectrophoresis-activated cell synchronizer device has been constructed that accepts an asynchronous mixture of cells, fractionates the cell populations according to the cell cycle phase, and elutes them through different outlets. The device utilizes electric fields that are 1–2 orders of magnitude below those used in electroporation and enriches asynchronous tumor cells in the G1 phase to 96% in one round of sorting, in a continuous flow manner (49).

## *2.2. Cell Separation with Chemical Blockade ("Arrest and Release" Strategy)*

*2.2.1. Mitotic Selection*

An alternative to overcome the objections of the mitosis-inhibiting (stathmokinetic) approaches involves mitotic selection (50). The stathmokinetic method will be discussed later. In monolayer cultures, cells are spread over a relatively large area. During mitosis cells become spherical and only a small area of cell membrane remains in contact with the containing vessel. The nuclear material is divided during mitosis (**Fig. 1.5**).

The mitotic cells can be completely detached by gently shaking and isolated from the supernatant medium by centrifugation. In actively dividing cells the percentage of mitotic cells known as the mitotic index is relatively low. The mitosis is relatively short compared to the duration of the cell cycle. It can be judged by multiplying the mitotic index by the cell cycle which is normally between 1.0 and 2.5 h. Assuming that the average durations of G1, S, and G2 + M are 8, 10, and 2 h, respectively, then the mitosis takes less than 10% of the cell cycle. To collect sufficient number of mitotic cells for synchronization purpose,

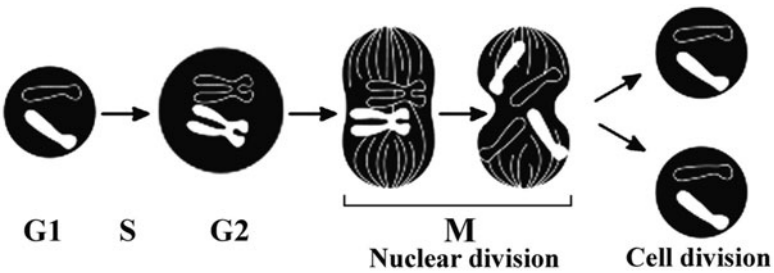


Fig. 1.5. Nuclear and cell division. The scheme does not show the duration of these processes, mitosis represent only a short period of time (1.0–2.5 h) of the cell cycle.

selection is limited only to those cell lines that are grown in a single layer on a flask or Petri dish containing the culture medium and detach during mitosis. Consequently, this method is applicable only to anchorage-dependent, monolayer cell cultures (e.g., HeLa, HaCaT, CHO).

Nevertheless, either alone or in combination with blocking agents such as hydroxyurea, the mitotic shake-off turned out to be an excellent method for synchronizing cells (38).

*2.2.2. Membrane Elution for Synchronization ("Baby Machine")*

This method is analogous to the mitotic shake-off in the sense that one can harvest synchronized cells without any chemical treatment. In this method for batch synchronization of membrane elution, growing cells are bound to a membrane. At division, one cell remains attached to the membrane, the other small daughter cell ("baby") is released into the medium (51, 52). These newborn cells have a G1 phase DNA content that reflects a normal cell cycle (11).

*2.2.3. Types of Chemical Blockade*

The idea behind *in vitro* chemical synchronization is the exposure of a random population of cells to agents that interfere with specific biosynthetic processes, such as DNA replication. The cells blocked in a specific stage of the cell cycle are then released by washing in control media or buffer, followed by the addition of exogenous substrates (e.g., nucleosides, nucleotides) to follow the wavelike rhythm of the cell cycle.

Cells separation by blocking metabolic reactions has been reviewed by Merrill in 1998 (53). The steady state of cell growth can be altered by the addition of drugs that block or delay the progression of the cell cycle in a specific phase. Methods can be grouped depending on which cell cycle phase has been arrested. Classes of batch synchronization methods arrest cells at

1. Mitosis by mitotic spindle poisons such as colchicine, vinca alkaloids (vincristine), nocodasol. Razoxane specifically inhibits the enzyme topoisomerase II resulting in the inhibition of cell division in the premitotic and early mitotic phases of the cell cycle.
2. Other synchronization methods affect DNA synthesis and are proposed to block the cell cycle in S phase (double thymidine block, hydroxyurea, aphidicolin).
3. The third class of chemical synchronization arrests cells at a specific point in the G1 phase, often at the "restriction point" (serum starvation).
4. Combined administration of blocking agents.

2.2.3.1. Chemical Blockade of Mitosis

*Roscovitine.* This is an olomoucine-related purine flavopiridol and is a highly potent inhibitor for the kinase activity of cyclin-dependent kinases (CDK1, CDK2, CDK5, and CDK7, but not

for CDK 4 and CDK 6) by competing with ATP at the ATP binding site of the kinase (54). Roscovitine is a potent inhibitor acting in G0/G1. However, roscovitine has been reported to prevent cell cycle progression of mammalian cells not only at the $G_1$–S but also in $G_2$–M checkpoints (55, 56).

*Mimosine*. The plant amino acid mimosine may inhibit initiation at origins of replication (57). Theoretical considerations argue against the use of batch synchronization methods as they are likely to disturb cell growth and prevent the understanding of the normal cell cycle (11).

*Colchicine*. One of the best known examples of chemical synchronization is the addition of colchicine (colcemid) which causes cell cycle arrest in metaphase by depolymerizing tubulin in microtubules. After treating cells with colcemid (or rasoxane, ICRF 159) cells accumulate in M phase and cannot proceed to anaphase. Sampling of cell populations at intervals after colcemid treatment showed a progressive shift of the flow cytometric profile from left to the right. Colchicine has been used to increase proportions of G2/M cells from 13 to 27–32% in pig mammary cells and up to 37% in fibroblasts (58).

*Vincristine (Oncovin, leurocristine)*. This vinca alkaloid from the Madagascar periwinkle *Catharanthus roseus* (*Vinca rosea)* is also a mitotic inhibitor, and is used in cancer chemotherapy. The mitodepressive effect and stathmokinetic action of cathinone from *Catha edulis* (59) and pantopon, a preparation of opiates (60), were reported on the meristematic region in the root tips of *Allium cepa* (garden onion).

Major objections against these and other stathmokinetic (mitosis inhibiting) approaches are that cell cycle blockades are likely to perturb and alter the behavior of the cell population in an unpredictable manner. Such a known example is the colcemid block of mitogenically stimulated B lymphocytes that resulted not only in G2 block but also in a G1 arrest. Moreover, tumorigenic lymphoblastoid cell lines have lost their sensitivity to growth inhibition by colcemid during early G1 (61).

#### 2.2.3.2. Cell Separation by the Inhibition of DNA Synthesis

One method that is generally used is the exposure of randomly proliferating cells to agents that interfere with specific biosynthetic activities, e.g., DNA replication. The cells blocked in the S phase are subsequently released by washing in control media, followed in some cases by the addition of exogenous tracers such as nucleosides. The removal of the blocking agent permits cells to move into succeeding segments of the cell cycle.

Metabolic reactions of cells are most often blocked by the inhibition of DNA synthesis and by nutritional deprivation. DNA synthesis can be inhibited during S phase by inhibitors of DNA replication such as excess thymidine (62), aminopterin (4-amino folic acid) (63–65), hydroxyurea (66, 67), methotrexate (68),

fluorodeoxyuridine (69), butyrate (12, 70–71), cytosine arabinoside (72), low temperature (73). The cell cycle is blocked by these inhibitors primarily in S phase resulting in viable cells. Their effects are variable and often debated. Best known nutrient deprivation methods are serum starvation and statin (e.g., lovastatin) treatment.

*Double thymidine block (early S phase block)*. A typical procedure for a double-thymidine block was described by Whitfield in 2002 (74). Cells (e.g., HeLa) at ~30% confluency are washed with buffer (PBS) growth medium, and cells are grown in the presence of 2 mM thymidine for 18 h. After the first block thymidine is removed, cells are washed and grown in fresh medium for 9 h to release cells from the block. The release is followed by the second block by the addition of 2 mM thymidine and cultivation for 17 h. As a result of this synchronization cells progress synchronously through G2 and mitotic phase and will be arrested at the beginning of S phase. Synchrony can be monitored by flow cytometry of propidium iodide-stained cells. After release from the thymidine block, >95% of the cells entered S phase (in 0–4 h), progressed into G2 phase (5–6 h), underwent a synchronous mitosis at 7–8 h, and reentered S phase after completing one full cell cycle at 14–16 h. Typically two to three additional synchronous cell cycles were obtained (74). Thymidine synchronization showed a constant rate of synthesis of DNA throughout S phase, but cells synchronized with aminopterin show a slower initial rate of DNA synthesis (65).

*Hydroxyurea*. Hydroxyurea is used to treat certain types of cancer or blood disorders. This medication may also be useful for chronic urinary tract infections or certain cases of psoriasis. In cell biology, hydroxyurea synchronization increases mitotic yield of cell lines. Large quantities of synchronized cells have been isolated in late G1 by growth in isoleucine-deficient medium followed by resuspension in fresh, complete medium containing either hydroxyurea (to $10^{-3}$ M) or cytosine arabinoside (to 5 μg/ml) (75).

The inhibitors that have been used most frequently for synchronization are hydroxyurea, which inhibits ribonucleotide reductase (76), and aphidicolin, an inhibitor of DNA polymerases (77). However, none of these agents has been regarded as truly satisfactory since both are chain elongation inhibitors that would not inhibit initiation of replication at the replication forks. Thus, most of the events of interest (i.e., initiation at early-firing origins) would have already occurred prior to release from the blocking agent. Unfortunately, drugs that specifically prevent either entry into the S period or initiation at origins have not yet been identified.

*Aphidicolin*. This tetracyclic diterpenoid produced by the fungus *Cephalosporium aphidicola* (78) selectively inhibits DNA

polymerase α (79). This enzyme is essential for nuclear replicative DNA synthesis, without affecting nuclear DNA repair synthesis and mitochondrial DNA replication (80, 81). Rodent and porcine fibroblasts can be reversibly synchronized at the S phase with aphidicolin treatment (82, 83). Aphidicolin turned out to be an effective agent in the synchronization of human HeLA (84) blocking the cell cycle at the transition from G1 to S phase (77). Cell synchronization is achieved by inhibition of DNA replication in **Chapter 6**.

*Butyrate*. A specific cell cycle synchronization was developed for a bovine kidney (MDBK) cell line. Exposure of MDBK cells to 10 mM butyrate caused inhibition of cell growth and cell cycle arrest in a reversible manner. Flow cytometric evidence was presented that butyrate affected the cell cycle at a specific point immediately after mitosis at the early stage of G1 phase. In comparison with other inhibitors, such as serum deprivation and aphidicolin, butyrate induced similar synchrony of cell populations (12). A protocol for cell cycle synchronization with butyrate and cell cycle analysis by flow cytometry will be given in **Chapter 8**.

2.2.3.3. Nutrient Deprivation

*Serum starvation (G0/G1 block)*. Removal of serum from a rapidly growing cell culture for about 24 h results in the accumulation of cells in G1 phase. Synchronized cells can then be released into S phase by the addition of serum. Nutritional serum starvation has been widely used for synchronizing cells by arresting them in the G0/G1 phase of the cell cycle, but it often reduced cell survival and increased DNA fragmentation (83) which caused high-embryonic losses after nuclear transfer (NT) (85). Regularly only non-tumor cells can be synchronized in $G_0/G_1$ by removal of growth factors ("serum starvation," amino acid depletion). In transformed cells proliferation is relatively independent of serum and growth factors, thus neoplastic cells may not cease proliferation upon serum deprivation, nor do they cease stringent $G_0$ arrest (86).

*Treatment with statins.* The mechanism by which lovastatin synchronizes cells is unknown. Lovastatin suppresses the synthesis of mevalonate by inhibiting 3-hydroxy-3-methylglutaryl-coenzyme A (HMG-CoA) reductase, the rate-limiting enzyme in the sterol-biosynthetic pathway. In addition to the deprivation of mevalonate by lovastatin, compactin (mevastatin), a related fungal toxin (87), and mevinolin (88), these statins also inhibit DNA replication (89–94). Lovastatin was successfully introduced as an early G1 synchronization agent with cell lines including normal and tumor cells of mouse, hamster and human origin (95). Statins as $G_1$ inhibitors prevent farnesylation and geranylation of proteins (96) and are effective CDK2 protein kinase inhibitors (97–99). Synchronization was achieved by the use of compactin

(87, 100) presumably by blocking DNA replication and mevalonate production.

*Other inhibitors.* It has been reported that roscovitine, a specific cyclin-dependent kinase 2 (CDK2) inhibitor more efficiently synchronized cells in the G0/G1 phase of the cell cycle than serum starvation and resulted in an increase in cloning efficiency as defined in terms of survival of fetuses and calves following embryo transfer (101).

2.2.3.4. Combined Administration of Blocking Agents

Blocking agents have been often applied for synchronization due to the simple procedure consisting of cell growth in the presence of the inhibitor. Cells blocked in one of the cell cycle phases (regularly in S phase) were then subsequently released by washing away the inhibitor and thereby permitting their simultaneous movement into succeeding segments of the cell cycle. Partial synchronization of cell division *in vitro* has been obtained with considerable success through the implementation of these techniques. The utilization of more than one antimetabolite was expected to improve the efficiency of synchronization.

*Thymidine–nocodazole.* Cells can be arrested in mitosis by blocking first in thymidine followed by release and then blocking in nocodazole. After release from the nocodazole block, most of the cells (>75%) divided synchronously within 2 h of release from the arrest, entered S phase by 10–12 h after release, and completed the next synchronous mitosis by 18–20 h, ultimately completing two full cell cycles (74).

*Thymidine–colcemid.* When successive treatment with excess thymidine and colcemid was applied all in one generation a high degree of synchrony was achieved by this method (102). The mitosis index of blastomeres increased from 9% metaphases (colchicine synchronization) to 18% (thymidine + colchicine synchronization) per embryo. The *in vitro* development of embryos was not affected by treatment (103).

*Citosine arabinoside–colcemid.* A number of studies have demonstrated that cytosine arabinoside (ara-C) inhibits mitotic activity in mammalian cells both *in vitro* (104) and *in vivo* (105, 106). The mitotic activity of Lieberkuhn's crypt epithelial components increased from 3 to 5% levels to peak values of 15% in rats treated with a single injection of either ara-C or colcemid. In animals treated with ara-C followed by colcemid the efficiency of synchronization was significantly improved, at least two-thirds of the epithelial cells were identified as dividing cells (107).

*Methotrexate versus serum deprivation and colcemid treatment.* Methotrexate or aphidicolin treatment induces a reversible blockade at the beginning of S phase which can be reversed upon drug removal with a consequent wave of synchronization (108). The combination of serum deprivation and aphidicolin was compared with low non-toxic concentrations (0.04–0.08 μM) of

methotrexate under standard culture conditions in cancer cell lines. Synchronization with methotrexate alone turned out to be a better choice for obtaining highly synchronous human cancer cell population than those induced by aphidicolin alone or by a combination of serum deprivation and aphidicolin (109). These experiments indicate that the combination of synchronization techniques and/or repeated perturbation of cell physiology do not necessarily contribute to a more homogeneous pool of synchronized cells. It is thus better to use the combination of methods that have less or no effect on the cell cycle. Such a combination is centrifugal elutriation with a nutrient starvation protocol. Nutrient starvation contributes to a better size selection and improves synchrony. Moreover, less cells will be needed for elutriation.

### 2.3. Synchronization of Embryonic Cells

Serum deprivation of embryonic stem cells before cell transplantation was adapted to decrease the rate of cell death after transplantation (110). To decide whether G0 or G1 cells function better as donor cells has been analyzed during the cell cycle of goat-transfected fibroblasts and determined the timing of transition from G0 to G1. Northern blot analysis showed that after serum starvation for 4 days quiescent cells started entering G1 and a few hours after addition of 10% serum to the medium cells were at the mid-G1 stage (111).

### 2.4. Synchronization at Low Temperature

Human fibroblasts which are in S phase at the time of switching to low temperature (30°C) complete their DNA synthesis and become arrested in the G1 phase of the cell cycle. The arrested cells can continue proliferation by restoration of the optimal growth temperature (37°C). At 30°C DNA replication was inhibited while the excision-repair process was operative but at a slightly reduced rate in comparison. This method was recommended for the study of S phase-dependent processes, as well as for repair studies in the absence of cell division (112). The effect of low incubation temperature on synchronization was also studied in cultures of *Plasmodium falciparum*. Growth seemed to be arrested when parasites reached maturation, but re-established their growth normally when returned to 37°C (113).

### 2.5. Comparison of Cell Synchrony Techniques

*Different methods–same cell culture*. This was done by taking aliquots from the same culture of exponentially growing CHO cells, which were then synchronized using mitotic selection, mitotic selection and hydroxyurea block, centrifugal elutriation, or an EPICS V cell sorter. It was concluded that, either alone or in combination with blocking agents such as hydroxyurea, elutriation and mitotic selection were both excellent methods for synchronizing cells (38).

The use of aphidicolin or hydroxyurea resulted in highly synchronized CHO cell populations, but methotrexate yielded inadequate synchronization (114). It was demonstrated that both aphidicolin and hydroxyurea were useful drugs for obtaining highly synchronized cell populations after an initial synchrony in mitosis. Aphidicolin was regarded as the best choice because of less toxicity to S phase cells when used in low concentrations.

*Selecting inhibitors for bone marrow cultures.* Methods for synchronization of bone marrow cells with fluorodeoxyuridine (FdU) and methotrexate (MTX) were compared. Fluorodeoxyuridine did not require cell washing for release of the DNA synthesis block and was found to be more beneficial for bone marrow cultures because it generally produced a higher mitotic yield and was less damaging to chromosomes than methotrexate (69). However, after FdU treatment flow cytometric analysis showed not only the accumulation of cells in early S phase over time, but also the increased radiation sensitivity of the entire population. Early S turned out to be the most radiosensitive phase of the cell cycle (115). Synchrony was tested *in vivo* in acute leukemic patients after a single injection of L-asparaginase, hydrocortisone, cyclophosphamide, cytosine arabinoside, methotrexate, and an exchange transfusion (62% of the total blood volume). L-Asparaginase and hydrocortisone were found to arrest the entry of cells into the S period. Cyclophosphamide inhibited DNA synthesis, arrested cells in mitosis, and inhibited the entry of cells into the S period. Cytosine arabinoside and methotrexate inhibited DNA synthesis. During the period of time the cells were inhibited in the S phase by these two drugs, cells continued to enter the S period. Thus, partial synchronization was achieved after cytosine arabinoside and methotrexate treatment (72).

*Selection among G1/S blocking agents.* For cytogenetic replication studies the timing of cell synchronization is restricted to G1 or early S phase. To get more precise information with regard to the point of G1/S transition different blocking systems have been investigated. Human amniotic fluid cells and fibroblast were temporarily blocked by replication inhibitors: thymidine (dT) surplus, fluorodeoxyuridine (FU), hydroxyurea (HU), and methotrexate uridine (MU). Most variation was found after HU treatment. MU synchronized cells before the onset of S phase. The arresting point of dT surplus and FdU was in early S phase (116).

### 2.6. Synchronization of Unicellular Organisms

*Synchronization of Escherichia coli.* To synchronize *E. coli* cells in culture, two major approaches have been routinely used. One involves temperature-sensitive alleles of the DNA replication protein DnaC (117) that interacts with DNA helicase, DnaB (118), required for the initiation of DNA replication. When the culture is shifted to nonpermissive temperature this will allow all replication forks to be completed without the initiation of new ones.

Subsequent shift to permissive temperature allows initiation of the synchronized culture (119). The other method is based on the attachment of cells to a membrane, while newborn cells are released to the medium. This technique is the adaptation of the "baby machine" (120, 121). Although cells are hardly perturbed, large quantities of cells cannot be collected by this method. Moreover, there are significant variations in stickiness among different *E. coli* strains (121). A new method of *E. coli* synchronization applies DL-serine hydroxamate, an aminoacid analog, which arrests DNA replication at initiation (122). Sporulation of bacteria and outgrowth of spores can be utilized for the synchronization of *B. subtilis* (**Chapter 11**).

*Synchronization of yeast.* Budding yeast can utilize a wide range of carbon sources (glucose, galactose, ethanol, and glycerol. These carbon sources may serve as a means to control the cell cycle, growth rates, and cell size which can be useful in the development of synchronization methods, which in turn may contribute to exploit yeasts in biotechnology.

The synchronization of yeast cells include: feeding and starving, magnesium exhaustion, repetitive heat shock, DNA division cycle block and release, α-factor mating pheromone block, cdc mutants arresting at specific cell cycle stages at a restrictive temperature, continuous synchrony by periodic feeding or dilution. These methods have been summarized by Walker in 1999 (123). An overview of the most commonly used methods to generate synchronized yeast cultures is presented in **Chapter 12**.

### 2.7. Effect of Synchronization on Transfection

Aphidicolin cell synchronization in G2/M phase led to a slight increase in plasma membrane permeabilization, to a threefold increase in percentage of transfected Chinese hamster cells, and to an eightfold increase in gene expression. This increase in cell transfection was specifically due to the G2/M synchronization process. Cell synchronization in G1 phase by sodium butyrate had no effect on cell permeabilization and transfection (124). S phase synchronized CHO cells also showed elevated transfection efficiency (125). The hypothesis that cell cycle synchronization increases transfection efficiency was confirmed in human trabecular meshwork cells. While efficiency of transfection increased about threefold in synchronized cells compared to controls, it still remained low (~3%) (126).

## References

1. Watson, J. D., and Crick, F. H. (1953) Molecular structure of nucleic acids: a structure for deoxyribonucleic acid. *Nature* **171**, 737–738.
2. Howard, A., and Pelc, S. (1953) Synthesis of deoxyribonucleic acid in normal and irradiated cells and its relation to chromosome breakage. *Heredity* **6**, 261–273.

3. Walker, P. M., and Yates, H. B. (1952) Nuclear components of dividing cells. *Proc. R. Soc. Lond. B Biol. Sci.* **140**, 274–299.
4. Swift, H. (1953) Nucleoproteins in the mitotic cycle. *Tex. Rep. Biol. Med.* **11**, 755–774.
5. Taylor, J. H., Woods, P. S., and Hughes, W. L. (1957) The organization and duplication of chromosomes as revealed by autoradiographic studies using tritium-labeled thymidine. *Proc. Natl. Acad. Sci. USA* **43**, 122–128.
6. Meselson, M., and Stahl, F. W. (1958) The replication of DNA in *Escherichia coli*. *Proc. Natl. Acad. Sci. USA* **44**, 671–682.
7. Howard, A., and Pelc, S. R. (1951) Nuclear incorporation of $P^{32}$ as demonstrated by autoradiographs. *Exp. Cell Res.* **2**, 178–187.
8. Baserga R. (1985) *The biology of cell reproduction*. Harvard University Press, Cambridge, MA.
9. Amon, A. (2002) Synchronization procedures. *Methods Enzymol.* **351**, 457–467.
10. Cooper, S. (2003) Rethinking synchronization of mammalian cells for cell cycle analysis. *Cell. Mol. Life Sci.* **60**, 1099–1106.
11. Coquelle, A., Mouhamad, S., Pequignot, M. O., Braun, T., Carvalho, G., Vivet, S., Métivier, D., Castedo, M., and Kroemer, G. (2006) Enrichment of non-synchronized cells in the G1, S and G2 phases of the cell cycle for the study of apoptosis. *Biochem. Pharmacol.* **72**, 1396–1404.
12. Li, C. J., and Elasser, T. H. (2006) Specific cell cycle synchronization with butyrate and cell cycle analysis by flow cytometry for Madin Darby Bovine Kidney (MDBK) cell line. *J. Anim. Vet. Adv.* **5**, 916–923.
13. Urbani, L., Sherwood, S. W., and Schimke, R. T. (1995) Dissociation of nuclear and cytoplasmic cell cycle progression by drugs employed in cell synchronization. *Exp. Cell Res.* **219**, 159–168.
14. Cooper, S. (2004a) Is whole-culture synchronization biology's 'perpetual-motion machine'? *Trends Biotechnol.* **22**, 266–269.
15. Cooper, S. (2004b) Rejoinder: whole-culture synchronization cannot, and does not, synchronize cells. *Trends Biotechnol.* **22**, 274–276.
16. Spellman, P. T., and Sherlock G. (2004a) Reply: whole-culture synchronization – effective tools for cell cycle studies. *Trends Biotechnol.* **22**, 270–273.
17. Spellman, P. T., and Sherlock G. (2004b) Final words: cell age and cell cycle are unlinked. *Trends Biotechnol.* **22**, 277–278.
18. Liu, S. V. (2005) Debating cell-synchronization methodologies: further points and alternative answers. *Trends Biotechnol.* **23**, 9–10.
19. Macdonald, H. R., and Miller, R. G. (1970) Synchronization of mouse L-cells by a velocity sedimentation technique. *Biophys. J.* **10**, 834–842.
20. Durand, R. E. (1975) Isolation of cell subpopulations from in vitro tumor models according to sedimentation velocity. *Cancer Res.* **35**, 1295–1300.
21. Tulp, A., and Welagen, J. J. (1976) Fractionation of ascites tumour cells at 1 g: separation of cells in specific stages of the life cycle. *Eur. J. Cancer.* **12**, 519–526.
22. Mitchison, J. M., and Vincent, W. S. (1965) Preparation of synchronous cell cultures by sedimentation. *Nature* **205**, 987–989.
23. Schindler, R., Ramseier, L., Schaer, J. C., and Grieder, A. (1970) Studies on the division cycle of mammalian cells. 3. Preparation of synchronously dividing cell populations by isotonic sucrose gradient centrifugation. *Exp. Cell Res.* **59**, 90–96.
24. Wolff, D. A., and Pertoft, H. (1972) Separation of HeLa cells by colloidal silica density gradient centrifugation. I. Separation and partial synchrony of mitotic cells. *J. Cell Biol.* **55**, 579–585.
25. Probst, H., and Maisenbacher, J. (1973) Use of zonal centrifugation for preparing synchronous cultures from Ehrlich ascites cells grown in vivo. *Exp. Cell Res.* **78**, 335–344.
26. Banfalvi, G. (2008) Cell cycle synchronization of animal cells and nuclei by centrifugal elutriation. *Nat. Protoc.* **3**, 663–673.
27. Lindahl, P. E. (1956) On counter streaming centrifugation in the separation of cells and cell fragments. *Biochim. Biophys. Acta* **21**, 411–415.
28. Sörenby, L., and Lindahl, P. E. (1964) On the concentrating of ascites tumour cells in stages of pre-mitosis and mitosis by counterstreaming centrifugation. *Exp. Cell Res.* **35**, 214–217.
29. Grabske, R. J., Lake, S., Gledhill, B. L., and Meistrich, M. L. (1975) Centrifugal elutriation: separation of spermatogenic cells on the basis of sedimentation velocity. *J. Cell Physiol.* **86**, 177–189.
30. Meistrich, M. L., Meyn, R. E., and Barlogie, B. (1977) Synchronization of mouse L-P59 cells by centrifugal elutriation separation. *Exp. Cell Res.* **105**, 169–177.
31. Grdina, D. J., Peters, L. J., Jones, S., and Chan, E. (1978) Separation of cells from a murine fibrosarcoma on the basis of size. I. Relationship between cell size and age as modified by growth in vivo or in vitro. *J. Natl. Cancer Inst.* **61**, 209–214.

32. Gohde, W., Meistrich, M. L., Meyn, R. E., Schumann, J., Johnston, D., and Barlogie, B. (1979) Cell-cycle phase-dependence of drug-induced cycle progression delay. *J. Histochem. Cytochem.* **27**, 470–473.
33. Shumaker, V. N. (1967) Zone centrifugation. *Adv. Biol. Phys.* **11**, 245–339.
34. Keng, P. C., Li, C. K. N., and Wheeler, K. T. (1980) Synchronization of 9L rat rain tumor cells by centrifugal elutriation. *Cell Biophys.* **2**, 191–206.
35. Banfalvi, G., Mikhailova, M., Poirier, L. A., and Chou, M. W. (1997) Multiple subphases of DNA replication in Chinese hamster ovary (CHO-K1) cells. *DNA Cell Biol.* **16**, 1493–1498.
36. Rehak, M., Csuka, I., Szepessy, E., and Banfalvi, G. (2000) Subphases of DNA replication in *Drosophila* cells. *DNA Cell Biol.* **19**, 607–612.
37. Day, A., Schneider, C., and Schneider, B. L. (2004) Yeast cell synchronization. *Methods Mol. Biol. Clifton, N.J.* **241**, 55–76.
38. Grdina, D. J., Meistrich, M. L., Meyn, R. E., Johnson, T. S., and White, R. A. (1984) Cell synchrony techniques. I. A comparison of methods. *Cell Tissue Kinet.* **17**, 223–236.
39. Continental conveyors Ltd. http://www.ccpl.in/?gclid=CL2u7qbjxp8CFVmHzAodFzb4ew
40. Rahman, M. http://www.abdserotec.com/uploads./Flow-Cytometry.pdf
41. Lee, G.-W., Hung, C.-I., Ke, B.-J., Huang, G.-R., Hwei, G.-R., Hwei, B.-H., and Lai, H.-F. (2001) Hydrodynamic focussing for a micromachined flow cytometer. *Trans. ASME.* **123**, 62–679.
42. Fiedler, S., Shirley, S. G., Schnelle, T., and Fuhr, G. (1998) Dielectrophoretic sorting of particles and cells in a microsystem. *Anal. Chem.* **70**, 1909–1915.
43. Fu, A. Y., Spence, C., Scherer, A., Arnold, F. H., and Quake, S. R. (1999) A microfabricated fluorescence-activated cell sorter. *Nat. Biotechnol.* **17**, 1109–1111.
44. Gawad, S., Schild, L., and Renaud, P. (2001) Micromachined impedance spectroscopy flow cytometer for cell analysis and particle sizing. *Lab. Chip.* **1**, 76–82.
45. Kruger, J., Singh, K., O'Neill, A., Jackson, C., Morrison, A., and O'Brien, P. (2002) Development of a microfluidic device for fluorescence activated cell sorting. *J. Micromech. Microeng.* **12**, 486–494.
46. Schrum, D. P., Culbertson, C. T., Jacobson, S. C., and Ramsey, J. M. (1999) Microchip flow cytometry using electrokinetic focusing. *Anal. Chem.* **71**, 4173–4177.
47. Morgan, H., Holmes, D., and Green, N. G. (2003) 3D focusing of nanoparticles in microfluidic channels. *IEE Proc. Nanobiotechnol.* **150**, 76–81.
48. Holmes, D., Sandison, M. E., Green, N. G., and Morgan, H. (2005) On-chip high-speed sorting of micron-sized particles for high-throughput analysis. *IEE Proc. Nanobiotechnol.* **152**, 129–135.
49. Kim, U., Shu, C. W., Dane, K. Y, Daugherty, P. S, Wang, J. Y., and Soh, H. T. (2007) Selection of mammalian cells based on their cell-cycle phase using dielectrophoresis. *Proc. Natl. Acad. Sci. USA* **104**, 20708–20712.
50. Teresima, T., and Tolmach, L. J. (1963) Growth and nucleic acid synthesis in synchronously dividing populations of HeLa cells. *Exp. Cell Res.* **30**, 344–362.
51. Thornton, M., Eward, K. L., and Helmstetter, C. E. (2002) Production of minimally disturbed synchronous cultures of hematopoietic cells. *Biotechniques* **32**, 1098–1100.
52. Cooper, S. (2002) Minimally disturbed, multicycle, and reproducible synchrony using a eukaryotic "baby machine". *Bioessays* **24**, 499–501.
53. Merrill, G. F. (1998) Cell synchronization. *Methods Cell Biol.* **57**, 229–249.
54. Mgbonyebi, O. P., Russo, J., and Russo, I. H. (1999) Roscovitine induces cell death and morphological changes indicative of apoptosis in MDA-MB-231 breast cancer cells. *Cancer Res.* **59**, 1903–1910.
55. Rudolph, B., Saffric, J. Z., Henglein, B., Muller, R., Ansorge, W., and Eilers, M. (1996) Activation of cyclin-dependent kinases by Myc mediates induction of cyclin A but not apoptosis. *EMBO J.* **15**, 3065–3076.
56. Azevedo, W. F., Leclerc, S., Meijer, L., Havlicek, I., Strnad, M., and Kim, S. H. (1997) Inhibition of cyclin-dependent kinases by a purine analogs: crystal structure of human cdk2 complexed with roscovitine. *Eur. J. Biochem.* **243**, 518–526.
57. Mosca, P. J., Dijkwel, P. A., and Hamlin, J. L. (1992) The plant amino acid mimosine may inhibit initiation at origins of replication in Chinese hamster cells. *Mol. Cell. Biol.* **12**, 4375–4383.
58. Boquest, A. C., Day, B. N., and Prather, R. S. (1999) Flow cytometric cell cycle analysis of cultured porcine fetal fibroblast cells. *Biol. Reprod.* **60**, 1013–1019.
59. Al-Meshal, I. A. (1987) Mitodepressive effect of (−)-cathinone, from *Catha edulis* (khat), on the meristematic region of *Allium cepa* root tips. *Toxicon* **4**, 451–454.

60. Kabarity, A., El-Bayoumi, A., and Habib, A. A. (1979) Mitodepressive effect and stathmokinetic action of pantopon hydrochloride. *Mutat. Res-Gen. Tox. En.* **2**, 143–148.
61. Kenter, A. L., Watson, J. V., Azim, T., and Rabbitts, T. H. (1986) Colcemid inhibits growth during early G1 in normal but not in tumorigenic lymphocytes. *Exp. Cell Res.* **167**, 241–251.
62. Viegas-Pequiqnot, E., and Dutrillaux, B. (1970) Une methode: simple pour obtenis des prophases et des prometaphases. *Ann. Genet.* **21**, 122–125.
63. Rueckert, R. R., and Mueller, G. C. (1960) Studies on unbalanced growth in tissue culture. I. Induction and consequences of thymidine deficiency. *Cancer Res.* **20**, 1584–1591.
64. Kishimoto, S., and Lieberman, I. (1965) Nuclear membranes of cultured mammalian cells. *J. Biol. Chem.* **25**, 103–107.
65. Adams, R. L. P. (1969) The effect of endogenous pools of thymidylate on the apparent rate of DNA synthesis. *Exp. Cell Res.* **56**, 55–58.
66. Gallo, J. H., Ordomez, J. V., Brown, G. E., and Testa, J. R. (1984) Synchronization of human leukemic cells: relevance for high resolution chromosome banding. *Hum. Genet.* **66**, 220–224.
67. Biegel, J. A., Leslie, D. S., Bigner, D. D., and Bigner, S. H. (1987) Hydroxyurea synchronization increases mitotic yield in human glioma cell lines. *Acta Neuropathol.* **73**, 309–312.
68. Yunis, J. J., Bloomfield, G. D., and Ensrud, K. (1981) All patients with acute nonlymphocytic leukemia may have a chromosomal defect. *N. Engl. J. Med.* **305**, 135–139.
69. Webber, L. M., and Garson, O. M. (1983) Fluorodeoxyuridine synchronization of bone marrow cultures. *Cancer Genet. Cytogenet.* **8**, 123–132.
70. Wright, J. A. (1973) Morphology and growth rate changes in Chinese hamster cells cultured in presence of sodium butyrate. *Exp. Cell Res.* **78**, 456–460.
71. Kruh, J., Defer, N., and Tichonicky, L. (1992) Molecular and cellular action of butyrate. *C. R. Seances Soc. Biol. Fil.* **186**, 12–25.
72. Lampkin, B. C., Nagao, T., and Mauer, A. M. (1971) Synchronization and recruitment in acute leukemia. *J. Clin. Invest.* **50**, 2204–2214.
73. Boucher, B., and Norman, C. S. (1980) Cold synchronization for the study of peripheral blood and bone marrow chromosomes in leukemia and other hematologic disease states. *Hum. Genet.* **54**, 207–211.
74. Whitfield, M. L., Sherlock, G., Saldanha, A. J., Murray, J. I., Ball, C. A., Alexander, K. E., Matese, J. C., Perou, C. M., Hurt, M. M., Brown, P. O., and Botstein, D. (2002) Identification of genes periodically expressed in the human cell cycle and their expression in tumors. *Mol. Biol. Cell.* **13**, 1977–2000.
75. Tobey, R. A., and Crissman, H. A. (1972) Preparation of large quantities of synchronized mammalian cells in late G1 in the pre-DNA replicative phase of the cell cycle. *Exp. Cell Res.* **75**, 460–464.
76. Skoog, L., and Nordenskjold, B. (1971) Effect of hydroxyurea and 1-0-D-arabinofuranosyl-cytosine on deoxyribonucleotide pools in mouse embryo cells. *Eur. J. Biochem.* **19**, 81–89.
77. Wang, T. F. (1991) Eukaryotic DNA polymerases. *Annu. Rev. Biochem.* **60**, 513–552.
78. Brundret, K. M., Dalziel, W., Hesp, B., Jarvis, J. A. J., and Neidle, S. (1972) *X*-Ray crystallographic determination of the structure of the antibiotic aphidicolin: a tetracyclic diterpenoid containing a new ring system. *J. Chem. Soc. Chem. Commun.* 1027–1028.
79. Nagano, H., and Ikegami, S. (1980) Aphidicolin: a specific inhibitor of eukaryotic DNA polymerase alpha. *Seikagaku* **52**, 1208–1216.
80. Sala, F., Parisi, B., Burroni, D., Amileni, A. R., Pedrali-Noy, G., and Spadari, S. (1980) Specific and reversible inhibition by aphidicolin in the alpha-like DNA polymerase of plant cells. *FEBS Lett.* **117**, 93–98.
81. Sala, F., Galli, M. G., Levi, M., Burroni, D., Parisi, B., Pedrali-Noy, G., and Spadari, S. (1981) Functional roles of the plant alpha-like and gamma-like DNA polymerases. *FEBS Lett.* **124**, 112–118.
82. Levenson, V., and Hamlin, J. (1993) A general protocol for evaluation the specific effects of DNA replication inhibitors. *Nucleic Acids Res.* **21**, 3997–4004.
83. Kues, W. A., Anger, M., Carnwarth, J. W., Motlik, J., and Nieman, H. (2000) Cell cycle synchronization of porcine fibroblasts: effects of serum deprivation and reversible cell cycle inhibitors. *Biol. Reprod.* **62**, 412–419.
84. Pedrali-Noy, G., Spadari, S., Miller-Faurès, A., Miller, A. O., Kruppa, J., and Koch, G. (1980) Synchronization of HeLa cell cultures by inhibition of DNA polymerase alpha with aphidicolin. *Nucleic Acids Res.* **8**, 377–387.

85. Lawrence, J. L., Schrick, F. N., Hopkins, F. M., Welborn, M. G., McCracken, M. D., Sonstegard, T., Wilson, T. J., and Edwards, J. L. (2005) Fetal losses and pathologic findings of clones derived from serum-starved versus serum-fed bovine ovarian granulosa cells. *Reprod. Biol.* **5**, 171–184.
86. Scher, C. D., Stone, M. E., and Stiles, C. D. (1979) Platelet-derived growth factor prevents Go growth arrest. *Nature* **281**, 390–392.
87. Endo, A., Kuroda, M., and Tansawa, K. (2004) Competitive inhibition of 3-hydroxy-3-methylglutaryl coenzyme A reductase by ML-236A and ML-236B. fungal metabolites having hypocholesterolemic activity. *Atheroscler. Suppl.* **5**, 39–42.
88. Langan, T. J., and Slater, M. C. (2005) Isoprenoids and astroglial cell cycling: diminished mevalonate availability and inhibition of dolichol-linked glycoprotein synthesis arrest cycling through distinct mechanisms. *J. Cell Physiol.* **149**, 284–292.
89. Larson, R. A., Chung, J., Scanu, A. M., and Vachnin, S. (1982) Neutrophils are required for the DNA synthetic response of human lymphocytes to mevalonic acid: evidence suggesting that a nonsterol product of mevalonate is involved. *Proc. Natl. Acad. Sci. USA* **79**, 3028–3032.
90. Habenicht, A. J., Glomset, J. A., and Ross, R. (1980) Relation of cholesterol and mevalonic acid to the cell cycle in smooth muscle and swiss 3T3 cells stimulated to divide by platelet-derived growth factor. *J. Biol. Chem.* **255**, 5134–5140.
91. Maltese, W. A., and Sheridan, K. M. (1987) Isoprenylated proteins in cultured cells: subcellular distribution and changes related to altered morphology and growth arrest induced by mevalonate deprivation. *J. Cell. Physiol.* **133**, 471–481.
92. Langan, T. J., and Volpe, J. J. (1987) Cell cycle-specific requirement for mevalonate, but not for cholesterol, for DNA synthesis in glial primary cultures. *J. Neurochem.* **49**, 513–521.
93. Doyle, J. W., and Kandutsch, A. A. (1988) Requirement for mevalonate in cycling cells: quantitative and temporal aspects. *J. Cell. Physiol.* **137**, 133–140.
94. Sinensky, M., and Logel, J. (1985) Defective macromolecule biosynthesis and cellcycle progression in a mammalian cell starved for mevalonate. *Proc. Natl. Acad. Sci. USA* **82**, 3257–3261.
95. Keyomarsi, K., Sandoval, L., Band, V., and Pardee, A. B. (1991) Synchronization of tumor and normal cells from G1 to multiple cell cycles by lovastatin. *Cancer Res.* **51**, 3602–3609.
96. Jakóbisiak, M., Bruno, S., Skierski, J., and Darzynkiewicz, Z. (1991) The cell cycle specific effects of lovastatin. *Proc. Natl. Acad. Sci. USA* **88**, 3628–3632.
97. Crissman, H. A., Gadbois, D. M., Tobey, R. A., and Bradbury, E. M. (1991) Transformed mammalian cells are deficient in kinase-mediated progression through the $G_1$ phase of the cell cycle. *Proc. Natl. Acad. Sci. USA* **88**, 7580–7585.
98. Bruno, S., Ardelt, B., Skierski, J. S., Traganos, F., and Darzynkiewicz, Z. (1992) Different effects of staurosporine, an inhibitor of protein kinases, on the cell cycle and chromatin structure of normal and leukemic lymphocytes. *Cancer Res.* **52**, 470–476.
99. Bruno, S., Traganos, F., and Darzynkiewicz, Z. (1996) Cell cycle synchronizing properties of staurosporine. *Methods Cell Sci.* **18**, 99–107.
100. Nagel, W. W., and Vallee, B. L. (1995) Cell cycle regulation of metallothionein in human colonic cancer cells. *Proc. Natl. Acad. Sci. USA* **92**, 579–583.
101. Gibbons, J., Arat, S., Rzucidlo, J., Miyoshi, K., Waltenburg, R. D., Respess, D. S., Tumlin, M., and Stice, S. L. (2002) Enhanced survivability of cloned calves derived from roscovitine-treated adult somatic cells. *Biol. Reprod.* **66**, 895–900.
102. Doida, Y., and Okada, S. (1967) Synchronization of L5178Y cells by successive treatment with excess thymidine and colcemid. *Exp. Cell Res.* **48**, 540–548.
103. Rottmann, O. J., and Arnold, S. (1983) Enhancing the mitotic index of blastomeres by thymidine synchronization. *Anim. Reprod. Sci.* **6**, 239–242.
104. Kim, J. H., and Eidinoff, M. L. (1965) Action of 1-(3-D-arabinofuranosylcytosine on the nucleic acid metabolism and viability of HeLa cells. *Cancer Res.* **25**, 698–702.
105. Lenaz, L., Sternberg, S. S., and Philips, F. S. (1969) Cytotoxic effects of 1-beta-D-arabinofuranosyl-5-fluorocytosine and of 1-beta-D-arabinofuranosylcytosine in proliferating tissues in mice. *Cancer Res.* **29**, 1790–1798.
106. Bertalanffy, F. D., and Gibson, M. H. L. (1971) The in vivo effects of arabinosylcytosine on the proliferation of murine B16 melanoma and Ehrlich ascites tumor. *Cancer Res.* **31**, 66–71.
107. Verbin, R. S., Diluiso, G., Liang, H., and Farber, E. (1972) Synchronization of cell

division in vivo through the combined use of cytosine arabinoside and colcemid. *Cancer Res.* **32**, 1489–1495.
108. Erba, E., Sen, S., Lorico, A., and D'Incalci, M. (1992) Potentiation of etoposide cytotoxicity against a human ovarian cancer cell line by pretreatment with non-toxic concentrations of methotrexate or aphidicolin. *Eur. J. Cancer.* **28**, 66–71.
109. Erba, E., and Sen, S. (1996) Synchronization of cancer cell lines with methotrexate in vitro. *Methods Cell Sci.* **18**, 149–163.
110. Zhang, E., Li, X., Zhang, S., Chen, L., and Zheng, X. (2005) Cell cycle synchronization of embryonic stem cells: effect of serum deprivation on the differentiation of embryonic bodies in vitro. *Biochem. Biophys. Res. Commun.* **333**, 1171–1177.
111. Memili, E., Behboodi, E., Overton, S. A., Kenney, A. M., O'Coin, M., Zahedi, A., Rowitch, D. H., and Echelard, Y. (2004) Synchronization of goat fibroblast cells at quiescent stage and determination of their transition from G0 to G1 by detection of cyclin D1 mRNA. *Cloning Stem Cells.* **6**, 58–66.
112. Enninga, I. C., Groenendijk, R. T., van Zeeland, A. A., and Simons, J. W. (1984) Use of low temperature for growth arrest and synchronization of human diploid fibroblasts. *Mutat. Res.* **130**, 343–352.
113. Rojas, M. O., and Wasserman, M. (2007) Effect of Low temperature on the in vitro growth of *Plasmodium falciparum*. *J. Eukaryot. Microbiol.* **40**, 149–152.
114. Fox, M. H., Read, R. A., and Bedford, J. S. (1987) Comparison of synchronized Chinese hamster ovary cells obtained by mitotic shake-off, hydroxyurea, aphidicolin, or methotrexate. *Cytometry* **8**, 315–320.
115. Miller, E. M., and Kinsella, T. J. (1992) Radiosensitization by fluorodeoxyuridine: effects of thymidylate synthase inhibition and cell synchronization. *Cancer Res.* **52**, 1687–1694.
116. Vogel, W., Schempp, W., and Sigwarth, I. (1978) Comparison of thymidine, fluorodeoxyuridine, hydroxyurea, and methotrexate blocking at the $G_1$/S phase transition of the cell cycle, studied by replication patterns. *Hum. Genet.* **45**, 193–198.
117. Carl, P. L. (1970) *Escherichia coli* mutants with temperature-sensitive synthesis of DNA. *Mol. Gen. Genet.* **109**, 107–122.
118. Wickner, S., and Hurwitz, J. (1975) Interaction of *Escherichia coli* dnaB and dnaC(D) gene products in vitro. *Proc. Natl. Acad. Sci. USA* **72**, 921–925.
119. Withers, H. L., and Bernander, R. (1998) Characterization of dnaC2 and dnaC28 mutants by flow cytometry. *J. Bacteriol.* **180**, 1624–1631.
120. Helmstetter, C. E., and Cummings, D. J. (1963) Bacterial synchronization by selection of cells at division. *Proc. Natl. Acad. Sci. USA* **50**, 767–774.
121. Helmstetter, C. E., Eenhuis, C., Theisen, P., Grimwade, J., and Leonard, A. C. (1992) Improved bacterial baby machine: application to *Escherichia coli* K-12. *J. Bacteriol.* **174**, 3445–3449.
122. Ferullo, D. J., Cooper, D. L., Moore, H. R., and Lovett, S. T. (2009) Cell cycle synchronization of *Escherichia coli* using the stringent response, with fluorescence labeling assays for DNA content and replication. *Methods* **48**, 8–13.
123. Walker, G. M. (1999) Synchronization of yeast cell populations. *Methods Cell Sci.* **21**, 87–93.
124. Golzio, M., Teissié, J., and Rols, M.-P. (2002) Cell synchronization effect on mammalian cell permeabilization and gene delivery by electric field. *Biochim. Biophys. Acta* **1563**, 23–28.
125. Grosjean, F., Batard, P., Jordan, M., and Wurm, F. M. (2002) S phase synchronized CHO cells show elevated transfection efficiency and expression using CaPi. *Cytotechnology* **38**, 57–62.
126. Hoffman, E. A., Poncius, A., McKay, B. S., and Stamer, W. D. (2004) Cell cycle synchronization and transfection efficiency of human trabecular meshwork cells. *Invest. Ophthalmol. Vis. Sci.* **45**, 4432.

# Chapter 2

# Synchronization of Mammalian Cells and Nuclei by Centrifugal Elutriation

Gaspar Banfalvi

## Abstract

Synchronized populations of large numbers of cells can be obtained by centrifugal elutriation on the basis of sedimentation properties of small round particles, with minimal perturbation of cellular functions. The physical characteristics of cell size and sedimentation velocity are operative in the technique of centrifugal elutriation also known as counterstreaming centrifugation. The elutriator is an advanced device for increasing the sedimentation rate to yield enhanced resolution of cell separation. A random population of cells is introduced into the elutriation chamber of an elutriator rotor running in a specially designed centrifuge. By increasing step by step the flow rate of the elutriation fluid, successive populations of relatively homogeneous cell size can be removed from the elutriation chamber and used as synchronized subpopulations. For cell synchronization by centrifugal elutriation early log S phase cell populations are most suitable where most of the cells are in G1 and S phase (>80%). Protocols for the synchronization of nuclei of murine pre-B cells and high-resolution centrifugal elutriation of CHO cells are given. The verification of purity and cell cycle positions of cells in elutriated fractions includes the measurement of DNA synthesis by [$^3$H]-thymidine incorporation and DNA content by propidium iodide flow cytometry.

**Key words:** Counterstreaming centrifugation, cell separation, velocity sedimentation, elutriator, resolution power.

## 1. Introduction

### *1.1. Definition of Terms: Elution, Elutriation, Centrifugal Elutriation*

Elution is an analytical process by which chemicals are emerging from a chromatography column and normally flow into a detector. The material obtained with the carrier (eluent) is the mobile phase and known as the eluate. In liquid column chromatography the eluent is a solvent (**Fig. 2.1a**). Elutriation is a technique to separate small particles suspended in a fluidized bed into different size groups by passing an increasing flow rate through the

G. Banfalvi (ed.), *Cell Cycle Synchronization*, Methods in Molecular Biology 761,
DOI 10.1007/978-1-61779-182-6_2, © Springer Science+Business Media, LLC 2011

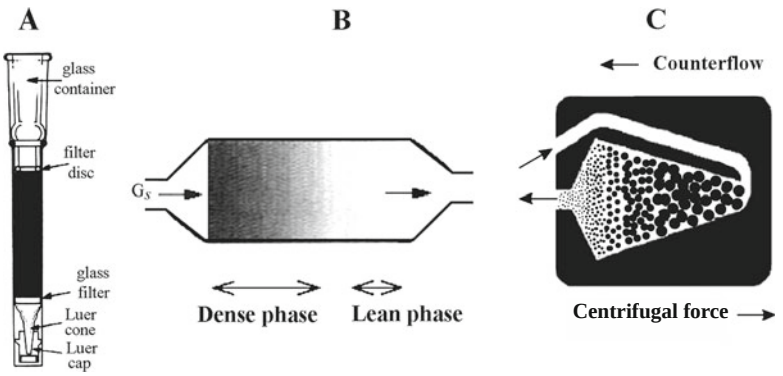


Fig. 2.1. Schematic views of elution, elutriation, and centrifugal elutriation. (**a**). For elution in column chromatography a liquid eluent is used. (**b**) Horizontal elutriation in a fluidized bed of particles with flux $G_S$. (**c**) Fractionation of cells by centrifugal elutriation. Cells are introduced with an initial lower flow rate which is opposed by the centrifugal force. By increasing the flow rate the floating cells in the elutriation chamber can be driven out and separated into 10–30 distinct size fractions.

elutriation chamber. In elutriation particles are suspended in a moving fluid which can be liquid or gas. In vertical elutriation smaller particles move upward with the fluid. Large particles will not be driven out of the elutriation chamber and tend to settle out on the walls or at the bottom of the elutriator due to the higher gravity exerted on their larger size. In horizontal position the suspended particles are passed through the elutriation chamber. By increasing stepwise the fluid velocity the particles can be separated into fractions (**Fig. 2.1b**). The principle of centrifugal elutriation is similar to elutriation except that the fluid is pumped into a rotating separation chamber that converges into an outlet tube (**Fig. 2.1c**).

### *1.2. Development and Application of Centrifugal Elutriation*

The first apparatus that exploited differences in velocity sedimentation for the separation of cells by counterstreaming centrifugation was described by Lindahl in 1948 (1). The Beckman Instrument Company modified this instrument and named it elutriator and termed the process centrifugal elutriation (2). Further refinement and a second chamber style known as the Sanderson chamber was introduced giving a better resolution especially with small cells (3). Centrifugal elutriation has been applied to separate hemopoietic cells, mouse tumor cells, testicular cells, and a variety of other specialized cells from other cells and cells in particular phases of the cell cycle reviewed first by Pretlow in 1979 (4). Several further applications have been described (5–9). The construction of the commercially available centrifugal elutriator resulted in a rapid purchase of these instruments especially in the United States in the second half of the 1970s, with high

expectations and significantly lower outcome than originally expected. The major reason of insufficient or lacking data is the missing technical skill necessary for the assembling and operation of these instruments and the use of such heterogeneous batch cultures that made the separation irreproducible. It is thus important to discuss first the circumstances that may cause experimental failures during the centrifugal elutriation.

### 1.3. Principles of Centrifugal Elutriation

Among the methods used to monitor cell cycle changes two distinct strategies prevailed (10). One is the chemical "arrest-and-release" approach that arrests cells at a certain stage of the cell cycle and then by the removal of the blocking agent by which synchronized cells are released to the next phase. In the alternative approach, cells are separated by physical means such as mitotic shake-up, gradient centrifugation, cell sorting, centrifugal elutriation. These methods have been overviewed in **Chapter 1**.

Counterflow centrifugal elutriation separates subpopulations of cells on the basis of cell volume and density. As there is only a slight change in cell density during the cell cycle, the principle of cell separation during elutriation is based on cell size (**Fig. 2.2**).

Before going to the point-by-point elutriation protocol, the following precautions are advised to avoid unnecessary mistakes and problems during the execution of this cell synchronization technique:

*Culture medium*. For test run and pilot experiments saline can be used to find out the right conditions (centrifugal force, flow rate) for cell fractionation. Although, any medium can be used for elutriation, it is advised that the elutriation fluid should be the physiological culture medium. To limit the cost of elutriation the fetal calf serum concentration can be reduced to 1%. Some investigators use cost-efficient 1% bovine serum albumin. The protein content prevents cells from clumping and the cellular debris from adhering to the chamber wall. Cell aggregates normally accumulate at the entrance of the elutriation chamber and may

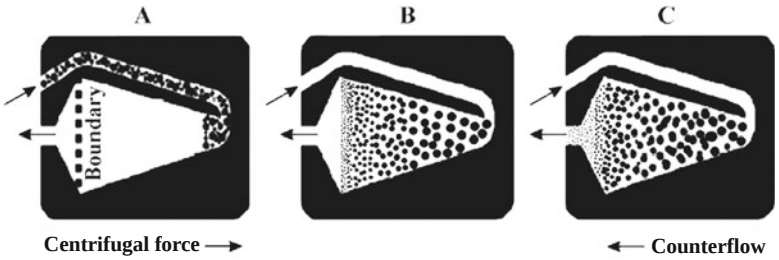


Fig. 2.2. Cell synchronization by centrifugal elutriation based on different cell size. The centrifugal force and the counter stream act in opposite directions in the elutriation chamber. (**a**) Early S phase cells enter the elutriation chamber. (**b**) Size gradient is balanced by centrifugal force and counterflow of elutriation by keeping the cells floating inside the chamber. (**c**) Increasing flow rate elutes smaller cells first followed by larger ones. Reproduced with permission of Banfalvi (11).

clog it. In such case the chamber has to be disassembled, whiped out with a soft paper towel, cleaned with a mild detergent, and reassembled taking care of the right position of the plastic insulation. High protein concentration may cause foaming and cell lysis. The culture medium should contain only soluble materials, any particle left in the medium may contribute to aggregation or will appear in one of the elutriated fractions obscuring the cell cycle profile.

*Cells.* Most significant cell growth takes place in S phase, it is thus not surprising that nearly 100% of G1 cells and more than 80% of S cells could be recovered by centrifugal elutriation (12). Best separation can be achieved by using cell populations maintained in early S phase of growth for several generations. This will reduce the number of aging and dying cells due to anoxia, the formation of artifacts, cell debris and will prevent clumpiness. Early S phase cells contribute to the reproduction of the results causing only small shift in the elutriation profile that can be attributed to minor differences in cell distribution.

Any suspension of cell line can be used for centrifugal elutriation. Cells that tend to stick together or attach to the culture substrate (e.g., Chinese hamster ovary cells) need more attention. These cells should be kept in suspension before synchronization by growing them in spinner flasks continuously stirred with a magnetic stirrer at speed high enough to prevent sedimentation and low enough to avoid cell breakage (**Fig. 2.3**). The resuspension of the cell suspension is also recommended by passing it several times through an 18-gauge needle right before loading in the elutriation chamber to ensure monodispersion. Once cells are in the chamber the flotation of cells keeps them separated.

### *1.4. Components of the Centrifugal Elutriation System*

The counterflow elutriation system (earlier Beckman, now Beckman-Coulter Inc.) consists of a centrifuge, elutriation rotor containing the elutriation chamber, stroboscope, peristaltic pump, manometer, sample mixing tube and the flow system (gauge for monitoring back pressure, injection and bypass valves, T-connector, rubber stoppers, and silastic tubing) (**Fig. 2.4**). Additionally the pump may be interfaced with a fraction collector. The cell separation is carried out in a specially designed centrifuge hosting either the standard JE-6B rotor or the larger JE-5.0 rotor. The standard elutriation chamber is available in two sizes. The small elutriation chamber has a capacity of approximately 4.5 ml and is suitable for the fractionation of $10^7$–$10^9$ cells. The large chamber is able to separate ten times more volume and cells. The geometry of the Sanderson chamber gives a better resolution for the separation of small cells in the range between $10^6$ and $10^8$ cells. The peristaltic pump is providing a gradually changing flow through the chamber with flow rates between 2 and 400 ml/min depending on the size of the chamber and the cells. The

Fig. 2.3. Spinner flasks for suspension cultures. Cell cultures (suspension or monolayer) are started in T-flasks containing 25 ml medium. After reaching confluency the cells of two flasks are combined in a smaller (200 ml) spinner flask that is sitting in the $CO_2$ incubator. Cells in suspension are grown under constant stirring in 100 ml medium starting at $\sim 10^5$ ml/ml density. Logarithmic growth is maintained by scaling up daily from 100 to 200 ml medium, then switching to a larger spinner flask (2 l) and doubling the volume of the medium to 400, 800, and if necessary 1,600 ml. Up to 3–4 $\times$ $10^8$ cells can be grown in 1 week before starting elutriation.

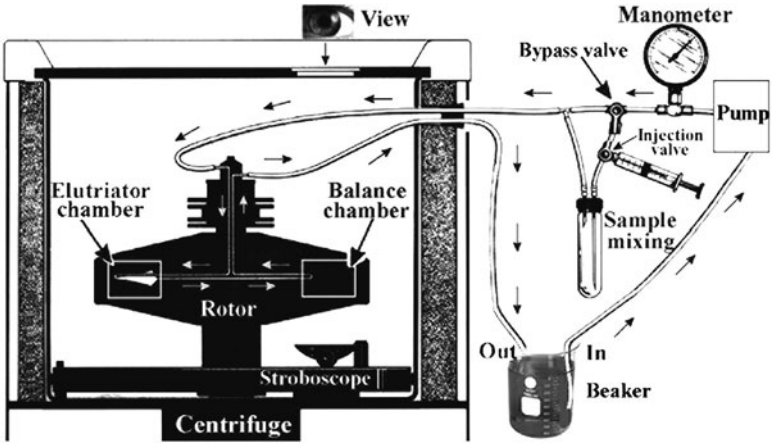


Fig. 2.4. Counterflow centrifugal elutriation system. The stroboscope is placed and fixed at the bottom of the centrifuge. The centrifuge is hosting the rotor that is running with constant speed. The pump is turned on and sterilization takes place by running 70% ethanol through the system followed by physiological buffer to remove traces of ethanol. The physiological buffer is then replaced by the elutriation fluid at an initial flow rate. The preliminary run also serves to remove bubbles from the system. The loading chamber serves as a sample mixer and in its bypass position traps small remaining bubbles and compensates pump pulsation. The bypass valve helps to remove residual bubbles from the sample mixer chamber. Reproduced with permission of Banfalvi (11).

**Table 2.1**
**Elutriation conditions for *Drosophila* and mammalian cells and murine pre-B nuclei**

| Cell type | Cell diameter (μm) | Flow rate (ml/min) | Centrifugal force of elutriation | | |
|---|---|---|---|---|---|
| | | | rpm | Rcf average (*g*) | Rcf maximum (*g*) |
| CHO | 11.9 | 12–49 | 2,000 | 569 | 753 |
| CHO | 11.9 | 19–52 | 2,200 | 575 | 683 |
| Indian muntjac | 11.4 | 12–50 | 2,200 | 575 | 683 |
| Murine pre-B | 10.2 | 11–73 | 2,200 | 688 | 911 |
| *Drosophila* S2 | 8.1 | 13–53 | 2,500 | 889 | 1,176 |
| Pre-B nuclei | 5.0 | 14–77 | 3,500 | 1,742 | 2,305 |

Temperature was 20°C for each elutriation.
Cell diameter refers to an average value of exponentially growing cells and average size of nuclei before synchronization, measured by multiparametric particle size counting. Rotational speed is given as revolution per minute (rpm), relative centrifugal force (Rcf) in *g*. Reproduced with permission of Banfalvi (11).

elutriation system uses either a constant centrifugal force and gradually increasing counterflow rate or a constant flow rate and reducing rotor speed to yield high resolution of synchronization. As the fine control of rotor speed reduction is not possible, constant speed and increasing flow rate are preferred. The rotor speed may vary between 1,800 and 3,500 rpm (~550–1,700×*g* relative centrifugal force) depending on cell size. Although, higher speed gives a better resolution, but the pump speed will also go up increasing the shearing force and the amount of cell debris. The relationship between cell size and centrifugal force is demonstrated in **Table 2.1**.

### *1.5. Monitoring the Efficiency of Centrifugal Elutriation*

Due to the close correlation between cell size and DNA content, the effectiveness of the separation can be tested by monitoring the results by cell number, cell size, and DNA content. The most simple method is to count the cells and estimate their size in a hemocytometer. This indispensable method visualizes cells and distinguishes among small and large cells as well as cell aggregates. Particle counters generally monitor changes in conductivity and help to automatize the counting procedure. Most of these devices provide information with respect to particle size and volume distribution. However, size distributions do not exclude errors generated by aggregation, coincidence and by nonspherical particles. Calibration was done by taking into consideration coincidence by counting the same cell population several times in

a Bürker chamber and by the particle counter. The ratio of cell count obtained by the cell number counted by the Bürker chamber over the cell number obtained by the particle counter serves then as a factor which is used to multiply the counter number to get the real cell number.

Flow cytometry is used to asses the quality of synchronization by monitoring size distribution with forward scatter analysis and concomitantly the DNA content of each elutriated fraction after staining with propidium iodide. Flow cytometry is also generally accepted for the evaluation of cellular processes (13, 14) for calculating proliferative parameters (15) to identify apoptotic cells by nuclear staining (16–18) or by the appearance of phosphatidylserine on cell surface (19) and monitor other cellular changes (20–22).

## 2. Materials

### 2.1. Disposables

1. 1.5 ml microcentrifuge tubes
2. 15 and 50 ml centrifuge tubes
3. 15 and 50 ml conical centrifuge tubes
4. Polystyrene test tubes
5. 25 and 75 $cm^2$ flasks for cell culture
6. 5 ml, 12 × 75 mm FACS tubes

### 2.2. Media and Solutions

1. RPMI 1640 growth medium
2. Fetal bovine serum (FBS). FBS was heat inactivated at 56°C for 30 min.
3. *Ham's medium*: Measure 10.64 g L-glutamine containing F12 powder for 1 l of 1× solution. Add 1.176 g/l of $NaHCO_3$ powder. Adjust pH to 7.1–7.2, as it will rise to 0.2–0.3 pH units during filtration. Filter-sterilize it immediately using a membrane with a porosity of 0.22 μm. Aseptically dispense into 100-ml sterile bottles. Store them in a cold room or in a refrigerator under 5°C until use. Before use, add 11 ml FBS albumin to each 100-ml F12 medium. F12 can be ordered as 1-, 5-, 10-, and 50-l liquid medium containing L-glutamine, without sodium hydrogen carbonate. Sterilized medium can be stored at 5°C for several weeks if unopened.
4. *Elutriation medium* (for 30 elutriation fractions): Prepare fresh 3.5 l of F12 culture medium in a 4-l flask containing 1% FBS. Omit filter sterilization, as fractionated cells are processed immediately after elutriation. Larger particles originating from F12 medium or from cell aggregates can be

removed by passing the medium and cell suspension through a 100-mesh stainless steel sieve.

5. *Phosphate-buffered saline (PBS)*: Instead of culture medium plus 1% FBS, $Ca^{2+}$- and $Mg^{2+}$-free PBS with 0.01% EDTA or without EDTA is successfully used as elutriation buffer. PBS contains 2.7 mM KCl, 4.3 mM sodium phosphate dibasic ($Na_2HPO_4$), 1.8 mM potassium phosphate monobasic ($KH_2PO_4$), 137 mM NaCl, pH 7.2. Sterilize in an autoclave.
6. *Saline*: Dissolve 9 g of NaCl in 1 l of distilled water and sterilize in an autoclave.
7. *Trypsin/EDTA solution*: Make up from 0.25% (wt/vol) trypsin, 1 mM EDTA in phosphate-buffered saline (PBS). Filter-sterilize. Stored at –20°C.
8. *PI solution for flow cytometry*: Dissolve 50 μg/ml of PI in 0.1 M ammonium citrate solution (not sterile).

## 3. Methods

### 3.1. Cell Growth

1. Keep the epithelial-like CHO-K1 cells (ATCC, CCL61) in suspension culture in spinner flasks using F12 Ham's medium supplemented with 10% heat-inactivated FBS at 37°C and 5% $CO_2$. Grow the murine pre-B cell line 70Z/3-M8 (23) in suspension culture at 37°C in RPMI 1640 medium supplemented with 10% FBS, 2 mg/ml mycophenolic acid, 150 mg/ml xanthine and 15 mg/ml hypoxanthine and $2 \times 10^{-5}$ M β-mercaptoethanol.
2. Maintain CHO cells as either monolayers in 75 $cm^2$ tissue culture flasks when smaller quantities of cells ($10^6$–$10^7$) are needed or in suspension in 250 ml and in 1-l spinner flasks if many cells are required, such as in elutriation ($2–3 \times 10^8$).
3. Maintain cells in logarithmic growth and high viability by culturing at densities between $1 \times 10^5$ and $4 \times 10^5$.
4. Replace media by splitting cells in the ratio of 1:2 daily. Grow CHO cells in suspension culture in 1 l spinner flasks containing a final volume of 800 ml F12 Ham's medium supplemented with 10% FBS. The suspension culture should initially contain $1–2 \times 10^5$ cells/ml at 37°C in 5% $CO_2$.
5. Grow cells for 24 h to a final concentration of $2–4 \times 10^5$ cells/ml for fractionation by centrifugal elutriation. Harvest cells by centrifugation at 600×*g* for 5 min at 5°C and resuspend in 10 ml of F12 medium containing 1% FBS. To avoid the presence of dead and fragmented cells in elutriated

fractions *see* **Note 1**. Remove cell aggregates by passing the cell suspension through a 100-mesh stainless steel sieve.

### 3.2. DNA Isolation

Isolate high molecular weight DNA from $10^6$ cells of elutriated fractions, determine the amount of DNA by a DyNA Quant fluorimeter (Hofer Scientific Instruments) using Hoechst 33258 dye, which binds to the minor groove of double-stranded DNA. Excite the bound dye with long UV light at 365 nm and measure its fluorescence at 458 nm with DNA from the calf thymus as standard.

### 3.3. Determination of DNA Content

(a) Isolate DNA from elutriated fractions by phenol extraction from an equal number of cells ($10^6$) from each elutriated fraction.

(b) Stain the DNA. The amount of DNA can be determined by specific dyes (e.g., Hoechst 33258).

(c) Excite the bond dye with UV light and measure DNA content. Use calf thymus DNA as DNA standard.

### 3.4. Measurement of Cell Number and Cell Size

Confirm the synchrony of elutriated fractions by measuring cell size in a Coulter Channelyzer or Coulter multisizer. The measurement of gradual and simultaneous increase both in cell size and in cell volume as well as the correlation between cell size and DNA content confirm that synchrony is maintained not only at low but also at increased and higher resolution.

### 3.5. Flow Cytometry

(a) Stain cells with 50 μg/ml of PI in 0.1 M ammonium citrate for 15 min at 0°C.

(b) Add an equal volume of 70% ethanol.

(c) Perform cell cycle analysis in a fluorescence-activated cell sorter. Use the flow cytometric profiles of elutriated fractions to calculate the nuclear DNA content expressed in average *C*-values (24). The *C*-value increases from 2C to 4C as the cell progresses through the S phase, providing quantitative measure of cell growth. When many fractions (>20) have to be processed within the same day, stained and fixed cells can be stored overnight in refrigerator (4°C) and flow cytometry can be performed next day.

### 3.6. Conditions Used for Centrifugal Elutriation

The elutriation system (earlier Beckman, now Beckman Coulter Inc.) is an advanced device that uses either a constant centrifugal force and gradually increasing counterflow rate or constant flow rate and reducing rotor speed to yield high resolution of synchronization. The cell separation is carried out in a specially designed centrifuge and rotor. This elutriator system was designed exclusively for research, not for diagnostic or therapeutic use.

### 3.6.1. Hardware

The hardware of the JE-6 elutriator system (JE-6B Rotor, elutriator, 6,000 rpm, 5,080×*g*, recoverable cells per run $10^9$) consists of the following subassemblies: centrifuge, rotor assembly, stroboscope, flow system, modified door for the Model J-21/J-21B or J2-21 centrifuges as well as various tools and lubricants. In our elutriation system, we used a J2-21 centrifuge and a JE-6B separation chamber (Beckman Coulter Inc.), in which the elutriation fluid was circulated at an initial flow rate of 16.5 ml/min using a MasterFlex peristaltic pump (Cole-Parmer Instrument Inc.) presterilized with 70% ethanol. Elutriation was performed at a rotor speed of 2,200 rpm (683×*g*) and temperature of 20°C for 4–5 h. Subpopulations of cells were eluted in F12 medium containing 1% FBS. We have also used the JE-5.0 elutriation system (JE-5.0 Rotor, Elutriator, 5,000 rpm, 4,704×*g*, retrievable cells per run $10^{10}$), including a Sanderson elutriation chamber (5 ml) and a J-6 M1 centrifuge (Beckman Instruments Inc.) (23). When the JE-5.0 elutriation chamber is used with the Avanti J-25 and Avanti J-26 XP series and with J6-MI centrifuges equipped with viewport door and strobe assembly, accelerated throughput, shorter run times can be achieved. The JE-6B low-volume elutriator rotor is excluded from the JE-5.0 elutriation system.

The protocol presented here has been developed to enable cell cycle studies in a variety of cell lines (25–27). The elutriation of 1–2 × $10^8$ cells in a JE-6B rotor and a J2-21 centrifuge was used most frequently in our experiments (28). The small JE-6B elutriation system was assembled according to the manufacturer's instructions. Only the flow system (gauge for monitoring back pressure, two three-way valves, T-connector, rubber stoppers, and several feet of silanistic tubing) was regularly disassembled after elutriation and reassembled before the next elutriation, as the centrifuge was normally used in several other experiments. For shaft, rotor, chamber, pressure ring, stroboscope, and flow system assembly and disassembly, see the instruction manual of the Beckman JE-6 or JE-5.0 elutriator rotor. The rotor speed and flow rate monogram in the manual give the necessary preliminary information on rotor speed (rpm), sedimentation rate, particle diameter (mm), and flow rate (ml/min).

### 3.6.2. Calibration of Peristaltic Pump

Among the preliminary experiments, the relationship between pump speed and flow rate has to be established. The calibration of the peristaltic pump is done by measuring the flow rates at different pump setting using elutriation buffer. It is recommended to do the calibration before the day of elutriation to lighten the burden of elutriation. The pump can be used within the linear range. In our case, linearity was maintained up to 80 ml/min.

*3.6.3. Particle Size Counting*

Particle size counters are recommended which produce a particulate size profile and average particle diameter for a given culture. The size limit is set for cells to count them above the limit and cell debris below the limit. The unit is cleaned and first a sample of solution (used for dilution) is analyzed, then the sample of the culture is profiled. The solution profile is subtracted from the culture profile to eliminate solution debris. This yields a debris count and a cell count. More sophisticated units include measurement of the mean particle diameter, which, for cell cultures above the size limit, equates to the average cell diameter.

We have used different counters to determine the sizes of the cells in each fraction. The counter is based on the principle of electronic particle counting, where the amplitude of a voltage pulse, caused by a change in impedance when a particle suspended in an electrolyte is drawn through an electrical field, is proportional to the volumetric size of the particle (29). From the change in impedance, the diameter and surface area of the particle are calculated, assuming that the particles are spherical.

## *3.7. Installation of Elutriation System*

*3.7.1. Installation of Stroboscope*

To operate the elutriation system, install the stroboscope first, as its chamber unit has to be placed at the bottom of the centrifuge. Turn the stroboscope unit in such a way that the flashlight will be under the observation port when the door of the centrifuge is closed. Rotate the wheels on the casting to tighten the chamber of the stroboscope. Run the cables of the stroboscope through the ports of the centrifuge inside the chamber and secure them with split rubber stoppers installed from outside. Connect the cables to the control unit of the stroboscope outside the centrifuge. Turn on the power switch and verify that the lamp of the photocell is lit (*see* **Note 2**).

*3.7.2. Installation of Elutriator Rotor*

Open the door of the centrifuge and install the assembled rotor containing the installed chambers (elutriator and bypass chambers). Place the rotor in the centrifuge (*see* **Note 3**).

*3.7.3. Installation of Flow Harness*

In addition to the port for the strobe control unit, there are two more ports in the centrifuge chamber, one for the tubing coming from the pump and the other for the outlet tubing. One can use only centrifuges that have these ports. Make sure that the tubing running from the pump to the rotor is placed in the upper (inlet) fitting and the outlet tubing in the lower fitting of the elutriator rotor (*see* **Note 4**). Connect the liquid lines. Secure tubings firmly with split rubber stoppers outside the centrifuge.

*3.7.4. Installation of Control Units*

The preliminary run serves to test whether the control units are functioning properly and the centrifuge is running smoothly. For the test run, check the control units of the centrifuge and set the

elutriation speed of the centrifuge. When the rotor is at speed, reset the counter, and push START button (*see* **Notes 5** and **6**). The rotor speed will be displayed in tens of rpm on the counter. Put the timer at "Hold" position to avoid untimely interruption of elutriation, the brake at "Maximum" and set the temperature at 20°C, and limit its change within ±1–2°C. On the stroboscope control, turn the FLASH DELAY potentiometer counterclockwise to 0 position and slowly turn it clockwise to bring the image of the elutriation chamber into view, seen through the viewport door of the centrifuge. If you have an old JE-6 rotor, the bypass chamber will come into view first. Keep turning the potentiometer till the separation chamber is seen. The separation chamber has two screws in it that make it distinguishable from the bypass chamber. Watch the pressure gauge in the flow harness (*see* **Notes 7** and **8**). Rise in pressure indicates the presence of air in the system (*see* **Note 9**). Stop the pump and/or decelerate the rotor. Note that not all the cables and ports are visualized in the scheme (**Fig. 2.4**). When the pressure is zero, the rotor speed is set at elutriation speed.

### *3.8. Synchronization of CHO Cells*

(1) Prepare 3,500 ml of fresh F12 elutriation medium in a 4,000-ml flask.

(2) Fill up a 3,000-ml flask with elutriation medium to the rim. Use this as the permanent medium reservoir. Cover it with aluminum foil until further use.

(3) Pour 400 ml of elutriation medium into a 500 ml beaker and use it as a temporary medium reservoir.

(4) Set up your centrifugal system (**Fig. 2.4**). Pump 100 ml of 70% ethanol through the system. Then pump through PBS solution (200 ml) to remove the 70% ethanol used to provide sterilization. Start the centrifugation to remove bubbles. Remove PBS and the bubbles by pumping 100 ml of elutriation medium through the elutriation system and discard this fraction (*see* **Note 9**).

(5) Replace the temporary medium reservoir with the permanent medium reservoir. Fill the cell reservoir (sample mixer) with medium using a large (30 ml) syringe. To flush all the air from the sample-mixing chamber, retract the short needle, so that the end is flushed with the inside of the rubber stopper. When the sample chamber is full and no more air is seen leaving the exit flow line, close the bypass valve to make sure that the liquid does not enter the sample chamber. Set the initial flow rate of the peristaltic pump at 16.5 ml/min. Keep the elutriation fluid circulating until the cells are introduced into the sample reservoir. Make sure once more that the bypass

valve is closed, the speed of the centrifuge is correct (2,200 rpm, 683 × *g*), the refrigeration of the centrifuge is on and set at 20°C, and the timer of the centrifuge is set at HOLD (endless) position. Turn the flash delay potentiometer of the stroboscope clockwise slowly from 0 position to bring the image of the separation chamber into view. Number empty culture bottles (or tubes) for collecting elutriation fractions (100 ml each) and stand in ice. Use the scale on the culture bottle as the volume measure.

(6) Load the sample reservoir by passing the concentrated cell suspension (1–2 × $10^8$ cells in 10 ml of Ham's medium containing 1% FBS in a 50-ml screw cap tube) through an 18-gauge needle three times just before loading to ensure monodispersion. Use a 10-ml Luer-lock syringe for injecting cells into the loading chamber. This also keeps the needle from jumping off the hypodermic syringe. The needle attaches to the body of the syringe via a screw-type twist. Remove the needle from the syringe. Close the bypass valve, as elution liquid is not allowed to enter the sample reservoir during loading. Attach the syringe directly to the Luer fitting on the injector valve for sample injection. Open the injector valve and inject resuspended cells into the sample reservoir. After injecting the cells slowly into the sample reservoir, close the injection valve. Air is not allowed to enter the system. As cells cannot be completely removed from the 50-ml tube and filled in the sample reservoir, those suspended cells that are left in the tube (~0.5 ml) serve as nonelutriated control.

(7) Load cells into the elutriation chamber. To load cells from the sample reservoir to the elutriation chamber, turn the sample chamber upside down and open the bypass valve. Start to collect the first 100 ml fraction flushed from the centrifuge. About 100 ml of liquid is required to remove one subpopulation of cells from the 4.5-ml separation chamber. View the loading of cells through the observation window of the door of the centrifuge. The appearance of a darkening cloud indicates the introduction of cells into the elutriation chamber. After loading, no more cells are allowed to enter the elutriation chamber. Close the bypass valve and turn back the loading chamber to its original position (*see* **Note 10**). The fraction collected during loading is discarded. This fraction contains cell debris and dead cells (*see* **Notes 11–12)**.

(8) To obtain the first elutriation fraction, increase the pump speed from 16.5 ml/min to 19 ml/min slowly by ~1 ml/min increments and collect the next 100 ml

media. Gradually increase the flow rate (or decrease rotor speed) to permit the elutriation of further fractions. Collect consecutively 100 ml effluent volumes from the centrifuge. Immediately after a fraction is collected, take 2 × 1-ml samples and add 9 ml of saline to each sample for Coulter counting and cell size measurement. Keep elutriated fractions in ice until further use and shake them gently from time to time to avoid cohesive sedimentation and loss of cells (*see* **Note 13**). We have obtained reproducible experiments by performing centrifugal elutriation at low, increased and high resolution and collecting 9, 16, and 30 elutriation fractions, respectively (**Fig. 2.5**). Only as many samples should be collected as the small team (2–3 persons) carrying out the elutriation can process on the same day (*see* **Note 14**).

(9) To finish elutriation, turn off rotor speed and let the high flow rate drive out residual particles from the elutriation chamber. Let the system run and collect 100 ml more liquid to remove all the remaining particles. Remove the medium at high flow rate and rinse the system with 200 ml of distilled water to lyse any cells left in the system. Cells left in the elutriator chamber may cause pellet formation (*see* **Note 11**).

(10) Although almost all parts of the elutriator rotor can be autoclaved, we rinse the system with 70% ethanol to sterilize it. Remove the ethanol by pumping and dry the passages with clean compressed air and leave the rotor assembled. Disconnect the liquid lines and remove the rotor and stroboscope chamber from the chamber. In case of longer storage, remove the elutriation chamber and the bypass (balance) chamber, but store the rest of the rotor assembled.

(11) Check the status of your elutriator system by a test run before doing cell separation (*see* **Note 15**).

### *3.9. Synchronization of Nuclei*

1. For the synchronization of isolated murine pre-B nuclei (average diameter 5 μm) use higher centrifugal force (3,500 rpm, 2,305×*g*).
2. Use a flow rate between 14 and 77 ml/min for murine pre-B nuclei (average diameter 5 μm) and apply a similar flow rate (11–73 ml/min), but a lower centrifugal force (2,200 rpm, 683×*g*) for murine pre-B cells (23, 33).

Due to the closer correlation between nuclear size and DNA content than between cell size and DNA content it could be of potential interest to elutriate subcellular particles to study the

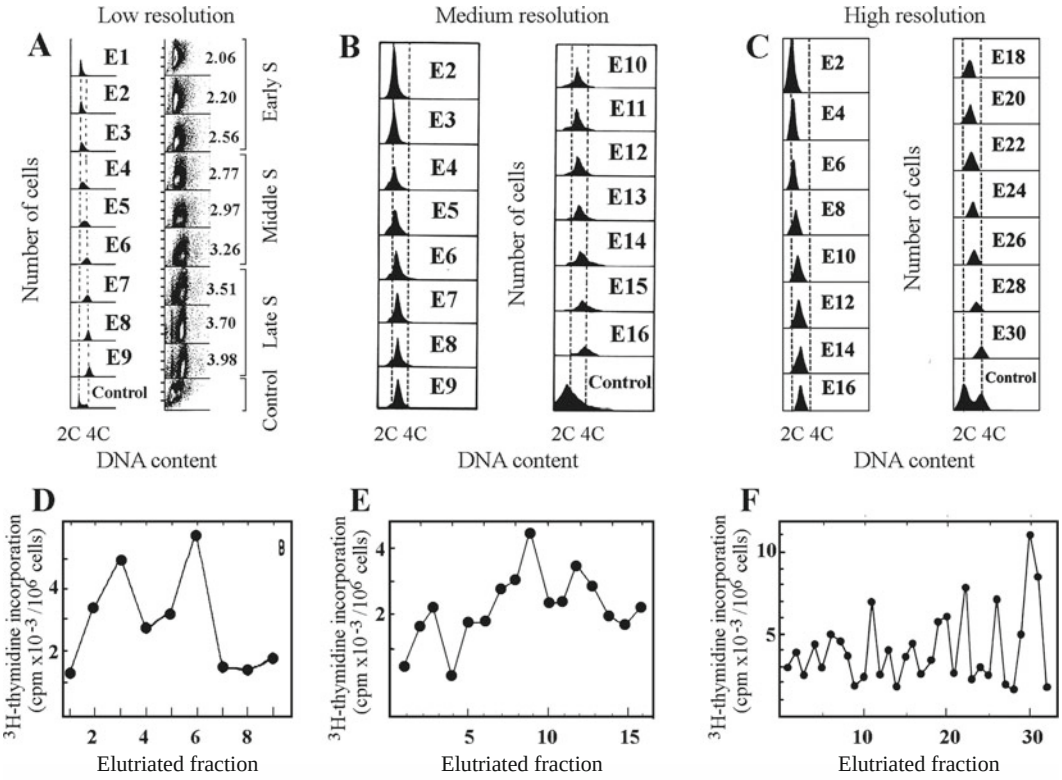


Fig. 2.5. Centrifugal elutriation at low, medium, and high resolution. Exponentially growing CHO cells were synchronized by counterflow centrifugal elutriation. **a** Flow cytometric profiles of DNA content at low (**a**), medium (**b**), and high resolution of elutriation. The cell number is indicated in the ordinate and the DNA content on the abscissa. The average *C*-value (haploid genome content) of elutriated fractions at low resolution (9 fractions, E1–E9) was calculated. For medium resolution 16 fractions (E2–E16) and at high resolution 30 elutriation fractions (E2–E30) were collected. DNA synthesis in elutriated fractions at low (**d**), medium (**e**), and high resolution (**f**). $^{3}$H-thymidine incorporation is shown in the ordinate and fraction number on the absicissa. 2*C*- and 4*C*-values were calculated from the flow cytometric profiles of elutriated fractions (24). Reproduced with the permission of Banfalvi et al. (30, 31); Szepessy et al. (32).

fine-tuning of nuclear control. The synchronization of nuclei is expected to open new vistas for the synchronization of protoplast preparations. The synchronization is based on the nuclear size that is increasing during DNA synthesis and nuclei can be separated by centrifugal elutriation. The introduction of a density gradient during elutriation is not recommended (*see* **Note 16**). To elutriate smaller particles either the centrifugal force has to be increased or the flow rate decreased. A lower flow rate would limit the resolution, while maximal pump speed (~500 ml/min) should also be avoided as the linearity between the pump speed and flow rate could not be maintained. Turbulence can be minimized by increasing the flow rate slowly from fraction to fraction (*see* **Note 17**).

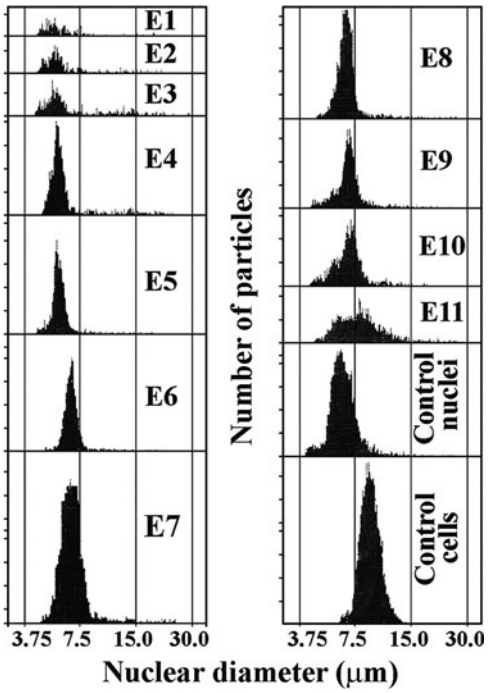


Fig. 2.6. Centrifugal elutriation of nuclei isolated from murine pre-B cells. Nuclear size is indicated on the abscissa, nuclear number or cell number is given on the ordinate. Cells ($1.15 \times 10^8$) were subjected to the isolation of nuclei. Elutriation of $6.86 \times 10^7$ nuclei was carried out in a JE-5.0 elutriation system equipped with a 5 ml Sandetson chamber and a MasterFlex (Cole-Parmer Instruments) peristaltic pump and a J-6 M1 centrifuge (Beckman Instruments Inc.). Elutriation took place at 20°C and 3,500 rpm ($2{,}305 \times g$). Eleven fractions (E1–E11) were collected, 100 ml each in RPMI medium 1640 supplemented with 1% FBS. After separation, nuclei were washed with PBS and counted by Coulter multisizer, and nuclear size analysis was carried out. Control nuclei and control cells were not subjected to elutriation. Reproduced with permission of Banfalvi (11).

### *3.10. Verification of Synchronization*

1. Assay the quality of synchronization after centrifugal elutriation in each elutriated fraction. Among the methods used for the isolation and detection of homogeneous populations of cells, several flow cytometric methods are generally accepted. Since its introduction, the PI flow cytometric assay has been widely used for the evaluation in different cellular processes in animal models (34) and plant cells (35).
2. Determine the DNA content by fluorometry (*see* **Section 3.3**).
3. Measure simultaneously the cell number and the increasing cell size. This third option offers the fastest measurement and is recommended when many fractions are collected and several measurements have to be carried out within a short period of time. A reliable combination is to choose at least two of the three options.

## 4. Notes

1. *Dead cells*. Avoid the presence of dead and fragmented cells in elutriated fractions. The cell culture has to be kept constantly in logarithmic growth. Best results are obtained when cells are recultivated every day.
2. *Installation of stroboscope*. Make sure that the cables run close to the wall of the centrifuge, so that the rotor cannot touch them. In case the photocell of the stroboscope does not work replace the flash lamp.
3. *Placing rotor in the centrifuge*. Be sure that the rotor is properly seated. If the pin of the rotor is improperly resting on one of the castellations, it will lift off when the drive starts. The centrifuge should be perfectly balanced and run smoothly. If you notice any vibration, the balance is imperfect. When the speed of the centrifuge is fluctuating, flow forces are not precisely balanced against centrifugal force to allow proper segregation. Check speed constancy and find the balance between centrifugal force and flow rate in preliminary test runs.
4. *Leaks*. These usually occur when (a) the chamber gasket is put backward; (b) the chamber screws are not tight; (c) tubings and connectors are not properly fitted; (d) there are nicks, scratches, irregularities on O-rings; and (e) permanently lubricated sealed bearings are washed with detergents, which can leach out the lubricant, resulting in a shortened bearing time.
   - *Seal inspection*. Clean the stained stationary seal housing (made of alumina) with soap and water or mild detergent. Abrasive materials should be used neither for cleaning nor for elutriation. Reassemble the bearing assembly (note that the seal mount has a left-handed thread). The seal should be replaced when any damage is visible.
   - *Cross leakage*. The most common problem in centrifugal elutriation is caused by defective or missing O-rings in the shaft assembly. Frequent disassembling and assembling of the elutriator system may result in defective O-rings and leaks. Make sure that all O-rings on the seal screw and transfer tube are in right place, lightly greased. Note, however, that overgreasing may clog the system. Once the subassemblies, as well as the flow system, have been assembled and the system proved to be completely sealed without any leakage in the preliminary run, it is not recommended to disassemble it after each elutriation.

– *High back pressure*. Insufficient spring pressure, which holds the rotating seal against the stationary seal, can be overcome by the back pressure, causing cross leakage. But the most common causes of high back pressure are the opening of liquid lines in the wrong direction and inadequate de-aeration.

5. *Rotor speed*. As the flow rate relative to rotor speed can be regulated on a much broader and finer scale, it is recommended that during elutriation the rotor speed is held constant rather than using decreasing rotor speed and constant flow rate.
6. *Oscillations in rotor speed*. To avoid temporary changes in rotor speed, constant electric voltage (110 or 220 V) can be secured by plugging the centrifuge to a stabilizer.
7. *Manometer*. Keep the manometer under constant observation at the beginning of elutriation to avoid pressure formation. In the elutriation system, the presence of bubbles is indicated by the sharp increase of the pressure. In such cases, quickly turn off the speed of the centrifuge, which will drive out the bubbles. Repeatedly lower the speed of the centrifuge to remove all the bubbles before elutriation.
8. *Tightness of tubing*. Do not make the connection between the tubing and the rotor too tight; leave some space for the movement for the tubing. As the speed of the elutriation rotors is not high (maximum 6,000 rpm, 5,080×*g*), vacuum in the centrifuge is not required and could not be maintained due to the liquid lines and electric cables.
9. *Removal of bubbles*. Be sure to fill all parts of the flow harness with liquid until all the bubbles have been removed. Prewarm the solutions and the centrifuge to the temperature where elutriation will be performed with the exception of the cells before their loading and the collected fractions are kept in ice.
10. *Loading cells*. During loading the cells into the elutriation chamber, one can line up cells exactly at the boundary inside the elutriation chamber (**Fig. 2.1a**): (a) a small increase of the flow rate will push forward the cell population to the boundary; (b) a small decrease of the flow rate will bring the population back to the boundary. The chamber should not be filled beyond the boundary line. Alternatively, the rotor speed could also be changed, but has an opposite effect as changing the flow rate. Such corrections during elutriation are recommended only for advanced users of the system. Basic principle: Do not change conditions during elutriation.
11. *Pellet formation*. Those particles that are not driven out from the separation chamber by the pumping will be

pelleted at the entrance of the elutriation chamber as soon as the peristaltic pump stops. The peristaltic pump should not be turned off during elutriation. To remove the sticky pellet, the elutriation chamber has to be disassembled and cleaned.

12. *Damaged cells.* These cells release DNA and tend to stick together. Clumping of cells leads to nonhomogeneous cell populations especially at the final stage of elutriation. Solution: Avoid rapid pipetting and fast resuspension of pelleted cells, which results in a significant loss of cell recovery, viability, release of chromosomal DNA, and stickiness of damaged cells. We have avoided DNase and EDTA treatment by the gentle treatment and loading of cells.
13. *Cell loss during elutriation.* The possible reasons are as follows: (a) cells are lysed (the system was not properly set up, check solutions for hypotony); (b) cells were left in the mixing chamber; (c) overloading the elutriation chamber results in the loss of smaller (G0/G1 and early S phase) cells; (d) the size gradient was not balanced and cells were not loaded in the elutriation chamber; (e) the centrifuge was stopped or decelerated. The particles concentrate near the increased cross-sectional area of the chamber. Flow velocity is greatest adjacent to the entrance port, the particle concentration is reduced in this area. This effect can be reduced by lowering the centrifugal force and the correspondent flow rates.
14. *High resolution of elutriation.* The danger of collecting too many elutriated fractions is that they cannot be processed. High resolution of elutriation needs the processing of many samples within the same day. Careful planning, the involvement of 2–3 persons in this highly coordinated work, some technical skill and experience are needed.
15. *Unable to judge.* This problem almost always arises when elutriation has not been done before. Consult the JE-6 or JE-5 instruction manual carefully before doing any or further installation. Carry out your first elutriation with an expert and/or discuss the details. Clarify the condition of your rotor by calling your nearest service office and ask for inspection.
16. *Application of density gradient.* Introduction of a density gradient would require a second reservoir. It is not recommended as a second reservoir would make the system too complex to handle. Growth medium with minimum FBS (1%) maintains cell viability and is dense enough to avoid contamination.

17. *Coriolis jetting effect.* Turbulence of particles inside the elutriation chamber can be minimized by increasing the flow rate slowly from fraction to fraction. The collection of many fractions (i.e., small increment in flow rate) also reduces turbulence and contributes to the increased resolution power of elutriation. A small shift (1–2 fractions) in the elutriation profile can be attributed to minor differences in cell growth. This difference can be reduced by strict cell culture conditions and corrected by calculating the *C*-value (haploid genome content) of each elutriated fraction from the corresponding flow cytometric profile (24).

## Acknowledgment

This work was supported by the OTKA grant TO42762 (G.B.).

### References

1. Lindahl, P. E. (1948) Principle of a counterstreaming centrifuge for the separation of particles of different sizes. *Nature* **161**, 648–649.
2. McEwen, C. R., Stallard, R. W., and Juhos, E. T. (1968) Separation of biological particles by centrifugal elutriation. *Anal. Biochem.* **23**, 369–377.
3. Sanderson, R. J., Bird, K. E., Palmer, N. F., and Brenman, J. (1976) Design principles for a counterflow centrifugation cell separation chamber. Appendix: a derivation of the equation of motion of a particle under combined centrifugal and hydrodynamic fields. *Anal. Biochem.* **71**, 615–622.
4. Pretlow, T. G. II, and Pretlow, T. P. (1979) Centrifugal elutriation (counterstreaming centrifugation) of cells. *Cell Biophys.* **1**, 195–210.
5. Meistrich, M. L. (1983) Experimental factors involved in separation by centrifugal elutriation. In: Pretlow, T. G. II, Pretlow, T. P. (eds.) *Cell separation*, Vol. 2, pp. 33–61. Academic, New York, NY.
6. Childs, G. V., Lloyd, J. M., Unabia, G., and Rougeau, D. (1988) Enrichment of corticotropes by counterflow centrifugation. *Endocrinology* **123**, 2885–2895.
7. Kauffman, M. G., Noga, S. J., Kelly, T. J., and Donnenberg, A. D. (1990) Isolation of cell cycle fractions by counterflow centrifugal elutriation. *Anal. Biochem.* **191**, 41–46.
8. Bauer, J. (1999) Advances in cell separation: recent developments in counterflow centrifugal elutriation and continuous flow cell separation. *J. Chromatogr. B Biomed. Sci. Appl.* **722**, 55–69.
9. Chianea, T., Assidjo, N. E., and Cardot, P. J. P. (2000) Sedimentation field-flow-fractionation: emergence of a new cell separation methodology. *Talanta* **51**, 835–847.
10. Uzbekov, R. E. (2004) Analysis of the cell cycle and a method employing synchronized cells for study of protein expression at various stages of the cell cycle. *Biochemistry* **69**, 485–496.
11. Banfalvi, G. (2008) Cell cycle synchronization of animal cells and nuclei by centrifugal elutriation. *Nat. Protoc.* **3**, 663–673.
12. Keng, P. C., Li, C. K., and Wheeler, K. T. (1980) Synchronization of 9L rat brain tumor cells by centrifugal elutriation. *Cell Biophys.* **2**, 191–206.
13. Riccardi, C., and Nicoletti, I. (2006) Analysis of apoptosis by propidium iodide staining and flow cytometry. *Nat. Protoc.* **1**, 1458–1461.
14. Doleel, J., Greilhuber, J., and Suda, J. (2007) Estimation of nuclear DNA content in plants using flow cytometry. *Nat. Protoc.* **2**, 2233–2244.

15. Terry, N. H. A., and White, R. A. (2006) Flow cytometry after bromodeoxyuridine labeling to measure S and G2.M phase durations plus doubling times in vitro and in vivo. *Nat. Protoc.* **1**, 859–869.
16. Schmid, I., Uittenbogaart, C., and Jamieson, B. D. (2006) Live-cell assay for detection of apoptosis by dual-laser flow cytometry using Hoechst 33342 and 7-aminoactinomycin D. *Nat. Protoc.* **1**, 187–190.
17. Mukhopadhyay, P., Rajesh, M., Haskó, G., Hawkins, B. J., Madesh, M., and Pacher, P. (2007) Simultaneous detection of apoptosis and mitochondrial superoxide production in live cells by flow cytometry and confocal microscopy. *Nat. Protoc.* **2**, 2295–2301.
18. Ferlini, C., and Scambia, G. (2007) Assay for apoptosis using the mitochondrial probes, Rhodamine123 and 10-N-nonyl acridine orange. *Nat. Protoc.* **2**, 3111–3114.
19. van Genderen, H., Kenis, H., Lux, P., Ungeth, L., Maassen, C., Deckers, N., Narula, J., Hofstra, L., and Reutelingsperger, C. (2006) In vitro measurement of cell death with the annexin A5 affinity assay. *Nat. Protoc.* **1**, 363–367.
20. Quah, B. J. C., Warren, H. S., and Parish, C. R. (2007) Monitoring lymphocyte proliferation in vitro and in vivo with the intracellular fluorescent dye carboxyfluorescein diacetate succinimidyl ester. *Nat. Protoc.* **2**, 2049–2056.
21. Chattopadhyay, P. K., Yu, J., and Roederer, M. (2006) Live-cell assay to detect antigen-specific CD4+ T-cell responses by CD154 expression *Nat. Protoc.* **1**, 1–6.
22. Pittet, M. J., Swirski, F. K., Reynolds, F., Josephson, L., and Weissleder, R. (2006) Labeling of immune cells for in vivo imaging using magnetofluorescent nanoparticles. *Nat. Protoc.* **1**, 73–79.
23. Offer, H., Zurer, I., Banfalvi, G., Rehak, M., Falcovitz, A., Milyavsky, M., Goldfinger, N., and Rotter, V. (2001) p53 modulates base excision repair activity in a cell cycle specific manner following genotoxic stress. *Cancer Res.* **61**, 88–96.
24. Basnakian, A., Banfalvi, G., and Sarkar, N. (1989) Contribution of DNA polymerase delta to DNA replication in permeable CHO cells synchronized in S phase. *Nucleic Acids Res.* **17**, 4757–4767.
25. Banfalvi, G., Nagy, G., Gacsi, M., Roszer, T., and Basnakian, A. (2006) Common pathway of chromatin condensation in mammalian cells. *DNA Cell Biol.* **25**, 295–301.
26. Rehak, M., Csuka, I., Szepessy, E., and Banfalvi, G. (2000) Subphases of DNA replication in *Drosophila* cells. *DNA Cell Biol.* **19**, 607–612.
27. Banfalvi, G. (2006) Structure of interphase chromosomes in the nuclei of *Drosophila* cells. *DNA Cell Biol.* **25**, 547–553.
28. Banfalvi, G., Littlefield, N., Hass, B., Mikhailova, M., Csuka, I., Szepessy, E., and Chou, W. M. (2000) Effect of cadmium on the relationship between replicative and repair DNA synthesis in synchronized CHO cells. *Eur. J. Biochem.* **267**, 6580–6585.
29. Coulter, W. H. (1957) High speed automatic blood cell counter and cell size analyzer. *Proc. Natl. Electron. Conf.* **12**, 1034–1040.
30. Banfalvi, G., Mikhailova, M., Poirier, L. A., and Chou, M. W. (1997) Multiple subphases of DNA replication in CHO cells. *DNA Cell Biol.* **16**, 1493–1498.
31. Banfalvi, G., Poirier, A. L., Mikhailova, M., and Chou, W. M. (1997) Relationship of repair and replicative DNA synthesis to cell cycle in Chinese hamster Ovary (CHO-K1) cells. *DNA Cell Biol.* **16**, 1155–1160.
32. Szepessy, E., Nagy, G., Jenei, Z., Serfozo, Z., Csuka, I., James, J., and Banfalvi, G. (2003) Multiple subphases of DNA repair and poly(ADP-ribose) synthesis in Chinese hamster ovary (CHO-K1) cells. *Eur. J. Cell Biol.* **82**, 201–207.
33. Banfalvi, G., Ujvarosi, K., Trencsenyi, G., Somogyi, C., Nagy, G., and Basnakian, A. G. (2007) Cell culture dependent toxicity and chromatin changes upon cadmium treatment in murine pre-B cells. *Apoptosis* **12**, 1219–1228.
34. Doleel, J., Greilhuber, J., and Suda, J. (2007) Estimation of nuclear DNA content in plants using flow cytometry. *Nat. Protoc.* **2**, 2233–2244.
35. Guidozzi, F. (1997) Enrichment of ovarian cancer cell suspensions by centrifugal elutriation after density gradient purification. *Int. J. Gynecol. Cancer* **7**, 100–105.

# Chapter 3

# Cytofluorometric Purification of Diploid and Tetraploid Cancer Cells

**Maria Castedo, Lorenzo Galluzzi, Ilio Vitale, Laura Senovilla, Didier Métivier, Mohamed Jèmaà, Santiago Rello-Varona, and Guido Kroemer**

## Abstract

During malignant transformation, cells can increase their ploidy and hence become polyploid (mostly tetraploid). Frequently, however, tetraploid cells undergo asymmetric divisions, in turn entailing a reduction in ploidy and the acquisition of a pseudo-diploid, aneuploid state. To investigate such a stepwise aneuploidization process, we developed a cytofluorometric method (based on the heterogeneity in cell size and/or chromatin content) that allows for the cloning and subsequent functional analysis of cells with distinct ploidies. Here, we detail this methodology, which has been instrumental for investigating the functional link between ploidy status and oncogenesis.

**Key words:** Cancer, CMFDA, CMTMR, H2B-GFP, p53, RKO.

## 1. Introduction

Tetraploid cells have been observed in some precancerous lesions including cervical dysplasia and Barrett's esophagus (1, 2). It has been hypothesized that tetraploidy constitutes a metastable state and that tetraploid cells progressively lose their chromosomes to reach a pseudo-diploid, yet aneuploid stage. Thus, tetraploidy might represent an intermediate stage between normal ploidy (euploidy) and cancer-associated aneuploidy (3–5).

A number of tumor suppressor genes including *TP53* have been demonstrated to actively repress tetraploidy (4). Accordingly, tetraploid cells that are isolated from (pre-)malignant

G. Banfalvi (ed.), *Cell Cycle Synchronization*, Methods in Molecular Biology 761,
DOI 10.1007/978-1-61779-182-6_3, 

lesions are frequently characterized by the genetic and/or functional inactivation of the p53 system (1, 2). Moreover, either the knockout of *TP53* (by homologous recombination) or the knockdown of the p53 protein (by RNA interference, RNAi) has been shown to stimulate the spontaneous tetraploidization of cancer cells and/or to facilitate the survival of tetraploid cells previously generated through karyokinesis or cytokinesis inhibition (3, 6–10). Along similar lines, we have recently shown that the absence of p53 is permissive for multipolar asymmetric divisions of tetraploid cells, resulting in the generation of daughter cells with an aneuploid, pseudo-diploid DNA content (11). Thus, multipolar mitoses (which reduce the tetraploid genome to pseudo-diploidy) are more frequent in conditions of p53 deficiency. Moreover, we discovered that tetraploid cells exhibit increased levels of the oncoprotein MOS, which is normally functional only during the meiosis of oocytes. Accordingly, RNAi-mediated downregulation of MOS prevented the occurrence of multipolar mitoses and stabilized the genome of p53-deficient tetraploid cells. These results demonstrate that prominent tumor suppressor gene products (exemplified by p53) and oncoproteins (exemplified by MOS) regulate ploidy, underscoring the importance of ploidy control for oncogenesis.

As a tool to elucidate the intricate relationship that links ploidy control to tumorigenesis, we developed cytofluorometric methods that – starting from genomically unstable cell populations – allow for the discrimination between diploid and tetraploid cells as well for the purification of viable cells that can be maintained in culture and subjected to functional analyses (8, 12–14).

In this context, it should be noted that the staining of chromatin or DNA with specific fluorescent dyes was not an option for this methodological development because such agents (and in particular their laser-mediated excitation) induce non-negligible extents of DNA damage, thereby activating a major DNA damage response that negatively affects cellular behavior and viability (15, 16). We reasoned that it should be possible to separate diploid cells (which have a 2n DNA content in the $G_0/G_1$ phase of the cell cycle and a 4n DNA content in $G_2/M$) from tetraploid cells (which have a 4n DNA content in $G_0/G_1$ and an 8n DNA content in $G_2/M$) based on their size, as determined by their cytofluorometric forward scatter (FSC), and we performed the following experiments to demonstrate our hypothesis.

We first admixed diploid cells that had been stained with CellTracker$^{TM}$ Green (CMFDA, a thiol-reactive fluorochrome that emits a green fluorescence) (**Fig. 3.1a**) with tetraploid cells that had been stained with CellTracker$^{TM}$ Orange (CMTMR, another thiol-reactive fluorochrome that emits an orange fluorescence) (**Fig. 3.1b**) at a 1:1 ratio (**Fig. 3.1c**).

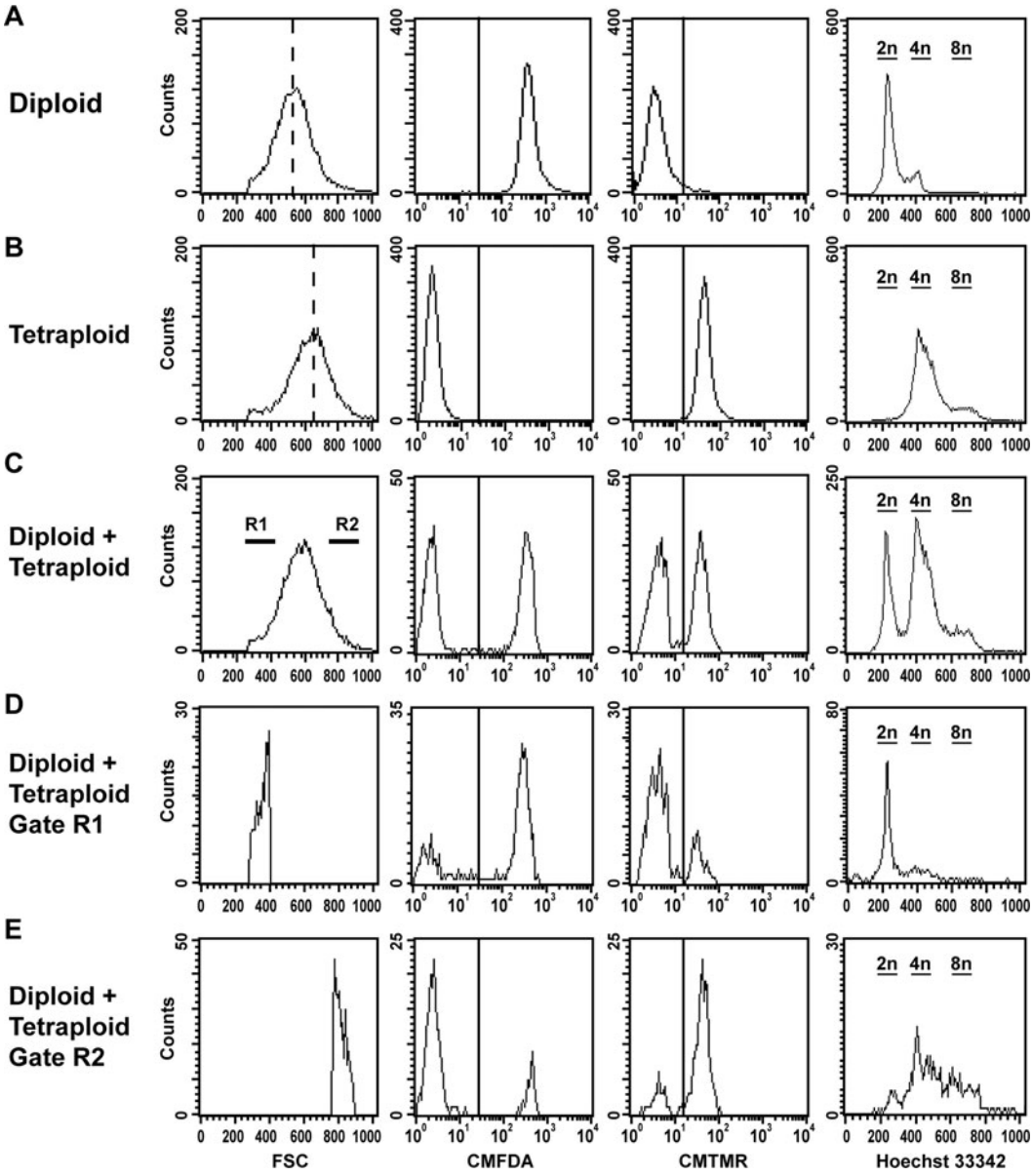


Fig. 3.1. Cytofluorometric separation of diploid and tetraploid cells based on their size. Two representative RKO diploid (**a**) and tetraploid (**b**) clones (obtained as described in **Section 3.1**) were labeled with CellTracker$^{TM}$ green (CMFDA) and CellTracker$^{TM}$ orange (CMTMR), respectively, as detailed in **Section 3.2**. Cells were subsequently stained with Hoechst 33342 and subjected to FACS analysis as described in **Section 3.1**. Cell size was estimated by measuring forward scatter (FSC). (**c**–**e**) Diploid and tetraploid cells represented in (**a**) and (**b**) were admixed at a 1:1 ratio and immediately analyzed by cytofluorometry as such (**c**) or upon gating on two sub-populations of cells differing in their size (R1 and R2 in the FSC histogram, panels (**d**) and (**e**), respectively). Dashed lines indicate FSC peak values. Please note that most cells belonging to the R1 sub-population are CMFDA positive and have a 2n DNA content, whereas the majority of those found in gate R2 is CMTMR positive and has a 4n DNA content.

The diploid and tetraploid cell populations as well as the heterogeneous population obtained by their combination were counterstained with the chromatinophylic dye Hoechst 33342 (emitting a blue fluorescent signal) to control ploidy (**Fig. 3.1a–c**). Starting from the 1:1 mix of diploid and tetraploid cells, we then separated two cell sub-populations upon gating on two regions of the Gaussian FSC frequency distribution that had either a small size (on the left side of the curve, R1) or a large size (on the right side of this curve, R2) (**Fig. 3.1c**). Notably, while most small cells (from the gate on R1) were CMFDA positive (>85%) and had a 2n DNA content (**Fig. 3.1d**), the majority of large cells (from the gate on R2) were CMTMR positive (>90%) and had a ≥4n DNA content (**Fig. 3.1e**), demonstrating that diploid and tetraploid cells can purified from heterogeneous populations based on their size.

After this first proof-of-principle experiment, we investigated whether we might purify freshly generated tetraploid cells by cytofluorometry. To this aim, we stably transfected human colon carcinoma RKO cells for the expression of a histone H2B-green fluorescent protein chimera (H2B-GFP), which allows to visualize chromatin and to quantify DNA without the use of genotoxic fluorochromes. These genetically engineered cells were then treated with nocodazole (a reversible inhibitor of microtubules that blocks karyokinesis and hence arrests mitosis), causing an increase in GFP fluorescence that was indicative of ongoing polyploidization (**Fig. 3.2a**).

On such a heterogeneous population (that could be represented as a GFP versus FSC dot plot), gates were placed around cells that were characterized by the smallest size and the lowest GFP fluorescence (R1), the peak population (R2) and the cells exhibiting the largest size and the highest GFP fluorescence (R3). Cell sorting from these gates resulted in the generation of three sub-populations that were enriched in cells with a 2n DNA content (R1), presented an equilibrated bimodal distribution (thereby being constituted by a similar amount of cells with a 2n and a 4n DNA content, R2), and contained a high proportion of cells with an 8n DNA content (R3), respectively (**Fig. 3.2b**). Cloning of the R1 and R3 populations by the limiting dilution technique revealed that the former contained a vast majority of diploid cells, whereas a sizeable fraction (generally >50%) of the latter consisted of tetraploid cells (**Fig. 3.2c**).

The possibility to purify diploid and tetraploid cells from an heterogeneous population was again explored by admixing them at a 1:1 ratio (**Fig. 3.3a**), followed by gating on three populations as defined by FSC and H2B-GFP fluorescence (**Fig. 3.3b**) and analysis of DNA content upon Hoechst 33342 staining (**Fig. 3.3c–f**). This approach revealed the possibility to distinguish diploid (R1) cells from their tetraploid counterparts (R3)

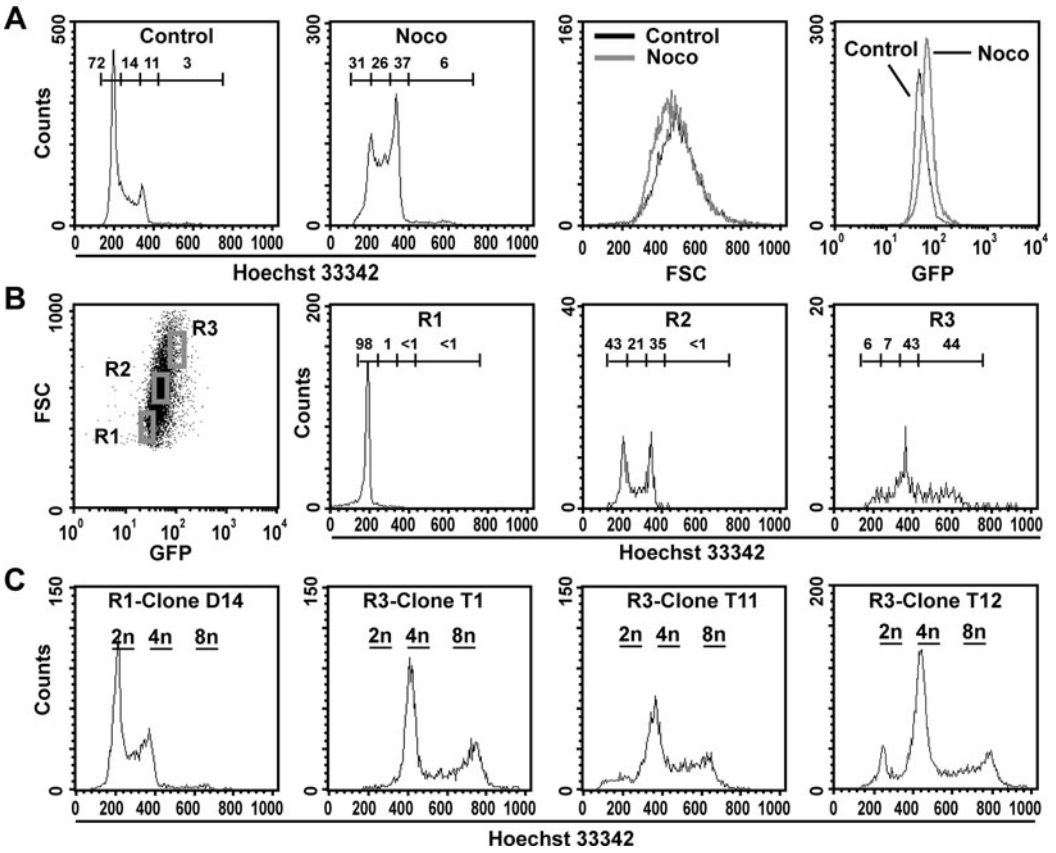


Fig. 3.2. Cytofluorometric separation of diploid cells expressing H2B-GFP in different phases of the cell cycle and *de novo* generated tetraploid cells. (**a**, **b**) Increase in the mean GFP fluorescence correlates to changes in the chromatin content. Diploid human colon carcinoma RKO cells stably expressing a H2B-GFP chimera and in the logarithmic growth phase were subjected (**a**) or not (**b**), to nocodazole (Noco)-mediated polyploidization followed by FACS-assisted analysis of DNA content (Hoechst 33342 staining), cell size (forward scatter, FSC), and GFP fluorescence, as described in **Section 3.1**. (**a**) From left to right, numbers indicate the percentage of cells characterized by $G_0/G_1$, S, $G_2$/M and polyploid DNA content. Please note that the accumulation of cells in the S and $G_2$/M phases of the cell cycle induced by nocodazole is associated to an increase in mean GFP fluorescence. (**b**) Separation of diploid and tetraploid cells based on FSC and H2B-GFP fluorescence. Untreated RKO cells stably expressing H2B-GFP were stained with Hoechst 33342 and analyzed by cytofluorometry upon gating on three distinct regions characterized by different FSC and GFP-dependent fluorescence. From left to right, numbers indicate the percentage of cells characterized by $G_0/G_1$, S, $G_2$/M and polyploid DNA content. Of note, cells derived from the R1 window were mostly diploid, cells belonging to R2 exhibited a bimodal distribution, and the R3 population was enriched in tetraploid cells. (**c**) Representative cell cycle profiles (assessed by Hoechst 33342 staining) of RKO cells cloned from the indicated sub-populations by the limiting dilution technique (as described in **Section 3.1**). Some tetraploid clones generated a sizeable and viable sub-tetraploid population, whose consistence allowed for the classification of clones according to genomic instability in stable (sub-tetraploid cells <10%) and unstable (sub-tetraploid cells >10%).

based on FSC and chromatin content (quantified thanks to the H2B-GFP chimera).

Intriguingly, we found that tetraploid clones frequently contain a sub-tetraploid population (**Figs. 3.2c** and **3.4**) that increases in consistence upon protracted culture and that is likely to arise from multipolar mitosis (11). By gating on cells with

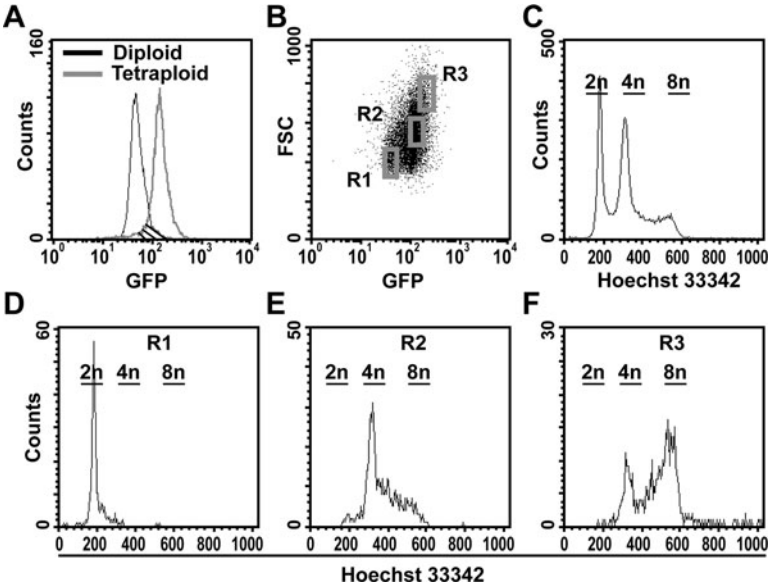


Fig. 3.3. Cytofluorometric separation of a 1:1 mixture of diploid and tetraploid populations expressing H2B-GFP. (**a**) GFP fluorescence of diploid and tetraploid human colon carcinoma RKO cells stably transfected for the expression of H2B-GFP (as detailed in **Section 3.3**). Cytofluorometric analysis revealed a limited overlay of the GFP signals derived from diploid and tetraploid cells (*hatched area*). (**b–f**) Diploid and tetraploid H2B-GFP-expressing RKO cells were mixed at a 1:1 ratio, stained with Hoechst 33342 (as described in **Section 3.1**) and then analyzed by cytofluorometry for size (forward scatter, FSC), GFP fluorescence (**b**), and DNA content, either as a mixed population as such (**c**) or upon sorting on the indicated windows (**d–f**), allowing for the purification of 2n, 4n, and 8n cell populations with a satisfactory degree of purity.

reduced FSC and H2B-GFP fluorescence, we could then obtain a near-to-diploid population of cells that apparently had been generated by tetraploid precursors (**Fig. 3.4**). By fluorescent *in situ* hybridization (FISH), we demonstrated that these cells were

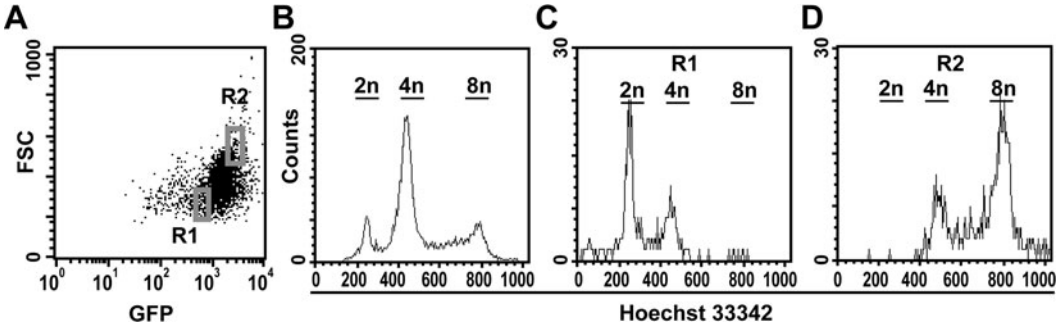


Fig. 3.4. *FACS separation of sub-tetraploid RKO cells from unstable tetraploid clones.* The unstable tetraploid H2B-GFP-expressing RKO clone T12 (obtained as described in **Fig. 3.2b**, **c**) was stained with Hoechst 33342 (as described in **Section 3.1**) and then analyzed by cytofluorometry for size (forward scatter, FSC), GFP fluorescence (**a**), and DNA content, either as a heterogeneous population as such (**b**) or upon sorting on the indicated windows (**c, d**), which allowed for the isolation of sub-tetraploid cells generated by multipolar and/or asymmetric divisions.

aneuploid and hence different from the parental diploid population (11), supporting the working hypothesis that tetraploid cells can generate an aneuploid offspring by multipolar and/or asymmetric divisions.

Here, we provide a detailed methodological description for the cytofluorometric analysis and purification of diploid and tetraploid cells that are contained in a mixed population of cells that differ in their ploidy status. For practical reasons, we describe the application of these techniques to human colon carcinoma RKO cells, a widely employed *in vitro* model of colon carcinogenesis that is characterized by a spontaneous rate of tetraploidy of 2–5%. With minor modifications, these methods can be promptly translated to other *in vitro* experimental models.

## 2. Materials

### 2.1. Common Materials

#### 2.1.1. Disposables

1. 1.5 ml microcentrifuge tubes
2. 15 and 50 ml conical centrifuge tubes
3. 25, 75, or 175 $cm^2$ flasks for cell culture
4. 5 ml, 12 × 75 mm FACS tubes
5. 6-, 12-, 24-, 96-well plates for cell culture

#### 2.1.2. Equipments

1. Bright-field inverted microscope: XDS-1R (Optika, Ponteranica, Italy), equipped with 10X, 25X, and 40X long working distance planachromatic objectives.
2. Cytofluorometer: FACSVantage (BD, San José, USA), equipped with a UV laser and a 70 mm nozzle, and controlled by the operational/analytical software CellQuest™ Pro (BD).

#### 2.1.3. Reagents

1. Alignment beads: AlignFlow™ Plus flow cytometry alignment beads, 6 μm, for 350–370 (UV) and 488 nm excitation (Gibco-Invitrogen, Carlsbad, USA), stock solution at ~$1.2 \times 10^8$ beads/ml, stored at 4°C under protection from light (*see* **Notes 1** and **2**).
2. Complete growth medium for RKO cells. McCoy's 5A medium: 4.5 g/l glucose and 4 mM L-glutamine (PAA Laboratories GmbH, Pasching, Austria) supplemented with 1 mM sodium pyruvate, 100 mM HEPES buffer, 100 U/ml penicillin G, 100 μg/ml streptomycin sulfate, and 10% fetal bovine serum (FBS) (*see* **Note 3**).

3. Phosphate buffered saline (PBS, 1X): 137 mM NaCl, 2.7 mM KCl, 4.3 mM $Na_2HPO_4$, 1.4 mM $KH_2PO_4$ in deionized water ($dH_2O$), adjust pH to 7.4 with 2 N NaOH.
4. Sheath fluid: FACSFlow™ (BD), store at room temperature (RT) (*see* **Note 4**).
5. Trypsin/EDTA: 0.25% trypsin, 0.38 g/l (1 mM) EDTA × 4 $Na^+$ in HBSS, store at –20°C (*see* **Notes 5** and **6**).

***2.2. Characterization and Selection of Diploid Versus Tetraploid RKO Cells***

1. Cytochalasin D (MP Biomedicals, Illkirch, France), stock solution in DMSO, 1 mg/ml, stored at –20°C (*see* **Notes 7** and **8**).
2. Hoechst 33342 (Molecular Probes-Invitrogen), stock solution in $dH_20$, 10 mg/ml, store at 4°C under protection from light (*see* **Notes 9** and **10**).
3. Nocodazole, stock solution in DMSO, 10 mM, store at –20°C under protection from light (*see* **Notes 11–13**).

***2.3. Cell Staining with CellTracker™ Probes***

1. CellTracker™ Green (CMFDA, Molecular Probes – Invitrogen), stock solution in DMSO, 10 mM, stored at –20°C (*see* **Notes 14** and **15**).
2. CellTracker™ Orange (CMTMR, from Molecular Probes – Invitrogen), stock solution in DMSO, 10 mM, stored at –20°C (*see* **Notes 14** and **15**).

***2.4. Stable Transfection with the pBOS-H2BGFP Vector***

1. Blasticidin S HCl (Gibco-Invitrogen), stock solution in 20 mM HEPES, 1 mg/ml, store at –20°C under protection from light (*see* **Notes 16–18**).
2. pBOS-H2BGFP (BD Biosciences, San José, USA), stock solution in $dH_20$, 1 mg/ml, store at 4°C (*see* **Note 19**).
3. Lipofectamine™ 2000 transfection reagent (Gibco-Invitrogen), store at 4°C (*see* **Note 20**).
4. Opti-MEM® reduced serum medium supplemented with Glutamax™ and phenol red (Gibco-Invitrogen), store at 4°C (*see* **Note 20**).

## 3. Methods

***3.1. Cell Culture***

1. Upon thawing, maintain RKO cells in complete growth medium in 75–175 $cm^2$ flasks (37°C, 5% $CO_2$) (*see* **Note 21**).
2. When confluence approaches 70–90%, detach cells with trypsin/EDTA (*see* **Notes 22–25**) to constitute fresh maintenance cultures (*see* **Note 26**) and to provide cells for experimental determinations.

3. Maintain cultures in 25–75 $cm^2$ flasks or in 6-, 12-, 24-, or 96-well plates, according to the specific experimental setting (*see* **Note 27**).

### 3.2. Characterization and Selection of Diploid Versus Tetraploid RKO Cells

1. Seed 0.5–1 × $10^6$ RKO cells in 5–10 ml growth medium in 25 $cm^2$ flasks and let adapt for 12–24 h (*see* **Note 28**).
2. Thereafter, discard culture supernatants and detach adherent cells with 3 ml trypsin/EDTA (*see* **Notes 22–25**).
3. Upon detachment, add 10–12 ml of growth medium and transfer cells to 15 ml centrifuge tubes (*see* **Note 29**).
4. Centrifuge samples at 300×*g* for 5 min (at room temperature, RT), discard supernatants, and resuspend cell pellets in 0.5–1 ml pre-warmed growth medium supplemented with 2 μM Hoechst 33342 (*see* **Note 30**).
5. Keep cells in staining conditions (37°C, 5% $CO_2$, under protection from light) for 30–45 min (*see* **Note 31**) and then transfer to FACS tubes for the cytofluorometric acquisition.
6. Analyze samples for DNA content by means of a classic cytofluorometer allowing for UV excitation (*see* **Note 32**), acquisition of light scattering data, and fluorescence recording in (at least) three separate channels (*e.g.*, green, red or orange, and blue) (*see* **Note 33**).
7. Perform acquisition and analysis by first gating on events that are characterized by normal light scattering parameters (forward scatter, FSC; and side scatter, SSC) (*see* **Notes 34** and **35**).
8. The RKO cell population is expected to contain 2–5% tetraploid cells, which can be cloned (and then amplified) by FACS-assisted sterile sorting or by the limiting dilution technique (*see* **Note 36**).
9. To this aim, count cells in a classical hemocytometer and seed at concentrations of 0.1, 1, and 3 cells/well in 96-well plates (200 μl growth medium/well) (*see* **Note 37**).
10. After 7–10 days, identify cells in wells by light microscopy-assisted inspection, amplify and characterize for ploidy by Hoechst 33342 staining (*see* **Section 3.1 – Steps 1–7** and **Notes 22–25, 28–35**).

### 3.3. Cell Staining with CellTracker™ Probes

1. Seed 0.5–1 × $10^6$ RKO cells of the desired ploidy in 5–10 ml growth medium in 25 $cm^2$ flasks and let adhere for 12–24 h (*see* **Notes 28** and **38**).
2. Remove culture supernatant and substitute with 5–10 ml fresh, pre-warmed growth medium supplemented with

7 μM CellTracker™ Green (CMFDA) or 15 μM CellTracker™ Orange (CMTMR) (*see* **Notes 39–41**).

3. Keep cells in staining conditions (37°C, 5% $CO_2$, under protection from light) for 15–45 min (*see* **Note 42**).
4. Remove unincorporated CellTracker™ by replacing the staining medium with 5–10 ml fresh, pre-warmed growth medium. Then incubate cells for additional 1–2 h in standard culture conditions (37°C, 5% $CO_2$) (*see* **Note 43**).
5. Wash cultures further 2–3 times with pre-warmed, sterile PBS (*see* **Note 44**).
6. Maintain cells overnight in standard culture conditions (37°C, 5% $CO_2$) and then collect (mix, if required by the experimental setup), stain with Hoechst 33342 and analyze by cytofluorometry as described above (*see* **Section 3.1**. – **Steps 2–7** and **Notes 22–25, 29–35**).

### *3.4. Stable Transfection with a H2B-GFP Encoding Plasmid*

1. Seed 2 × $10^5$ RKO cells in 12-well plates (in 1 ml growth medium per well) and let adhere for 12–24 h (*see* **Notes 28** and **45**).
2. Generate transfection complexes as follows (conditions on a per well basis):
   a. Dilute 4 μl Lipofectamine™ 2000 transfection reagent in 100 μl pre-warmed Opti-MEM® and incubate for 5–10 min at RT;
   b. Meanwhile, dissolve 2 μg pBOS-H2BGFP in 100 μl pre-warmed Opti-MEM®;
   c. At the end of the incubation period, combine the plasmid and Lipofectamine™ 2000 solutions (total volume = 200 μl), gently mix and keep for further 15–20 min at RT (*see* **Notes 46** and **47**).
3. While the DNA:Lipofectamine™ 2000 complexes are forming, remove culture supernatant in plates and substitute with 700 μl pre-warmed serum-free culture medium (*see* **Note 48**).
4. At the end of the complex formation period, add 200 μl transfection complexes dropwise to each well, whirl plates gently and keep in standard culture conditions (37°C, 5% $CO_2$) for 4–6 h (*see* **Note 49**).
5. In each well, supplement culture supernatant with 100 μl FBS to restore a final FBS concentration of 10% (as in normal growth medium) (*see* **Note 50**).
6. For the selection of stable transfectants, 24 h later collect cells by trypsinization (*see* **Section 3.1** – **Steps 2–3** and **Notes 23–25, 29, 51**) and seed into a cell culture support

of choice in growth medium supplemented with 20 μg/ml blasticidin S (*see* **Notes 52–54**).

7. Upon selection, monitor the ploidy of stably transfected cells by Hoechst 33442 staining, as described (*see* **Section 3.1 – Steps 1–7** and **Notes 22–25, 28–35**), or by metaphase spread and chromosome counting (as detailed in Refs. (17, 18)).

## 4. Notes

1. AlignFlow™ Plus flow cytometry alignment beads are provided as suspensions in water containing 0.05% Tween 20 and 2 mM sodium azide ($NaN_3$). Tween 20 is not currently listed as a carcinogen by the National Toxicology Program (NTP), the International Agency for Research on Cancer (IARC), or the Occupational Safety and Health Administration (OSHA), yet may behave as a mild irritant for the eyes, skin, and respiratory system. $NaN_3$ is toxic by ingestion and under acidic conditions may release the highly toxic gas hydrazoic acid.
2. Under appropriate storage conditions (4°C, under protection from light) AlignFlow™ Plus flow cytometry alignment beads are stable for at least 12 months.
3. Optimal growth conditions (*e.g.*, medium composition, supplements) vary according to the cell line of choice and may quite dramatically influence not only the growth rates but also the response to tetraploidizing agents. For this reason, we suggest to use the medium that is most suitable for the cell line of choice, as recommended by the American Type Culture Collection (ATCC, Manassas, USA).
4. FACSFlow™ is a mixture of multiple substances, any of which, at their given concentration, is considered to be hazardous to health.
5. EDTA is not currently listed as a carcinogen by NTP, IARC, or OSHA, yet may behave as a mild irritant for the eyes, skin, and respiratory system.
6. Under appropriate storage conditions (–20°C, under protection from light), Trypsin/EDTA is stable for at least 18 months.
7. Cytochalasin D is toxic and can be harmful or fatal if inhaled, swallowed, or absorbed through skin. Thus, cytochalasin D should always be handled using protective gloves, clothing, and eyewear.

8. The manufacturer recommends that cytochalasin D stock solutions, once prepared, are stored as single-use aliquots in tightly sealed vials and employed within 3 months. Whenever possible cytochalasin D solutions should be made up and used on the same day.
9. Hoechst 33342 is currently listed among substances that may cause concern to man owing to possible mutagenic effects but for which the available information is inadequate for making satisfactory assessments. It should be handled anyway with the maximal care, by using protective gloves, clothing, and eyewear.
10. As compared to other chromatinophilic dyes (*e.g.*, 4′,6-diamidino-2-phenylindole dihydrochloride, DAPI), Hoechst 33342 is particularly prone to photobleaching. Exposure to light of the stock solution should therefore be carefully prevented.
11. Nocodazole can be harmful or fatal if inhaled, swallowed, or absorbed through skin, and therefore should always be handled using protective gloves, clothing, and eyewear.
12. Undissolved nocodazole appears as a white powder and has a minimum shelf life of 2–3 years (stored at 4°C, under protection from light).
13. The commercial provider (Sigma-Aldrich) declares that nocodazole is stable in biological media for at least 7 days.
14. CMFDA and CMTMR are not currently listed as a carcinogen by NTP, IARC, or OSHA, yet may behave as mild irritants for the eyes and the respiratory system.
15. Undissolved CMFDA and CMTMR are stable for 1 year (stored at –20°C, under protection from light).
16. Blasticidin S is a nucleoside antibiotic isolated from *Streptomyces griseochromogenes*, which inhibits protein synthesis in both prokaryotic and eukaryotic cells (*see* also **Note 19**).
17. Blasticidin S is toxic, if swallowed, and should always be handled using protective gloves, clothing, and eyewear.
18. When stored properly at –20°C, blasticidin S is stable for up to 9 months. Media supplemented with blasticidin S can be stored at 4°C for up to 2 weeks. It is recommended by the manufacturer to avoid subjecting blasticidin to multiple freeze/thaw cycles.
19. The pBOS-H2BGFP vector is designed for stable expression in mammalian cells of a human histone H2B-green fluorescence protein (H2B-GFP) chimera driven by the strong EF-1α promoter. This vector also contains a blasticidin S-resistance gene for the selection of transfected cells (*see* also **Note 16**).

20. Lipofectamine™ 2000 and Opti-MEM® are generally considered as non hazardous, yet should always be handled using protective gloves, clothing, and eyewear.
21. It is recommendable to allow freshly thawed cells to re-adapt for 2–3 passages before using them in experimental assessments. Similarly, it is good practice to define a maximal number of passages and to discard maintenance cultures once this limit has been reached, to avoid genetic population drifts. This strategy requires an appropriate liquid nitrogen stock of cells, which should be generated from a homogenous and healthy population before the beginning of the experiments.
22. While 3 ml trypsin/EDTA are sufficient for 75 $cm^2$ flasks, 5–6 ml should be used for 175 $cm^2$ flasks.
23. Before the addition of trypsin/EDTA, adherent cells should be washed once with pre-warmed, sterile PBS. This step facilitates the subsequent trypsinization by minimizing the amount of FBS (which inactivates trypsin) within the flask.
24. Trypsinization time is a function of cell type, viability, and culture density. For RKO cells (and most cell lines), 5 min at 37°C are amply sufficient to fully detach a totally confluent, healthy population. It is, however, recommendable to check for complete cell detachment by visual inspection or by rapid observation in light microscopy.
25. Trypsinization-resistant cells can be mechanically detached with the help of a common scraper for cell culture (*see* also **Note 27**).
26. For maintenance, RKO cells can be split at 1:4–1:20 ratios, according to the experimental needs. Other cell lines are more sensitive and may have problems in recovering a normal growth rate if excessively diluted.
27. An alternative to 75 $cm^2$ flask is provided by 10 cm Ø Petri dishes. These are equal in surface to 75 $cm^2$ flasks but more accessible, which can be advantageous if cells need to be detached by scraping (*see* also **Note 25**).
28. Normally, RKO cells quickly adhere to cell culture supports and hence do not need prolonged adaptation times. This may not hold true for other cell types (*e.g.*, colon carcinoma HCT 116 cells), which should always allowed to adapt for 24–36 h prior to any experimental manipulation.
29. At this step, the FBS contained in the growth medium inactivates trypsin, thereby preventing trypsin-mediated damage of the plasma membrane, which can occur upon protracted trypsinization.

30. Hoechst 33342 is a cell-permeant chromatinophylic dye (absorption/emission peaks = 352/461 nm, *see* also **Note 32**) that optimally binds to DNA at pH 7.4. Unbound Hoechst 33342 has an emission peak in the 510–540 nm range (green). This fluorescence can be observed when excessive Hoechst 33342 concentrations are employed.
31. While some cell types (including RKO cells) take up Hoechst 33342 very readily (<15 min), others require >30 min for an appropriate staining. Nevertheless, staining with Hoechst 33342 should never be protracted for more than 45 min, as this may *per se* affect cell viability.
32. Due to its absorption properties, UV excitation at 360 nm is an absolute requirement for the use of Hoechst 33342 (*see* also **Note 30**).
33. In our experimental setting, the following channels are employed for fluorescence detection: FL1 for H2B-GFP and CFMDA; FL2 for CMTMR; FL4 for Hoechst 33342 (*see* also **Notes 39, 52**).
34. As a reminder, while FSC depends on cell size, SSC reflects the refractive index, which in turn is influenced by multiple parameters including cellular shape and intracellular complexity (*i.e.*, presence of cytoplasmic organelles and granules).
35. Cytofluorometers are provided with software for instrumental control and analysis. Unfortunately, the execution of nearly all these packages is limited to the computer that controls the cytofluorometer and, often, to a single operating system. A number of analytical software packages (for both Mac and PC-based systems) are available online free of charge. For PC users, we recommend WinMDI 2.9 (© 1993–2000, Joe Trotter), originally developed for Windows® 3.1 but compatible with new versions of the operating system (freely available at http://www.cyto.purdue.edu/flowcyt/software.htm).
36. If other cell lines are employed, tetraploidization can be chemically induced by short-term exposure to 100 nM nocodazole or 0.6 μg/ml cytochalasin D (an inhibitor of actin polymerization) as detailed in Refs. (7, 8, 10).
37. The use of (at least) three seeding concentrations is important to maximize the cloning efficiency.
38. Overconfluence is associated with poor dye uptake, mainly due to the limited plasma membrane surface that is available for exchanges with the staining medium. For this reason, cell density at staining should not exceed 50–60%.

39. CMFDA and CMTMR are characterized by absorption/emission peaks at 492/517 and 541/565 nm, respectively (*see* also **Note 33**).
40. Whereas CMFDA is colorless until processed by cytosolic esterases, CMTMR does not require enzymatic cleavage to activate fluorescence.
41. Cells loaded with CMFDA or CMTMR are both fluorescent and viable for at least 24 h.
42. Optimal staining time may vary according to cell type.
43. During this time, the acetate group of the dye undergoes modification or is secreted from the cell (*see* also **Note 44**).
44. This washing step is instrumental for further removing unincorporated CellTracker™ and/or excess acetate from the culture medium (*see* also **Note 43**).
45. Both over- and underconfluence are associated with poor transfection rates, the former due to limited uptake of transfection complexes, the latter because of liposome-mediated toxicity (which is favored when the cell:Lipofectamine™ 2000 ratio is low). For this reason, cell density at transfection should range between 70 and 80%.
46. When diluted Lipofectamine™ 2000 and the plasmid DNA are mixed, the solution may become cloudy.
47. Liposome-mediated plasmid transfection is carried out entirely at RT under a common safety cabinet. However, it is recommendable to keep the tubes containing plasmid stocks and the Lipofectamine™ 2000 reagent on ice (and to return them to storage conditions immediately after use), in order to minimize solvent evaporation and avoid liposome degradation.
48. For easily transfectable cell lines (*e.g.*, HeLa cells), complete growth medium (including FBS and antibiotics) can be used instead of serum-free culture medium (*see* also **Note 50**).
49. To avoid intra-well variations of transfection efficiency as well as local toxicity, transfection complexes (which exhibit a very high affinity for plasma membranes) should be added to cells very slowly and dropwise, while trying to cover the whole surface of the growth medium.
50. Approximately 20 μl FBS are sufficient if cells were moved to complete growth medium at **Step 3** (*see* also **Note 48**).
51. 300 μl trypsin/EDTA per well is largely sufficient for the detachment of cells from 12-well plates. In this context, 3 ml growth medium is appropriate for trypsin inactivation (*see* also **Note 29**).

52. As blasticidin S-resistant cells may appear independent of transfection (*see* also **Note 53**), we recommend to perform FACS-assisted sorting and selection of $GFP^+$ cells as soon as possible (transgene expression should be detectable as soon as 12–24 h after transfection). In this context, the use of $GFP^-$ parental cells is required for the identification of GFP-dependent fluorescence. As a note, GFP is characterized by absorption/emission peaks at 488/507 nm (*see* also **Note 33**).
53. To further reduce the possibility that H2B-$GFP^-$ cells might take over cultures, blasticidin S selection should never be discontinued even after the FACS-assisted selection of stable transfectants (*see* also **Note 52**).
54. Immunofluorescence microscopy-assisted observation of stably transfected cells should confirm that the GFP signal is spatially restricted to chromatin.

## Acknowledgments

GK is supported by the Ligue Nationale contre le Cancer (Equipe labellisée), Agence Nationale de la Recherche (ANR), Cancéropôle Ile-de-France, Fondation pour la Recherche Médicale (FRM), Institut National du Cancer (INCa), European Commission (Active p53, Apo-Sys, RIGHT, TransDeath, ChemoRes, ApopTrain), and Fondation pour la Recherche Médicale. MC is funded by the Association pour la recherche sur le cancer (ARC). LG, IV, and LS are supported by Apo-Sys, La Ligue contre le Cancer and FRM, respectively.

### References

1. Heselmeyer, K., Schrock, E., du Manoir, S., Blegen, H., Shah, K., Steinbeck, R., Auer, G., and Ried, T. (1996) Gain of chromosome 3q defines the transition from severe dysplasia to invasive carcinoma of the uterine cervix. *Proc. Natl. Acad. Sci. USA.* **93**, 479–484.
2. Maley, C. C., Galipeau, P. C., Li, X., Sanchez, C. A., Paulson, T. G., Blount, P. L., and Reid, B. J. (2004) The combination of genetic instability and clonal expansion predicts progression to esophageal adenocarcinoma. *Cancer Res.* **64**, 7629–7633.
3. Fujiwara, T., Bandi, M., Nitta, M., Ivanova, E. V., Bronson, R. T., and Pellman, D. (2005) Cytokinesis failure generating tetraploids promotes tumorigenesis in p53-null cells. *Nature* **437**, 1043–1047.
4. Margolis, R. L. (2005) Tetraploidy and tumor development. *Cancer Cell* **8**, 353–354.
5. Storchova, Z., and Pellman, D. (2004) From polyploidy to aneuploidy, genome instability and cancer. *Nat. Rev. Mol. Cell. Biol.* **5**, 45–54.
6. Andreassen, P. R., Lohez, O. D., Lacroix, F. B., and Margolis, R. L. (2001) Tetraploid state induces p53-dependent arrest of nontransformed mammalian cells in G1. *Mol. Biol. Cell* **12**, 1315–1328.
7. Castedo, M., Coquelle, A., Vitale, I., Vivet, S., Mouhamad, S., Viaud, S., Zitvogel, L.,

and Kroemer, G. (2006) Selective resistance of tetraploid cancer cells against DNA damage-induced apoptosis. *Ann. N Y Acad. Sci.* **1090**, 35–49.
8. Castedo, M., Coquelle, A., Vivet, S., Vitale, I., Kauffmann, A., Dessen, P., Pequignot, M. O., Casares, N., Valent, A., Mouhamad, S., Schmitt, E., Modjtahedi, N., Vainchenker, W., Zitvogel, L., Lazar, V., Garrido, C., and Kroemer, G. (2006) Apoptosis regulation in tetraploid cancer cells. *EMBO J.* **25**, 2584–2595.
9. Cross, S. M., Sanchez, C. A., Morgan, C. A., Schimke, M. K., Ramel, S., Idzerda, R. L., Raskind, W. H., and Reid, B. J. (1995) A p53-dependent mouse spindle checkpoint. *Science* **267**, 1353–1356.
10. Senovilla, L., Vitale, I., Galluzzi, L., Vivet, S., Joza, N., Younes, A. B., Rello-Varona, S., Castedo, M., and Kroemer, G. (2009) p53 represses the polyploidization of primary mammary epithelial cells by activating apoptosis. *Cell Cycle* **8**, 1380–1385.
11. Vitale, I., Senovilla, L., Jemaà, M., Michaud, M., Galluzzi, L., Kepp, O., Nanty, L., Criollo, A., Rello-Varona, S., Manic, G., Métivier, D., Vivet, S., Tajeddine, N., Valent, A., Castedo, M., and Kroemer, G. (2010) Multipolar mitosis of tetraploid cells: inhibition by p53 and dependency on Mos. *EMBO J.* **29**, 1272–1284.
12. Rello-Varona, S., Vitale, I., Kepp, O., Senovilla, L., Jemaa, M., Metivier, D., Castedo, M., and Kroemer, G. (2009) Preferential killing of tetraploid tumor cells by targeting the mitotic kinesin Eg5. *Cell Cycle* **8**, 1030–1035.
13. Vitale, I., Galluzzi, L., Vivet, S., Nanty, L., Dessen, P., Senovilla, L., Olaussen, K. A., Lazar, V., Prudhomme, M., Golsteyn, R. M., Castedo, M., and Kroemer, G. (2007) Inhibition of Chk1 kills tetraploid tumor cells through a p53-dependent pathway. *PLoS One* **2**, e1337.
14. Vitale, I., Senovilla, L., Galluzzi, L., Criollo, A., Vivet, S., Castedo, M., and Kroemer, G. (2008) Chk1 inhibition activates p53 through p38 MAPK in tetraploid cancer cells. *Cell Cycle* **7**, 1956–1961.
15. Cariello, N. F., Keohavong, P., Sanderson, B. J., and Thilly, W. G. (1988) DNA damage produced by ethidium bromide staining and exposure to ultraviolet light. *Nucleic Acids Res.* **16**, 4157.
16. Zhang, X., and Kiechle, F. (2001) Hoechst 33342-induced apoptosis is associated with decreased immunoreactive topoisomerase I and topoisomerase I-DNA complex formation. *Ann. Clin. Lab. Sci.* **31**, 187–198.
17. Mouhamad, S., Galluzzi, L., Zermati, Y., Castedo, M., and Kroemer, G. (2007) Apaf-1 deficiency causes chromosomal instability. *Cell Cycle* **6**, 3103–3107.
18. Zermati, Y., Mouhamad, S., Stergiou, L., Besse, B., Galluzzi, L., Boehrer, S., Pauleau, A. L., Rosselli, F., D'Amelio, M., Amendola, R., Castedo, M., Hengartner, M., Soria, J. C., Cecconi, F., and Kroemer, G. (2007) Nonapoptotic role for Apaf-1 in the DNA damage checkpoint. *Mol. Cell* **28**, 624–637.

# Chapter 4

# Large-Scale Mitotic Cell Synchronization

**Kalyan Dulla and Anna Santamaria**

## Abstract

Understanding cell growth and cell division involves the study of regulatory events that occur in a cell cycle phase-dependent manner. Studies analyzing cell cycle regulatory mechanisms and cell cycle progression invariably require synchronization of cell populations at specific cell cycle stages. Several methods have been established to synchronize cells, including serum deprivation, contact inhibition, centrifugal elutriation, and drug-dependent synchronization. Despite potential adverse cellular consequences of synchronizing cells by pharmacological agents, drug-dependent methods can be advantageous when studying later cell cycle events to ensure specific enrichment at selected mitotic stages. This chapter describes protocols used in our laboratory for isolating mitotic mammalian cells in a large-scale manner. In particular, we discuss the technical aspects of adherent or suspension cell isolation, the methods necessary to enrich cells at different mitotic stages and the optimized culture conditions.

**Key words:** Mitosis, large-scale synchronization, HeLa S3, HeLa S, spinner cultures, triple flasks, prometaphase, metaphase, anaphase/telophase.

## 1. Introduction

The cell cycle is the series of events that leads to genome duplication and cell division (1). In eukaryotic cells, containing a nucleus, the cell cycle is divided into interphase and M phase. Interphase proceeds in three stages, G1, S, and G2, in which the cell duplicates its DNA (during S phase) and grows. The result of the M phase of the cell cycle is the generation of two daughter cells that are genetically identical to each other as well as to their parental cell. This phase comprises mitosis and cytokinesis. Mitosis is the process by which a eukaryotic cell equally segregates its chromosomes. It is immediately followed by cytokinesis, which drives the division of the cytoplasm, cell membrane, and other

G. Banfalvi (ed.), *Cell Cycle Synchronization*, Methods in Molecular Biology 761,
DOI 10.1007/978-1-61779-182-6_4, 

organelles into two cells that will contain about the same amount of these cellular compartments. During M phase, activation of each successive stage phase is dependent on the proper progression and completion of the previous one. A large number of regulatory protein complexes and signaling pathways are devoted to ensure normal progression through the cell cycle and deregulation of this process may lead to tumorigenesis (1).

Elucidating the events and regulatory mechanisms of the cell cycle is an active field of investigation. Advances in the sensitivity and throughput of mass spectrometry-based methods and associated bioinformatic tools have made it feasible to perform large-scale analysis at a systems level (2, 3). The strength of proteomic approaches for the global analysis of the cell cycle, and mitosis in particular, has been demonstrated in several recent studies, as exemplified by an atlas of mitotic phosphorylation compared to interphase phosphorylation (4), the generation of quantitative datasets of spindle protein and kinase phosphoproteomes at distinct cell cycle and mitotic stages (5–8), the assignment of phosphorylation sites to individual kinases (9, 10), the analysis of the proteome and phosphoproteome of the human cell cycle (11), or the global analysis of phosphorylation states of the anaphase promoting complex in response to antimitotic drugs (12). All these studies required large amount of cells that are synchronized in various stages of the cell cycle, in particular, in specific mitotic stages. The latter proved difficult, due to the lack of methods for obtaining mammalian cells in later stages of mitosis in sufficient amounts.

Drug-independent methods allow successful synchronization with minimal perturbation of biological systems and several of these approaches are described in other chapters of this book. However, none of them allow distinction between different mitotic phases such as prometaphase, metaphase, and the later stages – anaphase and telophase. The "mitotic shake-off" method, for instance, originally described by Terasima and Tolmach (13), is useful for cells synchronized in mitosis, which on plating into culture dishes move into G1 in a synchronous manner. A drawback of this method is that only a small percentage of the cells is in mitosis at any given time and therefore the yield is extremely low, and as mentioned, it does not allow distinction between different mitotic stages. On the other hand, "centrifugal elutriation" (14) allows isolation of almost all cell types, adherent or suspension, based on their size, yielding large populations of phase-specific cells. For details of centrifugal elutriation, *see* also **Chapter 2**. Yet again, cells only in interphase but not in different mitotic stages could be discriminated with this method.

The methods presented here have been developed using HeLa S3 or HeLa suspension (S) (*see* **Section 2**). HeLa cells

are established, immortalized cells derived from a cervical cancer. HeLa cells are a common model system for mammalian cell cycle research and they are suitable for large-scale mitotic studies as they can be easily synchronized in mitosis. Here, we describe drug-derived protocols to synchronize cells at specific mitotic stages, as well as protocols that were developed to synchronize HeLa S cells, which can be grown in a larger scale in suspension cultures (**Note 1**).

## 2. Materials

### 2.1. Cell Lines

HeLa S3 and HeLa S (American Type Culture Collection, ATCC, Manassas, VA), were grown at 37°C in a humidifier incubator with a 5% $CO_2$ atmosphere in Dulbecco's modified Eagle's medium (DMEM), supplemented with 10% heat-inactivated fetal calf serum and penicillin–streptomycin (100 U/ml and 100 μg/ml, respectively).

### 2.2. Reagents, Solutions, and Media

1. Fetal calf serum (heat inactivated at 56°C for 30 min).
2. Pluronic F-68 nonionic surfactant.
3. FITC-labeled-α-Tubulin antibody.
4. MG132 cell-permeable proteasome inhibitor.
5. RO-3306 selective CDK1 inhibitor (Alexis Biochemicals).
6. Noscapine (also known as Narcotine, Nectodon, Nospen, and Anarcotine) benzylisoquinoline alkaloid.
7. Cell culture media: Dulbecco's Modified Eagle's Medium (DMEM), supplemented with 10% fetal calf serum (heat inactivated at 56°C for 30 min) and penicillin–streptomycin (100 U/ml and 100 μg/ml, respectively).
8. Phosphate Saline Buffer (PBS): 8 g NaCl, 0.2 g KCl, 1.44 g $Na_2HPO_4$, 0.24 g $KH_2PO_4$, in 1 l of distilled water, pH 7.4.
9. Mounting media for immunofluorescence: 50 mM Tris pH 8,6 (2.5 ml 1 M) + 2.5 ml water, 90% glycerol, 250 mg *p*-phenylenediamine (PPD) (5 mg/ml). Dissolve 250 mg PPD in Tris (protect from light). Add 45 ml glycerol 100% and mix vigorously.

### 2.3. Cell Culture Spinner and Culture Flasks

1. Triple flasks (Nunc).
2. Stirring platform (CELL SPIN).
3. Spinner flasks and other accessories.

### 2.4. Drug Stock Solutions

1. Thymidine stock solution: 200 mM (*see* **Note 2**) Store at room temperature or in aliquots at –20°C.
2. Nocodazole stock: concentration 500 mg/ml in DMSO. Store in aliquots at –20°C.
3. MG132 stock: concentration 20 mM in DMSO. Store in aliquots at –20°C.
4. RO-3306 stock: concentration 5 mg/ml in DMSO. Store in aliquots at –20°C in the dark.
5. Noscapine stock: concentration 100 mM in DMSO. Store in aliquots at –20°C.

## 3. Methods

### 3.1. Large-Scale Synchronization of Adherent HeLa S3 Cells

1. HeLa S3 cells are first seeded in 15 cm diameter culture dishes at a density of approximately $1 \times 10^7$ cells/dish.
2. For large-scale studies we use 10 culture triple flasks (*see* **Note 3**), containing three growth layers on top of each other with a total surface of 500 $cm^2$. Cells are expanded to culture triple flasks in a ratio of approximately 1:3 from the 15 cm diameter culture dishes.

A schematic representation of the protocols described below is depicted in **Fig. 4.1**.

#### 3.1.1. Synchronization of Cells in Prometaphase

Prometaphase begins when the nuclear envelope breaks down and continues until all sister chromatids are attached to the spindle microtubules in a bi-oriented fashion. To synchronize cells in prometaphase, treatment with the depolymerizing agent nocodazole is among the most common methods (15) (**Note 4**). Use low enough concentration (40 ng/ml) to affect microtubule dynamics and induce a spindle assembly checkpoint (SAC) arrest, but allow re-polymerization later on:

1. Wash cells that had been previously pre-synchronized in G1/S by the addition of 2 mM thymidine (*see* **Note 5**) for 16–24 h twice with 60 ml PBS/flask and once with 60 ml/flask pre-warmed drug-free fresh medium and release into fresh medium for 12–16 h.
2. 6 h after release (cells will be then in S phase), replace medium by fresh medium containing 40 ng/ml of nocodazole (*see* **Notes 6** and **7**). As cells will enter mitosis synchronously, the variability in the time that different cells are exposed to nocodazole before being harvested will be reduced.

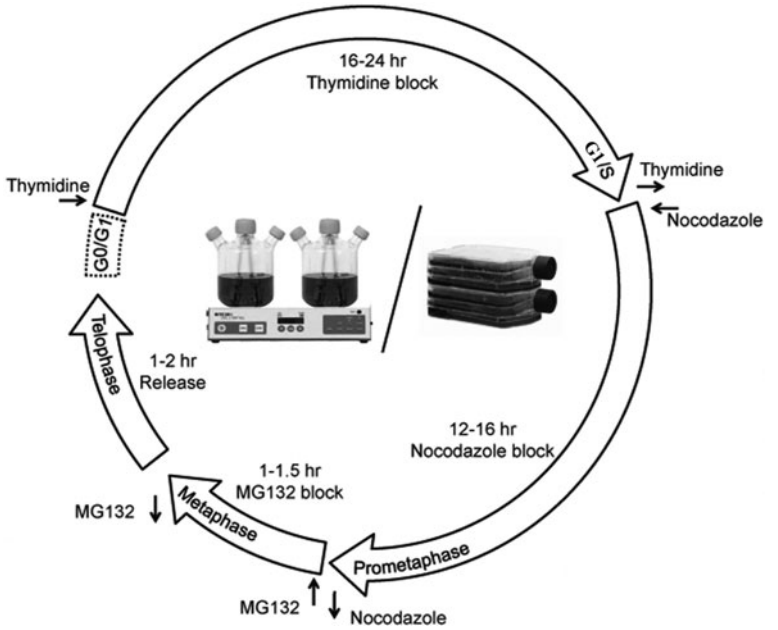


Fig. 4.1. Schematic representation of the synchronization protocols described in the text to isolate cells in a large-scale manner, in G1/S (thymidine block), prometaphase (nocodazole block), metaphase (nocodazole release into MG132), and telophase (MG132 release into fresh medium). Protocols are optimized for growing cells in triple flasks or spinner cultures.

3. Collect cells by mitotic shake-off. For this, remove the medium by decanting and add 3–5 ml PBS/flask.
4. Knock the flasks several times to the sidewall of the bench to detach the mitotic cells. This procedure yields about $1–2 \times 10^7$ mitotic cells per flask. The small volume of PBS added will help the detachment of cells from the flask. Too much or not enough liquid in the flasks results in a poorer mitotic yield or requires stronger strokes that result in the co-release of interphase cells. Also, cells should not be too confluent. The best results are obtained when cells are 60–70% confluent at the time of shake-off.

*3.1.2. Synchronization of Cells in Metaphase*

Metaphase is the period where chromosomes await at the metaphase equator to complete alignment, thereby switching off the spindle assembly checkpoint can be substituted by SAC. To enrich cells in metaphase, MG132, a reversible, cell-permeable proteasome inhibitor is used. Importantly, cells blocked by MG132 are characterized by an inactive SAC. This, combined with nocodazole-treated cells, allows the comparison between SAC dependent and independent events:

1. Isolate prometaphase-arrested cells by shake-off as described before. Subsequently, wash the cells twice with PBS and once

with fresh medium and release into fresh medium containing 20 μM MG132 for 60–90 min.

2. Harvest metaphase-arrested cells by centrifugation at 300×*g* for 3 min.

#### *3.1.3. Synchronization of Cells in Anaphase/Telophase*

In anaphase, sister chromatids are pulled apart to opposite poles of the mitotic spindle. Mitosis is completed in telophase when the chromosomes and other components are repackaged into the daughter nuclei. Synchronizing cells at late stages of mitosis is most difficult to achieve reproducibly due to their rather short duration (20–30 min). In addition, there are no drugs available to block cells efficiently in anaphase or telophase:

1. To isolate cells in late stages of mitosis (anaphase/telophase), wash metaphase-arrested cells (by MG132 treatment) twice with PBS and once with fresh medium and release into fresh drug-free medium for 60–90 min (*see* **Note 8**).
2. Harvest anaphase/telophase cells by centrifugation at 300×*g* for 3 min. Commonly, a proportion of 25/75% anaphase to telophase cells can be observed at this time.

### *3.2. Large-Scale Synchronization of HeLa S Cells Growing in Suspension*

Growth of cells in suspension (spinner) cultures allows synchronization of even larger amounts of cells. A disadvantage of suspension cultures compared to adherent cells is that the "shake-off" method of the rounded mitotic cells cannot be applied. As a result suspension cultures may contain higher proportion of interphase cells. To improve the purity of mitotic states, cells can be grown in medium supplemented with 20% FCS, instead of 10%. The increase in the growth stimulus helps the cells reaching prometaphase faster and more synchronously (8). In addition, cells can be grown in the presence of 0.1% Pluronic, which helps to minimize cell aggregation.

A schematic representation of the protocols described below is depicted in **Fig. 4.1**.

1. Expand cell cultures in spinner flasks which are operated at 45 rpm and kept inside the cell culture incubator at constant 37°C temperature and 5% $CO_2$ atmosphere. Seed cells in spinner flasks at a minimum density of $0.3 \times 10^6$ cells/ml and allow them to grow to a maximum density of $1.8 \times 10^6$ cells/ml and the medium is changed every 2 days.
2. Prior to synchronization, transfer cells to 400 ml of fresh medium containing 20% FCS at a density of $0.6 \times 10^6$ cells/ml (*see* **Note 3**).
3. Similar to the procedure described for HeLa S3 cells, first pre-synchronize HeLa S cells in G1/S by addition of 4 mM thymidine for 16–24 h (more than 90% of cells reach prometaphase within the 12 h of thymidine release).

4. Subsequently, wash cells with PBS and release into fresh medium. To minimize the time that cells stay at room temperature do the following: Transfer the medium (containing the cells) to eight 50 ml falcon tubes and centrifuge at 300×*g* for 3 min in two batches of four each. Discard the medium leaving less than 1 ml of old media and resuspend the cells in PBS (at room tempareture) with a 10 ml glass pipette. Again centrifuge and remove PBS and resuspend cells in fresh medium.
5. After 6 h, add nocodazole at a concentration of 40 ng/ml to arrest cells in prometaphase.
6. Harvest part of the population of prometaphase cells by centrifugation at 300×*g* for 3 min and wash the rest of cells as mentioned before and release into fresh medium containing 20 μM MG132 for 60–90 min.
7. Harvest part of the population of metaphase-arrested cells by centrifugation at 300×*g* for 3 min and wash the rest of cells once and release into fresh drug-free medium for 90–120 min. Note that the time to release cells in suspension from MG132 is longer than the one needed for adherent cells that had been shacken-off.

### *3.3. Immunofluorescence Staining of Cells in Suspension*

1. Before harvesting the cells at different mitotic stages, transfer 500 μl of cell suspension (from the total spinner culture) to a fresh 1.5 ml tube.
2. Spin down the cells at 300×*g* for 3 min.
3. Resuspend the cells in 500 μl fixing solution (1% paraformaldehyde and 3% sucrose) and incubate for 10 min at room temperature (*see* **Note 9**).
4. Centrifuge at 300×*g* for 3 min, discard the supernatant, and resuspend in 500 μl PBS. This cell suspension can be kept at 4°C for few days.
5. Transfer around 50 μl of cell suspension to a fresh eppendorf tube and add Triton X-100 (0.1% final concentration) and incubate for 15 min at room temperature with constant shaking. Note that starting with a too large amount of cells may create problems in mixing, and staining may not be uniform. On the other hand, the initial number of cells cannot be too low, as a considerable amount may be lost during the centrifugation steps.
6. Centrifuge again at 300×*g* for 3 min and discard the supernatant.
7. Resuspend the cell pellet in 100 μl of PBS-Tween 20 (0.2% final concentration) with 2% BSA.

8. Add 4′-6-diamidino-2-phenylindole (DAPI) and FITC-labeled anti-α-tubulin antibody at concentrations of 1 μg/ml and incubate for 1 h at room temperature with constant shaking.
9. Centrifuge at 300×*g* for 3 min and wash the cell pellet once with PBS to reduce background staining.
10. Keep cells at 4°C until analysis by immunofluorescence microscopy or examine directly. For this, mix 10 μl of stained cell suspension with 10 μl mounting solution, use 10 μl on a microscope glass slide, and place a glass coverslip on top.
11. Visualize under the microscope (*see* 7, 8) (**Note 10**).

## 4. Notes

1. The methods outlined here can also be applied to synchronize other cell types. However, when choosing a particular cell synchronization method, the cell cycle event to be studied, the doubling time of the cell type of interest, and the duration between each phase need to be considered.
2. The preparation of the thymidine stock requires extensive mixing at room temperature in a rotating wheel until the powder is completely dissolved.
3. The protocols described here have been optimized for the isolation of human mitotic spindles and for the study of dynamic phosphorylation of kinases at different mitotic stages, using HeLa S3 and HeLa S, respectively. These amounts can be scaled down or up accordingly to match the specific purpose of the experiment.
4. Generally, drug-induced mitotic states mimic normal mitotic stages but might not represent exactly unperturbed mitosis. Although both thymidine and nocodazole block/release methods are synchronization protocols commonly used that provide high proportions of synchronized cells and adequately reproduce cell cycle events, methods that induce cell cycle arrest in a particular phase of the cell cycle can potentially affect the protein of study or the biology of the cells.
5. Alternative methods to synchronize cells in G1/S phase are the DNA polymerase inhibitor aphidicolin (16) or hydroxyurea that targets the ribonucleotide reductase (17).
6. RO-3306 is an ATP-competitive inhibitor that has been proven to efficiently block cells in G2 by specifically inhibiting Cdk1/Cyclin B1 activity (18). It has been shown that treatment of HeLa S3 with RO-3306 for 20 h led to a

complete block of the cell cycle in the G2/M phase and removal of this inhibitor allowed rapid and synchronous entry into mitosis (18). To our knowledge, this inhibitor has not been used yet for cell synchronization in large-scale experiments. Provided that the same effect is displayed when larger amount of cells (or cells in suspension) are treated, this would help minimizing the possible adverse effects of nocodazole, providing a healthier mitotic population.

7. It is possible to successfully synchronize large amounts of HeLa S3 cells in a late prometaphase stage by the use of 25 μM noscapine (7). Noscapine is a microtubule-interacting agent that binds to tubulin and alters its conformation, thereby reducing the dynamics of microtubule turnover (19). As a consequence, cells arrest in a SAC-dependent late prometaphase stage, with a fairly normal mitotic spindle and most of the chromosomes aligned in the metaphase plate but few remaining near the spindle poles. The effect induced by noscapine treatment can be reverted by washing out the drug from the cells in culture. Approximately 30–60 min after noscapine wash out, most of the cells can be found in a stage close to metaphase and late mitotic stages (i.e., anaphase and telophase), respectively. Treatments for a maximum of 9–10 h with noscapine are recommended. If the goal is to isolate mitotic spindles, this method can be advantageous, as spindle structures remain organized upon noscapine treatment.
8. The actual time the cells take to reach telophase may slightly differ from experiment to experiment. So after 50 min, for every 10 min, 10 μl of cell suspension is pipetted onto a coverslip, mixed with quick stain (DAPI, 0.15% Triton X-100 in PBS) and observed under the microscope.
9. The protocol described here employs paraformaldehyde as fixation method. However, other cell fixation methods can be applied when staining with different antibodies as desired. We have successfully used the above-described protocol for fixation, using methanol as fixative.
10. The samples can be further benchmarked using Western blotting analysis of specific mitotic markers (8).

## Acknowledgments

We are thankful to Erich A. Nigg and Roman Körner for their support and critical reading of this chapter, and Herman H. Silljé, Albert Ries, and Elena Nigg for technical help to optimize these

protocols. We apologize for any omission in references. We also acknowledge funding by the Biozentrum of the University of Basel, the Max Planck Society, and by ENFIN, funded by the European Commission within its FP6 Program.

## References


1. Morgan, D. O. (2007) *The cell cycle: principles of control.* New Science Press, London.
2. Picotti, P., Bodenmiller, B., Mueller, L. N., Domon, B., and Aebersold, R. (2009) Full dynamic range proteome analysis of *S. cerevisiae* by targeted proteomics, *Cell* **138**, 795–806.
3. Choudhary, C., and Mann, M. (2010) Decoding signalling networks by mass spectrometry-based proteomics, *Nat. Rev. Mol. Cell Biol.* **11**, 427–439.
4. Dephoure, N., Zhou, C., Villen, J., Beausoleil, S. A., Bakalarski, C. E., Elledge, S. J., et al. (2008) A quantitative atlas of mitotic phosphorylation, *Proc. Natl. Acad. Sci. USA* **105**, 10762–10767.
5. Nousiainen, M., Sillje, H. H., Sauer, G., Nigg, E. A., and Korner, R. (2006) Phosphoproteome analysis of the human mitotic spindle, *Proc. Natl. Acad. Sci. USA* **103**, 5391–5396.
6. Daub, H., Olsen, J. V., Bairlein, M., Gnad, F., Oppermann, F. S., Korner, R., et al. (2008) Kinase-selective enrichment enables quantitative phosphoproteomics of the kinome across the cell cycle, *Mol. Cell* **31**, 438–448.
7. Malik, R., Lenobel, R., Santamaria, A., Ries, A., Nigg, E. A., and Korner, R. (2009) Quantitative analysis of the human spindle phosphoproteome at distinct mitotic stages, *J. Proteome Res.* **8**, 4553–4563.
8. Dulla, K., Daub, H., Hornberger, R., Nigg, E. A., and Korner, R. (2010) Quantitative site-specific phosphorylation dynamics of human protein kinases during mitotic progression, *Mol. Cell Proteomic.* **9**, 1167–1181.
9. Holt, L. J., Tuch, B. B., Villen, J., Johnson, A. D., Gygi, S. P., and Morgan, D. O. (2009) Global analysis of Cdk1 substrate phosphorylation sites provides insights into evolution, *Science* **325**, 1682–1686.
10. Santamaria, A., Wang, B., Elowe, S., Malik, R., Zhang, F., Bauer, M., Schmidt, A., Silljé H. H., Körner, R, Nigg, E. A., (2011) The Plk1-dependent phosphoproteome of the early mitotic spindle, *Mol. Cell Proteomic.* 10(1): M110.004457.
11. Olsen, J. V., Vermeulen, M., Santamaria, A., Kumar, C., Miller, M. L., Jensen, L. J., et al. (2010) Quantitative phosphoproteomics reveals widespread full phosphorylation site occupancy during mitosis, *Sci. Signal.* **3**, ra3.
12. Steen, J. A., Steen, H., Georgi, A., Parker, K., Springer, M., Kirchner, M., et al. (2008) Different phosphorylation states of the anaphase promoting complex in response to antimitotic drugs: a quantitative proteomic analysis, *Proc. Natl. Acad. Sci. USA* **105**, 6069–6074.
13. Terasima, T., and Tolmach, L. J. (1963) Growth and nucleic acid synthesis in synchronously dividing populations of HeLa cells, *Exp. Cell Res.* **30**, 344–362.
14. Banfalvi, G. (2008) Cell cycle synchronization of animal cells and nuclei by centrifugal elutriation, *Nat. Protoc.* **3**, 663–673.
15. Zieve, G. W., Turnbull, D., Mullins, J. M., and McIntosh, J. R. (1980) Production of large numbers of mitotic mammalian cells by use of the reversible microtubule inhibitor nocodazole. Nocodazole accumulated mitotic cells, *Exp. Cell Res.* **126**, 397–405.
16. Ikegami, S., Taguchi, T., Ohashi, M., Oguro, M., Nagano, H., and Mano, Y. (1978) Aphidicolin prevents mitotic cell division by interfering with the activity of DNA polymerase-alpha, *Nature* **275**, 458–460.
17. Reichard, P., and Ehrenberg, A. (1983) Ribonucleotide reductase – a radical enzyme, *Science* **221**, 514–519.
18. Vassilev, L. T., Tovar, C., Chen, S., Knezevic, D., Zhao, X., Sun, H., et al. (2006) Selective small-molecule inhibitor reveals critical mitotic functions of human CDK1, *Proc. Natl. Acad. Sci. USA* **103**, 10660–10665.
19. Ye, K., Ke, Y., Keshava, N., Shanks, J., Kapp, J. A., Tekmal, R. R., et al. (1998) Opium alkaloid noscapine is an antitumor agent that arrests metaphase and induces apoptosis in dividing cells, *Proc. Natl. Acad. Sci. USA* **95**, 1601–1606.

# Chapter 5

# Synchronization of Mammalian Cell Cultures by Serum Deprivation

**Thomas J. Langan and Richard C. Chou**

## Abstract

Mammalian cells are amenable to study the regulation of cell cycle progression *in vitro* by shifting them into the same phase of the cycle. Procedures to arrest cultured cells in specific phases of the cell cycle may be termed *in vitro* synchronization. The procedure described here was developed for the study of primary astrocytes and a glioma cell line, but is applicable to other mammalian cells. Its application allows astrocytes to reenter the cell cycle from a state of quiescence ($G_0$), and then, under carefully defined experimental conditions, to move together into subsequent phases such as the $G_1$ and S phases. A number of methods have been established to synchronize mammalian cell cultures, which include physical separation by centrifugal elutriation and mitotic shake off or chemically induced cell cycle arrest. Yet, there are intrinsic limitations associated with these methods. In the present protocol, we describe a simple, reliable, and reversible procedure to synchronize astrocyte and glioma cultures from newborn rat brain by serum deprivation. The procedure is similar, and generally applicable, to other mammalian cells. This protocol consists essentially of two parts: (1) proliferation of astrocytes under optimal conditions *in vitro* until reaching desired confluence; and (2) synchronization of cultures by serum downshift and arrested in the $G_0$ phase of the cell cycle. This procedure has been extended to the examination of cell cycle control in astroglioma cells and astrocytes from injured adult brain. It has also been employed in precursor cloning studies in developmental biology, suggesting wide applicability.

**Key words:** $G_0$, Astrocytes, Alzheimer's disease, cell cycle, glioma, oncogenesis, synchronization, serum deprivation.

## 1. Introduction

The regulation of the cell cycle is critical to the survival of mammalian species. Development of the mature organism from embryonic primordial cells is clearly a time of regulated sequences of cell division, and yet in mammals, only a minority of cells in fully mature individuals retain the capacity to reenter the cell

G. Banfalvi (ed.), *Cell Cycle Synchronization*, Methods in Molecular Biology 761,
DOI 10.1007/978-1-61779-182-6_5, 

cycle. These include skin cells, hepatocytes, epidermal cells in the intestinal tract, breast cells, and glial cells of the central nervous system (1, 2).

In conceptualizing cell fate in higher organisms, it has been suggested that certain cells enter a state of terminal differentiation, which can be abbreviated as $G_d$. Cells that can reenter the cell cycle, are in contrast considered to be in the $G_0$ phase of the cell cycle. This includes the several presumptively differentiated cells mentioned above (1–5). It is absolutely necessary for this minority of cells to remain in $G_0$ since inhibition of cell cycle reentry, as might, for example, occur in humans after massive radiation exposure, leading to death in several days (1, 2). In contrast, un-regulated proliferation of cells in $G_0$ can result in malignant transformation (1, 2). Thus, the cell types noted above contribute to many clinically significant types of cancers in humans, including melanoma and basal and squamous cell carcinoma of skin, bowel, breast, and intestinal tumors, and various grades of malignant astrocytoma in brain. More recently, it has been established

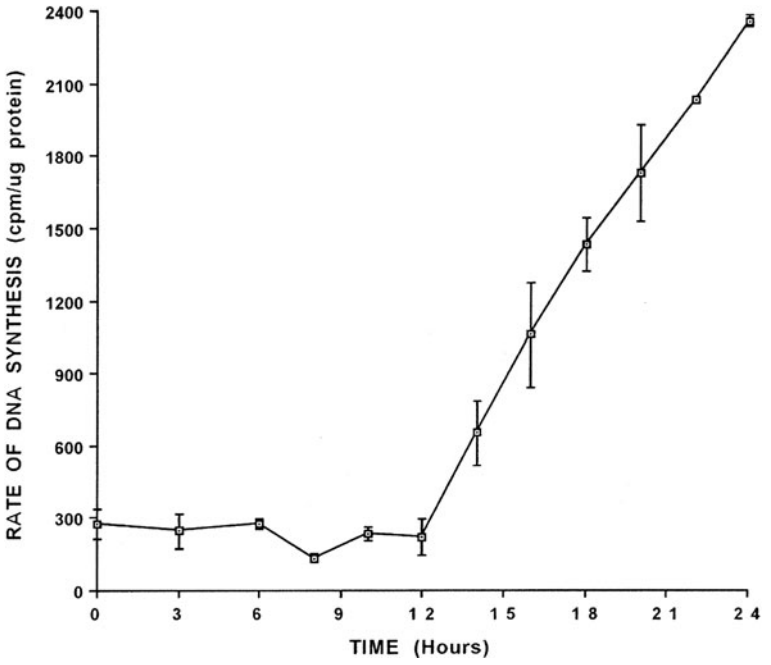


Fig. 5.1. Kinetic curve of primary astrocyte cell cycle. Primary astrocytes were plated in 6-well plates at a concentration of $10^4$ cells/cm$^2$ and allowed to grow to confluence of 30–50% in the presence of 10% BCS/DMEM and at 37°C and 5% $CO_2$/95% humidified air. After reaching the desired confluence, the cell cultures were serum downshifted from 10% BCS/DMEM to 0.1% BCS/DMEM for 48 h. At the end of the incubation, astrocytic cultures were allowed to reenter the cell cycle through serum up-shift in 10% BCS/DMEM. At various time points after serum up-shift, astrocytic cultures were pulse-labeled with $^3$H-thymidine at a final concentration of 1 $\mu$Ci/ml for 1 h prior to termination. Incorporation of $^3$H-thymidine into DNA of astrocytic cultures was measured as expressed as mean $\pm$ S.E.M. ($N = 4$–9).

that disordered cell cycle regulation is part of the pathogenesis of degenerative disorders, including Alzheimer's disease (5, 6).

This laboratory has focused on control of transition of primary astrocytes derived from newborn rat brain from $G_0$ into cell cycle reentry. In the 1970s, Arthur Pardee demonstrated that established cell lines could be rendered into a quiescent, or $G_0$ state, and argued that this capacity represents a unique mechanism of cell cycle control in normal animal cells (7). But it is clear that established cell lines differ fundamentally from normal cells, which tend to undergo either senescence or intro transformation with repeated culture (1, 2). We were able to extend this approach to primary brain cells extracted from the brains of newborn rodents (8). In so doing, we confirmed the value of serum depletion and shift-up to uncover regulation in cells more likely to represent their counterparts in intact organisms (1, 2, 8, 9). This simple technique of serum depletion is used to establish a $G_0$ state, followed by be re-addition of serum to enable reentry into $G_1$ and S phases (**Fig. 5.1**, *see* also **Notes 1–3**).

## 2. Materials

### 2.1. Mammalian Astrocytic Cell Cultures

1. Primary astrocytic cultures harvested from neonatal (not older than 48 h) Sprague Dawley rat pups (Harlan Sprague Dawley, Indianapolis, IN).
2. Glioma cell line, C6 (ATCC CCL 107, ATCC Walkerville, MD, USA).

### 2.2. Solutions

1. 10X Trypsin EDTA: 0.5% trypsin, 0.2% EDTA
2. Tris EDTA: 100 mM Tris–HCl, 25 mM EDTA, pH 7.4
3. 10% (v/v) bovine calf serum (BCS) in Dulbecco's Modified Eagle's Medium (DMEM)
4. 0.1% (v/v) BCS in DMEM (pH 7.4)
5. 30% (v/v) BCS in PBS (pH 7.4)
6. Phosphate buffer saline (PBS) (pH 7.4)
7. [Methyl-$^3$H]-thymidine (Amersham, Arlington Heights, IL) at final concentration 1 μCi/ ml of medium.

## 3. Methods

Perform the following procedures in a sterile environment.

1. Maintain neoatal rat astrocytic cultures (or C6 glioma cell cultures) (**Figs**. **5.1**, **5.2**, and **5.3**, and *see* also **Notes 3–5**),

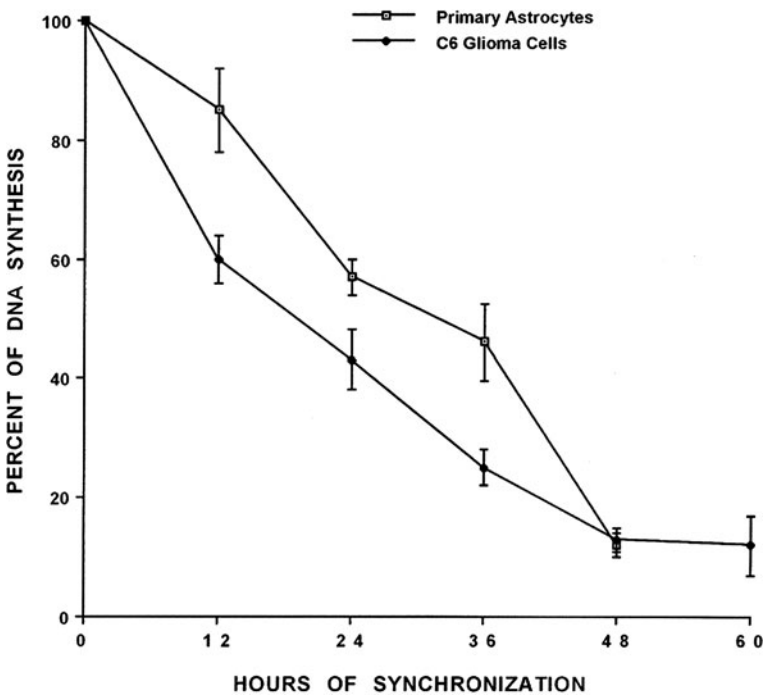


Fig. 5.2. Effect of serum deprivation on $^{3}$H-thymidine incorporation into DNA of primary astrocytic and C6G cell cultures. Both astrocytic cultures and C6 glioma cells were plated in the 6-well plates and allowed to grow to 30–50% confluence in the presence of 10% BCS/DMEM at 37°C and 5% $CO_2$/95% humidified air. At the end of the incubation, the media were removed and cultures were overlaid with 0.1% BCS/DMEM. Both cultures were incubated at 37°C and 5% $CO_2$/95% humidified air for various time periods. One hour prior to termination of incubation, cell cultures were pulse-labeled with $^{3}$H-thymidine at a final concentration of 1 $\mu$Ci/ml. Incorporated $^{3}$H-thymidine into DNA of astrocytic cultures at different time points was compared with the controls at T0. Results were expressed as means $\pm$ S.E.M. ($N = 4$–6 for primary astrocytes and 5–6 for C6G cells).

or other mammalian cells in primary or secondary cultures in 9 ml of 10% BCS in DMEM in T75 flasks.

2. Upon reaching complete confluence and ready for experimentation, aspirate media from the flasks and rinse cultures with 6 ml of Tris EDTA, followed by aspiration.
3. For trypsinization, add 6 ml of 1X Trypsin EDTA/Tris EDTA (pH 7.4) at 37°C to the cultures.
4. Agitate flasks gently by hand and incubate at 37°C and 5% $CO_2$/95% humidified air for 5 min.
5. Remove flasks from the incubator and rap them sharply against hood surface, thus causing cells to detach.
6. Triturate cells and add sufficient 30% BCS in PBS to achieve a final conc. of 10% BCS.

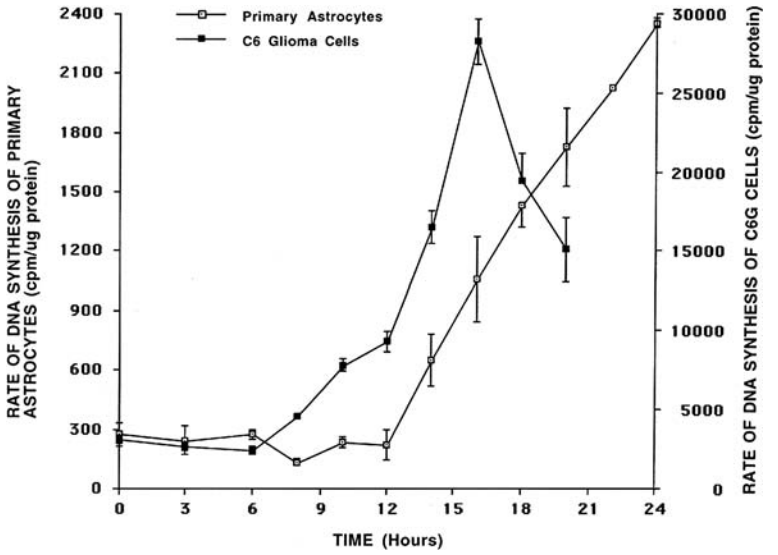


Fig. 5.3. Comparison of kinetic curves of primary astrocyte and C6G cell cycles. Both primary astrocytes and C6 glioma cells were plated in 6-well plates at concentrations of $10^4$ and $2 \times 10^3$ cells/cm$^2$, respectively, and allowed to grow to confluence of 30–50% in the presence of 10% BCS/DMEM and at 37°C and 5% $CO_2$/95% humidified air. After reaching the desired confluence, the cultures were serum downshifted from 10% BCS/DMEM to 0.1% BCS/DMEM for 48 h. At the end of the incubation, both cultures were allowed to reenter the cell cycle through serum shift-up in 10% BCS/DMEM. At various time points after serum shift-up, both cultures were pulse-labeled with $^3$H-thymidine at a final concentration of 1 μCi/ml for 1 h prior to termination. Incorporated $^3$H-thymidine into DNA of both cultures were measured and presented as mean ± S.E.M. ($N = 4$–9 for primary astrocytes and 5–7 for C6G cells).

7. Then spin cells in a tabletop centrifuge at 800×*g* and 4°C for 5 min.
8. Aspirate supernatants and cells and then resuspend them in 10% BCS in DMEM (usually about 40 ml media/flask to facilitate cell counting).
9. Triturate and filter cells through 20 μm mesh to remove debris and cell clumps, followed by cell count of cell suspension under a phase contrast microscope. Concentrations that work well during subsequent synchronization process are $1 \times 10^4$ cells/mm$^3$ for neonatal astrocytes and $2 \times 10^3$ cells/mm$^3$ for C6G cells (**Figs**. **5.1**, **5.2**, and **5.3**, *see* also **Notes 6** and 7). For replating astrocytic cultures, in 75 cm$^2$ flasks get a final volume of 9 ml, while 3 ml/well is satisfactory for 6-well plates (9.1 cm$^2$ total surface area/well).
10. Plate cells at desired densities and incubate at 37°C, and 5% $CO_2$/95% humidified air (*see* **Notes 7** and **8**).

11. After reaching a confluence of 30–50%, synchronize cell cultures through serum deprivation. Aspirate medium and rinse cells with PBS at 37°C. Overlay cells with 0.1% BCS in DMEM with the same volume as indicated above, and incubate at 37°C, and 5% $CO_2$/95% humidified air for about 48–72 h before starting the experiment (*see* **Notes** 7 and **8**).
12. At the end of the synchronization process, allow astrocytic cultures to reenter the cell cycle through serum shift-up in 10% BCS in DMEM at 37°C. The addition of 10% BCS in DMEM represents the start of the experiments (*see* **Notes 1, 8**, and **9**).
13. Assess rates of cell proliferation and degree of synchrony at any point of the cell cycle by pulse labeling cell cultures with 1 μCi/ml of $^3$H-thymidine for 1 h prior to termination of experiments. Counts of [methyl-$^3$H]-thymidine incorporated into the trichloroacetic acid-precipitated fraction is rapid and straightforward, resulting in determination cpm per μg protein (1, 9, 10). Alternatively, the fraction of cells in S phase can also be measured by pulse label with bromodeoxyuridine (BrDU) for 2.5 h, followed by immunocytochemical staining for BrDU (11) (*see* **Notes 8** and **9**). These techniques share the potential to shed new light on important questions about the pathogenesis of diseases (*see* **Note 10**).

## 4. Notes

1. Serum deprivation in this procedure decreases the rate of DNA synthesis in cultured neonatal astrocytic cells by about 88% at the end of the 48-h synchronization process, as based on $^3$H-thymidine incorporation (**Fig. 5.2**). By using immunofluorescent staining, BrDU pulse labeling demonstrated that the fraction of cells in S phase declined from 70 ± 3% ($N$ = 10, Total cell count = 100) to 15 ± 2 % ($N$ = 10, Total cell count = 105) under the same conditions.
2. Further serum deprivation beyond 48-h period rendered the neonatal astrocytic cells unable to reenter the cell cycle and caused subsequent cell death (data not shown).
3. Subsequent repletion of serum allowed neonatal astrocytic cells to reenter $G_1$ and S phases of the cell cycle in an approximately first order manner (2, 3, 10) (**Figs. 5.1** and **5.3**). In neonatal astrocytes, the DNA synthesis observed

in $G_1$ phase represents the basal level, persists until reaching the $G_1/S$ intersection, and lasts for 12 h. In an optimal synchronization procedure, repletion of 10% BCS in DMEM caused a 7- to 10-fold increase in DNA synthesis at the peak of S phase, when progressing from $G_1$ phase (**Figs**. **5.1** and **5.3**).

4. This procedure had been employed successfully in our hands in synchronizing the C6G cell line. The kinetics of cell cycle reentry in C6 glioma cells resembled those in neonatal astrocytes: an initial $G_1$ phase, followed by S phase, although the $G_1/S$ intersection shifted to an earlier time point (**Fig. 5.3**). Despite the shortening of $G_1$ phase, the peak of DNA synthesis in S phase was also 7- to 10-fold increase above the baseline in $G_1$ phase (**Fig. 5.3**). C6G cells were also able to sustain the synchronization process for much longer period (i.e., 60 h) than neonatal astrocytes with the ability to reenter the cell cycle (**Fig. 5.3**) following serum shift-up.
5. The present protocol arrests astrocytic cultures in $G_0$ phase of the cell cycle (8, 10, 11), as compared to a variety of other methods, which synchronize cell lines in other phases of the cell cycle, such as $G_1$ (12–14), S (5, 12), or M (15, 16) phase. This procedure is relatively free from major problems and satisfies the following criteria of synchronization, as set forth by Keyomarsi et al.: (a) both normal and tumor cells should be arrested at the same specific cell cycle phase; (b) the synchronization must be reversible and noncytotoxic; (c) the metabolic block should target a specific reaction and must be reversible; and (d) large quantities of synchronous cells should be obtained (12).
6. Astrocytic cultures undergoing synchronization are extremely sensitive to fluctuations in temperature, pH values, and $CO_2$ levels, all of which invariably affect molecular mechanisms involved in the progression of the cell cycle into quiescence (1–3). Therefore, a stable environment, provided by a rapidly equilibrating incubator, is essential for the success of synchronization by this method.
7. Other factors that determine the success of synchronization include the confluence and the rate of proliferation of the cell cultures before synchronization (4). Over-confluent, as well as rapidly growing, cultures often fail to survive synchronization or are unable to reenter the cell cycle after synchronization.
8. The optimal time for synchronization depends on the type of cell culture under study, and it is advisable to conduct simple kinetic studies on synchronization before

proceeding to actual experimentation. For example, in our kinetic studies, astrocytic cultures were synchronized for different periods of time. Based on the BRDU pulse labeling, the present protocol arrested about 85% of cultured astrocytes in $G_0$ phase (data not shown), which is well above the desired cell fraction (75%) for a successful cell synchronization process (13).

9. At the end of the synchronization process, the rate of DNA synthesis, as well as the potential of cultured cells to reenter the cell cycle, can be measured by $^3$H-thymidine pulsing as described above. Alternatively, the cell fractions in different phases of the cell cycle can be measured by flow cytometry in certain cell populations (11, 17). However, our laboratory has been unable to demonstrate distinct primary astrocytic cell populations in different phases of the cell cycle following synchronization by employing flow cytometry.
10. Our results (**Figs. 5.2** and **5.3** and ref. 9) have confirmed the utility of the serum deprivation protocol in determining differences between the kinetic curves of primary astrocytic cultures and C6 glioma cells following synchronization. The molecular basis of the difference between these two kinetic curves remained unidentified, but may well reflect a fundamental difference between normal and tumoral glial cells. And, as noted above, the initiation of cell cycling by astrocytes *in situ* is considered to be critical in the pathogenesis of Alzheimer's disease and other neurodegenerative processes (5, 6). Other laboratories have used serum deprivation to synchronize additional types of mammalian cells (2, 3, 10–13, 18–23). Thus, this procedure may eventually provide new insights into disease mechanisms related to oncogenesis and degenerative processes in other differentiated cells that retain the capacity to leave and then reenter $G_0$ (1–4).

## References


1. Alberts, B., Johnson, A., Lewis, J., Raff, M., Roberts, K., and Walter, P. (2002) Molecular biology of the cell. Fourth edition, Chap. 17. The cell cycle and programmed cell death, pp. 983–1026. Garland Science, NY.
2. Ashihara, T., and Baserga, R. (1979) Cell synchronization. *Methods Enzymol.* **58**, 248–262.
3. Bartholomew, J. C., Neff, N. T., and Ross, P. A. (1976) Stimulation of WI-38 cell cycle transit: effect of serum concentration and cell density. *J. Cell. Physiol.* **89**, 251–258.
4. Campbell, A. (1957) Synchronization of cell division. *Bacteriol. Rev.* **21**, 263–272.
5. Salomoni, P., and Callegari, F. (2010) Cell cycle control of mammalian neural stem cells: putting a speed limit on G1. *Trends Cell Biol.* **20**, 233–243.
6. Wang, W., Bu, B., Zhang, M., Yu, Z., and Tao, D. (2009) Neural cell cycle dysregulation and central nervous system diseases. *Progr Neurobiol.* **89**, 1–17.
7. Pardee, A. B. (1974) A restriction point for control of normal animal cell

proliferation. *Proc. Natl. Acad. Sci. USA* **71**, 1286–1290.
8. Langan, T. J., and Volpe, J. J. (1986) Obligatory relationship between the sterol biosynthetic pathway and DNA synthesis and cell proliferation in glial primary cultures. *J. Neurochem.* **46**, 1283–1291.
9. Li, V., Kelly, K., Schrot, R., and Langan, T. J. (1996) Cell cycle kinetics and commitment in newborn, adult, and tumoral astrocytes. *Brain Res.* **96**, 138–147.
10. Quesney-Huneeus, V., Galick, H. A., Siperstein, M. D., Erickson, S. K., Spencer, T. A., and Nelson, J. A. (1983) The dual role of mevalonate in the cell cycle. *J. Biol. Chem.* **258**, 378–385.
11. Merrill, G. F. (1998) Cell synchronization. In J. P. Mather and D. Barnes (Eds.), Methods in cell biology, Vol. 57, pp. 229–249. Academic Press, San Diego.
12. Keyomarsi, K., Sandoval, L., Band, V., and Pardee, A. B. (1991) Synchronization of tumor and normal cells from $G_1$ to multiple cell cycles by lovastatin. *Cancer Res.* **51**, 3602–3609.
13. Krek, W., and DeCaprio, J. A. (1995) Cell synchronization. *Methods Enzymol.* **254**, 114–124.
14. Pardee, A. B., and Keyomarsi, K. (1992) Modification of cell proliferation with inhibitors. *Curr. Opin. Cell Biol.* **4**, 186–191.
15. Langan, T. J., and Slater, M. C. (1991) Quiescent astroglia in long-term primary cultures re-enter the cell cycle and require a nonsterol isoprenoid in late $G_1$. *Brain Res.* **548**, 9–17.
16. Zieve, G. W., Turnbull, D., Mullins, J. M., and McIntosh, J. R. (1980) Production of large numbers of mitotic mammalian cells by use of the reversible microtubule inhibitor nocodazole. Nocodazole accumulated mitotic cells. *Exp. Cell Res.* **126**, 397–405.
17. Johnston, D. A., White, R. A., and Barlogie, B. A. (1978) Automatic processing and interpretation of DNA distributions: comparison of several techniques. *Comp. Biomed. Res.* **11**, 393–404.
18. Wilmut, I., Schnieke, A. E., McWhir, J., Kind, A. J., and Campbell, K. H. S. (1997) Viable offspring derived from fetal and adult mammalian cells. *Nature* **385**, 810–813.
19. Sanchez, I., Goya, L., Vallerga, A. K., and Firestone, G. L. (1993) Glucocorticoids reversibly arrest rat hepatoma cell growth by inducing an early $G_1$ block in cell cycle progression. *Cell Growth Differ.* **4**, 215–225.
20. Huberman, J. A. (1981) New views of the biochemistry of eucaryotic DNA replication revealed by aphidicolin, an unusual inhibitor of DNA polymerase alpha. *Cell* **23**, 647–648.
21. Mitchell, B. F., and Tupper, J. T. (1977) Synchronization of mouse 3T3 and SV40 3T3 cells by way of centrifugal elutriation. *Exp. Cell Res.* **106**, 351–355.
22. Terasima, T., and Tolmach, L. J. (1963) Growth and nucleic acid synthesis in synchronously dividing populations of HELA cells. *Exp. Cell Res.* **30**, 344–362.
23. Webber, L. M., and Garson, O. M. (1983) Fluorodeoxyuridine synchronization of bone marrow cultures. *Cancer Genet. Cytogenet.* **8**, 123–132.

# Chapter 6

# Cell Synchronization by Inhibitors of DNA Replication Induces Replication Stress and DNA Damage Response: Analysis by Flow Cytometry

**Zbigniew Darzynkiewicz, H. Dorota Halicka, Hong Zhao, and Monika Podhorecka**

## Abstract

Cell synchronization is often achieved by inhibition of DNA replication. The cells cultured in the presence of such inhibitors as hydroxyurea, aphidicolin, or thymidine become arrested at the entrance to S phase and upon release from the block they synchronously progress through S, $G_2$, and M. We recently reported that exposure of cells to these inhibitors at concentrations commonly used to synchronize cell populations led to phosphorylation of histone H2AX on *Ser*139 (induction of γH2AX) through activation of *ataxia telangiectasia mutated* and Rad3-related protein kinase (ATR). These findings imply that the induction of DNA replication stress by these inhibitors activates the DNA damage response signaling pathways and caution about interpreting data obtained with use of cells synchronized such way as representing unperturbed cells. The protocol presented in this chapter describes the methodology of assessment of phosphorylation of histone H2AX-*Ser*139, ATM/ATR substrate on *Ser/Thr* at SQ/TQ cluster domains as well as *ataxia telangiectasia mutated* (ATM) protein kinase in cells treated with inhibitors of DNA replication. Phosphorylation of these proteins is detected in individual cell immunocytochemically with phospho-specific antibody (Ab) and measured by flow cytometry. Concurrent measurement of cellular DNA content and phosphorylated proteins followed by multiparameter cytometric analysis allows one to correlate extent of their phosphorylation with cell cycle phase.

**Key words:** DNA repair, DNA double-strand breaks, flow cytometry, apoptosis, DNA fragmentation, $G_1$/S boundary.

## 1. Introduction

### *1.1. Virtues and Vices of Different Synchronization Methods*

Different approaches are being used to obtain populations of cells synchronized in the cell cycle (*see* reviews (1–4)). Each of these approaches offers some advantages but also suffers limitations.

G. Banfalvi (ed.), *Cell Cycle Synchronization*, Methods in Molecular Biology 761,
DOI 10.1007/978-1-61779-182-6_6, © Springer Science+Business Media, LLC 2011

One of widely used methods is based on isolation of mitotic cells by their detachment from flasks during culturing (5). Its virtue stems from the fact that cell progression through the cell cycle is not being perturbed. However, the technique is applicable to few cell lines, such as Chinese hamster ovary (CHO) or HeLa cells, that grow attached in cultures and detach during mitosis. Another technique selecting mitotic cells was designed for murine leukemic L1210 cells that grow in suspension but are being enforced to attach to polylysine-coated membranes. During mitosis the daughter cells detach from the mother cells, still attached to membranes, and float in culture medium (6, 7). It is unknown how widely this approach can be used because cells of other than L1210 lines cannot be synchronized this way (8). Cells of certain lines can be synchronized in $G_1$ by inhibitors of protein farnesylation and geranylgeranylation such as statins (9) or CDK2 protein kinase inhibitors (10–12). These techniques also are not universally applicable since many lines do not respond to statins or protein kinase inhibitors by reversible arrest in $G_1$.

Normal, non-tumor cells can be synchronized in $G_0/G_1$ by removal of growth factors, e.g., by "serum starvation" (13), or depletion of a particular amino acid (14), or by contact inhibition (15). These approaches generally fail to synchronize tumor cell lines. Moreover, the metabolism of so synchronized cells is often perturbed which affects their rate of progression through the cycle upon release from the arrest (16). It should also be noted that the cells synchronized in early $G_1$ or at mitosis start to lose synchrony while progressing through $G_1$ and thereby become less synchronous in S or $G_2$.

The approach based on separation of cells based on their size, centrifugal elutriation, is also being used to obtain synchronous cell populations (17, 18, *see* also **Chapter 2**). However, while this procedure does not perturb cell cycle progression the synchrony of uniformly sized elutriated cells is not always sufficiently narrow. Furthermore, elutriation requires rather complex and expensive instrumentation and an experienced operator. Density gradient centrifugation yields cell populations even less synchronized than the elutriation (19). Fluorescence-activated cell sorting (FACS) is also used to obtain synchronous cell populations, e.g., based on DNA content analysis upon supravital staining with fluorochromes such as Hoechst 33342 (20). However, Hoechst 33342 elicits DNA damage response (21), long-term toxicity (22), and undergoes redistribution from labeled to unlabeled cells in mixed cell populations (23).

Cell synchronization at mitosis by mitotic spindle poisons such as colchicines, vinca alkaloids, or nocodazole is another common approach (24, 25). The advantage of this approach is simplicity, low cost, and high degree of synchrony when one opts to obtain mitotic or immediately postmitotic cell populations

(26). As mentioned, so synchronized cell populations become less synchronous after progression through $G_1$. Furthermore, undesirable effects such as cytotoxicity and growth imbalance are seen during arrest in mitosis (27–29).

### 1.2. Inhibitors of DNA Replication

Among the most common approaches to obtain populations of synchronized cells, particularly in S phase, is cell synchronization with the use of DNA replication inhibitors such as hydroxyurea, methotrexate, aphidicolin, or high concentration of thymidine (30–33). A combination of replication inhibitors with other synchronizing agents is also widely used (25, 34). The advantage of cell synchronization by DNA replication inhibitors is the simplicity and low cost. However, the major drawback is the induction of growth imbalance (27, 35). While cells become arrested in their progression through S, their growth, in terms of RNA and protein synthesis, and cell enlargement continue which leads to perturbation of metabolic functions. Furthermore the cell cycle progression machinery of cells synchronized by DNA replication inhibitors is severely perturbed as reflected by unscheduled expression of cyclin proteins (36).

Inhibitors of DNA replication such as hydroxyurea, aphidicolin, thymidine, and aphidicolin were shown to induce phosphorylation of histone H2AX on Ser139 (37, 38). Phosphorylated H2AX is defined as γH2AX (39). Phosphorylation of H2AX and activation of *ataxia telangiectasia mutated* protein kinase (ATM) through its phosphorylation on Ser1981 (ATM-S1981$^P$) are the key markers signalizing DNA damage response (DDR) reflecting DNA damage that involves formation of DNA double-strand breaks (DSBs) (39, 40; reviews 41, 42). Both activation of ATM and H2AX phosphorylation can be detected immunocytochemically using phospho-specific Abs, and the extent of their phosphorylation reporting severity of DNA damage can be measured by flow or laser scanning cytometry (43–47). Since during replication stress H2AX is phosphorylated by ATM Rad3-related protein kinase (ATR) and not by ATM, the latter kinase remains not activated (37; *see* **Fig. 6.1**). While no phospho-specific Ab is available at present to directly detect activated ATR, its activation can be detected indirectly using Ab to ATM/ATR substrate that is phosphorylated on Ser/Thr at SQ/TQ cluster domains (sATM/ATR$^P$) (48). The response induced by DNA replication inhibitors thus can be assessed by detecting activation of ATR and phosphorylation of H2AX (expression of γH2AX) concurrent with the lack of activation of ATM (37). It should be noted, however, that in certain instances the DNA replication stress, e.g., as caused by UV light may also induce activation of ATM and DNA-dependent protein kinase (DNA-PKcs) (49).

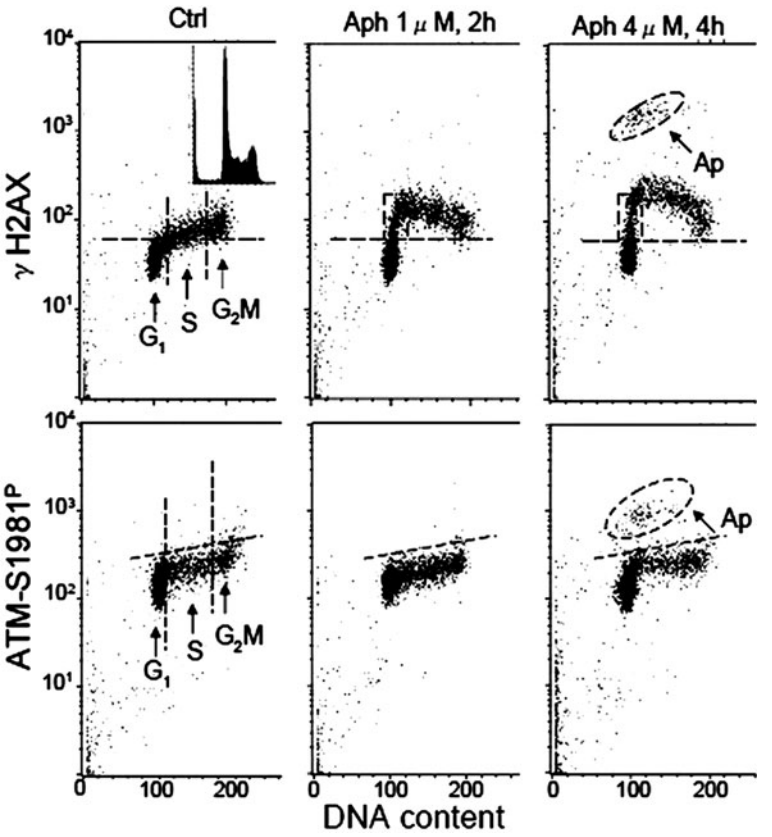


Fig. 6.1. Detection of histone H2AX phosphorylation and ATM activation in HL-60 cells treated with DNA polymerase alpha inhibitor aphidicolin (Aph). The cells were untreated (Ctrl) or treated in culture with 1 or 4 μM Aph and expression of γH2AX and ATM-S1981$^P$ was measured as described in the protocol (indirect immunofluorescence). The bivariate distributions (scatterplots) of γH2AX or ATM-S1981$^P$ immunofluorescence (IF) versus DNA content allow one to identify subpopulations of cells in $G_1$, S, and $G_2$M phases of the cell cycle as shown in *left panels*. The *horizontal line* in *top panels* represents the upper γH2AX IF threshold for 95% of $G_1$ phase cells from the untreated (Ctrl) cultures and the *dashed skewed line* (*bottom panels*) mark the upper threshold of ATM-S1981P IF for 95% of untreated (Ctrl) cells in all phases. The cellular DNA content histogram of the Ctrl cells is shown in the *left panel inset*. Increased expression of γH2AX is primarily seen in cells at the interphase of $G_1$ and S (marked by the *rectangular dashed outlines*) and also in S and $G_2$M in cells after treatment with Aph. No increase in expression of ATM-S1981$^P$ is apparent. Apoptotic cells (Ap, marked with *oval dashed line* boundaries) are detected as having markedly elevated expression of both γH2AX and ATM-S1981$^P$after treatment with 4 μM Aph for 4 h. Note that the γH2AX and ATM-S1981$^P$ coordinates are exponential while DNA content scale is linear.

### *1.3. Analysis of DDR Induced by DNA Replication Inhibitors*

The protocol presented in this chapter is designed to assess intensity of γH2AX and/or ATM-S1981$^P$ and/or phosphorylated ATM/ATR substrate (sATM/ATR$^P$) immunofluorescence (IF) for evaluation of the degree of DNA damage response. The detection of γH2AX, sATM/ATR$^P$, or ATM-S1981$^P$ is combined with differential staining of DNA to assess cellular DNA contents

which reveals the cell cycle phase (*see* **Note 1**). The procedure is based on either *indirect IF* detection of these phosphorylated proteins using the primary Ab unlabeled and the secondary Ab conjugated with FITC or Alexa Fluor 488, or using *direct IF* with the fluorochrome-tagged primary Abs (*see* **Note 2**). DNA is counterstained with propidium iodide (PI) whose emission spectrum (red) is separated from the green color emission of FITC or Alexa Fluor 488. The cells are briefly fixed in methanol-free formaldehyde and then transferred into 70% ethanol in which they can be kept briefly (≥2 h) or stored at –20°C for weeks or longer. Ethanol treatment makes the plasma membrane permeable to the γH2AX Ab; further permeabilization is achieved by including the detergent Triton X-100 into a solution used to incubate cells with the Ab. After incubation with the primary γH2AX Ab the cells are incubated with FITC or Alexa Fluor 488-labeled secondary Ab and their DNA is counterstained with PI in the presence of RNase A to remove RNA, which otherwise, similar as DNA, is also being stained with PI. Intensities of cellular green (FITC or Alexa Fluor 488) and red (PI) fluorescence are measured by flow cytometry.

It should be noted that H2AX undergoes constitutive phosphorylation in healthy cells, untreated by radiation or genotoxic agents. This constitutive expression of γH2AX, which is more pronounced in S and $G_2M$ than in $G_1$ cells, is considered to be in large part a reflection of oxidative DNA damage caused by the metabolically generated oxidants (50, 51). Moreover, DNA fragmentation during apoptosis (52) leads to formation of large quantity of DSBs inducing high level of H2AX phosphorylation (53; *see* **Fig. 6.1**). Strategies are presented to distinguish the DNA damage induced by DNA replication inhibitors from the constitutive damage occurring in untreated cells (*see* **Note 3**) or from the apoptosis-associated (AA) DSBs (*see* **Note 4**).

## 2. Materials

### *2.1. Reagents, Disposables*

1. Cells to be analyzed: $10^6$–$5 \times 10^6$ cells, untreated (control) and treated in culture with inhibitors of DNA replication (e.g., hydroxyurea, aphidicolin, or thymidine at their respective concentrations generally used to inhibit DNA synthesis and synchronize cells at the entrance to S phase) suspended in 1 ml of tissue culture medium.
2. Methanol-free formaldehyde (Polysciences, Warrington, PA).
3. Phosphate-buffered saline (PBS).

4. Bovine serum albumin (BSA).
5. Antibodies (Abs). Commercially available phospho-specific Abs:
   - mono- as well as poly-clonal, unconjugated Abs,
   - FITC- or Alexa Fluor 488-conjugated, applicable to cytometry, that can be used to detect γH2AX, ATM-S1981$^{P}$, or ATM/ATR substrate,
   - FITC- or Alexa 488-tagged secondary Abs to be used in conjunction with the non-conjugated primary Abs to these phosphorylated proteins.
6. DNase-free RNase A
7. 12 × 75 mm polypropylene tubes

### 2.2. Solutions

1. Methanol-free formaldehyde fixative: Prepare 1% (v/v) solution of methanol-free formaldehyde in PBS. This solution may be stored at 4°C for up to 2 weeks.
2. BSA-T-PBS: Dissolve BSA in PBS to obtain 1% (w/v) BSA solution. Add Triton X-100 to obtain 0.2% (v/v) of its concentration. This solution may be stored at 4°C for up to 2 weeks.
3. Propidium iodide (PI) stock solution: Dissolve PI in distilled water to obtain 1 mg/ml solution. This solution can be stored at 4°C in the dark (e.g., in the tube wrapped in aluminum foil) for several months.
4. PI staining solution: Dissolve RNase A (DNase-free) in PBS to obtain 0.1% (w/v; 100 mg/ml) solution. Add an appropriate aliquot of PI stock solution (e.g., 5 μl/1 ml) to obtain its 5 μg/ml final concentration. Store the PI staining solution in the dark. This solution may be stored at 4°C for up to 2 weeks.

### 2.3. Instrumentation

1. Flow cytometers of different types, offered by several manufacturers, can be used to measure cell fluorescence following staining according to the protocol given below.
2. Centrifuge and rotor using 300×*g*.

## 3. Methods

1. Centrifuge cells collected from tissue culture (suspended in culture medium) at 300×*g* for 4 min at room temperature. Suspend cell pellet (1–2 × $10^6$ cells) in 0.5 ml of PBS.
2. With a Pasteur pipette transfer this cell suspension into polypropylene tube (*see* **Note 5**) containing 4.5 ml of ice-cold 1% methanol-free formaldehyde solution in PBS. Keep on ice for 15 min.

3. Centrifuge at 300×*g* for 4 min at room temperature and suspend cell pellet in 4.5 ml of PBS. Centrifuge again as above and suspend cell pellet in 0.5 ml of PBS. With a Pasteur pipette, transfer the suspension to a tube containing 4.5 ml of ice-cold 70% ethanol. The cells should be maintained in 70% ethanol for 1 h but may be stored in 70% ethanol at –20°C for several weeks.
4. Centrifuge at 300×*g* for 4 min at room temperature, remove the ethanol, and suspend cell pellet in 2 ml of BSA-T-PBS solution.
5. Centrifuge at 300×*g* for 4 min at room temperature and suspend the cells again in 2 ml of BSA-T-PBS. Keep at room temperature for 5 min.
6. Centrifuge at 300×*g* for 4 min at room temperature and suspend the cells in 100 μl of BSA-T-PBS containing 1 μg of the primary γH2AX Ab (*see* **Notes 2** and **6**).
7. Cap the tubes to prevent drying and incubate them overnight at 4°C (*see* **Note 7**).
8. Add 2 ml of BSA-T-PBS and centrifuge at 300×*g* for 4 min at room temperature.
9. Centrifuge at 300×*g* for 4 min at room temperature and suspend the cells in 2 ml of BSA-T-PBS.
10. Centrifuge at 300×*g* for 4 min at room temperature and suspend the cells pellet in 100 μl of BSA-T-PBS containing the appropriate (anti-mouse or anti-rabbit, depending on the source of the primary Ab) FITC- or Alexa Fluor 488-tagged secondary Ab (*see* **Note 6**).
11. Incubate for 1 h at room temperature, occasionally gently shaking. Add 5 ml of BSA-T-PBS and after 2 min centrifuge at 300×*g* for 4 min at room temperature.
12. Suspend the cells in 1 ml of the PI staining solution. Incubate at room temperature for 30 min in the dark.
13. Set up and adjust the flow cytometer for excitation with light at blue wavelength (488-nm laser line or BG-12 excitation filter).
14. Measure intensity of green (530 ± 20 nm) and red (>600 nm) fluorescence of the cells by flow cytometry. Record the data.

## 4. Notes

1. On the bivariate distributions (scatterplots) subpopulations of cells in $G_1$, versus S versus $G_2/M$ are distinguished based on differences in their DNA content (intensity of PI

fluorescence; *see* **Fig. 6.1**). To assess the mean extent of DNA damage for cells at a particular phase of the cycle the mean values of γH2AX or ATM-S1981$^P$ or sATM/ATR$^P$ IF are calculated separately for $G_1$, S, and $G_2$/M cells distinguished based on differences in DNA content, by the computer-interactive "gating" analysis. The gating analysis should be carried out to obtain mean values of γH2AX or ATM-S1981$^P$ or sATM/ATR$^P$ IF for $G_1$ (DNA Index; DI = 0.9–1.1), S (DI = 1.2–1.8), and $G_2$M (DI = 1.9–2.1) cell subpopulations.

2. If primary Ab conjugated with fluorochrome (e.g., with FITC or Alexa Fluor 488) is being used replace the unlabeled Ab in Step 5 with the conjugated one and move to Step 10, omitting Steps 6–9.

3. As mentioned in **Section 1** the low level of expression of γH2AX or ATM-S1981$^P$ IF seen in cells that have not been treated with exogenous inducers of DDR represents the constitutive ("background") H2AX phosphorylation and ATM activation. To quantify the γH2AX or ATM-S1981$^P$ IF induced by DNA replication inhibitors the constitutive component of γH2AX or ATM-S1981$^P$ IF has to be subtracted. Toward this end the means of γH2AX or ATM-S1981$^P$ IF of $G_1$, S, and $G_2$/M phase of the untreated cells are subtracted from the respective means of the $G_1$, S, and $G_2$/M subpopulations of the inhibitor-treated cells, respectively (*see* **Fig. 6.1**) After the subtraction the extent of increase in intensity of γH2AX (ΔγH2AX IF) or ATM-S1981$^P$ (ΔATM-S1981$^P$ IF) over the untreated sample represents the treatment-induced phosphorylation of this protein, per each phase of the cell cycle. Alternatively, one can express the inhibitor-induced phosphorylation of H2AX or sATM/ATR as a percent (or multiplicity) of the increase of the mean IF value of the inhibitor treated to the mean of the untreated cells, in the respective phases of the cell cycle. The irrelevant isotype control may be used to estimate the nonspecific Ab binding component, although its use may be unnecessary when one is interested only in the assessment of the inhibitor-induced increase (Δ) in IF.

4. DNA undergoes extensive fragmentation during apoptosis (52) which leads to the appearance of a multitude of DSBs in apoptotic cells, triggering H2AX phosphorylation and ATM activation (53). It is often desirable, therefore, to distinguish between primary DSBs induced by DNA damaging agents such as DNA replication inhibitors versus DSBs generated during apoptosis. The following attributes of γH2AF IF allow one to distinguish the cells with the inhibitor-induced H2AX phosphorylation from the cells that have

phosphorylation of this histone triggered by apoptosis-associated (AA) DNA fragmentation: (i) The γH2AX IF induced by replication inhibitors is seen rather early during the treatment (30 min–2 h) whereas AA γH2AX IF is seen later (>3 h) (53); (b) The intensity AA γH2AX IF is much higher than that of the inhibitor-induced γH2AX IF, unless the cells are at late stage of apoptosis (53, *see* **Fig. 6.1**); (c) The induction of AA γH2AX IF is prevented by cell treatment with the caspase inhibitor z-VAD-FMK, which precludes activation of endonuclease responsible for DNA fragmentation (53); (d) The AA H2AX phosphorylation occurs concurrently with activation of caspase-3. Multiparameter analysis [activated (cleaved) caspase-3 versus γH2AX IF], thus, allows one to distinguish cells in which DSBs were caused by inducers of DNA damage (active caspase-3 is undetectable) from the cells that have H2AX phosphorylation and ATM activation additionally triggered in response to apoptotic DNA fragmentation (active caspase-3 is present); (e) ATM is activated in response to AA DNA fragmentation whereas is not activated during replication stress (37). These strategies are discussed in more detail elsewhere (47).

5. If the sample initially contains a small number of cells they may be lost during repeated centrifugations. Polypropylene or siliconized glass tubes are recommended to minimize cell loss. Since transferring cells from one tube to another causes electrostatic attachment of a large fraction of cells to the surface of each new tube, all steps of the procedure, including fixation, preferentially should be done in the same tube. Addition of 1% (w/v) BSA to rinsing solutions also decreases cell loss. When the sample contains very few cells, carrier cells (e.g., chick erythrocytes) may be included; they may be recognized during analysis based on differences in DNA content (intensity of PI fluorescence).
6. Quality of the primary and of secondary antibody is of utmost importance. The ability to detect γH2AX, sATM/ATR$^{P}$, or ATM-S1981$^{P}$ is often lost during improper transport or storage conditions of the Ab. We occasionally observed that the Abs provided by the vendor were defective. Also of importance is use of the Abs at optimal concentration. It is recommended that with the first use of every new batch of the primary or secondary Ab to test them at serial dilution (e.g., within the range between 0.2 and 2.0 μg/100 μl) to find their optimal titer for detection of these phospho-proteins. The optimal titer is recognized as giving maximal signal-to-noise ratio, i.e., the maximal ratio of the mean IF intensity of the drug treated to the untreated

cells. Not always the titer recommended by the vendor is the optimal one.

7. Alternatively, incubate for 1 h at 22–24°C. The overnight incubation at 4°C, however, appears to yield somewhat higher intensity of γH2AX IF, sATM/ATR$^{P}$, or ATM-S1981$^{P}$ IF compared to 1 h incubation.

## Acknowledgment

This project is supported by NCI CA RO1 28 704.

### References

1. Grdina, D. J., Meistrich, M. L., Meyn, R. E., Johnson, T. S., and White, R. A. (1987) Cell synchrony techniques. A comparison of methods. In: Techniques in Cell Cycle Analysis, Gray, J. W. and Darzynkiewicz, Z. (eds). Humana Press Inc, Clifton, NJ, pp. 367–402.
2. Davis, P. K., Ho, A., and Dowdy, S. F. (2001) Biological methods for cell-cycle synchronization of mammalian cells. *BioTechniques* **30**, 1322–1331.
3. Merril, G. F. (1998) Cell synchronization. *Methods Cell Biol.* **57**, 229–249.
4. Amon, A. (2002) Synchronization procedures. *Methods Enzymol.* **351**, 457–467.
5. Terasima, T., and Tolmach, L. J. (1963) Growth and nucleic acid synthesis in synchronously dividing populations of HeLa cells. *Exp. Cell Res.* **30**, 344–362.
6. Edward, K. L., Van Ert, M. N., Thornton, M., and Helmstetter, C. E. (2004) Cyclin mRNA stability does not vary during the cell cycle. *Cell Cycle* **3,** 1057–1060.
7. Thornton, M., Edward, K. L., and Helmstetter, C. E. (2002) Production of minimally disturbed synchronous cultures of hematopoetic cells. *BioTechniques* **32**, 1098–10100.
8. Huang, X., Dai, W., and Darzynkiewicz, Z. (2005) Enforced adhesion of hematopoietic cells to culture dish induces endomitosis and polyploidy. *Cell Cycle* **4**, 801–805.
9. Jakóbisiak, M., Bruno, S., Skierski, J., and Darzynkiewicz, Z. (1991) The cell cycle specific effects of lovastatin. *Proc. Natl. Acad. Sci. USA* **88**, 3628–3632.
10. Crissman, H. A., Gadbois, D. M., Tobey, R. A., and Bradbury, E. M. (1991) Transformed mammalian cells are deficient in kinase-mediated progression through the $G_1$ phase of the cell cycle. *Proc. Natl. Acad. Sci. USA* **88**, 7580–7585.
11. Bruno, S., Ardelt, B., Skierski, J. S., Traganos, F., and Darzynkiewicz, Z. (1992) Different effects of staurosporine, an inhibitor of protein kinases, on the cell cycle and chromatin structure of normal and leukemic lymphocytes. *Cancer Res.* **52**, 470–476.
12. Bruno, S., Traganos, F., and Darzynkiewicz, Z. (1996) Cell cycle synchronizing properties of staurosporine. *Methods Cell Sci.* **18**, 99–107.
13. Griffin, M. J. (1976) Synchronization of some human cell strains by serum and calcium starvation. *In Vitro* **12**, 393–400.
14. Tobey, R. A., and Crissman, H. A. (1972) Use of flow microfluorimetry in detailed analysis of effects of chemical agents on cell cycle progression. *Cancer Res.* **32**, 2726–2731.
15. Holley, R. W., and Kiernan, M. A. (1968) "Contact inhibition" of cell division in 3T3 cells. *Proc. Natl. Acad. Sci. USA* **60**, 300–305.
16. Pardee, A. B., and Keyomarsi, K. (1992) Modification of cell proliferation with inhibitors. *Curr. Opin. Cell Biol.* **4**, 186–191.
17. Mitchell, B. F., and Tupper, J. T. (1977) Synchronization of mouse 3T3 and SV40 3T3 cell by way of centrifugal elutriation. *Exp. Cell Res.* **106**, 351–355.
18. Banfalvi, G. (2008) Cell cycle synchronization of animal cells and nuclei by centrifugal elutriation. *Nat. Protoc.* **3**, 663–673.

19. Cymerman, U., and Beer, J. B. (1980) Some problems in using density gradient centrifugation for synchronization of L5178Y-S cells. *Neoplasma* **27**, 429–436.
20. Juan, G., Hernando, E., and Cordon-Cardo, C. (2002) Separation of live cells in different phases of the cell cycle for gene expression analysis. *Cytometry* **49**, 170–175.
21. Zhao, H., Traganos, F., Dobrucki, J., Wlodkowic, D., and Darzynkiewicz Z. (2009) Induction of DNA damage response by the supravital probes of nucleic acids. *Cytometry A* **75A**, 510–519.
22. Zhang, X., Chen, J., Davis, B., and Kiechle, F. (1999) Hoechst 33342 induces apoptosis in HL-60 cells and inhibits topoisomerase I in vivo. *Arch. Pathol. Lab. Med.* **123**, 921–927.
23. Mohorko, N., Kregar-Velikonja, N., Repovs, G., Gorensek, M., and Bresjanac, M. (2005) An in vitro study of Hoechst 33342 redistribution and its effects on cell viability. *Hum. Exp. Toxicol.* **24**, 573–580.
24. Samake, S., and Smith, L. C. (1996) Synchronization of cell division in eight-cell bovine embryos produced in vitro: effects of nocodazole. *Mol. Reprod. Dev.* **44**, 486–492.
25. Harper, J. V. (2005) Synchronization of cell populations in $G_1$/S and $G_2$/M phases of the cell cycle. *Methods Mol. Biol.* **296**, 157–165.
26. Darzynkiewicz, Z., Crissman, H., Traganos, F., and Stainkamp, J. (1982) Cell heterogeneity during the cell cycle. *J. Cell Physiol.* **112**, 465–474.
27. Urbani, L., Sherwood, S. W., and Schimke, R. T. (1995) Dissociation of nuclear and cytoplasmic cell cycle progression by drugs employed in cell synchronization. *Exp. Cell Res.* **219**, 159–168.
28. Chou, L. F., and Chou, W. G. (1999) DNA-end binding activity of Ku in synchronized cells. *Cell Biol. Int.* **23**, 663–670.
29. Piotrowska, K., Modlinski, J. A., Korwin-Kossakowski, M., and Karasiewicz, J. (2000) Effects of preactivation of ooplasts or synchronization of blastomere nuclei in $G_1$ on preimplantation development of rabbit serial nuclear transfer embryos. *Biol. Reprod.* **63**, 677–682.
30. Tobey, R. A., Oishi, N., and Crissman, H. A. (1990) Cell cycle synchronization: reversible induction of $G_2$ synchrony in cultured rodent and human diploid fibroblasts. *Proc. Natl. Acad. Sci. USA* **87**, 5104–5109.
31. Vogel, W., Schempp, W., and Sigwarth, I. (1978) Comparison of thymidine, fluorodeoxyuridine, hydroxyurea, and methotrexate blocking at the $G_1$/S phase transition of the cell cycle, studied by replication patterns. *Hum. Genet.* **45**, 193–198.
32. Fox, M. H., Read, R. A., and Bedford, J. S. (1987) Comparison of synchronized Chinese hamster ovary cells obtained by mitotic shake-off, hydroxyurea, aphidicolin, or methotrexate. *Cytometry* **8**, 315–320.
33. Matherly, L. H., Schuetz, J. D., Westin, E., and Goldman, I. D. (1989) A method for the synchronization of cultured cells with aphidicolin: application to the large-scale synchronization of L1210 cells and the study of the cell cycle regulation of thymidylate synthase and dihydrofolate reductase. *Anal. Biochem.* **182**, 338–345.
34. Kues, W. A., Anger, M., Carnawath, J. W., Paul, D., Motlik, J., and Niemann, H. (2000) Cell cycle synchronization of porcine fetal fibroblasts: effects of serum deprivation and reversible cell cycle inhibitors. *Biol. Reprod.* **62**, 412–419.
35. Cohen, L. S., and Studzinski, G. P. (1967) Correlation between cell enlargement and nucleic acid and protein content of HeLa cells in unbalanced growth produced by inhibitors of DNA synthesis. *J. Cell Physiol.* **69**, 331–339.
36. Gong, J., Traganos, F., and Darzynkiewicz, Z. (1995) Growth imbalance and altered expression of cyclins B1, A. E and D3 in MOLT-4 cells synchronized in the cell cycle by inhibitors of DNA replication. *Cell Growth Differ.* **6**, 1485–1492.
37. Kurose, A., Tanaka, T., Huang, X., Traganos, F., Dai, W., and Darzynkiewicz, Z. (2006) Effects of hydroxyurea and aphidicolin on phosphorylation of ATM on *Ser* 1981 and histone H2AX on *Ser* 139 in relation to cell cycle phase and induction of apoptosis. *Cytometry A* **69A**, 212–221.
38. Kurose, A., Tanaka, T., Huang, X., Traganos, F., and Darzynkiewicz, Z. (2006) Synchronization in the cell cycle by inhibitors of DNA replication induces histone H2AX phosphorylation, an indication of DNA damage. *Cell Prolif.* **39**, 231–240.
39. Rogakou, E. P., Pilch, D. R., Orr, A. H., Ivanova, V. S., and Bonner, W. M. (1998) DNA double-stranded breaks induce histone H2AX phosphorylation on serine139. *J. Biol. Chem.* **273**, 5858–5868.
40. Sedelnikova, O. A., Rogakou, E. P., Panuytin, I. G., and Bonner, W. (2002) Quantitative detection of $^{125}$IUdr-induced DNA double-strand breaks with γ-H2AX antibody. *Radiation Res.* **158**, 486–494.
41. Mah, L.-J., El-Osta, A., and Karagiannis, T. C. (2010) GammaH2AX: a sensitive

molecular marker of DNA damage and repair. *Leukemia* **24**, 679–686.
42. Lavin, M. F., and Kozlov, S. (2007) ATM activation and DNA damage response. *Cell Cycle* **6**, 931–942.
43. Zhao, H., Traganos, F., and Darzynkiewicz, Z. (2010) Kinetics of the UV-induced DNA damage response in relation to cell cycle phase. Correlation with DNA replication. *Cytometry A* **77A**, 285–293.
44. Tanaka, T., Huang, X., Halicka, H. D., Zhao, H., Traganos, F., Albino, A. P., Dai, W., and Darzynkiewicz, Z. (2007) Cytometry of ATM activation and histone H2AX phosphorylation to estimate extent of DNA damage induced by exogenous agents. *Cytometry A* **71A**, 648–661.
45. MacPhail, S. H., Banath, J. P., Yu, T. Y., Chu, E. H., Lambur, H., and Olive, P. L. (2003) Expression of phosphorylated histone H2AX in cultured cell lines following exposure to X-rays. *Int. J. Radiat. Biol.* **79**, 351–358.
46. Zhao, H., Traganos, F., and Darzynkiewicz, Z. (2008) Kinetics of histone H2AX phosphorylation and Chk2 activation in A549 cells treated with topotecan and mitoxantrone in relation to the cell cycle phase. *Cytometry A* **73A**, 480–489.
47. Kurose, A., Tanaka, T., Huang, X., Halicka, H. D., Traganos, F., Dai, W., and Darzynkiewicz, Z. (2005) Assessment of ATM phosphorylation on *Ser*-1981 induced by DNA topoisomerase I and II inhibitors in relation to *Ser*-139-histone H2AX phosphorylation, cell cycle phase and apoptosis. *Cytometry A* **68A**, 1–9.
48. Traven, A., and Heierhorst, J. (2005) SQ/TQ cluster domains: concentrated ATM/ATR kinase phosphorylation site regions in DNA-damage-response proteins. *BioEssays* **27**, 397–407.
49. Yajima, H., Lee, K. J., Zhang, S., Kobayashi, J., and Chen, B. P. (2009) DNA double-strand break formation upon UV-induced replication stress activates ATM and DNA-PKcs kinases. *J. Mol. Biol.* **385**, 800–810.
50. Tanaka, T., Halicka, H. D., Huang, X., Traganos, F., and Darzynkiewicz, Z. (2006) Constitutive histone H2AX phosphorylation and ATM activation, the reporters of DNA damage by endogenous oxidants. *Cell Cycle* **5**, 1940–1945.
51. Zhao, H., Tanaka, T., Halicka, H. D., Traganos, F., Zarebski, M., Dobrucki, J., and Darzynkiewicz, Z. (2007) Cytometric assessment of DNA damage by exogenous and endogenous oxidants reports the aging-related processes. *Cytometry A* **71A**, 905–914.
52. Kajstura, M., Halicka, H. D., Pryjma, J., and Darzynkiewicz, Z. (2007) Discontinuous fragmentation of nuclear DNA during apoptosis revealed by discrete "sub-$G_1$" peaks on DNA content histograms. *Cytometry A* **71A**, 125–131.
53. Tanaka, T., Kurose, A., Huang, X., Dai, W., and Darzynkiewicz, Z. (2006) ATM kinase activation and histone H2AX phosphorylation as indicators of DNA damage by DNA topoisomerase I inhibitor topotecan and during apoptosis. *Cell Prolif.* **39**, 49–60.

# Chapter 7

# Chromosome Formation During Fertilization in Eggs of the Teleost *Oryzias latipes*

**Takashi Iwamatsu**

## Abstract

Upon fertilization, eggs shift their cell cycle from the meiotic to the mitotic pattern for embryogenesis. The information on chromosome formation has been accumulated by various experiments using inhibitors to affect formation and behavior of chromosomes in the cycle of cell proliferation. Based on experimental results on meiosis and early stages of development of the teleost *Oryzias latipes*, we discuss the roles of the activities of histone H1 kinase, microtubule-associated protein kinase, DNA polymerase, DNA topoisomerase, and other cytoplasmic factors that play a crucial role in formation and separation of chromosomes.

**Key words:** Teleost, meiosis, fertilization, DNA replication, chromosomal formation, chromosomal separation, aphidicolin, camptothecin.

## 1. Introduction

### *1.1. Meiosis in Non-mammalian Vertebrates*

In the ovary, proliferating oogonia shift from a mitotic cell cycle to a meiotic cell cycle as they differentiate to follicle-enclosed oocytes. Then in response to junctional interactions with the surrounding follicle cells, oocytes interrupt their first meiotic cell division at prophase (Pro I arrest) while they continue to grow until substances and structures indispensable for early embryonic development are fully accumulated. This process is aided by the hormonally cooperative actions of gonadotropins and the follicle cells that are in intimate contact with the oocyte. In most animal species the oocyte in the preovulatory follicle is arrested at metaphase of the first or second meiotic division, and meiosis is completed upon fertilization followed by initiation of embryonic mitotic divisions.

G. Banfalvi (ed.), *Cell Cycle Synchronization*, Methods in Molecular Biology 761,
DOI 10.1007/978-1-61779-182-6_7, 

In non-mammalian vertebrates, meiosis of fully grown oocytes remains arrested at the germinal vesicle (GV) stage until the oocytes acquire the ability to respond to maturation-inducing hormone (MIS) secreted by mature follicle cells. When expression of maturation-promoting factor (MPF) (1) is induced in the ooplasm upon stimulation by MIS, fully grown fish oocytes begin to undergo cytoplasmic maturation. In response to MIS, the fully grown oocytes, which have a supply of inactive MPF (a complex of p32cdc2 and cyclin B), form active MPF through the *de novo* synthesis of cyclin B and then resume meiosis (germinal vesicle breakdown, GVBD) (**Fig. 7.1**) (2). Thus, meiosis is released from Pro I arrest and then proceeds to metaphase of the second meiotic division (Meta II) (Pro I–Meta II transition), at which time meiosis stops again (Meta II arrest). During the period from GVBD to Meta II arrest, maturing preovulatory oocytes acquire fertilizability (the ability to respond to sperm penetration), and a cytostatic factor (Mos protein kinase) (3–5) is *de novo* synthesized from dormant maternal mRNA stored in the ooplasm. Meta II-arrested vertebrate oocytes are ovulated as eggs and complete meiosis with extrusion of the second polar 2 body upon sperm penetration. Resumption of meiosis in the oocyte involves the activation of MPF, inactivation of which is associated with degradation of cyclin B upon fertilization. Proteasomes participate in degradation of cyclin B, the decrease in MPF activity and completion of the first meiotic division (polar body extrusion) in goldfish (6) and rat (7) oocytes. Thus, upon fertilization, eggs shift their cell cycle from the meiotic to the mitotic pattern for

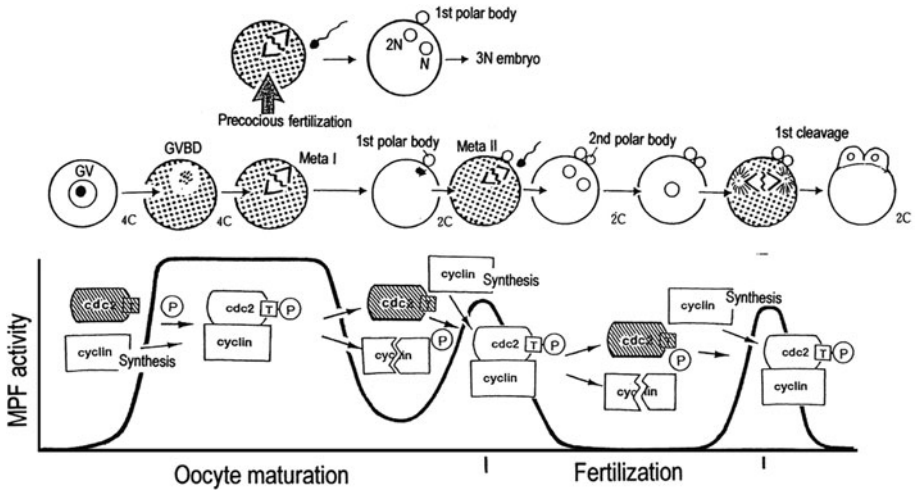


Fig. 7.1. Profile of maturation-promoting factor (MPF) activity in early *Oryzias* development. Maturation-inducing hormone (MIS) releases oocytes from the first arrest allowing them to proceed through the two consecutive meiotic cell divisions without DNA replication. An increase in MPF activity is required for entry into the meiotic metaphases (Meta I and Meta II). The mature oocytes (eggs) arrest again at the second meiotic metaphase (Meta II) until fertilization. Upon fertilization or precocious fertilization, the egg shifts from meiotic cell division to mitotic cell division. Reproduced in part with permission from Springer Science+Business Media, LLC (140).

embryogenesis. At the G2/M transition, MPF induces mitosis by phosphorylation of a variety of structural and regulatory proteins that control mitotic processes such as chromosome condensation, spindle assembly, and nuclear envelope breakdown (8).

It has been generally believed that at the final step of fertilization, chromosomes of the zygote nucleus are formed around the time of karyogamy. Two types of karyogamy occur in the process of fertilization in different species (9): the male and the female pronuclei associate in the central region of the egg cytoplasm with or without pronuclear membrane fusion. In fish eggs, which have discoidal cleavage, chromosome formation begins within the fused zygote nucleus in the period from the termination of DNA replication to the pronuclear karyogamy. The condensed chromatins are first visible by electron microscopy at the early stage of pronuclear membrane fusion (10). Although most of the investigations mentioned here concern fish oocytes or eggs, some exciting new data on chromosome formation during fertilization in other organisms will be described. We expect readers to find pivotal questions for understanding the mechanisms of chromosome formation during fertilization.

To elucidate the factors involved in cytoplasmic control of chromosome formation during early development of the fish, we have examined chromosomal behavior at various developmental and experimental conditions by applying the following materials and methods.

### *1.2. Chromosome Behavior in the Precocious Fertilization of Preovulatory Oocytes*

Non-activated oocytes penetrated by a spermatozoon contain two metaphase chromosome arrays within 20 min post-insemination. In mammalian oocytes, the cytoplasm develops the ability to transform the highly condensed chromatin of the sperm into metaphase chromosomes (11). Similar observations on the transformation of sperm nuclei into metaphase chromosomes in non-activated immature oocytes have been reported previously for *Urechis* (12), an amphibian (13, 14), and mammals (mouse) (15, 16). Early experiments in amphibians in which the nucleus was transplanted into non-activated oocytes with MPF and CSF activity also revealed that the nuclei were transformed to metaphase chromosomes (17–19). Based on these findings, Masui et al. (20) proposed that the ooplasmic activity that promotes condensation of metaphase chromosomes could be sustained only at low levels of intracellular $Ca^{2+}$. According to data obtained in a cell-free system from the amphibian oocyte, the levels of free $Ca^{2+}$ may play an important role in controlling nuclear behavior (21). We also verified the role of intracellular $Ca^{2+}$ in chromosomal condensation in *Oryzias* oocytes. Oocyte activation, probably dependent on the loss of MPF activity caused by an increase in the intracellular $Ca^{2+}$ concentration and pH, is indispensable for the transformation of gamete nuclei into pronuclei. Both an internal calcium increase and an internal pH rise are responsible for meiosis reinitiation from prophase I (*see* (9)).

In vertebrate oocytes, MPF activity appears as a result of mixing the nucleoplasm with the cytoplasm after GVBD, and it diffuses throughout the ooplasm based on observations that chromosomal formation from incorporated sperm nuclei could be observed during the period after GVBD but not before or at the time of GVBD. This is different from the situation of marine invertebrates such as the brittle star (22), the starfish, the oyster, and the surf clam (138, 139), in which maturing oocytes may have the ability to form female meiotic chromosomes only within the restricted cytoplasm containing the GV materials but not form male chromosomes from the incorporated sperm nucleus. The requirement for GV material for chromosomal formation has been demonstrated experimentally in previous studies on fish oocytes (23, 24) in which no chromosomes from the penetrated sperm nucleus could be found in blastomeres formed from inseminated oocytes that had been matured without GVBD. A similar finding, that the development of chromosomal condensation activity depends upon the release of some component(s) from the GV, has been reported by Ziegler and Masui (18) for amphibian oocytes.

During fertilization processes, dynamic responses take place in nuclei of both the egg and the spermatozoon: the resumption of meiosis, breakdown of the poreless nuclear envelope (25, 26), reduction of disulfide bonds in protamines (27, 28), decondensation of chromatin, replacement of protamines by histones (29–34), reformation of the nuclear envelope (25), DNA replication (35–39), and chromosome formation (40). In mitosis, the formation and behavior of chromosomes involve consecutive changes such as cohesion, condensation, and separation of chromosomes following DNA replication.

### *1.3. DNA Synthesis in the Period from Sperm Penetration to Karyogamy*

In fish eggs, chromatin decondensation and transformation of the penetrated sperm nucleus to the pronucleus take place in cytoplasm lacking MPF activity between 3 and 30 min postinsemination. The sperm nucleus undergoes breakdown of the nuclear envelope and transforms to a large male pronucleus by reformation of the nuclear envelope under these cytoplasmic conditions. Judging from the results of experiments (41) with inhibitors, DNA synthesis, transcription, protein synthesis, and phosphorylation-sensitive 6-DMAP may not be required for nuclear behavior in fertilization processes from sperm penetration to karyogamy.

When fertilized during maturation, oocytes of the starfish initiate the first DNA replication shortly after the end of meiosis (42). Why the penetrated sperm nucleus neither transforms into the male pronucleus (or meiotic chromosomes in harmony with the oocyte nucleus) nor initiates DNA replication until meiosis finishes in the oyster and the starfish is not known at present.

Starfish oocytes that are naturally fertilizable at any stage of meiosis are endowed with a built-in stability of the cell cycle driving mechanism that can be looked upon as a substitute for the metaphase arrest observed in most vertebrate eggs (128).

In zygotes of many animals, DNA synthesis occurs simultaneously in both female and male pronuclei as they migrate toward each other after fertilization and before pronuclear fusion (43–45). The timing of DNA replication in mammals has been determined by measuring the incorporation of $^{3}$H-thymidine or 5-bromodeoxyuridine (BrdU) into pronuclei. It is 7–11 h post-fertilization (pf) (46) or 8–13 h pf (35) in the mouse, 5–6.5 h pf (47) in the golden hamster, and 3–5 h pf (44) or 3–6 h pf (48) in the rabbit. In the sea urchin *Arbacia*, DNA synthesis normally follows pronuclear fusion and occurs in the zygote nucleus about 16 min post-insemination at 20°C (49). Increases in both the intracellular $Ca^{2+}$ concentration and the pH appear to be required for the initiation of DNA synthesis in sea urchin eggs (50). These increases synchronize with the decline in MPF (histone H1 kinase) activity and act as regulatory signals for cell cycle control and stimulation of DNA replication (51). In normal mitotic cell cycles, MPF is held in its inactive form by tyrosine phosphorylation of its p34cdc2 subunit until DNA replication is completed (52–54). In this connection, calyculin A induces an increase in MPF activity and chromosome condensation (55) and specifically inhibits the protein phosphatases (pp1 and pp2) that are involved in the initiation of DNA replication in *Xenopus* egg extracts (56).

In unfertilized *Oryzias* eggs with an adequate amount of fluorescent-labeled BrdU microinjected into the cortical cytoplasm in advance of fertilization, the earliest BrdU fluorescence is detected in developing pronuclei of eggs 15 min post-insemination (57). The synchronized DNA synthesis of the migrating female and male pronuclei is observed in eggs that were microinjected with BrdU 25 min post-insemination, as previously reported for the hamster egg (36). However, eggs no longer show labeled pronuclei when injected with BrdU after 30 min post-insemination. If fertilized eggs with BrdU microinjected into the cytoplasm are incubated in 10 μg/ml aphidicolin saline at 27°C, no incorporation of BrdU into the pronuclei is observed at the end of a 30-min incubation. These results reveal that DNA synthesis occurs during a period between 15 and 30 min post-insemination in *Oryzias* eggs.

### *1.4. Chromosome Formation in the Period from Sperm Penetration to Karyogamy*

In fertilized eggs, the changes in the sperm nucleus occur synchronously with the progression of meiotic division from Meta II to interphase in the egg nucleus, being perhaps controlled by cytoplasmic factors such as MPF and MAP (microtubule-associated protein) kinase activities (58–61). The interaction of

increased intracellular $Ca^{2+}$ with ooplasmic components upon fertilization brings about a loss of the MPF activity which in turn induces the formation of metaphase chromosomes (21). The data obtained with fish eggs also confirm the important roles of MPF activity in regulating nuclear envelope disassembly, chromosome condensation, and spindle formation for the first cleavage (41).

During the fertilization processes in an *Oryzias* hybrid between *O. latipes* and *O. javanicus*, chromosome condensation occurs more slowly in the *O. javanicus* male pronucleus than in the female *O. latipes* pronucleus in the cytoplasm of *O. latipes* eggs (62). This time lag leads to the preferential elimination of *O. javanicus* chromosomes in the hybrid cells (63). This may infer that the hybrid zygotes lack some cytoplasmic factors involved in DNA replication or chromosome condensation and needed to form the individual sister chromatids of *O. javanicus* in the ooplasm of *O. latipes*. The resulting probably aberrant *O. javanicus* chromosomes would be lost from blastomeres during cleavage because they missed the proper timing of normal chromosome formation. Similarly, human sperm chromosomal regions replicate later than the female regions in the golden hamster egg (38). According to the results of genetic and cytoplasmic approaches in *Drosophila*, the correct timing of DNA replication may be essential for the assembly of chromatin that is fully competent to undergo chromosome condensation in mitosis (64).

### 1.5. Effects of Inhibitors on Chromosomal Behavior in the Zygote

For the faithful segregation of chromosomes with their pivotal genetic informations, metaphase chromosomes consisting of two separable sister chromatids are formed during or soon after chromosome duplication. At the onset of the metaphase to anaphase transition, the cohesion between the condensed sister chromatids is dissolved, thereby allowing the chromosomes to be pulled apart toward opposite poles of the blastodisc by the spindle microtubules. Specific inhibitors of various enzymes that participate in chromosome formation are used to examine the behavior of chromosomes during cell division, since the behavior of chromosomes must reflect their structural features. The relationship between the changes in gamete nuclei and MPF activity has been analyzed using inhibitors of DNA synthesis and chromosome segregation during fertilization.

#### 1.5.1. DNA Polymerase α Inhibitor, Aphidicolin

Eukaryotic DNA polymerase α that is located in the GV of fully grown oocytes of the toad (65), the frog (66–68), the sea urchin (69), and the starfish (70, 71) shifts to the endoplasmic reticulum or granules in the cytoplasm when the GV breaks down (65, 72). Aphidicolin is a specific inhibitor of DNA polymerase α and is known to inhibit replicative DNA synthesis, namely DNA replication but not RNA and protein (73–76). In aphidicolin-treated

starfish *Asterina pectinifera* zygotes (77), the mitotic spindle (mitotic apparatus) develops and grows, but although the chromatin mass is free of the nuclear envelope, it does not associate with the mitotic apparatus and remains as a linear rod-like chromatin structure near the first cleavage furrow. In the advanced stages of cleavage in aphidicolin-treated embryos, observations by electron microscopy show that the nuclear envelope is not reformed after Meta I, and the chromatin mass is dispersed in the cytoplasm, indicating that aphidicolin causes achromosomal cleavage in fertilized starfish eggs (78, 79). In the presence of aphidicolin, the cell cycle of the egg cytoplasm progresses independently of the DNA synthesis blockade and the formation of abnormal chromosomes, so that the subsequent cleavages give rise to achromosomal blastomeres. This abnormality of chromosome separation reflects the formation of incomplete chromosomes which is induced by aphidicolin treatment only during the limited period of the restricted pronuclear migration (about 10 min) from the end of DNA synthesis to the encounter of the pronuclei. Aphidicolin seems to interfere with reformation of the nuclear envelope, the resolution of intramolecular DNA folding, and the organization of kinetochores (80, 81), subsequent to the inhibition of DNA synthesis.

Aphidicolin prevents chromosomal DNA replication but does not prevent meiotic maturation divisions in oocytes of the starfish (82). During fertilization of fish eggs, the morphological processes of the second meiotic division also occur normally in the presence of aphidicolin. On the other hand, in non-activated, fertilized eggs with high histone H1 kinase and MAP kinase activities, the compact nucleus (haploid) of a penetrated spermatozoon is also directly transformed to the same meiotic metaphase chromosomes (Meta III) as female meiotic Meta II in the presence of aphidicolin. The male chromosomes that are formed without formation of a male pronucleus and without DNA synthesis are normally segregated into two anaphase chromosomal masses, when the egg is artificially activated (57). Thus the difference between meiotic and mitotic chromosomes that are formed under conditions preventing DNA synthesis is whether or not the chromosomes are separable in the cell division. This difference infers at least a possibility that aphidicolin may intervene in the short process (only about 10 min) of forming separable chromosomes while DNA synthesis is inhibited in mitosis, unlike the simple pairing of homologous chromosomes in meiosis.

As already found in simian virus 40, complete separation of parental DNA strands is not observed when the polymerization reaction is inhibited by aphidicolin, which induces supercoiling in replicative intermediate DNA (83). From the results obtained using novobiocin and aphidicolin, Droge et al. (83) conclude that DNA synthesis and strand separation are closely linked.

### 1.5.2. DNA Topoisomerase Inhibitors

In fish eggs, the effects of camptothecin (inhibitor of DNA topoisomerase I (topo I)) (84–86), etoposide, and β-lapachone (inhibitors of DNA topoisomerase II (topo II)) on formation of individual sister chromosomes were examined (87). Results of these experiments revealed that only camptothecin-treated eggs displayed an aberrant segregation of chromosomes in the first cleavage, as seen in aphidicolin-treated eggs. A similar effect has been obtained in fertilized starfish eggs exposed to a different topo I inhibitor, kalihinol F, that does not inhibit topo II and chromosomal DNA synthesis (87). In the starfish, inseparable metaphase chromosomes are formed at the first cleavage, when fertilized eggs are exposed to kalihinol F during the second meiotic period for about 20 min after the extrusion of the first polar body and formation of the female pronucleus. This period precedes chromosomal DNA synthesis and pronuclear fusion (43–47). These results indicate that topo I inhibition cannot affect the formation process of meiotic sister chromosomes in non-activated fish eggs (57), suggesting that the enzyme topo I has a pivotal function in the formation of mitotic chromosomes in starfish and fish embryos.

What step in chromosome formation could be affected by topo I inhibitor? So far the mechanism of action of topo I inhibitors in formation of inseparable sister chromatids remains unknown. Camptothecin inhibits the relaxation of supercoiled DNA induced by topo I (88) during DNA synthesis in HeLa cells by more than 80% (89) as well as the DNA rejoining step catalyzed by eukaryotic topo I (84, 85). A possible function of topo I in DNA replication is also suggested by its swivel-like enzymatic activity (90). The abnormality of metaphase chromosomes may be related to (i) the formation of a camptothecin-induced cleavage complex or (ii) the specific interference by camptothecin in the swivel mechanism of topo I, which possibly leads to the inhibition of both DNA and RNA syntheses (89, 91). Topo I activity is also required for proper chromosomal segregation in a prokaryote *Escherichia coli* (92, 93). Further experiments examining the function of topo I on formation and segregation of chromosomes will help to elucidate the mechanism of formation of chromosomes capable of normal segregation in cell division.

Although a topo II inhibitor had no inhibitory effects on the formation of individual meiotic or mitotic chromosomes in fertilized fish eggs, there have been extensive investigations on the participation of topo II in successful sister chromosome segregation in meiosis and mitosis of the yeast (94–97), *Drosophila* (98), surf clam (99), frog eggs (100, 101), mouse oocytes (102–106), Chinese hamster eggs (107), and kangaroo rat eggs (108). Intertwined both positively and negatively supercoiled DNA can be relaxed by topo II which transiently breaks and rejoins double-stranded DNA in the presence of ATP (109–113). Topo II is required in the mitotic cell division cycle for untangling

intertwined sister chromosomes following the completion of DNA synthesis (114–117). According to the two-step scaffolding model (118), topo II α is initially required for the decatenation of DNA fibers to generate individual chromosomes and then condensin complexes transform the prophase chromosomes into mature mitotic forms. In chromosomal formation, the structural maintenance of chromosome (SMC) protein complexes, condensins and cohesins, plays central roles in chromosome condensation and sister chromatid cohesion, respectively. Recently, aberrant segregation has been considered to result from incomplete formation of mitotic chromosomes from newly replicated DNA in the absence of the activity of key components such as DNA topoisomerases and condensin (119).

Although a tremendous number of genetic and biochemical investigations have been carried out during the last 30 years (120–122), the mechanism of chromosomal formation during the fertilization processes remains to be unraveled. There is also little information on how the architecture of mitotic chromosomes might be organized following DNA replication in pronuclei during the fertilization processes. During the fertilization of the surf clam, the female and male nuclei behave differently within the same ooplasmic conditions. The oocyte nucleus undergoes consecutive meiotic divisions independent of the behavior of the sperm nucleus. More biochemical information on the existence of a presumptive regulatory factor (9) or cytoplasmic compartment in the oocyte should also provide a deeper insight into the intracellular mechanism of chromosomal formation during fertilization. In particular, elucidation of the loss or non-disjunction of chromosomes in interspecific hybrid zygotes could solve a crucial question on the specific molecular mechanism for formation of complete individual chromosomes; however, we are still too early in the research to answer this mysterious question. Further investigations using gene targeting methodology to clarify chromosome formation have made it possible to test which key components are required for the processes of fertilization including the steps from DNA replication to chromosome formation in embryogenesis.

## 2. Materials

### *2.1. Reagents*

1. Alkaline phosphatase-conjugated goat anti-mouse immunoglobulin G (Tago, Burlingame, CA, USA)
2. Alkaline phosphatase-conjugated rabbit anti-mouse immunoglobulin G (Amersham, Little Chalfont, Buckinghamshire, UK)
3. Aphidicolin (Wakojunyaku-kogyo, Osaka, Japan)

4. [$\gamma$-$^{32}$P]-ATP (NEN Research Products, Boston, MA, USA)
5. Biotinylated anti-mouse sheep IgG (Amersham)
6. Chloretone (acetone chloroform; Nakarai Chemicals, Kyoto)
7. FITC-conjugated goat antibody against mouse IgG (Amersham)
8. FITC-conjugated streptavidin (Amersham)
9. Hoechst 33258 (Hoechst AG, Melbourne, VIC, Australia)
10. Monoclonal antibody against α-tubulin YL1/2 (Sera Laboratory, Crawley Down, Sussex, England)
11. Monoclonal antibody against BrdU (Becton Dickinson Immunocytometry Systems, CA, USA)
12. Monoclonal mouse antibody against single-stranded DNA (Chemicon International, El Segundo, CA, USA)
13. MS222 (meta-aminobenzoic acid ethyl ester methane sulfonate; Sandoz Ltd., Switzerland)
14. Polyvinylidene difluoride membrane (Immobilon; Millipore, Bedford, MA, USA)
15. RX-H X-ray film (Fuji, Tokyo, Japan)
16. All other chemicals are commercial chemical substances and personal gifts

### 2.2. Gametes

1. Mature medaka fish *Oryzias latipes* (Local fish farmer, Yamato-kouriyama, Nara Prefecture, Japan). Keep fish under artificial reproductive conditions (26–28°C, 14 h illumination) for at least 2 weeks before use.
2. Isolate oocytes into saline (123) from ovaries of females that had spawned every day. Under these reproductive conditions, oocytes are at the GVBD stage 5–6 h before the onset of light (124).
3. Prepare sperm suspension (2–3 × $10^7$ cells/ml) for insemination by removing testes from mature males and releasing spermatozoa into saline or a test solution contained in a depression glass slide.

## 3. Methods

### 3.1. Experimental Procedures in Oocytes

1. Transfer female fish that had spawned every day into a dark, cold (water temperature, 10°C) chamber 10 h before the onset of light.

2. Return them 10 h later to an aquarium at 27°C (R27).
3. Fix aliquots of oocytes obtained from the ovaries at various times after R27 immediately with 2% glutaraldehyde–1.5% paraformaldehyde (0.1 M phosphate buffer, pH 7.4) for cytological observation.
4. Inseminate the remaining oocytes at given time intervals after R27.
5. Calculate the rates of egg activation and sperm penetration on the basis of the numbers of activated oocytes and the percentage of oocytes with sperm nucleus in the cortical cytoplasm at the end of 30 min immersion in sperm suspension.

### 3.2. Treatment of Eggs with Drugs

1. Pretreat unfertilized eggs with 10 μg/ml actinomycin D (RNA synthesis inhibitor), 10 μg/ml aphidicolin (inhibitor of DNA polymerase α), 25 μg/ml cycloheximide (protein synthesis inhibitor), or 5 mM 6-dimethyl-aminopurine (6-DMAP; protein phosphorylation inhibitor) for 30 min (27°C) prior to insemination, as mature eggs became overripe during the long treatment.
2. Just before each experiment, dilute stock solutions of 1 mg/ml actinomycin D and 10 mg/ml aphidicolin in dimethyl sulfoxide (DMSO) with saline. Dissolve the other drugs directly in saline just before each experiment.
3. Inseminate and incubate the pretreated eggs in saline containing each drug at the same concentration as during pretreatment (*see* **Note 1**). Present values as mean+SE μm.
4. Prepare a stock solution of each inhibitor (aphidicolin, camptothecin, etoposide, and β-lapachone) by dissolving it in DMSO.
5. For testing, dilute each stock solution in saline to yield a concentration of 10 μg/ml of inhibitor and 0.1% DMSO. This concentration of DMSO has no effect on the morphological events of fertilization, including formation of spindle and chromosomes for the first cleavage.
6. Preincubate eggs for 30 min at 27°C by immersion in the test solutions.
7. Inseminate the pretreated eggs by spermatozoa suspended in the same solution.
8. In another experiment, pretreat unfertilized eggs by immersing in saline containing 10 μg/ml of inhibitor and 0.25% anesthetic MS222 for 30 min and then inseminate by spermatozoa suspended in the same saline: 0.25% MS222 saline (10 ml) supplemented with 0.08 ml of 1 N NaOH and buffered to pH 7 with 10 mM HEPES buffer.

9. To ascertain the time during fertilization that eggs were sensitive to aphidicolin, expose eggs to 10 μg/ml aphidicolin saline for given times post-insemination at 27°C.

### 3.3. Cytological Assessment of Oocytes Before and After Activation

1. Examine the nuclear states of the oocytes by staining them with Hoechst 33258 dye (0.1–0.2 μg/ml of 50% glycerol) after gametes were fixed in 4% glutaraldehyde in 0.1 M phosphate buffer (pH 7) for at least 30 min at room temperature.
2. For examination of the cortical cytoplasm, use a pair of scalpels under a binocular dissecting microscope (×20) to isolate the cortex at the animal pole region from the yolk mass of fixed eggs in distilled water.
3. Mount the cortical cytoplasm with a small amount of distilled water on a clean glass slide (125).
4. Measure the distribution (diameter) of chromosomes and the diameter of interphase nuclei with nuclear envelopes by micrometer under a fluorescence microscope (Olympus BH-2, ×400).
5. To prepare cells for observation of chromosomes, place morulae in a depression glass slide coated with Sigmacoat and containing L15 culture medium with 0.4% bovine serum albumin and 0.0003% colchicine.
6. Cut the chorions deeply at the vegetal pole region with a pair of scalpels, and separate cells by carefully vibrating the chorions with forceps before the cells are pushed out of the opening cut in each chorion.
7. After removal of empty chorions, incubate the cell suspension for 60–90 min at 27°C.
8. Wash cells five times for 15–20 min at room temperature in 3 ml of 0.7% Na-citrate.
9. Collect swollen cells in a small pipette.
10. Mount the cell suspension on a cold Carnoy's fixative and spread cells by gently blowing on the slide.
11. Then dry the slide immediately over a flame on alcohol lamp.
12. After the slide is completely dried, stain the chromosomes with Hoechst dye and observe under fluorescent microscope.
13. For examination of the aster and spindle, fix eggs in 0.25% glutaraldehyde, 4% paraformaldehyde, 3% Triton X-100, 3 μM taxol, 5 mM ethyleneglycol-bis-(β-aminoethylether)-*N*,*N*,*N*′,*N*′-tetraacetic acid (EGTA), 1 mM $MgCl_2$, 80 mM piperazine-*N*,*N*′-bis[2-ethanesulfonic acid]

(PIPES), pH 6.8 (MTSB), for 6 h at room temperature and store in methanol (–20°C) for approximately 12 h.

14. Rinse the fixed eggs in PBS (136 mM NaCl, 2.5 mM KCl, 8 mM $Na_2HPO_4$, 1.5 mM $KH_2PO_4$, pH 7.4).
15. Stain their microtubules immunologically by incubating the eggs in PBS containing 0.1% Tween-20, a monoclonal antibody against α-tubulin YL1/2 (1:100), and a fluorescein isothiocyanate (FITC)-conjugated goat antibody against mouse IgG for 12 h at 4°C.
16. Following five rinses in PBS for 5 min each, incubate the eggs in PBS containing 50% glycerol and 0.1 μg/ml Hoechst 33582 for 20 min at room temperature.
17. Isolate the slightly thickened cortex of the animal pole region from the spherical yolk mass of the eggs by dissecting with a pair of scalpels.
18. Mount samples on a clean glass slide and cover with a coverslip.
19. Observe the samples by fluorescence microscopy.

### 3.4. Anesthetization of Eggs

1. In order to anesthetize mature eggs, dissolve 5 mM chloretone or 0.25% MS222 in saline.
2. Adjust the 5 mM chloretone saline to pH 4.4 with 50 mM acetate buffer and supplement 10 ml of 0.25% MS222 saline with 0.1 ml of 1 N NaOH buffered to pH 7 with 20 mM HEPES–Na HEPES buffer.
3. Pretreat unfertilized eggs with anesthetic saline for 30 min (27°C) and then inseminate for 1 min with spermatozoa ($2 \times 10^7$ spermatozoa/ml) suspended in anesthetic saline.
4. Rinse eggs for 4 min in anesthetic saline.
5. Incubate eggs in regular saline or saline containing a test drug.

### 3.5. Microinjection into the Egg

1. For microinjection into the egg, treat spermatozoa with 0.001% dodecylsulfate saline to damage the plasma membrane by sucking repeatedly in a small pore pipette for about 3 min on ice and rinse three times in saline by centrifugation (1,000×*g*, 5 min).
2. Rinse unfertilized eggs three times in calcium- and magnesium-free (CMF) saline (128.3 mM NaCl, 27 mM KCl, 6.0 mM $NaHCO_3$, 0.2 mM EDTA, 4 mM HEPES-NaOH, pH 7).
3. Microinject about 1 nl of aequorin solution into the cortical cytoplasm by pressure (126).

4. Prepare aequorin solution by mixing 0.64% recombinant hcp-aequorin solution containing 50 mM KCl, 0.1 mM EDTA, and 10 mM MOPS, pH 7.3 (gift of Dr. O. Shimomura), with 1/4–1/5 vol of 20 mM $MgCl_2$ solution to remove free EDTA from the solution just before use.
5. Place the microinjected eggs in Mg-free physiological saline containing 0.2 mM $CaCl_2$ for 1 h to allow the injected aequorin to diffuse uniformly throughout the cortical cytoplasm.
6. Keep eggs in CMF saline in complete darkness.
7. In order to induce $Ca^{2+}$ release and exocytosis (CABD) in the aequorin-loaded cytoplasm of unfertilized eggs, microinject about 0.3 nl of 0.5 mM $CaCl_2$ into the cortical cytoplasm at the animal pole of an egg held in CMF saline. Observe the easily visible CABD carefully as the disappearance of the cortical alveoli in translucent eggs with a binocular dissecting microscope.

### 3.6. DNA Synthesis

Measure the initiation time of DNA synthesis by detecting the fluorescently labeled nucleus of fertilized eggs from the time of sperm penetration.

1. In this experiment, microinject approximately 60 nl of saline containing 10 mM 5-bromo-2′-deoxyuridine (BrdU) into the cortical cytoplasm at the animal pole region, as soon as exocytosis of cortical alveoli starts upon insemination.
2. Then fix eggs with 4% paraformaldehyde, 10% methanol, and 100 mM phosphate buffer, pH 7.0 (PMP fixative), for 6 h at room temperature.
3. To determine the duration of DNA synthesis, also microinject approximately 60 nl of 10 mM BrdU into the cortical cytoplasm at the animal pole region of dechorionated eggs, 20, 25, 30, and 40 min post-insemination. DNA synthesis is the period from sperm penetration to karyogamy.
4. Prepare dechorionated eggs according to a simplified procedure (127), by cutting off the chorion at the vegetal pole side with small scissors during exocytosis upon insemination.
5. Then, transfer BrdU-injected eggs into PMP fixative at the stage of karyogamy for 40 min post-insemination and fix for 6 h at room temperature.
6. Stain the BrdU-injected eggs with an anti-BrdU monoclonal mouse antibody.
7. Then counterstain the entire DNA with 0.1 μg/ml Hoechst 33582 (128).

8. After rinsing away the fixative, dissect out the cortical cytoplasms at the animal pole region from the egg yolk mass.
9. Subsequently incubate in a few drops of 4 N HCl for 2 h in a moist chamber to denature the DNA.
10. Following acid denaturation, rinse the slides three times with PBS.
11. Successively incubate the cortical cytoplasms on the slide in the moist chamber at 25–27°C with the reagents listed below:
    (a) monoclonal mouse antibody against BrdU (1:6 in PBS) for 2 h,
    (b) biotinylated anti-mouse sheep IgG (1:50) for 1 h,
    (c) FITC-conjugated streptavidin (1:100) for 30 min,
    (d) monoclonal mouse antibody against single-stranded DNA (1:10) for 1 h,
    (e) Hoechst 33582 containing 50% glycerol for 20 min at room temperature.
12. Rinse each incubation three times with PBS.

### 3.7. P13suc1 Precipitation

1. Rinse 30 eggs quickly three times in cold (0–4°C) extraction buffer (100 mM β-sodium glycerophosphate, 40 mM Mes, pH 6.8, 30 mM EGTA, 65 mM $MgCl_2$, 3 μg/ml leupeptin, 100 μM phenylmethylsulfonyl fluoride (PMSF), and 1 mM DTT) in an Eppendorf tube (*see* **Note 2**).
2. Then add 60 μl of fresh extraction buffer.
3. Homogenize samples for 5 s (0–4°C) and immediately place in liquid nitrogen.
4. Thaw samples and centrifuge at 15,000×*g* for 15 min at 4°C.
5. Supplement 60 μl of each supernatant with 6 μl of 1 M HEPES (pH 7.5) and mix with 10 μl of a 50% (v/v) suspension of p13suc1 beads, equilibrated previously with extraction buffer.
6. Following incubation overnight at 4°C, wash the beads three times in cold washing buffer (modified extraction buffer supplemented with 0.2% Tween-20, 100 mM HEPES, pH 7.5), with an exchange of Eppendorf tube at the second wash.
7. Boil the washed beads for 3 min.
8. Analyze the beads by polyacrylamide gel electrophoresis (PAGE) in the presence of SDS (SDS-PAGE 12.5% gel) (129).
9. Following electrophoresis immunoblot with anti-cyclin B antibody, anti-cdc2 antibody, or anti-cdk antibody (130).

### 3.8. Histone H1 Kinase and MBP Kinase Assay

Histone H1 kinase assays were performed according to a modified procedure described elsewhere (131) and detailed below:

1. To detect histone kinase activity, transfer each group of 20 eggs into an Eppendorf tube.
2. Wash eggs rapidly three times within 10 s in an excess of extraction buffer (100 mM β-glycerophosphate, 40 mM Mes–Mes Na, 65 mM $MgCl_2$, 30 mM EGTA, 100 μM PMSF, 3 μg/ml leupeptin, and 1 mM DDT at 0–4°C) in the Eppendorf tube (132).
3. Place eggs in 50 μl of extraction buffer (two eggs in 5 μl), homogenate for 5 s (0–4°C), and freeze immediately in liquid nitrogen.
4. Immediately after thawing, spin down 10 μl of sample at 15,000×*g* for 15 min at 4°C.
5. Mix sample with 40 μl of a reaction medium containing 1.25 μM [γ-$^{32}$P]-ATP (1.36 mCi/μmol), 5.6 mM 2-mercaptoethanol, 25 mM Tris–HCl, pH 7.4, 5.6 mM adenosine triphosphate (ATP), 0.6 μM cAMP-dependent protein kinase inhibitor, 0.1 mM histone type III-S or 2 mg/ml lysine-rich histone H1, and 1.5 μCi/50 μl [γ-$^{32}$P]-ATP.
6. After various incubation times at 30°C, stop the kinase reaction by the addition of 5 μl of 3 M phosphoric acid.
7. Absorb aliquots of samples onto P81 phosphocellulose paper (Whatman).
8. After extensive washing with 0.1 M phosphoric acid, measure the radioactivity remaining on the paper by liquid scintillation counting.
9. Measure MAP kinase activity by incubation of a final volume of 40 μl with 40 μg of myelin basic protein (MBP), 50 μM [γ-$^{32}$P]-ATP (2.5 mCi/μmol), and 5 μM protein kinase A inhibitor peptide for 15 min at room temperature.
10. Boil an aliquot of samples for 3 min, then separate the proteins by SDS-PAGE.
11. Visualize phosphorylation of histone H1 by autoradiography, which is performed on dried gels with RX-H X-ray film.

### 3.9. Immunoblotting

1. Analyze samples of 30 eggs in each group. Following SDS/PAGE (12.5% separation gel) after precipitation with p13suc1 beads and electrotransfer to Immobilon, rinse the blots in 150 mM NaCl and 20 mM Tris–HCl (pH 7.5) and block for 1 h with 5% non-fat dry milk dissolved in TTBS (150 mM NaCl, 0.1% Tween-20, 0.01% $NaN_3$, and 20 mM Tris–HCl, pH 7.5).

2. After rinsing in TTBS for 10 min, incubate the membranes with an anti-cyclin B (1:1,000 dilution of *Xenopus* cyclin B1 antibody; X1-158) or a 1:1,000 cdk2 antibody(α-goldfish cdk 2C1-42) overnight at room temperature.
3. After three rinses in TTBS, incubate with 1:1,000 or 1:2,000 dilution of alkaline phosphatase-conjugated rabbit or goat anti-mouse immunoglobulin G (IgG) for 2 h.
4. Finally, wash three more times by treating the membranes with 0.2 mM 5-bromo-4-chloro-3-indolylphosphate *p*-toluidine salt and nitroblue tetrazolium in 100 mM Tris–HCl buffer (pH 9.8) containing 1.0 mM $MgCl_2$ for visualization of phosphatase activity (AP-kit; Bio-Rad, Tokyo, Japan).

### 3.10. Chromosome Formation in Meiosis

To understand the formation and segregation of chromosomes in meiosis and mitosis, a number of cytological approaches have been developed using fertilized oocytes in which chromosomal formation is inhibited by chemical agents. The meiotic cell cycle that produces haploid gametes consists of two consecutive divisions in the absence of DNA replication.

1. The fully grown oocytes of a teleost, *Oryzias latipes*, gradually enlarge with the progression of meiotic divisions from the germinal vesicle (GV) stage (meiotic prophase I) to Meta II (meiotic metaphase II) for about 7 h (27°C) after MIS stimulation.
2. Two hours before GV breakdown (GVBD), thread-like lamp-brush chromosomes are scattered throughout the nucleoplasm of the GV as illustrated in **Fig. 7.2** (*see* **Note 3**).
3. One hour later, the thread-like chromosomes condense to diminutive chromosomes that are shortened but remained *in situ* scattered within the GV. In oocytes just at the time of GVBD, divalent chromosomes aggregate at the central region of the GV. The aggregation of condensed chromosomes begins concurrently with nuclear envelope breakdown and the disappearance of the nucleoli.
4. One to two hours after GVBD, chromosomes at prometaphase (pro-Meta I) or metaphase (Meta I) of the first meiotic division are distributed on the spindle or arranged on the equatorial plate of the first meiotic spindle, respectively.
5. Most oocytes 3–4 h after GVBD are at Meta I or anaphase I (Ana I) of the first meiotic stage (*see* **Notes 4** and **5**).
6. About 5 h after GVBD, the oocytes ovulate. Following the extrusion of the first polar body, Meta II chromosomes of the egg align on the equatorial plate of the second meiotic apparatus, which occurs without intervening telophase and prophase stages (*see* **Notes 6** and **7**).

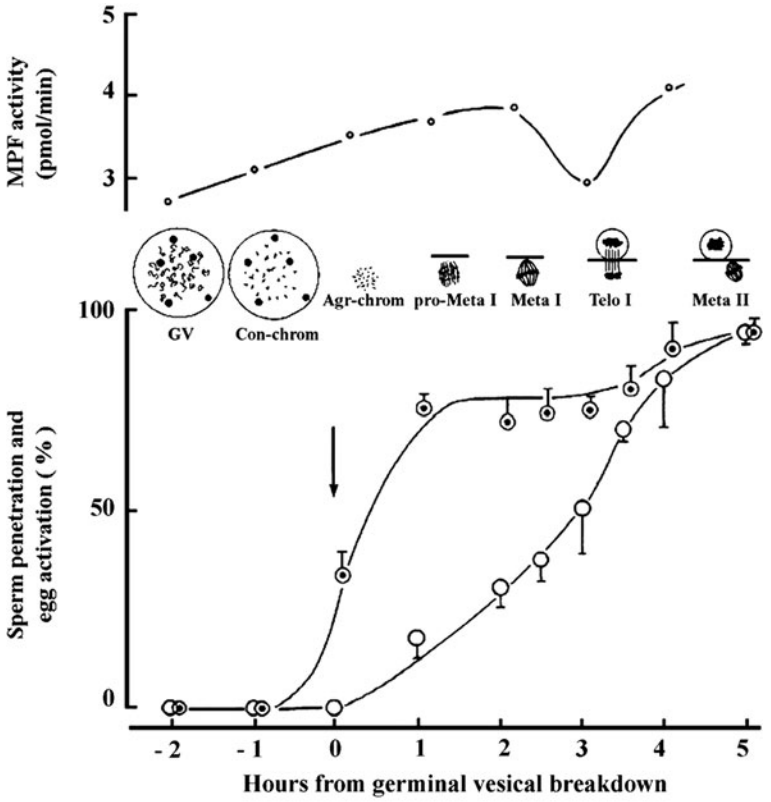


Fig. 7.2. Sperm penetration and oocyte response in the precocious fertilization of *Oryzias latipes*. The state of meiotic divisions from germinal vesicle (GV) breakdown (GVBD) to metaphase of the second meiotic division (Meta II), including condensation (con-chrom) and aggregation (agr-chrom) of chromosomes. Sperm penetration (*double circles*) is first seen at GVBD, and oocyte activation follows (*open circles*) 1 h later. This material is reproduced with permission from John Wiley & Sons, Inc. (141).

### *3.11. Susceptibility of Metaphase Chromosomes to Aphidicolin in Fertilized Eggs*

The treatment of fish eggs with aphidicolin that prevents both DNA replication and the cyclic change in MPF activity during fertilization also inhibits the formation of individual sister chromosomes that are normally separated into blastomeres at the time of the subsequent first cleavage (57).

1. To examine the time at which aphidicolin is effective in causing formation of aberrant chromosomes, treat unfertilized eggs with aphidicolin for 30 min (27°C).
2. Then inseminate in a sperm suspension containing aphidicolin (**Fig. 7.3**).
3. At the end of incubation with aphidicolin for a given time post-insemination, rinse fertilized eggs and further incubate in regular saline until 70 min post-insemination, the time of the first cleavage.

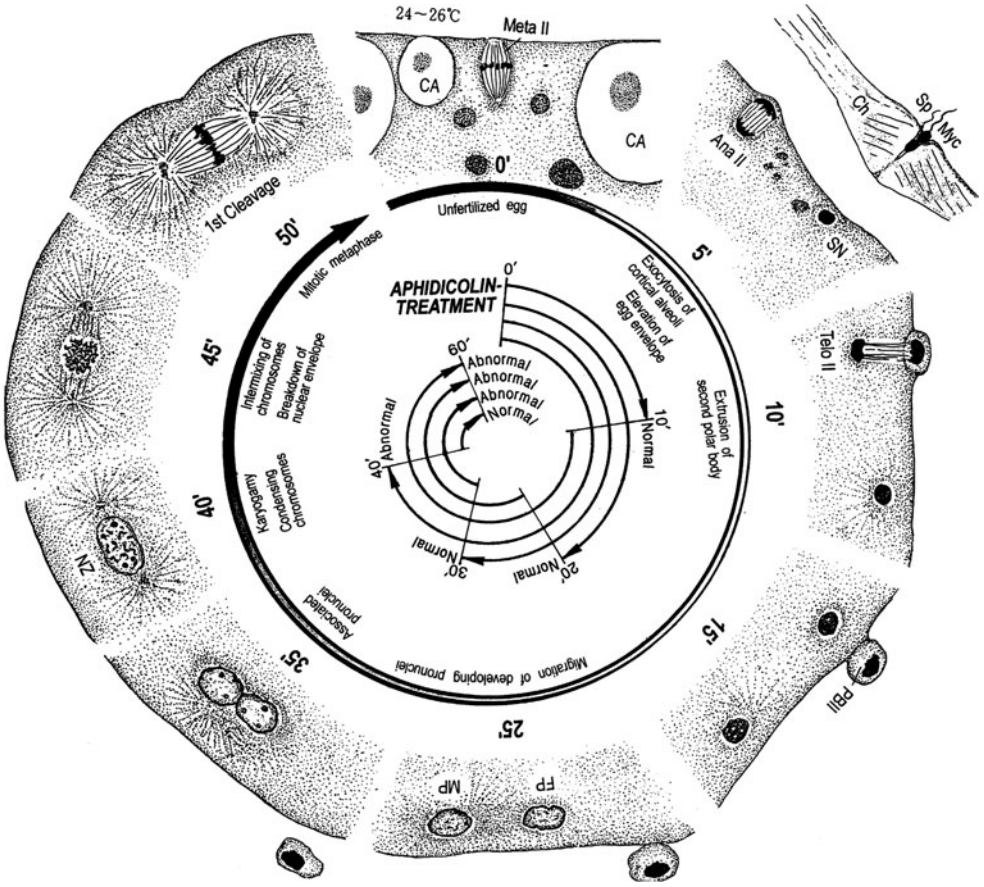


Fig. 7.3. Schematic illustration of nuclear behavior during fertilization of fish eggs. Numbers indicate the time (minutes) from insemination (0′) to the first cleavage (50′). The *large encircling arrow* indicates MPF activity (*shade of black*). In the central part of the illustration, the experimental procedure and the results of aphidicolin treatment are represented by the length of the *small arrows* indicating the time intervals of treatment. The effects of respective aphidicolin treatments are represented at the end of each arrow as "normal" or "abnormal" segregation of chromosomes (from (75); see text).

4. Transfer eggs from aphidicolin-containing saline to regular saline within 30 min post-insemination, to form normal interphase nuclei in each blastomere (*see* **Note 9**).
5. In another experiment, immerse dechorionated eggs into saline containing aphidicolin at given times post-insemination.
6. Transfer from regular saline to saline containing the inhibitor within 30 min post-insemination and incubate until 70 min post-insemination (*see* **Note 10**).

In the fertilization of the fish *Oryzias* (**Fig. 7.3**), the nucleus of the spermatozoon (Sp) penetrates into the egg cytoplasm beneath the micropyle (Myc) in the chorion (Ch) 5 s post-insemination, and then meiotic chromosomes following Ana II aggregate compactly as the second polar body is extruded in the perivitelline

space (Ps) 15 min post-insemination. Between 10 and 20 min post-insemination, the female pronucleus begins to migrate away from the second polar body toward the swollen male pronucleus. The female pronucleus encounters the male pronucleus at the center of the blastodisc about 35 min post-insemination. The female and male pronuclei containing several nucleolus-like bodies fuse at adjacent regions of their nuclear envelopes 40 min post-insemination. In the initial stage of nuclear fusion, chromatin condensation is not yet distinct. In the oval-shaped zygote nucleus of the most advanced stage, condensing chromatin masses are first detected throughout the nucleoplasm (10). Forty-three minutes post-insemination, the irregularly shaped zygote nucleus, which starts to shrink, still contains the condensed chromosomes and nucleolus-like bodies. Forty-five minutes post-insemination, the zygote nucleus has a highly convoluted and collapsed nuclear envelope but no nucleolus-like bodies. In eggs at a more advanced stage, metaphase chromosomes are arranged on the equatorial plate of the first cleavage, and the sister chromatids are disentangled and then pulled to opposite poles of the zygote. Cytokinesis occurs about 60 min post-insemination.

These results show that in fertilized eggs the normal formation of individual metaphase chromosomes was susceptible to disruption by aphidicolin in a critical period between 30 and 40 min post-insemination (**Fig. 7.3**). This is the limited period from the termination of DNA synthesis to the appearance of condensed chromatids in the zygote nucleus, corresponding to the period in which MPF has high activity to phosphorylate topo II α (80) or topo I. In the blastomeres of *Xenopus* embryos that are treated with aphidicolin, non-replicated chromatids are also frequently stretched out during the separation of chromatids at anaphase and telophase (81). Thus, the effect of aphidicolin on sister chromosome formation during fertilization does not seem to be species specific.

## 4. Notes

1. When ovarian intrafollicular oocytes of *O. latipes* are inseminated after mechanical removal of follicular cell layers including the micropylar cell, by use of a pair of fine forceps, the spermatozoon can penetrate into the egg cytoplasm through the opened micropyle. Morphology and behavior of nuclei did not change in the period from sperm penetration to karyogamy.

2. The concentrations of EGTA and $MgCl_2$ in the buffer were modified to inhibit egg activation, as medaka eggs contain calcium and magnesium at high concentrations, probably in the yolk mass.
3. If oocytes are penetrated by a spermatozoon before or at the stage of GVBD, they fail to activate. The penetrated sperm nucleus is only slightly swollen in the cytoplasm of the non-activated oocytes.
4. Upon sperm penetration 1 h after GVBD, most oocytes in pro-Meta I undergo no or only partial activation with restricted exocytosis of cortical alveoli at a restricted region of the animal hemisphere. In these oocytes normal pronuclei are not formed. The partial activation may be due to an incomplete increase in the intracellular $Ca^{2+}$ which partially inactivates MPF.
5. In contrast, Meta I oocytes normally undergo full activation upon insemination. Meiotic Meta II chromosomes and the incorporated sperm nucleus transform into a diploid female pronucleus and a haploid male pronucleus by decondensation of the sperm chromatin immediately after the extrusion of the first polar body. Therefore, the ability to undergo normal exocytosis of cortical alveoli is intimately related to the loss of MPF activity which allows the cytoplasm to form pronuclei (**Figs**. **7.1** and **7.2**).
6. The association of these abilities of the oocyte may be mediated by common cytoplasmic factors, such as intracellular $Ca^{2+}$, inositol 1,4,5-triphosphate ($IP_3$), pH, and/or the sensitivity of these oocytes. In mouse oocytes, the increase in intracellular calcium can differ depending on the stage of maturation, and the oocytes appear to develop an increased sensitivity to $IP_3$ during the course of maturation (133).
7. When a fertilizable fish oocyte is activated upon insemination, an incorporated sperm nucleus rapidly transforms into a pronucleus. A diploid female pronucleus (2n) is formed after the extrusion of the first polar body. The diploid female and the haploid male pronuclei undergo karyogamy to form a triploid zygote nucleus (134, 135, **Fig. 7.1**). In a study on the mouse (136), intrafollicular oocytes precociously fertilized before completion of Meta I also skip the second meiotic division and develop to polyploid embryos. Thus after Meta I, intrafollicular oocytes that have not completed the first meiotic division acquire the competence essential for the formation of female and male pronuclei or condensed chromosomes and can skip the second meiotic division upon activation by sperm penetration (135).

8. When inseminated at pro-Meta I or Meta I 2 h after GVBD, 25% of fish oocytes exhibit normal activation by sperm penetration, followed by the extrusion of the first polar body, formation of female and male pronuclei, and karyogamy within 60 min post-insemination (140).
9. Unlike oyster (137, 138) and the surf clam (139) oocytes, which do not allow the incorporated sperm nucleus to undergo pronucleus formation until completion of meiotic division, these preovulatory fish and mouse oocytes do not possess the negative regulatory system within the ooplasm to insure the completion of meiosis. Therefore, these vertebrate oocytes must be protected from extracellular factors until at least Meta II (the time of ovulation) by their follicular cell layers. The extracellular factors include sperm entry and mechanical stimulations that induce a rise in intracellular $Ca^{2+}$ and pH which would disturb the meiotic process. Thus the oocytes normally ovulate in a safe condition in which the final meiotic division is completed upon external stimulation.
10. During the transfer of eggs from aphidicolin-containing saline to regular saline a mass of elongated thread-like chromatids or a condensed, compact chromatin mass was observed near the furrow between blastomeres in the eggs that were treated with aphidicolin until 40 min post-insemination or later.
11. Most of these aphidicolin-treated eggs showed aberrant thread-like chromatids elongated near the cleavage furrow, while all eggs that were exposed to the inhibitor 40 min post-insemination or were cleaved later showed normal chromosome segregation (57).

## Acknowledgments

The author is grateful to the collaborators Drs. T. Haraguchi, S. Ikegami, T. Kishimoto, H. Kobayashi, S. Oda, H. Ohta, Y. Shibata, and M. Yamashita for their help in preparing the manuscript.

### References

1. Masui, Y. and Clarke, H.J. (1979) Oocyte maturation. *Int. Rev. Cytol.* 57, 185–282.
2. Yamashita, M. (2000) Toward modeling of a general mechanism of MPF formation during oocyte maturation in vertebrates. *Zool. Sci.* 17, 841–851.
3. Sagata, N., Oskarsson, M., Copeland, T., Brumbaugh, J. and Woude, G.F.V. (1988)

Function of c-mos protooncogene product in meiotic maturation in *Xenopus* oocytes. *Nature* 335, 519–525.
4. Freeman, R.S., Kanki, J.P., Ballantyne, S.M., Pickham, K.M. and Donophue, D.J. (1989) Effects of the v-mos on *Xenopus* development: meiotic induction in oocytes and mitotic arrest in cleaving embryos. *J. Cell Biol.* 111, 533–541.
5. Sheets, M.D., Wu, M. and Wickens, M. (1995) Polyadenylation of c-mos mRNA as a control point in *Xenopus* meiotic maturation. *Nature* 274, 511–516.
6. Tokumoto, T., Yamashita, M., Tokumoto, M., Tanaka, H., Katsu, Y., Horiguchi, R., et al. (1997) Initiation of cyclin B degradation by the 26S proteasome upon egg activation. *J. Cell Biol.* 138, 1313–1322.
7. Josefsberg, L.B.-Y., Galiani, D., Dantes, A., Amsterdam, A. and Deckel, N. (2000) The proteasome is involved in the first metaphase-to-anaphase transition of meiosis in rat oocytes. *Biol. Reprod.* 62, 1270–1277.
8. Mueller, P.R., Coleman, T.R. and Dunphy, W.G. (1995) Cell cycle regulation of a *Xenopus* Wee1-like kinase. *Mol. Biol. Cell* 6, 119–134.
9. Longo, F.J. (1997) Fertilization. Chapman & Hall, New York, NY.
10. Iwamatsu, T. and Kobayashi, H. (2002) Electron microscopic observations of karyogamy in the fish egg. *Dev. Growth Differ.* 44, 357–363.
11. Clarke, H.J. and Masui, Y. (1986) Transformation of sperm nuclei to metaphase chromosomes in the cytoplasm of maturing oocytes of the mouse. *J. Cell Biol.* 102, 1039–1046.
12. Das, N.K. and Baker, C. (1976) Mitotic chromosome condensation in the sperm nucleus during postfertilization maturation division in *Urechis* eggs. *J. Cell Biol.* 68, 155–159.
13. Tchou, S. and Chen, C.H. (1942) Fertilization of artificially ovulated premature eggs of *Bufo. Sci. Rec. China* (K'e hsuch chi u) 1, 203–208.
14. Elinson, R.P. (1977) Fertilization of immature frog eggs: cleavage and development following subsequent activation. *J. Embryol. Exp. Morphol.* 37, 187–201.
15. Iwamatsu, T. and Chang, M.C. (1972) Sperm penetration *in vitro* of mouse oocytes at various times during maturation. *J. Reprod. Fertil.* 31, 237–247.
16. Abeydeera, L.R., Niwa, K. and Okuda, K. (1993) Maturation-promoting factor (MPF) is responsible for the transformation of sperm nuclei to metaphase chromosomes in maturing bovine oocytes *in vitro*. *J. Reprod. Fertil.* 98, 409–414.
17. Gurdon, J.B. (1968) Changes in somatic cell nuclei inserted into growing and maturing amphibian oocytes. *J. Embryol. Exp. Morphol.* 20, 401–414.
18. Ziegler, D. and Masui, Y. (1973) Control of chromosome behavior in amphibian oocytes. II. The effect of inhibitors of RNA and protein synthesis on the induction of chromosome condensation. *J. Cell Biol.* 68, 620–628.
19. Moriya, M. and Katagiri, Ch. (1976) Microinjection of toad sperm into oocytes undergoing maturation division. *Dev. Growth Differ.* 18, 349–356.
20. Masui, Y., Lohka, M.J. and Shuibuya, E.K. (1984) Roles of Ca ions and ooplasmic factors in the resumption of metaphase-arrested meiosis in *Rana pipiens* oocytes. *Symp. Soc. Exp. Biol.* 38, 45–66.
21. Lohka, M.J. and Masui, Y. (1984) Effects of $Ca^{2+}$ ions on the formation of metaphase chromosomes and sperm pronuclei in cell-free preparations from unactivated Rana pipiens eggs. *Dev. Biol.* 103, 434–442.
22. Yamashita, M. (1983) Electron microscopic observations during monospermic fertilization process of the brittle-star *Amphipholis kochii* Lutken. *J. Exp. Zool.* 228, 109–120.
23. Iwamatsu, T. (1966) Role of the germinal vesicle materials on the acquisition of developmental capacity of the fish oocyte. *Embryologia* 9, 205–221.
24. Iwamatsu, T. and Ohta, T. (1980) The changes in sperm nuclei after penetrating fish oocytes matured without germinal vesicle material in their cytoplasm. *Gamete Res.* 3, 121–132.
25. Longo, F.J. (1973) The onset of DNA synthesis and its relation to morphogenetic events of the pronuclei in activated eggs of the sea urchin, *Arbacia punctulata*. *Dev. Biol.* 30, 56–67.
26. Longo, F.J. and Kuncle, M. (1978) Transformation of sperm nuclei upon insemination. *Curr. Topics Dev. Biol.* 12, 149–184.
27. Wolgemuth, D.J. (1983) Synthetic activities of the mammalian early embryo: molecular and genetic alterations following fertilization. In: Mechanisms and control of animal fertilization (J.F. Hartmann, Ed.). pp. 415–452, Academic Press, New York.
28. Ohsumi, K., Katagiri, Ch. and Yanagimachi, R. (1996) Development of pronuclei from human spermatozoa injected microsurgically into frog (*Xenopus*) eggs. *J. Exp. Zool.* 237, 319–325.

29. Kopecny, V. and Pavlok, A. (1975) Autoradiographic study of mouse spermatozoan arginine-rich nuclear protein in fertilization. *J. Exp. Zool.* 191, 85–96.
30. Poccia, D., Salik, J. and Krystal, G. (1981) Transitions in histone variants of the male pronucleus following fertilization and evidence for a maternal store of cleavage-stage histones in the sea urchin egg. *Dev. Biol.* 82, 287–296.
31. Rodman, T.C., Pruslin, F.H., Hoffmann, H.P. and Allfrey, V.G. (1981) Turnover of basic chromosomal proteins in fertilized eggs – a cytoimmunochemical study of events *in vitro*. *J. Cell Biol.* 90, 351–361.
32. Zirkin, B.R., Soucek, D.A., Chang, T.S.K. and Perreault, S.D. (1985) *in vitro* and *in vivo* studies of mammalian sperm nuclear decondensation. *Gamete Res.* 11, 349–365.
33. Ohsumi, K. and Katagiri, Ch. (1991) Occurrence of H1 subtypes specific to pronuclei and cleavage-stage cell nuclei of anuran amphibians. *Dev. Biol.* 147, 110–120.
34. Philpott, A. and Leno, G.H. (1992) Nucleoplasmin remodels sperm chromatin in *Xenopus* egg extracts. *Cell* 69, 759–767.
35. Luthardt, F.W. and Donahue, R.P. (1973) Pronuclear DNA synthesis in mouse eggs: an autoradiographic study. *Exp. Cell Res.* 82, 143–151.
36. Naish, S.J., Perreault, S.D., Foehner, L. and Zirkin, B.R. (1987) DNA synthesis in the fertilizing hamster sperm nucleus: sperm template availability and egg cytoplasmic control. *Biol. Reprod.* 36, 245–253.
37. Barnes, F.L., Callos, P., Powell, R., Westhusin, W.A. and Shepherd, D. (1993) Influence of recipient oocyte cell cycle stage on DNA synthesis, nuclear envelope breakdown, chromosome constitution, and development in nuclear transplant bovine embryos. *Mol. Reprod. Dev.* 36, 33–41.
38. Campbell, K.H.S., Loi, P., Cappai, P. and Wilmut, I. (1994) Improved development to blastocyst of ovine nuclear transfer embryos reconstructed during the presumptive S phase of enucleated activated oocytes. *Biol. Reprod.* 50, 1385–1393.
39. Laurincik J., Kopecny, V. and Hyttel, P. (1994) Pronucleus development an DNA synthesis in bovine zygotes *in vitro*. *Theriogenology* 42, 1285–1293.
40. Hirano, T. (2000) Chromosome cohesion, condensation, and separation. *Annu. Rev. Biochem.* 69, 115–144.
41. Iwamatsu, T., Shibata, Y. and Yamashita, M. (1999) Studies on fertilization of the teleost. II. Nuclear behavior and changes in histone H1 kinase. *Dev. Growth Differ.* 41, 473–482.
42. Nomura, A., Maruyama, Y.K. and Yoneda, M. (1991) Initiation of DNA replication cycle in fertilized eggs of the starfish, *Asterina pectinifera*. *Dev. Biol.* 143, 289–296.
43. Simmel, E.B. and Karnofsky, D.A. (1961) Observation on the uptake of tritiated thymidine in the pronuclei of fertilized sand dollar embryos. *J. Biophys. Biochem. Cytol.* 10, 59–65.
44. Oprecue, S. and Thibault, C. (1965) Duplication de l'AND dans les oeufs de lapine après la fecundation. *Ann. Biol. Anim. Biochim. Biophys.* 5, 151–156.
45. Howlett, S.K. and Bolton, V.N. (1985) Sequence and regulation of morphological and molecular events during the first cell cycle of mouse embryogenesis. *J. Embryol. Exp. Morphol.* 67, 175–206.
46. Abramczuk, J. and Sawicki, W. (1975) Pronuclear synthesis of DNA in fertilized and parthenogenetically activated mouse eggs: a cytophotometric study. *Exp. Cell Res.* 92, 361–372.
47. Balkan, W. and Martin, R.H. (1982) Timing of human sperm chromosome replication following fertilization of hamster eggs *in vitro*. *Gamete Res.* 6, 115–119.
48. Szollosi, D. (1966) Time and duration of DNA synthesis in rabbit eggs after sperm penetration. *Anat. Rec.* 154, 209–212.
49. Longo, F.J. and Plunkett, W. (1973) The onset of DNA synthesis and its relation to morphogenetic events of the pronuclei in activated eggs of the sea urchin, *Arbacia punctulata*. *Dev. Biol.* 30, 56–67.
50. Whitaker, M.J. and Steinhardt, R.A. (1981) The relation between the increase in reduced nicotinamide nucleotides and the initiation of DNA synthesis in sea urchin eggs. *Cell* 25, 95–103.
51. Collas, P., Chang, T., Long, C. and Robl, J.M. (1995) Inactivation of Histone H1 Kinase by $Ca^{2+}$ in rabbit oocytes. *Mol. Reprod. Dev.* 40, 253–258.
52. Gould, K.L. and Nurse, P. (1989) Tyrosine phosphorylation of the fission yeast $cdc2^{+}$ protein kinase regulates entry into mitosis. *Nature* 342, 39–45.
53. Enoch, T. and Nurse, P. (1990) Mutation of fission yeast cell cycle control genes abolishes dependence of mitosis on DNA replication. *Cell* 60, 665–673.
54. Pagano, M., Pepperkok, R., Verde, F., Ansorge, W. and Graetta, G. (1992) Cyclin A is required at two points in the human cell cycle. *EMBO J.* 11, 961–971.

55. Tosuji, H., Mabuchi, I., Fusetani, N. and Nakazawa, H. (1992) Calyculin A induces contractile ring-like apparatus formation and condensation of chromosomes in unfertilized sea urchin eggs. *Proc. Natl. Acad. Sci. USA* 89, 10613–10617.
56. Someya, A., Tanaka, N. and Okuyama, A. (1993) Inhibition of initiation of DNA replication in Xenopus egg extracts by a phosphatase inhibitor, Calyculin A. *Biochem. Biophys. Res. Commun.* 196, 85–91.
57. Iwamatsu, T., Shibata, Y., Hara, O., Yamashita, M. and Ikegami, S. (2002) Studies on fertilization in the teleost. IV. Effects of aphidicolin and camptothecin on chromosome formation in fertilized medaka eggs. *Dev. Growth Differ.* 44, 293–302.
58. Doree, M., Peaucellier, G. and Picard, A. (1983) Activity of the maturation-promoting factor and the extent of protein phosphorylation oscillate simultaneously during meiotic maturation of starfish oocytes. *Dev. Biol.* 99, 489–501.
59. Gerhart, J.C., Wu, M. and Kirschner, M.W. (1984) Cell cycle dynamics of an M phase-specific cytoplasmic factor in *Xenopus laevis* oocytes and eggs. *J. Cell Biol.* 98, 1247–1255.
60. Newport, J.W. and Kirschner, M.W. (1984) Regulation of the cell cycle during early *Xenopus* development. *Cell* 37, 731–742.
61. Picard, A., Labbe, J.C., Peaucellier, G., et al. (1987) Changes in the activity of the maturation-promoting factor are correlated with those of a major cAMP- and calcium independent protein kinase during the first mitotic cell cycles in the starfish embryo. *Dev. Growth Differ.* 29, 93–103.
62. Iwamatsu, T., Kobayashi, H., Yamashita, M., Shibata, Y. and Yusa, A. (2003) Experimental hybridization among Oryzias species. II. Karyogamy and abnormality of chromosome separation in the cleavage of interspecific hybrids between *Oryzias latipes* and *O. javanicus*. *Zool. Sci.* 20, 1381–1387.
63. Sakai, C., Konno, F., Nakano, O., Iwai, T., Yokota, T., Lee, J., Nishida-Umehara, C., Kuroiwa, A., Mtsuda, Y. and Yamashita, M. (2007) Chromosome elimination in the interspecific hybrid medeka between *Oryzias latipes* and *O. hubbsi*. *Chromosome Res.* 15, 697–709.
64. Loupart, M.-L., Krause, S.A. and Heck, M.M.S. (2000) Aberrant replication timing induces chromosome condensation in *Drosophila* ORC2 mutants. *Curr. Biol.* 10, 1547–1556.
65. Nagano, H., Okano, K., Ikegami, S. and Katagiri, C. (1982) Changes in intracellular location of DNA polymerase-alpha during oocyte maturation of the toad, *Bufo bufo japonicus*. *Biochem. Biophys. Res. Commun.* 106, 683–690.
66. Fox, A.M., Breaux, C.B. and Benbow, R.M. (1980) Intracellular localization of DNA polymerase activities within large oocytes of the frog, *Xenopus laevis*. *Dev. Biol.* 80, 79–95.
67. Grippo, P.C. Taddei, C., Locorotondo, G. and Gambino-Giuffrida, A. (1977) Cellular localization of DNA polymerase activities in full-grown oocytes and embryos of *Xenopus laevis*. *Exp. Cell Res.* 190, 247–252.
68. Martini, G., Tato, F., Attardi, D.G. and Tocchini-Valentini, G.P. (1976) Nuclear localization of DNA polymerase alpha in *Xenopus laevis*. *Biochem. Biophys. Res. Commun.* 72, 875–879.
69. Shioda, M., Nagano, H. and Mano, Y. (1977) Cytoplasmic location of DNA polymerase-α and -βof sea urchin eggs. *Biochem. Biophys. Res. Commun.* 78, 1362–1368.
70. Haraguchi, T. and Nagano, H. (1983) Isolation and characterization of DNA polymerases from mature oocytes of the starfish, *Asterina pectinifera*. *J. Biochem.* 93, 87–697.
71. Oishi, N. and Shimada, H. (1983) Intracellular localization of DNA polymerases in the oocyte of starfish, *Asterina pectinifera*. *Dev. Growth Differ.* 25, 547–551.
72. Iwamatsu, T., Haraguchi, T. and Nagano, H. (2010) Cytoplasmic location of DNA polymerase in oocytes of the teleost fish, *Oryzias latipes*. *Aichi Univ. Educat. (Nai. Sci.)* 59, 1–8.
73. Ikegami, S., Taguchi, T., Ohashi, M., Oguro, M., Nagano, H. and Mano, Y. (1978) Aphidicolin prevents mitotic cell division by interfering with the activity of DNA polymerase-α. *Nature* 275, 458–460.
74. Ikegami, S., Amemiya, S., Oguro, M., Nagano, H. and Mano, Y. (1979) Inhibition by aphidicolin of cell cycle progression and DNA replication in sea urchin embryos. *J. Cell. Physiol.* 100, 439–444.
75. Oguro, M., Suzuki-Hori, C., Nagano, H., Mano, Y. and Ikegami, S. (1979) The mode of inhibitory action by aphidicolin on eukaryotic DNA polymerase-α. *Eur. J. Biochem.* 97, 603–607.
76. Brachet, J. and De Ptrocellis, B. (1981) The effects of aphidicolin, an inhibitor of DNA replication, on sea urchin development. *Exp. Cell Res.* 135, 179–189.
77. Yamada, H., Hirai, S., Ikegami, S., Kawarada, Y., Okuhara, E. and Nagano, H. (1985) The fate of DNA originally existing in the zygote

nucleus during a chromosomal cleavage of fertilized echinoderm eggs in the presence of aphidicolin: Microscopic studies with anti-DNA antibody. *J. Cell Physiol.* 124, 9–12.
78. Nagano, H., Hirai, S., Okano, K. and Ikegami, S. (1981) Achromosomal cleavage of fertilized starfish eggs in the presence of aphidicolin. *Dev. Biol.* 85, 409–415.
79. Saiki, T., Kyozuka, K., Osanai, K. and Hamaguchi, Y. (1991) Chromosomal behavior in starfish (*Asterina pectinifera*) zygotes under the effect of aphidicolin, an inhibitor of DNA polymerase. *Exp. Cell Res.* 192, 380–388.
80. Wells, N.J. and Hickson, I.D. (1995) Human topoisomerase II alpha is phosphorylated in a cell-cycle phase-dependent manner by a proline-directed kinase. *Eur. J. Biochem.* 23, 491–497.
81. Clute, P. and Masui, Y. (1997) Microtubule dependence of chromosome cycles in *Xenopus laevis* blastomeres under the influence of a DNA synthesis inhibitor, aphidicolin. *Dev. Biol.* 185, 1–13.
82. Taguchi, T., Ohashi, M., Oguro, M., Nagano, H. and Mano, Y. (1978) Aphidicolin prevents mitotic cell division by interfering with the activity of DNA polymerase-α. *Nature* 275, 458–460.
83. Droge, P., Sogo, J.M. and Stahl, H. (1985) Inhibition of DNA synthesis by aphidicolin induces supercoiling in simian virus 40 replicative intermediates. *EMBO J.* 4, 3241–3246.
84. Wang, J.C. (1985) DNA topoisomerases. *Annu. Rev. Biochem.* 54, 665–697.
85. Drlica, K. and Franco, R.J. (1988) Inhibitors of DNA topoisomerases. *Biochemistry* 27, 2253–2259.
86. Gupta, M., Fujimori, A. and Pommier, Y. (1995) Eukaryotic DNA topoisomerases I. *Biochim. Biophys. Acta* 1262, 1–14.
87. Ohta, E., Ohta, S., Hongo, T., Hamaguchi, Y., Ando, T., Shioda, M. and Ikegami, S. (2003) Inhibition of chromosome separation in fertilized starfish eggs by kalihinol F, a topoisomerase I inhibitor obtained from a marine sponge. *Biosci. Biotechnol. Biochem.* 67, 2365–2372.
88. Horowitz, M.S. and Horowitz, S.B. (1971) Intracellular degradation of HeLa and adenovirus type 2 DNA induced by camptothecin. *Biochem. Biophys. Res. Commun.* 45, 723–727.
89. Annunziato, T.A. (1989) Inhibitors of topoisomerases I and II arrest DNA replication, but do not prevent nucleosome assembly *in vivo*. *J. Cell Sci.* 93, 593–603.
90. Gellert, M. (1981) DNA topoisomerases. *Annu. Rev. Biochem.* 50, 879–910.
91. Hsian, Y.-H., Hertzberg, R., Hecht, S. and Liu, L.F. (1985) Camptothecin induces protein-linked DNA breaks via mammalian DNA topoisomerase I. *J. Biol. Chem.* 260, 14873–14878.
92. Zhu, Q., Pongpech, P. and DiGate, R.J. (2001) Type I topoisomerase activity is required for proper chromosomal segregation in *Escherichia coli*. *Proc. Natl. Acad. Sci. USA* 98, 9766–9771.
93. Usongo, V., Nolent, F., Sanscartier, P., Tanguay, C., Broccoli, S., Baaklini, I., Drlica, K. and Drolet, M. (2008) Depletion of RNase H1 activity in *Escherichia coli* lacking DNA topoisomerase I leads to defects in DNA supercoiling and segregation. *Mol. Microbiol.* 69, 968–981.
94. Uemura, T., Ohkura, H., Adachi, Y., Morino, K., Shiozaki, K. and Yanagida, M. (1987) DNA topoisomerase II is required for condensation and separation of mitotic chromosomes in *S. pombe*. *Cell* 50, 917–925.
95. Holm, C., Goto, T., Wang, J.C. and Botstein, D. (1985) DNA topoisomerase II is required at the time of mitosis in yeast. *Cell* 41, 553–563.
96. Holm, C., Stearns, T. and Botstein, D. (1989) DNA topoisomerase II must act at mitosis to prevent nondisjunction and chromosome breakage. *Mol. Cell. Biol.* 9, 159–168.
97. Rose, D., Thomas, W. and Holm, C. (1990) Segregation of recombined chromosomes in meiosis I requires DNA topoisomerase II. *Cell* 60, 1009–1017
98. Bhat, M.A., Philp, A.V., Glover, D.M. and Bellen, H.J. (1996) Chromatid segregation at anaphase required the barren product, a novel chromosome-associated protein that interacts with topoisomerase II. *Cell* 87, 1103–1114.
99. Wright, S.J. and Schatten, G. (1990) Teniposide, a topoisomerase II inhibitor, prevents chromosome condensation and separation but not decondensation in fertilized surf clam (*Spisula solidissima*) oocytes. *Dev. Biol.* 142, 224–232.
100. Shamu, C.E. and Murray, A.W. (1992) Sister chromatid separation in frog egg extracts requires DNA topoisomerase II activity during anaphase. *J. Cell Biol.* 117, 921–934.
101. Buchenau, P., Saumweber, H. and Arndt-Jovin, D.L. (1993) Consequences of TOPO II inhibition in early embryogenesis of *Drosophila* revealed by *in vivo* confocal laser scanning microscopy. *J. Cell Sci.* 104, 1175–1185.
102. Kallio, M. and Lahdtie, J. (1996) Fragmentation of centromeric DNA and prevention

of homologous chromosome separation in male meiosis *in vivo* by the topoisomerase II inhibitor etoposide. *Mutagenesis* 11, 435–443.
103. Kallio, M. and Lahdtie, J. (1997) Effects of the DNA topoisomerase II inhibitor merbarone in male mouse meiotic divisions *in vivo*: cell cycle arrest and induction of aneuploidy. *Environ. Mol. Mutagen.* 29, 16–27.
104. Mailhes, J.B., Marchetti, F., Young, D. and London, S.N. (1996) Numerical and structural chromosome aberrations induced by etoposide (VP-16) during oocyte maturation of mice: transmission to 1-cell zygotes and damage to dictyate oocytes. *Mutagenesis* 11, 357–361.
105. Marchetti, F., Bishop, J.B., Lowe, X., Generoso, W.M., Hozier, J. and Wyrobek, A.J. (2001) Etoposide induces heritable chromosomal aberrations and aneuploidy during male meiosis in the mouse. *Proc. Natl. Acad. Sci. USA* 98, 3952–3957.
106. Tateno, H. and Kamiguchi, Y. (2001) Abnormal chromosome migration and chromosome aberrations in mouse oocytes during meiosis II in the presence of topoisomerase II inhibitor ICRF-193. *Mutat. Res.* 502, 1–9.
107. Charron, M. and Hancock, R. (1990) DNA topoisomerase II is required for formation of mitotic chromosomes in Chinese hamster ovary cells: studies using the inhibitor 4′-demethylepipodophyllotoxin 9-(4,6-*0*-thenylidene-β-D-glucopyranoside). *Biochemistry* 29, 9531–9537.
108. Downes, C.S., Mullinger, A.M. and Johnson, R.T. (1991) Inhibitors of DNA topoisomerase II prevent chromatid separation in mammalian cells but do not prevent exit from mitosis. *Proc. Natl. Acad. Sci. USA* 88, 8895–8899.
109. Baldi, M.I., Benedetti, P., Mattoccia, E. and Tocchi-Valentini, G.P. (1980) in vitro catenation and decatenation of DNA and a novel eukaryotic ATP-dependent topoisomerase. *Cell* 20, 461–467.
110. Hsieh, T. (1983) Knotting of the circular duplex DNA by type II DNA topoisomerase from *Drosophila melanogaster*. *J. Biol. Chem.* 258, 8413–8420.
111. Hsieh, T.-S. and Brutlag, D. (1980) ATP-dependent DNA topoisomerase from D. melanogaster reversibly catenates duplex DNA rings. *Cell* 27, 115–125.
112. Kreuzer, K.N. and Cozzarelli, N.R. (1980) Formation and resolution of DNA catenanes by DNA gyrase. *Cell* 20, 245–254.
113. Liu, L.F., Davis, J.I. and Calendar, R. (1981) Novel topologically knotted DNA from bacteriophage P4 capsids: studies with DNA topoisomerases. *Nucleic Acids Res.* 9, 3979–3989.
114. Sundin, O. and Varshavsky, A. (1980) Terminal stages of SV40 replication proceed via multiply intercatenated dimmers. *Cell* 21, 103–114.
115. Sundin, O. and Varshavsky, A. (1981) Arrest of segregation leads to accumulation of highly intertwined catenated dimmers: dissection of the final stage of SV40 DNA replication. *Cell* 25, 659–669.
116. DiNardo, S., Voelkel, K. and Sternglanz, R. (1984) DNA topoisomerase II mutant of *Saccharomyces cerevisiae*: Topoisomerase II is required for segregation of daughter molecules at the termination of DNA replication. *Proc. Natl. Acad. Sci. USA* 81, 2616–2620.
117. Weaver, D.T., Fields-Berry, S.C. and DePamphilis, M.L. (1985) The termination region for SV40 DNA replication directs the mode of separation for the two sibling molecules. *Cell* 41, 565–575.
118. Maeshima, K. and Laemmli, U.K. (2003) A two-step scaffolding for mitotic chromosome assembly. *Dev. Cell* 4, 467–480.
119. Xu, Y.-X. and Manley, J.L. (2007) New insights into mitotic chromosome condensation. A role for the prolyl isomerase Pin 1. *Cell Cycle* 6, 2896–2901.
120. Kelly, T.J. and Brown, G.W. (2000) Regulation of chromosome replication. *Annu. Rev. Biochem.* 69, 829–880.
121. Hirano, T. (2005) SMC proteins and chromosome mechanics: from bacteria to humans. *Philos. Trans. R. Soc. B* 36, 507–514.
122. Yanagida, M. (2005) Basic mechanism of eukaryotic chromosome segregation. *Philos. Trans. R. Soc. B* 360, 609–1615.
123. Iwamatsu, T., Ohta, T., Nakayama, N. and Shoji, H. (1976) Studies of oocyte maturation of the medaka, *Oryzias latipes*. III. Cytoplasmic and nuclear change of oocyte during *in vitro* maturation. *Ann. Zool. Jpn.* 49, 28–37.
124. Iwamatsu, T. (1978) Studies on oocyte maturation of the medaka, *Oryzias latipes*. VI. Relationship between the circadian cycle of oocyte maturation and activity of the pituitary gland. *J. Exp. Zool.* 206, 355–363.
125. Iwamatsu, T., Onitake, K. and Nakashima, S. (1992) Polarity of responsiveness in sperm and artificial stimuli in medaka eggs. *J. Exp. Zool.* 264, 351–358.
126. Iwamatsu, T., Yoshimoto, Y. and Hiramoto, Y. (1988) Cytoplasmic $Ca^{2+}$ release induced

by microinjection of $Ca^{2+}$ and effects of microinjected divalent cations on $Ca^{2+}$ sequestration and exocytosis of cortical alveoli in the medaka egg. *Dev. Biol.* 125, 451–457.
127. Iwamatsu, T., Fluck, R.A. and Mori, T. (1933) Mechanical dechorionation of fertilized eggs for experimental embryology in the medaka. *Zool. Sci.* 10, 945–951.
128. Nomura, A., Yoneda, M. and Tanaka, S. (1993) DNA replication in fertilized eggs of the starfish *Asterina pectinifera*. *Dev. Biol.* 159, 288–297.
129. Laemmli, U.K. (1970) Cleavage of structural proteins during the assembly of the head of bacteriophage T4. *Nature* 277, 680–685.
130. Yamashita, M., Yoshikuni, M., Hirai, T., Fukuda, S. and Nagahama, Y. (1991) A monoclonal antibody against the PSTAIR sequence of p34cdc2, catalytic subunit of maturation-promoting factor and key regulator of the cell cycle. *Dev. Growth Differ.* 33, 617–624.
131. Yamashita, M., Jiang, J., Onozato, H., Nakanishi, T. and Nagahama, Y. (1992) M phase-specific histone H1 kinase in fish oocytes: purification, components and biochemical properties. *Eur. J. Biochem.* 205, 537–543.
132. Iwamatsu, T., Sugiura, T., Sugitani, K. and Hori, R. (1995) Inorganic contents of the medaka egg before and after cortical reaction. *Fish Biol. J. Medaka* 7, 21–24.
133. Mehlman, L.M. and Kline, D. (1994) Regulation of intracellular calcium in the mouse egg: calcium release in response to sperm or inositol triphosphate is enhanced after meiotic maturation. *Biol. Reprod.* 51, 1088–1198.
134. Iwamatsu, T. (1965) On fertilizability of preovulation eggs of the medaka, *Oryzias latipes*. *Embryologia* 8, 327–336.
135. Iwamatsu, T. (1997) Abbreviation of the second meiotic division by precocious fertilization in fish oocytes. *J. Exp. Zool.* 277, 450–459.
136. Eppig, J.J., Schultz, M.R., O'Brien, M. and Chesnel, F. (1994) Relationship between the developmental programs controlling nuclear and cytoplasmic maturation of mouse oocytes. *Dev. Biol.* 164, 1–9.
137. Kuraishi, R. and Osanai, K. (1988) Behavior of sperm nuclei in meiotic eggs of the oyster, *Crassostrea gigas*. *Bull. Mar. Biol. Stn. Asamushi* 18, 57–65.
138. Longo, F.J., Mathews, L. and Hedgecock, D. (1993) Morphogenesis of maternal and paternal genomes in fertilized oyster eggs (Crassostrea gigas): effects of cytochalasin B at different periods during meiotic maturation. *Biol. Bull.* 185, 197–214.
139. Longo, F.J. and Anderson, E. (1970) An ultrastructural analysis of fertilization in the surf clam, Spisula solidissima. I. Polar body formation and development of the female pronucleus. *J. Ultrastruct. Res.* 33, 495–514.
140. Iwamatsu, T. (2000) Fertilization in fishes. In: Fertilization in Protozoa and Metazoan Animals – Cellular and Molecular Aspects. (J.J. Tarin and A. Cana, Eds.). pp. 89–145, Springer-Verlag.
141. Iwamatsu, T. (1997) Abbreviation of the second meiotic division by precocious fertilization in fish oocytes. *J. Exp. Zool.* 277, 450–459.

# Chapter 8

# Specific Cell Cycle Synchronization with Butyrate and Cell Cycle Analysis

**Congjun Li**

## Abstract

Synchronized cells have been invaluable in many kinds of cell cycle and cell proliferation studies. Butyrate induces cell cycle arrest and apoptosis in Madin Darby Bovine Kidney (MDBK) cells. We explore the possibility of using butyrate-blocked cells to obtain synchronized cells and we characterize the properties of butyrate-induced cell cycle arrest. The site of growth inhibition and cell cycle arrest was analyzed using 5-bromo-2′-deoxyuridine (BrdU) incorporation and flow cytometry analyses. Exposure of MDBK cells to 10 mM butyrate caused growth inhibition and cell cycle arrest in a reversible manner. Butyrate affected the cell cycle at a specific point both immediately after mitosis and at a very early stage of the G1 phase. After release from butyrate arrest, MDBK cells underwent synchronous cycles of DNA synthesis and transited through the S phase. It takes at least 8 h for butyrate-induced G1-synchronized cells to begin the progression into the S phase. One cycle of cell division for MDBK cells is about 20 h. By combining BrdU incorporation and DNA content analysis, not only can the overlapping of different cell populations be eliminated, but the frequency and nature of individual cells that have synthesized DNA can also be determined.

**Key words:** Bovine kidney epithelial cell, BrdU incorporation, butyrate, cell cycle synchronization, flow cytometry.

## 1. Introduction

An optimal cell cycle synchronization protocol is required in order to study the proliferative biomarkers of the cell cycle. Highly synchronized cell populations greatly facilitate cell cycle analysis (1, 2). A number of agents and protocols have been described to block cell cycle progression reversibly. These protocols and agents can be used to either arrest actively dividing cells in chemotherapeutic protocols or devise synchronizing regimens for cultured

G. Banfalvi (ed.), *Cell Cycle Synchronization*, Methods in Molecular Biology 761,
DOI 10.1007/978-1-61779-182-6_8, 

cells (3). Most of these agents have an extensive history as chemotherapeutic agents, and their mechanisms of action are well understood. Among the most widely used protocols are the use of nutritional or serum deprivation to arrest cells in G0/G1, the use of DNA synthesis inhibitors to block the cell cycle at the early S phase, and the use of nocodazole – a mitotic inhibitor – to synchronize cells at the G2/M phases. However, not all agents that produce cell cycle blocks are suitable for different kinds of block-and-release experiments or different kinds of cell types. We have recently reported that butyrate can arrest MDBK cells specifically at the early G1 phase (4). However, the properties of butyrate-induced cell cycle arrest and cell cycle progression after release have not been characterized. To obtain cell populations at specific cell cycle stages and to develop a model for studies of cell growth regulation, we examined synchronization protocol of butyrate-induced cell cycle arrest and demonstrated that butyrate blocks the cell cycle at the very early G1 phase and that butyrate-induced cell cycle block is reversible. Using butyrate-synchronized cells, we also determined that the cell division cycle of MDBK cells is about 20 h. The use of flow cytometry allows us to monitor the progression of the cell cycle and to characterize the cell cycle arrest induced by butyrate.

## 2. Materials

1. Madin Darby bovine kidney epithelial cells (MDBK, American Type Culture Collection) were cultured in a 25 $cm^2$ flask, and the medium was renewed twice per week. Cell cultures were maintained in a water-jacked incubator with 5% $CO_2$ at 37°C. The cells were used for treatment testing at approximately 50% confluence during the exponential phase of growth.
2. Dulbecco's Modified Eagle's Medium (DMEM) supplemented with 5% fetal bovine serum.
3. Solution of trypsin (0.25%).
4. Sodium butyrate dissolved in molecular-grade water was prepared as 1 M stock and stored in single-use aliquots at –20°C.
5. BrdU Flow kits (BD Pharmingen, San Diego, CA).
6. 25 $cm^2$ flask with 0.2 μm vent cap.

## 3. Methods

### 3.1. Cell Treatment

Adding up to 10 mM sodium butyrate into the cell culture medium did not cause a measurable pH change. Duplicated flasks of cells were used for treatment.

### 3.2. Flow Cytometric Analysis with Measurement of DNA Content

1. Flow cytometry analysis can be done with the measurements of increased DNA content in proliferating cells going through cell cycle phases and with the combined measurements of increased DNA content in proliferating cells going through cell cycle phases and immunostaining on the newly synthesized DNA containing BrdU, which reflects the cell cycle progression status. Cellular DNA content increases from the original amount of the two copies (2C) in the G1 phase to twice the amount of four copies (4C) in the G2/M phases, with intermediate DNA content in the S phase cells. To measure the DNA content, cells were stained with a fluorescent dye (propidium iodide) that directly binds to the DNA in the nucleus. Measuring the fluorescence by flow cytometry provided a measure of the amount of dye taken up by the cells and, indirectly, the amount of DNA content. The cells collected by trypsinization were washed with an ice-cold PBS (pH 7.4) buffer. The cells were then resuspended in the PBS buffer and two volumes of ice-cold 100% ethanol were added dropwise into tubes and mixed with cells in suspension by slow vortexing. After ethanol fixation, the cells were centrifuged (400 $\times g$, 5 min) and washed in the PBS buffer once. The cells were then resuspended at $10^6$/ml. 50 μg/ml of RNase A was then added to each sample and the samples were incubated at 37°C for 30 min. After incubation, 20 μg of propidium iodide was added to each tube for at least 30 min to provide the nuclear signal for fluorescence-activated cell sorting (flow cytometry). After staining the cells with propidium iodide, the tubes were transferred to ice or stored at 4°C and protected from light. The stained cells can be analyzed within 48 h or stored for up to 2 weeks. However, in this case, the stained cells require nylon mesh filtration (Filcons, BD Cat. No. 340627) to remove cell clumps or syringing (25 gauge) to break up cell clumps. Flow cytometric data are acquired using a flow cytometer equipped with a 488 nm argon laser. In our laboratory, we used the FC500 from Beckman Coulter (Beckman Coulter Inc., Palatine, IL). This laser permits the excitation of the fluorescent dye, propidium iodide (FL2). In the meantime,

forward angle (FS) and side-scattered (SSC) are also generated from illuminated cells.

2. Cell cycle analysis of DNA histograms: a pragmatic approach: The problem with deconvoluting the DNA content of cells into their component parts is the overlapping of the cell populations. There are a variety of computer programs available for the analysis of DNA histograms. We use Cylchred, a cell cycle analysis software (University of Wales College of Medicine) for this purpose, which is a freeware that can be downloaded from several web sites. The package accepts histograms in an FCS single parameter binary format with up to 1,024 channels. Cylchred has been available in a DOS environment since 1996 and also works with Windows operating systems. The measure function of this program invokes the main cell cycle algorithm and displays the derived components on the histogram with the associated data in the result window. **Figure 8.1** shows the deconvoluted DNA histograms with the associated data.

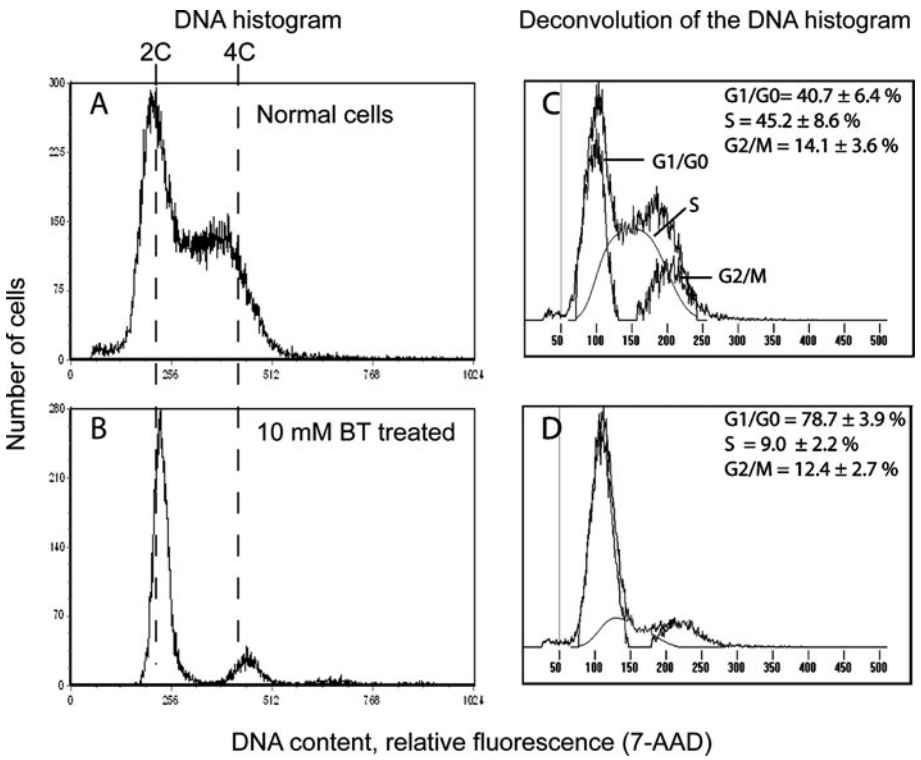


Fig. 8.1. Deconvolution of the DNA histogram using Cylchred software (University of Wales College of Medicine). One set of representative histogram plots of the flow cytometry analysis (DNA content) of MDBK cells: (**a** and **c**) Histogram and its deconvolution of the flow cytometric analysis of the exponential growing cells. (**b** and **d**) Histogram plot and the deconvolution of flow cytometry analysis of MDBK cells treated with 10 mM sodium butyrate.

### 3.3. 5-Bromo-2′-Deoxyuridine (BrdU) Incorporation and Flow Cytometric Analysis of Cells

1. The most accurate method of measuring the relative number of cells in the different cell cycle stages is to pulse-label the cells with BrdU and to use an antibody to BrdU. BrdU is a thymidine (TdR) analogue and is incorporated into cellular DNA through the same pathway. DNA synthesis can be visualized *in situ* by direct immunofluorescence using an antibody against BrdU (5).
2. By combining the immunofluorescent staining of the incorporated BrdU and DNA content stained by the DNA marker, we can not only analyze cell cycle synchrony with high resolution but also monitor the cell cycle progression after the cells are released from the treatments.
3. Asynchronously growing MDBK cells were treated with butyrate for 24 h.
4. Cells were washed with a fresh medium to eliminate the dead cells and then replaced with a fresh medium with 5% fetal bovine serum.
5. Cells were pulse-labeled with BrdU using BrdU Flow kits (BD Pharmingen, San Diego, CA) by following the manufacturer's instructions. In summary, to pulse-label the cells, 10 μl of BrdU solution (1 mM BrdU in PBS) was carefully added directly to each ml of culture media and cultured for 40 min.
6. To stain cells with fluorescence-labeled antibody, cells were collected with trypsinization, fixed, and permeabilized with a BD Cytofix/Cytoperm buffer supplied with the kits.
7. The cells were then treated with DNase to expose the incorporated BrdU (30 μg of DNase to each sample, incubated at 37°C for 1 h).
8. After washing with 1 ml of 1X BD Perm/wash buffer, the cells were resuspended with 50 μl of BD Perm/wash buffer containing diluted fluorescent (fluorescent isothiocyanate, FITC) anti-BrdU antibody and incubated for 20 min at room temperature.
9. After washing with the BD Perm/wash buffer, the cells were resuspended in 20 μl of 7-AAD solution (supplied with kits) to stain the cellular DNA content.
10. Cell DNA content and BrdU labeling were acquired using flow cytometry (FC500, Beckman Coulter Inc.). The 488 nM argon laser permits the excitation of the fluorescent isothiocyanate (FITC) (FL1) and DNA content marker 7-ADD (FL3). Fluorescent signals from the 7-ADD are normally acquired in the linear signal amplification mode, and fluorescent signals generated by other fluorochromes such as FITC are typically acquired in a logarithmic mode.

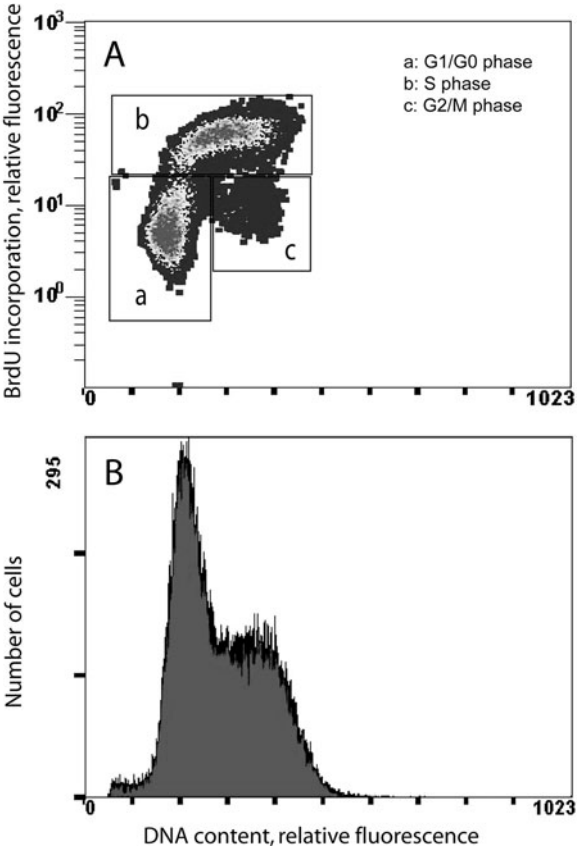


Fig. 8.2. Density and histogram plots of the flow cytometry analysis of normal proliferating cell population. (**A**) Pulse-label with BrdU and using an antibody to BrdU accurately measure the relative number of cells in different stages of the cell cycle. For flow cytometric analysis, the cells were first pulse-labeled with BrdU for 30 min. The collected cells were first stained with diluted fluorescent (fluorescent isothiocyanate, FITC) anti-BrdU antibody and then stained with a DNA marker (7-ADD). The fluorescent signal generated by FITC was acquired in a logarithmic mode, and the fluorescent signal from the DNA-content marker 7-ADD was normally acquired in the linear signal amplification mode. Cells were separated into three clusters by double staining analysis. (a) G1/G0 cells, with 2C DNA content and without any DNA synthesis activity; (b) S phase cells, with DNA content between 2C and 4C (two and four copies of DNA content, respectively) and high BrdU incorporation (DNA synthesis) activity; (c) G2/M cells, with 4C DNA content and also without DNA synthesis activity. (**B**) Histogram, the flow cytometric analysis of the cell cycle by DNA content for the same cell preparation.

11. Collected data were analyzed using Cytomic RXP (Beckman Coulter Inc.).

**Figure 8.2** shows the representative data from the normal growing cell population to show that a second fluorescence parameter (BrdU) provides more flexibility for the quantitative

cell cycle analysis of populations. The fluorescent signal generated by FITC was acquired in a logarithmic mode and the fluorescent signal from the DNA-content marker 7-ADD was acquired in the linear signal amplification mode. Using double color staining (immunofluorescent staining of the BrdU incorporation and fluorescent staining of the total DNA), cells can be separated into three major clusters. The first is a cell population with two copies of DNA and without any DNA synthesis activity, e.g., the cells in the G1/G0 phases (cluster a). The second is the cell population (G2/M phases) that has four copies of DNA and is without any synthesis activity (cluster c). The last is a cell population (cluster b) that has the DNA content between clusters a and c, but has a strong shift of immunofluorescent staining of the newly synthesized DNA. Those cells are in the S phase. All data are displayed in density plots. In comparison with the profiles from the DNA content analysis, the immunofluorescent staining of incorporated BrdU and flow cytometric analysis provides a high-resolution technique to eliminate the overlap between different cell populations and to determine the frequency and nature of individual cells that have synthesized DNA.

12. Asynchronously growing MDBK cells were incubated for 24 h in the presence of 10 mM butyrate.
13. The cells were washed with a fresh medium to eliminate the dead cells and then were replaced in a fresh medium with 5% fetal bovine serum.
14. The cells were pulse-labeled with BrdU at indicated time points and were collected for flow cytometric analysis. **Figure 8.2a, b** is the flow cytometric data representing the 1 and 6 h time points after release from butyrate. The average flow cytometric cell cycle distribution from four experiments showed an arrest of the cells in the G1 phase with the majority of the cells in the G0/G1 phases (81.0 ± 2.9%), while 8.9 ± 1% and 10.1 ± 2.4% of the cells were in the S and G2/M phases, respectively. However, during the first 8 h post-release, the G1-synchronized cells progressed very little into the succeeding stage. Only 18.5 ± 3.7% of the cells at 6 h post-release and 38.1 ± 5.5% of the cells at 8 h post-release progressed into the S phase (data not shown). These data indicated that butyrate blocks the cell cycle at a very early G1 phase and may induce some of the cells into the G0 phase.

**Figure 8.3** shows the flow cytometric data representing data acquired from normal cells (without butyrate treatment) and cells treated for 24 h with 5 and 10 mM butyrate. These data confirmed that cells respond to butyrate treatment in a dose-dependent manner. Data are displayed in contour plots.

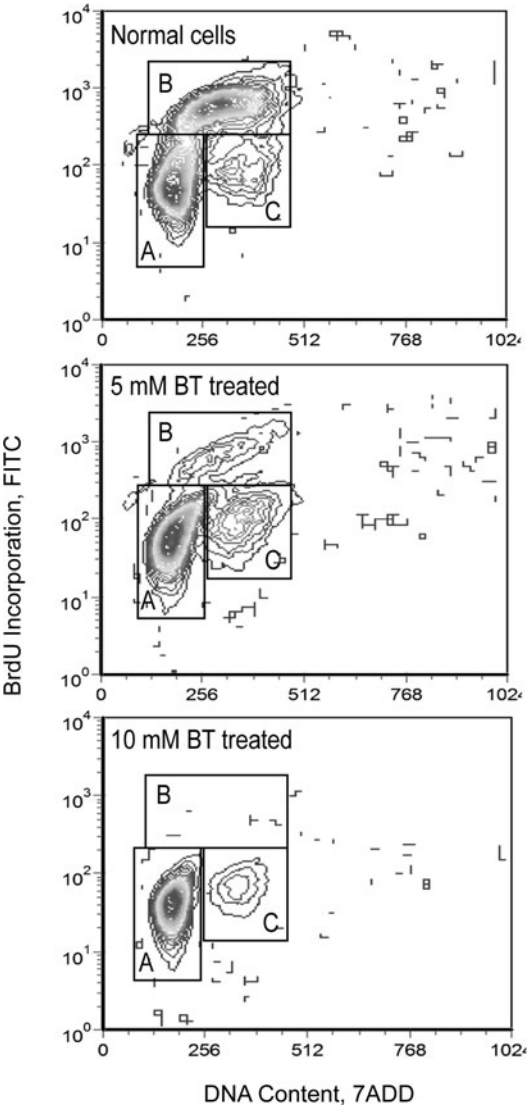


Fig. 8.3. MDBK cell response to different concentrations of butyrate treatments. Cells were treated with butyrate at 0, 5, and 10 mM for 24 h and then pulse-labeled with BrdU. The collected cells were first stained with a diluted fluorescent (fluorescent isothiocyanate, FITC) anti-BrdU antibody and then stained with a DNA marker (7-ADD). Cell DNA content and BrdU pulse-labeling were analyzed using flow cytometry (FC500, Beckman Coulter Inc., Palatine, IL) and collected data were analyzed using Cytomic RXP (Beckman Coulter Inc.). The fluorescent signal generated by FITC was acquired in a logarithmic mode, and the fluorescent signal from the DNA-content marker 7-ADD was normally acquired in the linear signal amplification mode. Data are displayed in contour plots.

### 3.4. Cell Cycle Progression after Release from Aphidicolin Treatment

1. One cycle of cell division for MDBK cells takes about 20 h. Using butyrate-induced synchronized cells, we determined the length of the cell division cycle of MDBK cells (**Fig. 8.4**).
2. After release from the butyrate treatment, the cells were collected at various times post-release and processed for cycle analysis by flow cytometry. Monitoring the cell cycle progression for 24 h after the removal of butyrate showed that the synchronized G1 cells underwent synchronous cycles of DNA synthesis and transited through the S phase (**Fig. 8.5**).

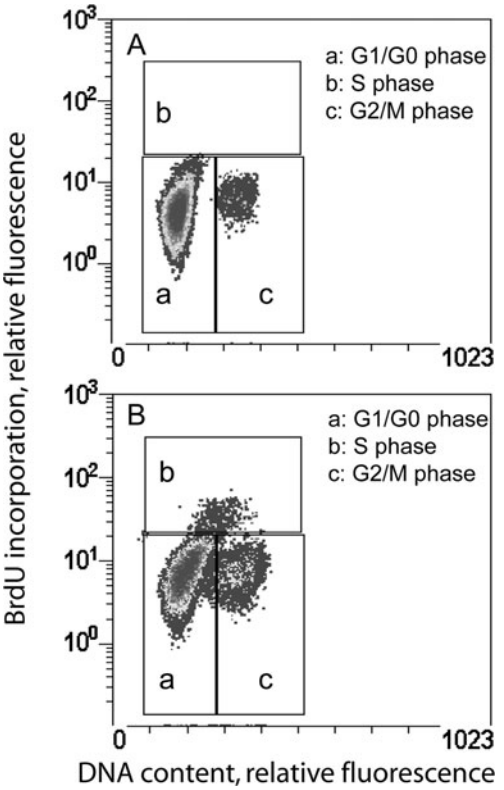


Fig. 8.4. The cell cycle progression after release from aphidicolin treatment. The cells were first incubated in a serum-deprived medium for 48 h and replaced with a fresh medium with 5% fetal bovine serum and 10 μg/ml aphidicolin for another 24 h. The cells were released into fresh medium containing 5% fetal bovine serum. At the indicated time point, cells were pulse-labeled with BrdU. Collected cells were first stained with a diluted fluorescent (fluorescent isothiocyanate, FITC) anti-BrdU antibody and then stained with a DNA marker (7-ADD). (**a**) A representative flow cytometric analysis of the cells 1 h after release from butyrate. (**b**) A representative flow cytometric analysis of cells 6 h after release from butyrate. The cell cycle progression during the first 8 h after release from butyrate. Data are from three individual experiments and are presented as mean ± SEM.

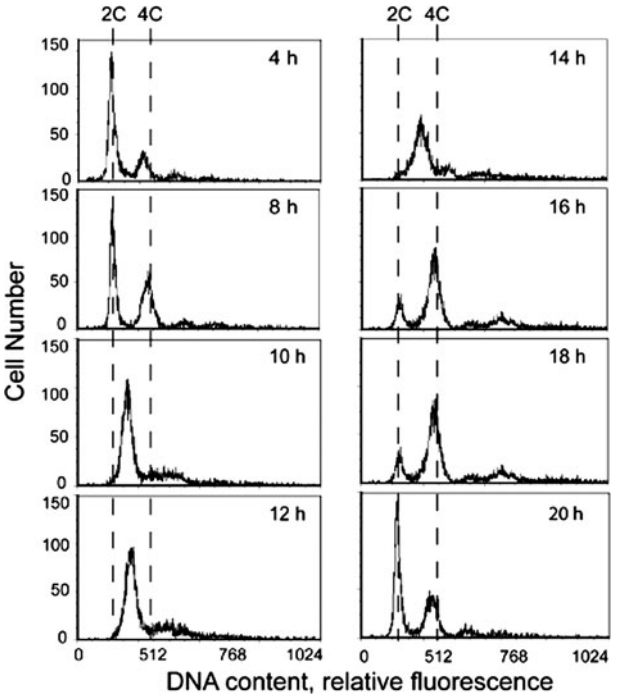


Fig. 8.5. Cell cycle determination using butyrate-synchronized MDBK cells. After release from the butyrate treatment, the cells were collected at indicated times post-release and processed for cycle analysis by flow cytometry. 2C and 4C: two and four copies of DNA content, respectively.

3. Synchronized G1 cells remained in the G1 phase for at least 8 h, with a weak increase in the S phase and a weak decrease in the G1 phase between 6 and 8 h.
4. At 10 h post-release, almost all of the cells progressed into the S phase. Between 16 and 18 h post-release, the majority of the cells were in the G2/M phase.
5. At 20 h post-release, the G1 cell population becomes dominant population of the cells again.

These results demonstrated that butyrate blocks the cells at an early stage in G1 and prevents their cell cycle progression. Once released from butyrate, the cell cycle block was reversed and the cells progressed in synchrony into the next cell cycle phases. It took about 8 h to complete the S phase and about 20 h for one cycle of cell division in MDBK cells.

## 4. Notes

1. The study was undertaken in order to examine the cell cycle characteristics of the Madin Darby Bovine Kidney (MDBK) cell line after culture in the presence of 10 mM butyrate.

The study demonstrated that the Madin Darby Bovine Kidney (MDBK) cells, a commonly used cell line in veterinary research, can be effectively synchronized at the G1 phase using butyrate (4). However, since different cells may respond to butyrate differently, a titration must be performed to optimize the condition and dosage of butyrate.

2. There are also significant (from 10 to 15% of total cell population) M/G2 cell populations accumulated after the butyrate treatment. However, by vigorously tapping the flasks 10 times to remove any loosely attached mitotic cells before collecting the cells by trypsinization, one can reduce the M/G2 population.
3. Among the most common experimental approaches to cell cycle study is to arrest cell growth using incubation in a low-serum medium or a cell cycle inhibitor such as aphidicolin. It is generally accepted that serum deprivation produces cell arrest at a point in the G1 phase (6). Aphidicolin is a DNA synthesis inhibitor that blocks the cell cycle at the very early S phase (not at the G1/S boundary) by inhibiting the activity of the DNA polymerase α complex in eukaryotic cells (7, 8). Nocodazole, an inhibitor of microtubule formation, has been extensively used for cell synchronization for many different cell types (9, 10). Nocodazole-treated cells gradually progress into mitosis, but without cell division. After a short treatment of 3–4 h, accumulated M phase cells can be collected by shake-off. With these time points for comparison, we have also clearly shown that the major population of butyrate-treated cells is arrested at the very early G1 phase, possibly immediately after mitosis, and some cells may be in G0. Because G1 is a decisive stage for the capacity of cells to progress in the cell cycle, butyrate can be an invaluable tool to study cell cycle regulatory events.

## References


1. Futcher, B. (1999) Cell cycle synchronization. *Methods Cell Sci.* **21**, 79–86.
2. Uzbekov, R., Chartrain, I., Philippe, M., and Arlot-Bonnemains, Y. (1998) Cell cycle analysis and synchronization of the *Xenopus* cell line XL2. *Exp. Cell Res.* **242**, 60–68.
3. Levenson, V., and Hamlin, J. L. (1993) A general protocol for evaluating the specific effects of DNA replication inhibitors. *Nucleic Acids Res.* **21**, 3997–4004.
4. Li, C. J., and Elsasser, T. H. (2005) Butyrate-induced apoptosis and cell cycle arrest in bovine kidney epithelial cells: involvement of caspase and proteasome pathways. *J. Anim. Sci.* **83**, 89–97.
5. Sun, W. H., and DePamphilis, M. L. (2004) Methods for detecting cells in S phase. *Methods Mol. Biol.* **241**, 37–53.
6. Cooper, S., and Shedden, K. (2003) Microarray analysis of gene expression during the cell cycle. *Cell Chromosome* **2**, 1.
7. Kobayashi, T., Rein, T., and DePamphilis, M. L. (1998) Identification of primary initiation sites for DNA replication in the hamster dihydrofolate reductase gene initiation zone. *Mol. Cell. Biol.* **18**, 3266–3277.
8. Li, C. J., Bogan, J. A., Natale, D. A., and DePamphilis, M. L. (2000) Selective activation of pre-replication complexes *in vitro* at

specific sites in mammalian nuclei. *J. Cell Sci.* **113**, 887–898.
9. Li, C. J., and DePamphilis, M. L. (2002) Mammalian Orc1 protein is selectively released from chromatin and ubiquitinated during the S-to-M transition in the cell division cycle. *Mol. Cell. Biol.* **22**, 105–116.
10. Mendez, J., Zou-Yang, X. H., Kim, S. Y., Hidaka, M., Tansey, W. P., and Stillman, B. (2002) Human origin recognition complex large subunit is degraded by ubiquitin-mediated proteolysis after initiation of DNA replication. *Mol. Cell* **9**, 481–491.

# Chapter 9

# Analysis of Nuclear Uracil–DNA Glycosylase (nUDG) Turnover During the Cell Cycle

**Jennifer A. Fischer and Salvatore Caradonna**

## Abstract

Uracil–DNA glycosylases (UDG/UNG) are enzymes that remove uracil from DNA and initiate base-excision repair. These enzymes play a key role in maintaining genomic integrity by reducing the mutagenic events caused by G:C to A:T transition mutations. The recent finding that a family of RNA editing enzymes (AID/APOBECs) can deaminate cytosine in DNA has raised the interest in these base-excision repair enzymes. The methodology presented here focuses on determining the regulation of the nuclear isoform of uracil–DNA glycosylase (nUDG), a 36,000 Da protein. In synchronized HeLa cells, nUDG protein levels decrease to barely detectable levels during the S phase of the cell cycle. Immunoblot analysis of immunoprecipitated or affinity-isolated nUDG reveals ubiquitin-conjugated nUDG when proteolysis is inhibited by agents that block proteasomal-dependent protein degradation.

**Key words:** Uracil–DNA glycosylase, cell cycle, ubiquitin conjugation, immunoprecipitation, cell transfection.

## 1. Introduction

Research concerning the removal of uracil moieties from DNA and the subsequent repair has been an area of interest to a number of investigators. Uracil misincorporation and cytosine deamination are potentially mutagenic events that can occur with significant frequency under various cellular conditions. Thus to preserve genomic integrity, it is critical that the cell contains enzymes to recognize and repair this damage (1). Uracil–DNA glycosylases catalyze the first step in the base-excision repair pathway to remove uracil from DNA. In mammalian cells there are at least three structurally distinct families of UDGs (2). These

G. Banfalvi (ed.), *Cell Cycle Synchronization*, Methods in Molecular Biology 761,
DOI 10.1007/978-1-61779-182-6_9, © Springer Science+Business Media, LLC 2011

enzymes hydrolyze the *N*-glycosyl bond between the uracil base and the deoxyribose moiety. The resulting apyrimidinic site is then repaired by the sequential actions of an AP endonuclease, phosphodiesterase, DNA polymerase, and DNA ligase (3).

The discovery that regulated generation of uracil in DNA is part of certain cellular processes has raised awareness of this base-excision repair pathway. B lymphocytes require the generation of G:U mismatches in selected regions of immunoglobulin genes to promote both somatic hypermutation and class-switch recombination (4, 5). Activation-induced cytidine deaminase (AID), which is specific for B cells, is required for both processes in maturing lymphocytes.

Cytosine deamination to uracil in DNA appears to be a form of innate immunity to HIV infection. Using a murine leukemia virus model system Harris and coworkers show that the CEM15/APOBEC3G DNA deaminase can be packaged into virions during virus production (6). The presence of this APOBEC family member triggers deamination of cytosine to uracil within the virus minus-strand cDNA after infection and during retroviral replication. This was shown to lead to HIV genome destruction, possibly due to uracil–DNA glycosylase action on the overabundance of uracil moieties. Research in our laboratory has focused on the post-translational mechanisms that alter the stability of the nuclear isoform of UDG (nUDG, UNG2). We have shown that nUDG turnover is a function of cell cycle phase and in certain cell lines a function of drug-induced stress during DNA replication (7, 8).

## 2. Materials

### 2.1. Cell Culture

1. Dulbecco's modified Eagle's medium (DMEM) containing 10% fetal bovine serum (FBS) both purchased from GIBCO/Invitrogen. Sodium pyruvate is added to 1 mM Dulbecco's phosphate-buffered saline (PBS), Trypsin/EDTA (0.25%/1 mM).
2. The HeLa S3 cell line (CCL2.2) was obtained from the American Type Culture Collection and the 293H (11631-017) cell line was purchased from Invitrogen Corp.
3. Mycoplasma PCR Detection Kit (MP0035).

### 2.2. Reagents Used in Cell Synchronization

1. Nocodazole is dissolved in dimethyl sulfoxide (DMSO) to a final concentration of 1 mg/ml. The solution is stored at –20°C in aliquots and used within 1 year.

2. Aphidicolin is dissolved in DMSO to a final concentration of 1 mg/ml. Aliquots are stored at –20°C and used within 2 months.
3. *N*-acetyl-leu-leu-Norleu-al (LLnL, Sigma A6185) is dissolved in DMSO at a final concentration of 10 mM. Aliquots are stored at –20°C and used within 1 month. Carbobenzoxy-L-leucyl-L-leucyl-L-leucinal (Z-LLL-CHO, MG132, 474790) is purchased from Calbiochem and dissolved in DMSO at a final concentration of 10 mM. Aliquots are stored at –20°C and used within 1 month.
4. [Methyl-$^3$H]-thymidine is purchased from PerkinElmer (81.5 Ci/mmol, 1 μCi/μl). Stocks are stored at +4°C in airtight containers. Trichloroacetic acid (TCA) is dissolved in $H_2O$ to make a 100% solution (i.e., 500 g TCA plus 227 ml $H_2O$). Solution is stored at +4°C and diluted as needed. GF/C (Z242349 Whatman glass microfiber filters, 2.5 cm) were used.

### 2.3. Protein Extraction, SDS-PAGE, and Western Blotting

1. NP40 extraction buffer (for extraction of proteins from cells): 50 mM Tris–HCl, pH 7.5, 250 mM NaCl, 0.1% NP40, 5 mM EDTA, and 50 mM sodium fluoride. Calbiochem protease inhibitor cocktail set III, EDTA-free and Calbiochem phosphatase inhibitor cocktail set III. Bio-Rad protein assay dye reagent concentrate. Bovine serum albumin (BSA) was used for standard curve in protein determination.
2. Polyacrylamide gel solutions: 40% ProtoGel (37.5:1 acrylamide:bisacrylamide), 4X Resolving Buffer (separating gel), ProtoGel Stacking Buffer (stacking gel). *N*-,*N*-,*N*′-,*N*′-tetramethylethylenediamine (TEMED), molecular biology grade. 10% ammonium persulfate (electrophoresis grade) made up fresh on a weekly basis. SDS-PAGE sample loading buffer (3X stock concentrations): 240 mM Tris–HCl pH 6.8, 6% SDS, 30% glycerol, and 0.6 mg/ml bromophenol blue. 2-Mercaptoethanol (BME), electrophoresis grade. Running buffer (5X stock diluted to 1X the day of use). 5X stock (4 l, stored at room temperature): 60 g Tris base, 288 g glycine, and 20 g SDS (all reagents electrophoresis grade). Prestained protein molecular weight markers: Fermentas Spectra Multicolor Broad Range Protein Ladder.
3. Protein transfer and immunostaining. Blotting membrane: InVitrolon PVDF membrane from Invitrogen. Whatman 3MM chromatography paper.

Transfer (Electroblot) buffer, 1X (for 5 l): 15.15 g Tris base, 72 g glycine, and 1 l methanol. Transfer buffer is made up and stored at 4°C in a carboy. 10X TBS (Tris-buffered saline, for 1 l): 100 ml

of 1 M Tris–HCl, pH 8.0, 87.66 g NaCl, volume brought to 1 l and stored at 4°C. TBST (Tris-buffered saline plus Tween-20): Make up 4 l and store at 4°C (use within a month). 400 ml 10X TBS and 2 ml Tween-20. We cut the tips off a 1 ml pipet tip, slowly pipet the Tween-20 into the stirring solution, and let the tips swirl in the solution to remove remaining detergent. Bring the volume up to 4 l.

TBST–5% skim milk block: 5 g of non-fat skim milk in 100 ml of TBST. Make this up fresh daily. There is a high degree of variability in background levels due to non-fat skim milk from different commercial vendors. We use Carnation packets or Non-fat dry milk from Cell Signaling Technology Corp. Polyclonal AU1 antibody is from Covance Corp. Ab225 antibody against the amino-terminal end of nUDG is prepared for us by Covance Corp. using our bacterially expressed protein. Detection of immunostaining is done using Amersham's ECL Western Blotting Detection Reagents.

### 2.4. Ubiquitination of nUDG

1. pCINeo vector is purchased from Promega Corp. Lipofectamine 2000 is purchased from Invitrogen. Primers for cloning are purchased from Integrated DNA Technologies.
2. NiNTA-agarose is purchased from Qiagen Corp. Buffer A: 6 M guanidine-HCl, 0.1 M sodium phosphate, and 10 mM imidazole, pH 8.0. Buffer TI: 25 mM Tris–HCl, 20 mM imidazole, pH 6.8.

## 3. Methods

### 3.1. Maintenance of Cell Cultures

1. HeLa S3 cells are maintained in DMEM media supplemented with 10% calf serum. Cells are cultured in a humidified atmosphere of 5% $CO_2$ at 37°C. 293H cells and HT-29 cells are maintained in DMEM media supplemented with 10% fetal calf serum. We routinely passage cells at 3–4 day intervals, reseeding flasks at a 1–10 dilution. Cells are not carried for more than 10–15 passages and are not allowed to become totally confluent. We do not use antibiotics (*see* **Note 1**).
2. The day before the experiment, cells are seeded into dishes. For experiments requiring 6 cm dishes, cells are seeded at between 1 and $2 \times 10^6$ per dish. For 10 cm dishes cells are seeded at between 5 and $6 \times 10^6$ per dish. Experiments are carried out using the growth conditions described above.

### 3.2. Synchronization of Cells at Different Points in the Cell Cycle

1. To arrest cells at the $G_2$/M border, HeLa S3 cells are treated with 100 ng/ml of nocodazole for times ranging from 12 to 20 h (*see* **Note 2**).
2. Cells are released from nocodazole block by washing twice in media free of the drug. Cells will tend to float off the surface at this point so it is essential to wash the cells off the surface using a sterile pipet and spinning the cells down, washing again and pelleting the cells. Cells are replated and immediately placed in the incubator (*see* **Note 3**).
3. Individual plates are harvested at the appropriate times. Since at the early time points cells have not adhered they are harvested in the media, spun down, and washed once in ice-cold PBS. Cells are pelleted by centrifugation, the wash is aspirated, and the pellets are frozen at –80°C until extraction (*see* **Note 3**).
4. To synchronize cells at the $G_1$/S border, HeLa S3 cells are treated with aphidicolin at a final concentration of 5 μg/ml for 20 h.
5. After this time period, cells are washed three times with complete media minus the drug. Media is added and cells allowed to incubate for the appropriate time intervals before harvesting. Since aphidicolin does not disrupt adherence to the plates, washing of cells is done on the plates without the need for centrifugation.
6. To examine the post-translational fate of nUDG prior to proteolysis, cells are treated with inhibitors to prevent proteasomal degradation. Cells are treated with 100 ng/ml of nocodazole for 6 h and then treated with either LLnL at 50 μM or MG132 at 25 μM for an additional 6 h. At the appropriate time the cells are harvested as described above (*see* **Note 4**).
7. A convenient method to monitor progression through S phase is by pulse-labeling individual cultures with [$^3$H]-thymidine at time intervals that correspond to the experimental time points (*see* **Note 5**). Plates are seeded and treated as appropriate, outlined above. At individual time points 10 μCi of [$^3$H]-thymidine is added to the cell culture and incubated for 30 min. After this time the cells are washed once with ice-cold PBS, scraped, and pelleted by centrifugation. The cell pellet is resuspended in 400 μl of PBS and 100 μl of 10% TCA. The mixture is incubated on ice for 15 min and then filtered through a pre-wet (10% TCA) GF/C filter on an appropriate filtration apparatus. The filter is washed with 10 ml of 10% ice-cold TCA and finally with 1–2 ml of 100% acetone. Filters are dried and counted.

### 3.3. Protein Analysis by SDS-PAGE and Western Blot

1. Cell extracts are prepared in NP40 buffer containing Calbiochem protease inhibitor cocktail set III (1–200 dilution) and 1 mM PMSF as well as Calbiochem phosphatase inhibitor cocktail set III (1–200 dilution). The –80°C stored pellets are resuspended directly in prepared NP40 buffer and sonicated using a Branson sonifier and cup horn, 90% pulse, and mid-range intensity setting. The extract is pulsed 8–10 times and incubated on ice for 30 min. After this period the extract is centrifuged in a microfuge, top speed for 5 min. The supernatant is reserved for further use and the pellet is stored at –80°C (*see* **Note 6**). Total protein concentration per sample is determined using the BioRad Bradford protein assay reagent and BSA for the standard curve.
2. The BioRad SDS-PAGE Mini-PROTEAN Electrophoresis Cell is routinely used and polyacrylamide reagents from National Diagnostics. Glass plates are washed with glass detergent dried and cleaned with 100% ethanol and dried. The apparatus is put together and a mark is made to indicate the height of the separating gel (usually 1.75 cm from the shorter glass plate). Formulation for 12% separating gel utilizes per 10 ml, 3 ml of 40% ProtoGel (37.5:1 acrylamide:bisacrylamide), 2.5 ml of 4X resolving buffer, and 4.4 ml of $H_2O$. The solution is degassed for 5 min by using a rubber stopper with a cut plastic pipet through the hole. House vacuum is applied to the stoppered 50 ml flask. Polymerization is initiated with the addition of 0.10 ml of 10% (w/v) ammonium persulfate (made fresh weekly) and 0.01 ml of TEMED. Working quickly at this point, the solution is poured between the glass plates with a plastic pipet up to the mark. This solution is overlaid with water-saturated butanol to a depth of 1–2 mm. Polymerization can be seen within 15 min. After 30 min the (4%) stacking gel is prepared using per 10 ml, 1.0 ml of 40% ProtoGel, 2.8 ml of ProtoGel Stacking Buffer, and 6.1 ml of $H_2O$. The solution is degassed as described above and polymerization initiated by the addition of 0.05 ml fresh ammonium persulfate and 0.01 ml of TEMED. The overlay is removed, stacking gel is poured in using a plastic pipet, and a comb is slowly inserted at an angle, to avoid trapping of bubbles (*see* **Note 7**). Gels are allowed to set for a minimum of 1 h before placing in the buffer tank apparatus. Gels can be stored overnight wrapped in parafilm with the comb still in the stacking gel.
3. Appropriate volumes of extract, based on total protein, are mixed with either 2X or 3X SDS-PAGE buffer and 1% BME. The samples are heated to 80°C for 5 min and briefly centrifuged. During this time the polyacrylamide gel is

assembled into the buffer tank assembly with the comb still in place. Running buffer is added and the comb is gently removed allowing the running buffer to enter the wells. The wells are washed out using a plastic pipet, slowly pipeting up and down. Samples are loaded and appropriate protein markers are used. We routinely use prestained markers (Fermentas) which makes it easy to monitor progress of electrophoresis and orientation of the gel and the blot throughout the procedure. Electrophoresis is conducted at 150–200 V, until the dye is at the bottom or just run off (usually around an hour to an hour and a half).

4. Transfer of proteins, subsequent to SDS-PAGE fractionation, to a solid support is accomplished using a Mini Trans-Blot Cell from BioRad. The electrophoretic apparatus is taken apart and the gel carefully removed from the plates. Stacking gel is removed with a single-edged razor and the gel is soaked in cold transfer buffer for 5 min at room temperature with gentle rocking (*see* **Note 8**). During this time a piece of PVDF (*see* **Note 9**) membrane is removed, wetted in methanol, and soaked in a tray of transfer buffer (insure that the membrane is submerged by rocking the tray). A second tray is set up containing the gel holder cassette (black side down). A 1 l beaker of cold transfer buffer is placed near the tray and used to wet the sponges and the 3MM paper. Lay down a wetted sponge and three pieces of wetted 3MM paper (two come with the PVDF) in this order. Using a cut plastic 10 ml pipet (size should be a little longer than the cassette, lengthwise) roll over the paper and insure that all bubbles are out. Place the soaked polyacrylamide gel on the 3 MM paper (top side toward you). Roll the gel out gently to remove all air bubbles. Carefully place the wet PVDF membrane on the gel. Again gently roll all air bubbles out (*see* **Note 10**). Place one piece of wet 3MM paper on the PVDF, gently roll over the surface again, turn the gel 90°, and roll out the air bubbles from this direction. Carefully place the second wetted sponge on top. Close and lock the cassette. Place the frozen ice-block container (stored at –80°C containing $H_2O$ to three-quarters full) in the tank, add a small stir bar, and add transfer buffer to about 75% full (it helps to have a third tray under the transfer tank to collect any spillover and avoid electrical issues once on the stir plate). Carefully place the cassette in the tank (black to back). Connect the lid making sure the red electrode is on the red side and the black electrode is on the black side. Run the transfer at 100 V for 1 h with stirring. A power supply that maintains about 200 mA is required. Insure that the amperage is registering. If it is not the

connections are faulty. Under these conditions the temperature of the transfer is between 10 and 15°C for the whole run.

5. After the run the PVDF membrane is submerged in TBS and transferred to 5% skim milk in TBST. The membrane is blocked for 30 min at room temperature with rocking. The blocking solution is discarded and a new block is added to the tray containing the membrane. Primary antibody is added at a dilution that is dependent on the antibody. Appropriate dilutions should be determined empirically for the particular protein species being examined. Incubation is done overnight at room temperature with rocking. A 0.01% thimerosal is included in the overnight incubation to prevent growth of any bacterial contamination. After the incubation period the membrane is washed in TBST twice and then incubated in TBST for 5 min with rocking. This is repeated twice more. The membrane is again blocked in 5% skim milk/TBST for 15–20 min, the block is discarded, and secondary antibody is added with new blocking solution. The membrane is incubated for 1 h at room temperature with rocking. The washing steps are repeated exactly as above. The membrane is placed in TBS and rocked while the ECL developing solution is prepared. The membrane and the tray are emptied of TBS and shaken to remove as much liquid as possible. The membrane is then incubated with 4 ml of ECL solution for 1 min. The membrane is gently shaken and laid on a piece of saran wrap transfer side down (the side that touched the polyacrylamide gel). The membrane is wrapped in the saran wrap and taped (transfer side up) in an appropriate x-ray cassette or holder such as technal poof-printer (*see* **Note 11**). Tape the wrapped membrane and transfer side up on the inside glass of the proof-printer along with a fluorescent ruler (used to align the gel and the film). Expose to film in an appropriate dark room by placing the film on the membrane and closing the proof-printer and applying even pressure. Make sure the correct film side is in contact with the membrane. Develop the film in an x-ray processor. Use the imprint of the ruler on the film to correctly align the colored markers on the membrane. Examples of these procedures are illustrated in **Figs**. **9.1** and **9.2**.

### *3.4. Determination of nUDG Ubiquitination in Cells as a Function of the Cell Cycle*

1. For ectopic expression of nUDG, a eukaryotic expression vector is constructed to contain the open reading frame of nUDG. The DNA containing the open reading frame is cloned into the pCINeo vector.
2. The protein is designed to contain an in-frame epitope tag at the C-terminus of the protein. PCR and appropriate primers

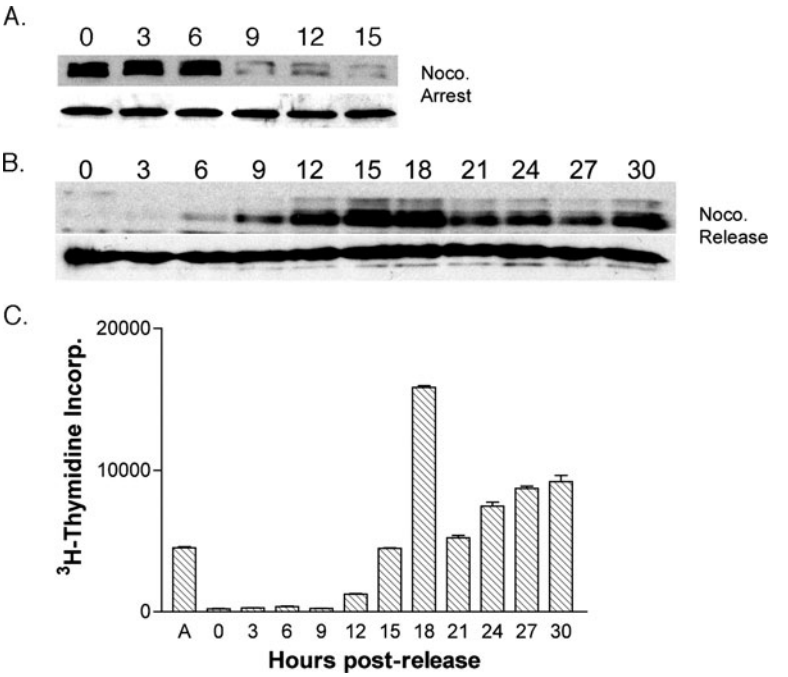


Fig. 9.1. Analysis of the steady-state levels of nUDG during nocodazole block and release. (**a**) HeLa cells were incubated with nocodazole and harvested at 3 h intervals post-arrest (indicated by *numbers* above each lane). Immunoblot analysis was performed using equivalent amounts of cell extract to detect nUDG protein levels at the indicated times. As a control to insure that equivalent amounts of protein were applied to each lane, the nitrocellulose was stripped of antibody and reprobed with antisera against glyceraldehyde-3-phosphate dehydrogenase (GAPDH). As seen in the *lower panel* of (**a**), equivalent amounts of total protein were applied per lane. (**b**) HeLa cells were treated with nocodazole for 12 h. The drug was then removed and the cells were released from $G_2$/M phase arrest. Extracts from cells harvested at 3 h intervals post-release were analyzed by Western blot. The numbers above each lane indicate hours post-release. *Lower panel*: GAPDH immunostain loading control. (**c**) To verify that release from nocodazole block occurred when the drug was removed, parallel cultures ($2 \times 10^5$ cells per 6 cm dish) were pulse-labeled with $^3$H-thymidine and the DNA extracted and analyzed for $^3$H-dTMP incorporation. Cells were treated for 12 h with nocodazole. The cells were then washed twice with media free of nocodazole and at the indicated times (in hours), cells were harvested and incorporation (reported as cpm $\times 10^{-3}$) was determined. "A" indicates a 20 min labeling of an asynchronous population of HeLa cells. 0 hour indicates a 20 min pulse immediately after nocodazole release. Values indicate the means averaged from triplicate pulse-labeled cultures.

are used to incorporate the epitope tag (DTYRYI) at the 3′ end of the sequence. This epitope is recognized by the antibody, AU1 (*see* **Note 12**).

3. A eukaryotic expression vector, that contains a His-tagged ubiquitin construct, was generously provided by Dr. Dirk Bohmann (*see* **Note 13**). The vector consists of a CMV promoter/enhancer region driving the transcription of an

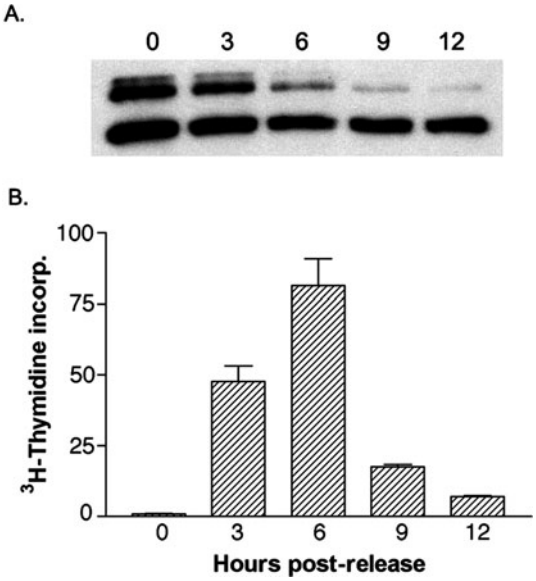


Fig. 9.2. Analysis of steady-state levels of nUDG during release from an aphidicolin block. (**a**) HeLa cells were treated with aphidicolin for 18 h. Cells were then washed three times with DMEM minus serum. Complete media was added and cells were harvested at the indicated times in hours. Western blot analysis was then performed on cell extracts using antisera (C8) that recognizes both forms of UDG (nuclear and mitochondrial). As seen in the figure, the upper bands (nUDG) significantly diminish by 6 h post-release from aphidicolin block. In contrast the lower band (mitochondrial UDG) maintains a relatively constant level up to 12 h post-release. (**b**) Parallel cultures ($1 \times 10^6$ cells per 10 cm dish) were pulse-labeled with $^3$H-thymidine at the indicated hours post-release from the aphidicolin block. The cells were harvested and the DNA was extracted and analyzed for $^3$H-dTMP incorporation (reported as cpm $\times 10^{-3}$). Values indicate the means averaged from triplicate pulse-labeled cultures.

mRNA encoding a multimeric precursor protein composed of eight ubiquitin units with an amino-terminally added pHis tag (six histidine residues, pMT107) to each ubiquitin unit (9).

4. The constructs are transiently cotransfected into 293H cells using lipofectAMINE 2000. Twenty four hours prior to transfection, 293H cells are plated in 6 cm dishes at $2 \times 10^6$ cells/dish. Cells are transfected with 3 μg of nUDG construct (vector alone or AU-tagged nUDG) and 5 μg of pMT107. Cells are allowed to incubate with the DNA complexes for 24 h. The media is then changed and in selected plates the proteasome inhibitor, MG132, is added to a final concentration of 25 μM. Cells are incubated for an additional 12 h before harvesting. Cells are scraped into cold PBS and pelleted.
5. To detect pHis-Ub-conjugated UDG1A, the procedures as outlined by the Tansey laboratory are followed (10). Cell

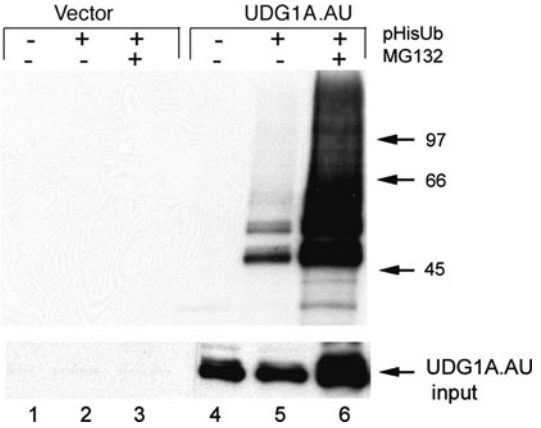


Fig. 9.3. *In vivo* ubiquitination of epitope-tagged nUDG. AU-tagged nUDG containing plasmid constructs were co-transfected with pHis-tagged ubiquitin plasmid constructs as described in experimental procedures. Extracts derived from transfected cells were subjected to Ni-NTA agarose affinity fractionation under denaturing conditions. Fractionated protein was analyzed by Western blot using AU1 antibody as probe. *Lower panel* – total cell extracts, prior to Ni-NTA fractionation, were analyzed for AU-tagged nUDG expression by Western blot analysis. About 10% of the extracts used as input for fractionation are represented here.

pellets are resuspended in buffer A, sonicated, and allowed to bind to Ni-NTA agarose for 3 h at room temperature. The agarose is washed with buffer A, buffer A/buffer TI, and buffer TI. The protein–agarose complex is resuspended in SDS-PAGE buffer and proteins analyzed by Western blot using AU1 antibody. Typical results from this procedure are presented in **Fig. 9.3**.

## 4. Notes

1. Stocks of cells used in the lab are routinely banked at an early passage after being tested for mycoplasma contamination using PCR methods.
2. Insure that chemical inhibitors are used before the expiration date as stated by the company for the particular solution or dry form.
3. Be consistent throughout the protocol. If you wash the cell monolayer on the plate do this throughout the time course. If cells come off the plate and have to be washed in suspension, do this for all the points in the time course.
4. These inhibitors produce a significant percentage of cell death. Drugs should be titered for the particular cell line to

minimize cell killing and still produce the desired response (i.e., inhibition of proteolysis).

5. The down side to these experiments is the need to use radioactivity. All appropriate protection and approvals must be in place before using even low-energy radioactivity. Cell cytometry can be a replacement protocol. Most universities have central facilities for cell cycle analysis.
6. Initial experiments need to establish correct fractionation of the protein of interest under every condition tested. The bulk of nUDG is readily extracted into the supernatant under these procedures at all the time points. However, a small consistent fraction does remain in the pellet.
7. Acrylamide is a neurotoxin and should be treated as such. Adjust volumes as appropriate for the particular apparatus being used.
8. Besides the toxicity of acrylamide, finger prints leave proteins behind that can obscure results, particularly when using sensitive systems such as ECL; wear gloves for all gel and membrane handling.
9. Nitrocellulose can also be used. PVDF appears more stable for stripping and reprobing. It is also more useful when proteins are further analyzed (i.e., mass spectrometry).
10. Take great care to remove bubbles because transfer is interrupted if air is trapped between the gel and the membrane. This usually occurs right at the spot of your protein of interest.
11. Technal proof-printer: http://www.kpsurplus.com/products/view/12208
12. When reverse translating from amino acid sequence to nucleotide sequence (i.e., codons for DTYRYI) make sure to check with codon usage charts for the particular species that will be expressing this protein. Choose the codon with the highest percentage used by that species.
13. Expression vectors obtained from other labs should be checked either by restriction mapping, sequence analysis, or transient transfection and Western blot analysis before being used in further experiments.

## References

1. Lindahl, T., and Wood, R. D. (1999) Quality control by DNA repair. *Science* **286**, 1897–1905.
2. Pearl, L. H. (2000) Structure and function in the uracil-DNA glycosylase superfamily. *Mutat. Res.* **460**, 165–181.
3. Krokan, H. E., Standal, R., and Slupphaug, G. (1997) DNA glycosylases in the base excision repair of DNA. *Biochem. J.* **325**, 1–16.
4. Rada, C., Williams, G. T., Nilsen, H., Barnes, D. E., Lindahl, T., and Neuberger, M. S. (2002) Immunoglobulin isotype switching

is inhibited and somatic hypermutation perturbed in UNG-deficient mice. *Curr. Biol.* **12**, 1748–1755.
5. Di Noia, J., and Neuberger, M. S. (2002) Altering the pathway of immunoglobulin hypermutation by inhibiting uracil-DNA glycosylase. *Nature* **419**, 43–48.
6. Harris, R. S., Sheehy, A. M., Craig, H. M., Petersen-Mahrt, S. K., Watt, I. N., Neuberger, M. S., and Malim, M. H. (2003) DNA deamination mediates innate immunity to retroviral infection. *Cell* **113**, 803–809.
7. Fischer, J. A., Muller-Weeks, S., and Caradonna, S. (2004) Proteolytic degradation of the nuclear isoform of uracil-DNA glycosylase occurs during the S phase of the cell cycle. *DNA Repair* (Amst) **3**, 505–513.
8. Fischer, J. A., Muller-Weeks, S., and Caradonna, S. J. (2006) Fluorodeoxyuridine modulates cellular expression of the DNA base excision repair enzyme uracil-DNA glycosylase. *Cancer Res.* **66**, 8829–8837.
9. Treier, M., Staszewski, L. M., and Bohmann, D. (1994) Ubiquitin-dependent c-Jun degradation in vivo is mediated by the delta domain. *Cell* **78**, 787–798.
10. Salghetti, S. E., Kim, S. Y., and Tansey, W. P. (1999) Destruction of Myc by ubiquitin-mediated proteolysis: cancer-associated and transforming mutations stabilize Myc. *EMBO J.* **18**, 717–726.

# Chapter 10

# Synchronization of HeLa Cells

**Hoi Tang Ma and Randy Y.C. Poon**

## Abstract

HeLa is one of the oldest and most commonly used cell lines in biomedical research. Owing to the ease of which they can be effectively synchronized by various methods, HeLa cells have been used extensively for studies of the cell cycle. Here we describe several protocols for synchronization of HeLa cells from different phases of the cell cycle. Synchronization in $G_1$ phase can be achieved with the HMG-CoA reductase inhibitor lovastatin, S phase with a double thymidine block procedure, and $G_2$ phase with the CDK inhibitor RO3306. Cells can also be enriched in mitosis by treating with nocodazole and mechanical shake-off. Release of the cells from these blocks enables researchers to follow gene expression and other events through the cell cycle. We also describe several protocols, including flow cytometry, BrdU labeling, immunoblotting, and time-lapse microscopy, for validating the synchrony of the cells and monitoring the progression of the cell cycle after release.

**Key words:** Cell cycle, cyclin, cyclin-dependent kinases, flow cytometry, synchronization.

## 1. Introduction

HeLa is one of the oldest and most commonly used cell lines in biomedical research. The cell line was originally derived from human cervical carcinoma taken from an individual named Henrietta Lacks (1). Due to the presence of the human papillomaviruses E6 and E7 proteins, proper control of both cell cycle checkpoints and apoptosis is impaired (2). Partly due of this, HeLa cells are relatively easy to be synchronized by many methods, making them good model systems for studying cell cycle regulation. In addition to looking at individual gene products, whole genome approaches have been performed using synchronized HeLa cells, including microarray analysis of gene expression (3, 4), miRNA expression

G. Banfalvi (ed.), *Cell Cycle Synchronization*, Methods in Molecular Biology 761,
DOI 10.1007/978-1-61779-182-6_10, 

patterns (5), as well as proteomic analysis of protein modifications (6).

Synchronization involves the isolation of cells in specific cell cycle phases based on either physical properties or perturbation of cell cycle progression with biochemical constraints. Methods based on physical characteristics have the advantage that cells are not exposed to pharmacological agents. For example, centrifugal elutriation can be used to separate cells from different points of the cell cycle based on cell size (7, 8). A major limitation of this method is that specially designated equipments are required.

Several chemicals are effective for synchronization because they are able to reversibly inhibit unique steps of the cell cycle. Releasing the blockade allows the population to progress synchronously into the cell cycle. Although these synchronizations are relatively easy to perform, a caveat is that gene expression and post-translational modifications may be altered after blocking the cell cycle, making them very different from that of the unperturbed cell cycle. Another limitation of synchronization using chemicals is that while synchrony is good immediately after the time of release, it deteriorates progressively at later time points. Therefore, experiments should ideally be designed to use more than one synchronization methods from different parts of the cell cycle.

We describe below protocols for blocking HeLa cells in $G_1$ phase, S phase, $G_2$ phase, or mitosis, and for releasing them synchronously into the cell cycle. Unlike cells such as fibroblasts, HeLa cells cannot be synchronized at $G_0$ with methods based on serum starvation or contact inhibition.

To trap HeLa cells in S phase, inhibitors of DNA synthesis including thymidine, aphidicolin, and hydroxyurea are frequently used. High concentration of thymidine interrupts the deoxynucleotide metabolism pathway, thereby halting DNA replication. As treatment with thymidine arrests cells throughout S phase, a double thymidine block procedure (which involves releasing cells from a first thymidine block before trapping them with a second thymidine block) is generally used to induce a more synchronized early S phase blockade.

Cyclin-dependent kinase 1 (CDK1) is the key engine that drive cells from $G_2$ phase into mitosis. Accordingly, inhibition of CDK1 activity with a specific inhibitor called RO3306 blocks cells in $G_2$ phase (9). As RO3306 is a reversible inhibitor, the cells can then be released synchronously into mitosis when the drug is washed out.

In HeLa cells, mitosis typically only lasts for 40–60 min. But cells can be trapped in mitosis by the continued activation of the spindle-assembly checkpoint. The checkpoint is activated by unattached kinetochores or the absence of tension between the paired kinetochores. Hence spindle poisons such as nocodazole

(which prevents microtubule assembly) can activate the checkpoint and trap cells in a prometaphase-like state. Several critical factors should be considered when using nocodazole to synchronize HeLa cells. As nocodazole displays a relatively high cytotoxic activity, it is used in combination with other synchronization methods (such as the double thymidine block described here) to minimize the incubation time. Furthermore, as nocodazole-blocked cells can exit mitosis precociously by mitotic slippage, the synchronization protocol also relies on the isolation of mitotic cells based on their physical properties (by using mechanical shake-off). In fact, mechanical shake-off is one of the oldest synchronization procedure devised for mammalian cells (10).

Finally, the method described here for synchronizing HeLa cells in $G_1$ phase is based on lovastatin. Lovastatin is an inhibitor of HMG-CoA reductase (11, 12), an enzyme which catalyzes the conversion of HMG-CoA to mevalonate. Cells are released from the lovastatin-mediated blockade by the removal of lovastatin and addition of mevalonic acid (mevalonate).

An important aspect of synchronization experiments is to validate the degree of synchronization and to monitor the progression of cells through the cell cycle. Here we describe protocols for analyzing the cell cycle by flow cytometry after propidium iodide staining. This provides basic information about the DNA contents of the cell population after synchronization. A more accurate method of cell cycle analysis based on BrdU labeling and flow cytometry is also detailed below. Biochemically, cell-free extracts can be prepared and the periodic fluctuation of cell cycle markers can be analyzed by immunoblotting. Finally, fine details of progression through mitosis can be monitored using time-lapse microscopy.

## 2. Materials

### 2.1. Stock Solutions and Reagents

1. BrdU: 10 mM in $H_2O$ (**Note 1**).
2. BrdU antibody (DAKO, Glostrup, Denmark).
3. Cell lysis buffer: 50 mM Tris–HCl (pH 7.5), 250 mM NaCl, 5 mM EDTA, and 50 mM NaF, and 0.2% NP40. Add fresh: 1 mM PMSF, 1 μg/ml leupeptin, 2 μg/ml aprotinin, 10 μg/ml soybean trypsin inhibitor, 15 μg/ml benzamidine, 10 μg/ml chymostatin, and 10 μg/ml pepstatin.
4. Deoxycytidine: 240 mM in $H_2O$.

5. FITC-conjugated rabbit anti-mouse immunoglobulins (DAKO).
6. Lovastatin (Mevinolin): 10 mM (**Note 2**).
7. Mevalonic acid (Sigma): 0.5 M (**Note 3**).
8. Nocodazole (Sigma): 5 mg/ml in DMSO (**Note 1**).
9. PBS (phosphate-buffered saline): 137 mM NaCl, 2.7 mM KCl, 10 mM sodium phosphate dibasic, and 2 mM potassium phosphate monobasic, pH 7.4.
10. PBST: PBS with 0.5% Tween 20 and 0.05% w/v BSA.
11. PI/RNase A solution: 40 μg/ml propidium iodide and 40 μg/ml RNase A in TE (make fresh).
12. Propidium iodide (Sigma): 4 mg/ml in $H_2O$ (**Note 1**).
13. RNase A: 10 mg/ml in 0.01 M NaOAc (pH 5.2); heat to 100°C for 15 min to remove DNase; then add 0.1 volume of 1 M Tris–HCl (pH 7.4).
14. RO3306 (Alexis, SanDiego, CA, USA): 10 mM in DMSO (**Note 4**).
15. SDS sample buffer: 10% w/v SDS, 1 M Tris–HCl (pH 6.8), 50% v/v glycerol, and bromophenol blue (to taste). Add 50 μl/ml 2-mercaptoethanol before use.
16. TE: 10 mM Tris–HCl (pH 7.5) and 0.1 mM EDTA.
17. Thymidine: 100 mM in DMEM (**Note 5**).

### 2.2. Cell Culture

All solutions and equipment coming into contact with the cells must be sterile. Proper sterile technique should be used accordingly:

1. HeLa cells (American Type Culture Collection, Manassas, VA, USA). Cells are grown in a humidified incubator at 37°C in 5% $CO_2$.
2. HeLa cells stably expressing histone H2B-GFP or similar cell lines for live cell imaging.
3. Growth medium: Dulbecco's Modified Eagle Medium (DMEM) containing 10% heat-inactivated calf serum and 30 U/ml penicillin–streptomycin.
4. Trypsin (0.25% with EDTA).
5. Tissue culture plates and standard tissue culture consumables.

### 2.3. Equipments

1. Standard tissue culture facility.
2. Centrifuge that can accommodate 15 and 50 ml centrifuge tubes.
3. Microcentrifuge that can reach 16,000 × *g* at 4°C.

4. Flow cytometer equipped with 488 nm laser.
5. Inverted fluorescence wide-field microscope equipped controlled environment chamber and camera for time-lapse analysis.

## 3. Methods

### 3.1. Synchronization from Early S: Double Thymidine Block

1. Grow HeLa cells in 100-mm plates with 10 ml growth medium to ~40% confluency (*see* **Note 6**).
2. Add 200 μl of 100 mM thymidine (2 mM final concentration).
3. Incubate for 14 h.
4. Aspirate the medium and wash the cells twice with 10 ml PBS.
5. Add 10 ml growth medium supplemented with 24 μM deoxycytidine.
6. Incubate for 9 h.
7. Add 200 μl of 100 mM thymidine.
8. Incubate for 14 h.
9. Aspirate the medium and wash the cells twice with 10 ml PBS.
10. Add 10 ml growth medium supplemented with 24 μM deoxycytidine and return the cells to the incubator.
11. Harvest the cells at different time points for analysis.

Typically, cells are harvested every 2 or 3 h for up to 24 h. This should cover at least one cell cycle. As significant loss of synchrony occurs after one cell cycle, it is not very meaningful to follow the cells with longer time points (*see* **Note 7**).

### 3.2. Synchronization from $G_2$: RO3306

Here we describe a method that involves first blocking the cells with a double thymidine block procedure before releasing them into a RO3306 block. Alternatively, asynchronously growing cells can be treated directly with RO3306 for 16–20 h. The main challenge is that cells can escape the $G_2$ arrest and undergo genome reduplication if they are exposed to RO3306 for a long period of time (13):

1. Synchronize cells at early S phase with the double thymidine block procedure (**Section 3.1**).
2. After release from the second thymidine block, incubate the cells for 2 h.
3. Add RO3306 to 10 μM final concentration (*see* **Note 8**).

4. Incubate for 10 h.
5. Aspirate the medium and wash the cells twice with 10 ml PBS.
6. Add 10 ml of growth medium.
7. Harvest the cells at different time points for analysis.

Cells treated with RO3306 are trapped in late $G_2$ phase. As cells rapidly enter mitosis after release from the block, this synchronization procedure is best suited for studying entry and exit of mitosis. After release from the block, the cells can be harvested every 15 min for up to 4 h. Progression through mitosis can also be tracked with time-lapse microscopy (see below).

### 3.3. Synchronization from Mitosis: Nocodazole

While it is possible to treat asynchronously growing HeLa cells with nocodazole directly, the yield and purity of the mitotic population are rather low. On the one hand, many cells remain in interphase if the nocodazole treatment is too short. On the other hand, cells may undergo mitotic slippage and apoptosis following a long nocodazole treatment. In the method described here, cells were first synchronized with a double thymidine block procedure before releasing into the nocodazole block.

1. Synchronize cells at early S phase with the double thymidine block procedure (**Section 3.1**).
2. After release from the second thymidine block, allow the cells to grow for 2 h.
3. Add nocodazole to a final concentration of 0.1 μg/ml.
4. Incubate for 10 h.
5. Collect the mitotic cells by mechanical shake-off and transfer the medium to a centrifuge tube (*see* **Note 9**).
6. Add 10 ml PBS to the plate and repeat the shake-off procedure.
7. Combine the PBS with the medium and pellet the cells by centrifugation.
8. Wash the cell pellet twice with 10 ml growth medium by resuspension and centrifugation.
9. Resuspend the cell pellet with 10 ml growth medium and put onto a plate.
10. Harvest the cells at different time points for analysis.

### 3.4. Synchronization from $G_1$: Lovastatin

1. Grow HeLa cells in 100-mm plates in 10 ml of growth medium to ~50% confluency.
2. Add 20 μM of lovastatin.
3. Allow the cells to grow for 24 h.
4. Aspirate the medium and wash the cells twice with 10 ml of PBS.

5. Add 10 ml fresh growth medium supplemented with 6 mM mevalonic acid.
6. Harvest the cells at different time points for analysis.

### 3.5. Assessment of Synchronization: Flow Cytometry (Propidium Iodide)

The position of the synchronized cell cycle can be determined by the DNA content of the cells. While $G_1$ cells contain two copies of the halpoid genome (2 N), cells in $G_2$ and mitosis contain four copies (4 N). After staining with propidium iodide, the amount of DNA in cells can be quantified with flow cytometry:

1. Collect medium to a 15-ml centrifugation tube.
2. Wash the plates with 2 ml PBS and combine with the medium.
3. Add 2 ml trypsin and incubate for 1 min.
4. Add back the medium. Dislodge cells from the plate by pipetting up and down.
5. Collect the cells by centrifugation at 1.5 krpm for 5 min.
6. Wash the cells twice with 10 ml of ice-cold PBS containing 1% calf serum by resuspension and centrifugation.
7. Resuspend the cell pellet with the residue buffer (~0.1 ml) (*see* **Note 10**).
8. Add 1 ml cold 80% ethanol dropwise with continuous vortexing.
9. Keep the cells on ice for 15 min (fixed cells can then be stored indefinitely at 4°C).
10. Centrifuge the cells at 1.5 krpm for 5 min. Drain the pellet thoroughly.
11. Resuspend the pellet in 0.5 ml PI/RNase A solution.
12. Incubate at 37°C for 30 min.
13. Analyze with flow cytometry (*see* **Note 11**).

### 3.6. Assessment of Synchronization: Flow Cytometry (BrdU)

The DNA contents of $G_1$ cells (2N) can readily be distinguished from those in $G_2/M$ (4N) by propidium iodide staining and flow cytometry. However, the DNA contents of $G_1$ and $G_2/M$ cells overlap with a significant portion of S phase cells. Cells in early S phase contain DNA contents indistinguishable from $G_1$ cells. Likewise, cells in late S phase contain similar amount of DNA as $G_2/M$ cells. Although several computer algorithms are available to estimate the S phase population from the DNA distribution profile, they at best provide a good approximation. Their use is particularly limiting for synchronized cells. The BrdU labeling method described here provides more precise information on the percentage of cells in $G_1$, S, and $G_2/M$. BrdU (5-bromo-2-deoxyuridine) is a thymidine analogue that can be incorporated into newly synthesized DNA. If a brief pulse of BrdU is used,

only S phase cells will be labeled. The BrdU-positive cells are then detected by antibodies against BrdU:

1. Add 10 μM BrdU at 30 min before harvesting cells at each time point.
2. Harvest and fix cells as described in **Section 3.5** Steps 1–9.
3. Collect the cells by centrifugation at 1.5 krpm for 5 min.
4. Wash the cells twice with 10 ml PBS by resuspension and centrifugation. Remove all supernatant.
5. Add 500 μl of freshly diluted 2 M HCl.
6. Incubate at 25°C for 20 min.
7. Wash the cells twice with 10 ml PBS and once with 10 ml PBST by resuspension and centrifugation.
8. Resuspend the cell pellet with the residue buffer (~0.1 ml).
9. Add 2 μl anti-BrdU antibody.
10. Incubate at 25°C for 30 min.
11. Wash twice with 10 ml PBST by resuspension and centrifugation.
12. Resuspend the cell pellet in the residue buffer (~0.1 ml).
13. Add 2.5 μl of FITC-conjugated rabbit anti-mouse immunoglobulins.
14. Incubate at 25°C for 30 min.
15. Wash the cells once with 10 ml PBST by resuspension and centrifugation.
16. Stain the cells with propidium iodide as described in **Section 3.5** Steps 10–12.
17. Analyze with bivariate flow cytometry.

### *3.7. Assessment of Synchronization: Cyclins*

Another way to evaluate the synchrony of cells is through the detection of proteins that vary periodically during the cell cycle. Given that cyclins are components of the engine that drives the cell cycle, we are using this as an example. Cyclin E1 accumulates during $G_1$ and decreases during S phase. In contrast, cyclin A2 increases during S phase and is destroyed during mitosis. The accumulation and destruction of cyclin B1 are slightly later than cyclin A2:

1. Harvest cells as described in **Section 3.5** Steps 1–6.
2. Resuspend the cells with 1 ml PBS and transfer to a microfuge tube.
3. Centrifuge at 16,000 × *g* for 1 min.
4. Aspirate the PBS and store the microfuge tube at –80°C until all the samples are ready.
5. Add ~2 pellet volume of cell lysis buffer into the microfuge tube. Vortex to mix.

6. Incubate on ice for 30 min.
7. Centrifuge at 16,000 × *g* at 4°C for 30 min.
8. Transfer the supernatant to a new tube.
9. Measure the protein concentration of the lysates. Dilute to 1 mg/ml with SDS sample buffer (*see* **Note 12**).
10. Run the samples on SDS-PAGE and analyze by immunoblotting with specific antibodies against cyclin A2, cyclin B1, and cyclin E1 (*see* **Note 13**).

### *3.8. Assessment of Synchronization: Time-Lapse Microscopy*

As they have the same DNA contents, cells in $G_2$ and mitosis cannot be distinguished by flow cytometry after propidium iodide staining. To differentiate these two populations, mitotic markers such as phosphorylated histone $H3^{Ser10}$ can be analyzed. Antibodies that specifically recognize phosphorylated form histone $H3^{Ser10}$ are commercially available and can be used in conjunction with either immunoblotting or flow cytometry.

Another method for monitoring mitosis is based on microscopic analysis of the chromosomes. Here we describe a method using time-lapse microscopy, thereby allowing the tracking individual cells into and out of mitosis after RO3306 synchronization. For this purpose, HeLa cells expressing GFP (green fluorescent protein)-tagged histone H2B are used in the following method:

1. Synchronize cells in $G_2$ with RO3306 as described in **Section 3.2**. An extra plate is needed to set aside for the time-lapse microscopy.
2. Setup the fluorescence microscope and equilibrate the growth chamber with 5% $CO_2$ at 37°C (*see* **Note 14**).
3. After release from the RO3306 block, place the plate immediately into the growth chamber.
4. Focus the microscope at the optical plane of the chromatin. As the cells are going to round up during mitosis, it is not a good idea to focus the images based on the bright field.
5. Images are taken every 3 min for 2–4 h (*see* **Note 15**).

## 4. Notes

1. Mutagen. Handle with care and use gloves.
2. Inactive lactone form of mevinolin is activated by dissolving 52 mg in 1.04 ml EtOH. Add 813 μl of 1 M NaOH and then neutralized with 1 M HCl to pH 7.2. Bring the solution to 13 ml with $H_2O$ to make a 10 mM stock solution. Store at –20°C. It has been reported that *in vitro* activation of mevinolin lactone may not be necessary (12, 14).

In that case, simply dissolve 52 mg of mevinolin in 13 ml 70% EtOH.

3. Dissolve 1 g of mevanlonic acid lactone in 3.5 ml of EtOH. Add 4.2 ml of 1 M NaOH. Bring the solution to 15.4 ml with $H_2O$ to make a 0.5 M stock solution.
4. RO3306 is sensitive to light and freeze–thaw cycle. We keep the stocks in small aliquots wrapped with aluminum foils at –80°C.
5. Dissolve thymidine and filter sterile to make the 100 mM stock solution. Incubation at 37°C may help to solubilize the thymidine.
6. The synchronization procedures described in these protocols are for using 100-mm plates. Cells obtained from one 100-mm plate at each time point should be sufficient for both flow cytometry analysis and immunoblotting. The procedures can be scaled up proportionally.
7. It is possible to break up a 24-h experiment into two independent sessions. Alternatively, it is possible for two researchers to work in shifts to harvest the cells at different time points. However, we found that the best results are obtained when all the cells are harvested by the same researcher.
8. For HeLa cells, CDK1 but not other CDKs is inhibited with 10 μM of RO3306 (9, 13). The exact concentration of RO3306 used should be determined for each stock.
9. The basis of synchronization by nocodazole treatment is that mitotic cells are rounded and attach less well to the plate than cells in interphase. It is possible to collect the mitotic cells by blasting them off with the medium using a pipette. Alternatively, shakers that hold plates and flasks can be used securely. It is also possible to hold the plates on a vortex and shake for 20 s with the highest setting. In any case, the cells should be examined under a light microscope before and after the mechanical shake-off to ensure that most of the mitotic cells are detached.
10. It is crucial to resuspend the cells very well before adding ethanol to avoid crumbing.
11. As cells from different phases of the cell cycle may be missing in the synchronized population, it is a good idea to first use asynchronously growing cells to setup the DNA profile.
12. Many reagents are available for measuring the concentration of the lysates. We use BCA protein assay reagent from Pierce (Rockford, IL, USA) using BSA as standards.

13. Cyclins are readily detectable in HeLa cells using commercially available monoclonal antibodies: cyclin A2 (E23), cyclin B1 (V152), and cyclin E2 (HE12).
14. We use a TE2000E-PFS inverted fluorescent microscope (Nikon, Tokyo, Japan) equipped with a SPOT BOOST$^{TM}$ EMCCD camera (Diagnostic Instrument, Sterling Heights, MI, USA) and a INU-NI-F1 temperature, humidity, and $CO_2$ control system (Tokai Hit, Shizuoka, Japan). Data acquisition and analysis are carried out using the Metamorph software (Molecular Devices, Downingtown, PA, USA).
15. A critical parameter in every time-lapse microscopy experiment is photobleaching and UV damage to the cells. The exposure time should be minimized.

## References


1. Skloot, R. (2010) The immortal life of Henrietta Lacks. New York: Random House.
2. McLaughlin-Drubin, M. E., and Munger, K. (2009) Oncogenic activities of human papillomaviruses. *Virus Res.* **143**, 195–208.
3. Chaudhry, M. A., Chodosh, L. A., McKenna, W. G., and Muschel, R. J. (2002) Gene expression profiling of HeLa cells in G1 or G2 phases. *Oncogene* **21**, 1934–1942.
4. Whitfield, M. L., Sherlock, G., Saldanha, A. J., Murray, J. I., Ball, C. A., Alexander, K. E. et al. (2002) Identification of genes periodically expressed in the human cell cycle and their expression in tumors. *Mol. Biol. Cell* **13**, 1977–2000.
5. Zhou, J. Y., Ma, W. L., Liang, S., Zeng, Y., Shi, R., Yu, H. L., et al. (2009) Analysis of microRNA expression profiles during the cell cycle in synchronized HeLa cells. *BMB Rep.* **42**, 593–598.
6. Chen, X., Simon, E. S., Xiang, Y., Kachman, M., Andrews, P. C., and Wang, Y. (2010) Quantitative proteomics analysis of cell cycle-regulated Golgi disassembly and reassembly. *J. Biol. Chem.* **285**, 7197–7207.
7. Wahl, A. F., and Donaldson, K. L. (2001) Centrifugal elutriation to obtain synchronous populations of cells. *Curr. Protoc. Cell Biol.* Chapter 8, Unit 8.5.
8. Banfalvi, G. (2008) Cell cycle synchronization of animal cells and nuclei by centrifugal elutriation. *Nat. Protoc.* **3**, 663–673.
9. Vassilev, L. T., Tovar, C., Chen, S., Knezevic, D., Zhao, X., Sun, H., et al. (2006) Selective small-molecule inhibitor reveals critical mitotic functions of human CDK1. *Proc. Natl. Acad. Sci. USA* **103**, 10660–10665.
10. Terasima, T., and Tolmach, L. J. (1963) Growth and nucleic acid synthesis in synchronously dividing populations of HeLa cells. *Exp. Cell Res.* **30**, 344–362.
11. Keyomarsi, K., Sandoval, L., Band, V., and Pardee, A. B. (1991) Synchronization of tumor and normal cells from G1 to multiple cell cycles by lovastatin. *Cancer Res.* **51**, 3602–3609.
12. Javanmoghadam-Kamrani, S., and Keyomarsi, K. (2008) Synchronization of the cell cycle using lovastatin. *Cell Cycle* **7**, 2434–2440.
13. Ma, H. T., Tsang, Y. H., Marxer, M., and Poon, R. Y. C. (2009) Cyclin A2-cyclin-dependent kinase 2 cooperates with the PLK1-SCFbeta-TrCP1-EMI1-anaphase-promoting complex/cyclosome axis to promote genome reduplication in the absence of mitosis. *Mol. Cell Biol.* **29**, 6500–6514.
14. Mikulski, S. M., Viera, A., Darzynkiewicz, Z., and Shogen, K. (1992) Synergism between a novel amphibian oocyte ribonuclease and lovastatin in inducing cytostatic and cytotoxic effects in human lung and pancreatic carcinoma cell lines. *Br. J. Cancer* **66**, 304–310.

# Chapter 11

# Synchronization of *Bacillus subtilis* Cells by Spore Germination and Outgrowth

Gaspar Banfalvi

## Abstract

This protocol defines conditions under which the germination of spores can be used to synchronize *Bacillus subtilis* cells, utilizing the time-ordered sequence of events taking place during the transition from spore to vegetative cells. The transition stages involve: phase change, swelling, emergence, initial division, and elongation. By using this method we have obtained two distinctive synchronized cell cycles, while the synchrony faded away in the third cycle. The advantage of using spore outgrowth and germination is that a highly synchronized population of bacterial cells can be obtained. The limitations of this method are that it can be applied only for sporulating bacteria and synchrony lasts for only a limited period of time exceeding not more than two cycles.

**Key words:** Endospore formation, spore outgrowth, transition stage, vegetative cells, permeabilization, DNA synthesis, spectrophotometry.

## 1. Introduction

The process of vegetative bacterial cells converted into a dormant structure is called sporogenesis, and the return to the vegetative stage is known as spore germination. Contrary to endospores vegetative cells are capable to active growth. Endospore formation is typical to three genera of Gram-positive bacteria: Bacillus (*B. anthracis, B. subtilis*), *Clostridium* (*C. botulinum, C. perfingens, C. tetani*), and Sporosarcina. *Bacillus subtilis* is a sporulating model organism for differentiation, gene/protein regulation, and cell cycle events (1). That sporulation and spore germination can be used as a model system to study the transition between different cell forms has been described four decades ago (2–4).

G. Banfalvi (ed.), *Cell Cycle Synchronization*, Methods in Molecular Biology 761,
DOI 10.1007/978-1-61779-182-6_11, 

In spore-forming bacteria "*de novo*" nucleotide synthesis is not operative in the early stage of transition from spore to vegetative stage known as germination (5). After the germination stage, the nucleoside triphosphate levels increase rapidly by the utilization of the nucleoside and nucleoside monophosphate pools of the dormant spores (6). Consequently, DNA synthesis resumes only after the formation of these substrates. The processes of germination and spore outgrowth take place in a time-ordered sequence allowing to follow closely the transition between spore and vegetative stages (7–13).

The process of germination of the bacterial spore is known as a change from the heat resistant to a heat-labile stage which does not represent the true vegetative cell. The transition has been divided into two distinct stages. The term germination is known as the first stage and the transformation of germinated spores into vegetative cells is called outgrowth (14) or post-germinative development (15). One of the most important reactions in this chain is the initiation of germination also referred to as trigger reaction. The germination process can be triggered by heavy metals, heat, hydrostatic pressure, a variety of chemicals of nutrient and nonnutrient origin (16). Although little is known about the mechanism of activation, it is believed that molecular rearrangements taking place inside the spores develop into the germination process. The triggering is operationally similar to the opposite process of sporulation representing a stage of no return. One of the best triggering agents is L-alanine when present in high concentration in the germination medium. It was demonstrated that a short exposure to L-alanine caused a subsequent germination in spores of *Bacillus cereus* (17). The quintessential germination receptor in *B. subtilis* is GerA that is activated by a single germinant, L-alanine and inhibited by its stereoisomer, D-alanine (18). Most of what is known about Ger receptor function has been derived from studies in the gerA operon (19). A homologous gerA operon of *B. subtilis* was isolated from *Bacillus thuringiensis* (20).

The germination process involves loss of resistance to injuring agents such as heat or heavy metals; loss of refractability; decrease in the optical density of the spore suspension; increase in stainability (21, 22); decrease in dry weight due to the loss of picolinic acid, calcium, and mucopeptides (23); the initiation of respiration (24); as well as imbibition of water (25). These changes point to initial biochemical steps preceding visual signs of germination. Outgrowth includes four stages occurring in the following order: swelling, emergence from the spore coat, elongation of the emergent organism, and finally division of the elongated organism.

As the bacterial endospore metabolism, structure, and composition differ from that of the vegetative cell, sporulation and spore germination can be applied as a sample model system to

study biochemical mechanism regulating these transitions. The differentiation is cyclic and can serve the purpose of synchronizing those bacteria that undergo sporulation. This chapter describes how germination and outgrowth of *B. subtilis* ATCC23857 (strain 168, indole$^-$) can be adapted for cell cycle synchronization. Studies have shown that in cells of *B. subtilis* 168, rendered permeable to small molecules by treatment with toluene, the incorporation of [$^3$H]dTTP incorporation depended on the presence of ATP and was sensitive to the inhibitor of DNA replication (6-((*p*-hydroxyphenyl)azo))uracil (HP-Ura) and to the gyrase inhibitor novobiocin (26).

## 2. Materials

### 2.1. Disposables, Instruments

1. 1.5 ml microcentrifuge tubes.
2. 5, 15 and 50 ml conical centrifuge tubes.
3. Glass culture tubes and flasks.
4. Whatman GF/C glass microfiber filters diameter 2.4 cm.
5. Rotating incubator.
6. Microcentrifuge tubes.
7. Spectrophotometer and cuvettes.

### 2.2. Solutions, Buffers

1. 60 Ci/mmol $^3$H-dTTP, 100 Ci/mmol $^3$H-thymidine.
2. Pre-mixed scintillation solution.
3. Buffer for DNA synthesis: phosphate buffer ($K_2HPO_4$/$KH_2PO_4$), 0.5 M, pH 7.5, 0.2 mM $MgSO_4$, 15 mM ATP, 0.4 mM dNTP (dATP, dGTP, dCTP, each), 2 mM HP-Ura, 2 mM 1-β-D-arabinofuranosylcytosine-5′-triphosphate (ara-dCTP) (**Notes 1**–**3**).

### 2.3. Lyophilized Spores

1. Keep spores of *B. subtilis* 168 in 1.5 ml microcentrifuge tubes in 50% glycerol at –20°C (*see* **Note 4**).
2. Lyophilized spores: 10 mg spores plus 1 ml 50% glycerol (10 mg/ml).

### 2.4. Germination of Spores

1. Sterile germination medium in 1 l: 14 g $K_2HPO_4$, 6 g $KH_2PO_4$, 2 g $(NH_4)_2SO_4$, 1 g trisodium citrate, 0.5 g $MgSO_4{\cdot}7H_2O$, 8 mg $FeCl_3$ $6H_2O$, 0.5 g L-alanine, 50 mg L-arginine, 50 mg L-asparagine, 100 mg sodium glutamate, 50 mg L-histidine, 5 mg L-methionine, 50 mg L-phenylalanine, 5 mg L-serine, 100 mg L-threonine, 50 mg L-tryptophan pH 7.4.

2. Germination mixture: 30 ml germination medium, plus 0.3 ml 50% glucose and 1.5 ml 10 mg/ml spores (*see* **Note 5**).

### 2.5. Monitoring of Germination

Monitor germination by the decrease in optical density at 525 nm in a spectrophotometer (*see* **Note 6**).

### 2.6. Cell Culture Medium

1. Antibiotic medium 3 (Penassay broth): 5 g/l tryptone, 1.5 g/l yeast extract, 1.5 g/l beef extract, 3.5 g/l sodium chloride, 1 g/l dextrose, 3.68 g/l potassium phosphate dibasic, 1.32 g/l potassium phosphate monobasic, pH adjusted to 6.9.
2. Medium C, pH 7.4 in 1 l: 14.0 g $K_2HPO_4$, 6.0 g $KH_2PO_4$, 2 g $(NH_4)_2SO_4$, 1 g trisodium citrate, 0.2 g $MgSO_4 \cdot 7H_2O$, 5 g glucose, 0.5 g casamino acids, and 50 mg indole.

## 3. Methods

### 3.1. Cell Growth

1. To 50 ml Penassay broth, add 10 μl spores in 50% glycerol, grow overnight in a 250 ml Erlenmeyer flask at 37°C in an orbital incubator shaker at 100 rpm.
2. From the overnight culture take 4 ml and add to 200 ml medium C in a 1 l flask and grow at 37°C in the orbital shaker at 100 rpm.

### 3.2. Preparation of Toluene-Treated Cells

1. At $3 \times 10^7$ cells/ml density take 25 ml cells each in six 50 ml conical tubes and harvest them in a Beckmann J21 centrifuge at room temperature (5,000 × *g*, 5 min).
2. Decant the supernatant and resuspend the pellet of each tube in 2 ml of 0.1 M phosphate buffer, pH 7.4. Pool the suspension in one 15 ml tube and spin down cells.
3. Resuspend cells in 3 ml 0.1 M phosphate buffer, pH 7.4, add 30 μl toluene. Shake the mixture for 10 min at room temperature then chill it in ice.
4. Add 10 ml cold 0.1 M phosphate buffer, pH 7.4, spin in centrifuge and resuspend cells in 1.5 ml of the phosphate buffer. The density of cells (1.5 ml/$4.5 \times 10^9$) should be around $3 \times 10^9$ cells/ml.
5. Distribute toluene-treated cells in 100 μl aliquots, freeze them in liquid nitrogen (*see* **Note 7**).

### 3.3. Spore Germination and Outgrowth

1. Subject homogenized lyophilized spores (20 mg + 2 ml $H_2O$) in a 5 ml test tube to sonication (e.g., Bronson sonicator, model B-12), with a microtip and setting for 5 min at 1 min intervals while immersed in ice water bath.

2. Prewarm sonicated spores to 37°C for 5 min and heat-activate at 80°C for 20 min.
3. Centrifuge heat-activated spores at 5,000 × *g* for 10 min at +4°C.
4. Resuspend the pellet of spores in sterile 2 ml $H_2O$ (to 10 mg/ml).
5. Initiate germination in a 250 ml Erlenmeyer flask by adding to 30 ml germination medium 0.3 ml 50% glucose and 1.5 ml 10 mg/ml heat activated spores. Place germination mixture in a rotary shaker with the temperature set at 37°C and a rotary speed of 100 rpm.
6. Monitor germination by measuring the optical density at 525 nm in a spectrophotometer.

### 3.4. DNA Polymerase Assay in Permeable Cells of B. subtilis

To assure that in outgrowing spores of *B. subtilis* 168 replicative DNA synthesis is dealt with, measure DNA synthesis in permeable cells in the presence and absence of ATP. Use the protocol of **Table 11.1** to demonstrate that in toluene-treated permeable *B. subtilis* cells DNA synthesis is an ATP-dependent replicative process and replicative DNA synthesis can be blocked by inhibitors of semiconservative replication such as HP-Ura.

### 3.5. DNA Synthesis in Outgrowing Spores

1. $^3$H-thymidine incorporation is advised to be measured from zero level absorption every 10 min by adding 5 μl $^3$H-thymidine to 0.3 ml germination medium and 0.2 ml germination mixture incubated at 37°C for 10 min.
2. Terminate DNA synthesis by adding 5 ml 0.3 M ice-cold trichloroacetic acid (TCA).
3. Collect precipitate on Whatman GF/C glass fiber filter, wash three times with 5 ml portions of 0.3 M TCA and then with absolute alcohol.
4. Dry filters under an infrared lamp and determine radioactivity with a toluene-based scintillation fluid.

A typical spore germination and outgrowth curve as well as the DNA synthesis profile are shown in **Fig. 11.1**. A lag period can be seen between the addition of the germination-inducing medium and the first sign of germination manifested as a decrease of absorption corresponding to the observation of Woese and Morowitz (27). The germination phase (**Fig. 11.1a**) continues till the absorption reaches its minimum referred to as zero level (**Fig. 11.1b**). The zero level of absorption is followed by spore outgrowth involving RNA and protein synthesis and finally DNA synthesis. The outgrowth consists of several subphases (**Fig. 11.1c–f**) including swelling and emergence from spore coat (**Fig. 11.1c**), elongation of the emerging vegetative cells from the spore coats proceeding to the early phase of logarithmic growth

**Table 11.1**
**DNA polymerase assay to prove semiconservative replication in *B. subtilis* 168 toluene-treated cells**

| Number of sample | $^3$H-dTTP (μl) | $H_2O$ (μl) | $KPO_4$ (μl) | $MgSO_4$ (μl) | ATP (μl) | dNTP (μl) | HP-Ura (μl) | +ara-dCTP-dCTP (μl) | *B. subtilis* (μl) | Counts (cpm) |
|---|---|---|---|---|---|---|---|---|---|---|
| 1 | 5 | 55 | 14 | 6 | 10 | – | – | – | 10 | 54 ± 21 |
| 2 | 5 | 55 | 14 | 6 | – | 10 | – | – | 10 | 36 ± 16 |
| 3 | 5 | 45 | 14 | 6 | 10 | 10 | – | – | 10 | 1,180 ± 38 |
| 4 | 5 | 35 | 14 | 6 | 10 | 10 | 10 | – | 10 | 337 ± 29 |
| 5 | 5 | 35 | 14 | 6 | 10 | 10 | – | 10 | 10 | 78 ± 26 |

The final volume of each reaction mixture was 100 μl. Incubation lasted for 30 min at 37°C. Termination took place by the addition of ice-cold 0.3 M trichloroacetic acid (TCA). Precipitate was collected on Whatman GF/C glass fiber filters washed with three 5 ml portions of 0.3 M TCA and then with 3 × 5 ml ethanol. Filters were dried under an infrared lamp and the radioactivity was determined in a toluene-based scintillation fluid.

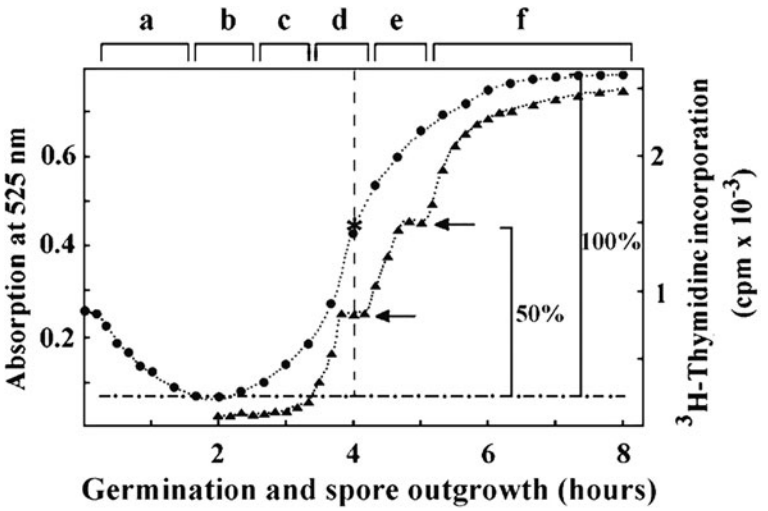


Fig. 11.1. Synchronization of *B. subtilis* 168 cells by germination and spore outgrowth. Lyophilized spores were homogenized, heat activated, and germinated as described in **Section 3**. Germination is given as decrease in optical density vs. time. The germination and outgrowth curve consists of (a) phase change (germination), (b) swelling stage (zero level), (c) emergence, (d) first cell cycle, (e) second cell cycle, (f) stationary phase (●···●). DNA synthesis showing (b) the lack of $^3$H-thymidine incorporation in the swelling stage, (c) emergence, (d) initiation of DNA synthesis and the first cell cycle, (e) elongation and second cell cycle, (f) stationary phase (▲···▲). The swelling stage is regarded as the zero level of absorption (—●—). For the best synchrony, stop outgrowth of spores after the swelling stage when the optical density at 525 nm starts to increase and does not exceed twice the value of its original absorption before germination. The upper limit of synchrony corresponds to the inflexion point of DNA synthesis (~50% of maximal outgrowth) is indicated by the *asterisk* (*). The *two arrows* (←) indicate the end of the first and second round of the cell cycle.

and cell division (**Fig. 11.1d**), to mid logarithmic phase and cell growth (**Fig. 11.1e**) and to late log and the stationary phase (**Fig. 11.1f**). Synchrony is indicated by the biphasic curve of $^3$H-thymidine incorporation, involving back-to-back division cycles such that the population doubles in number every generation time (**Fig. 11.1d**, **e**). Synchrony is lost in late logarithmic and stationary phase (**Fig. 11.1f**) (*see* **Note 8**).

## 4. Notes

1. Prepare solutions with distilled water as solvent with an electric conductance of <0.055 mS and an organic content of less than five parts per billion.
2. Phosphate buffer is best stored at 4°C and can be used for up to 2 months.

3. Neutralize dNTP solutions (dATP, dGTP, dCTP) dissolved in distilled water with 0.1 M NaOH to pH 7.5.
4. Freshly harvested spores germinate more reproducibly, but spores kept in glycerol also give reproducible results. For long-term use, store spores in 50% glycerol at –20°C.
5. To start germination, initial absorbance values at 525 nm should be between 0.25 and 0.3 optical density.
6. To obtain best synchrony stop outgrowing spores after the swelling stage. The best choice regarding synchrony is to take outgrowing spores after zero-level absorption when the OD 525 nm value starts to increase and reaches the initial optical density of spores before germination.
7. After toluene treatment work as quickly as possible, toluene-treated cells are vulnerable. For short-term storage (1 day) keep toluene-treated cells in dry ice–ethanol mixture, for long term store permeable *B. subtilis* cells at –80°C or in liquid nitrogen.
8. Do not use outgrowing spores after the inflexion point of the growth curve as the vegetative culture will be already in stationary phase.

## References


1. Graumann, P. (Ed.). (2007) *Bacillus: Cellular and molecular biology* (1st Ed.). Caister Academic Press, Wymondham. http://www.horizonpress.com/bac
2. Hansen, J. N., Spiegelman, G., and Halvorson, H. O. (1970) Bacterial spore outgrowth: Its regulation. *Science* **168**, 1291–1298.
3. Keynan, A. (1973) The transformation of bacterial endospores into vegetative cells. *Symp. Soc. Gen. Microbiol.* **23**, 85–123.
4. Mandelstam, J. (1976) Bacterial sporulation: A problem in the biochemistry and genetics of a primitive developmental system. *Proc. R. Soc. B.* **193**, 89–106.
5. Nelson, D. L., and Kornberg, A. (1970) Biochemical studies of bacterial sporulation and germination. XVIII. Free amino acids in spores. *J. Biol. Chem.* **245**, 1128–1136.
6. Setlow, P., and Kornberg, A. (1970) Biochemical studies of bacterial sporulation and germination. XXIII. Nucleotide metabolism during spore germination. *J. Biol. Chem.* **245**, 3645–3652.
7. Balassa, G. (1965) Synthesis macromoleculaires au cours de la germination des spores de *B. subtilis*. I. *Cinctique Annales De I'lnstitut Pasteur* **109**, 13–35.
8. Balassa, G. (1969) Biochemical genetics of bacterial sporulation. I. Unidirectional pleiotropic interactions among genes controlling sporulation in *Bacillus subtilis*. *Mol. Gen. Genet.* **104**, 73–103.
9. Kobayashi, I, Steinberg, W., Higa, A., Halvorson, H. O., and Levinthal, C. (1965) Sequential synthesis of macromolecules during outgrowth of bacterial spores. In *Spores IZZ*, pp. 200–212. L. L. Campbell and H. O. Halvorson (Eds.). Washington, DC: American Society for Microbiology.
10. Torriani, A., and Levinthal, C. (1967) Ordered synthesis of proteins during outgrowth of spores of *B. Cereus*. *J. Bacteriol.* **94**, 176–183.
11. Armstrong, R. L., and Sueoka, N. (1968) Phase transition in ribonucleic acid synthesis during germination of *B. subtilis* spores. *Proc. Natl. Acad. Sci. USA* **59**, 153–160.
12. Steinberg, W., and Halvorson, H. O. (1968) Timing of enzyme synthesis during outgrowth of *Bacillus Cereus*. I. Ordered enzyme synthesis. *J. Bacteriol.* **95**, 469–478.
13. Kennett, R. N., and Sueoka, N. (1971) Gene expression during outgrowth of *B. subtilis* spores. The relationship between order on the chromosome and temporal sequence of enzyme synthesis. *J. Mol. Biol.* **60**, 31–44.

14. Campbell, L. L., Jr. (1957) In *Spores*, p. 33. H. Halvorson (Ed.). Washington, DC: American Institute of Biological Sciences.
15. Levinson, H. S., and Hyatt, M. T. (1956) Correlation of respiratory activity with phases of spore germination and growth in *Bacillus megaterium* as influenced by manganese and L-alanine. *J. Bacteriol.* **72**, 176–183.
16. Halvorson, H. O. (1959) Symposium on initiation of bacterial growth. *Bacteriol. Rev.* **23**, 267–272.
17. Harrell, W. K., and Halvorson, H. (1955) Studies on the role of L-alanine in the germination of spores of *Bacillus terminalis*. *J. Bacteriol.* **69**, 275–279.
18. Yasuda, Y., and Tochikubo, K. (1984) Relation between D-glucose and L- and D-alanine in the initiation of germination of *Bacillus subtilis* spores. *Microbiol. Immunol.* **28**, 197–207.
19. McCann, K. P., Robinson, C., Sammons, R. L., Smith, D. A., and Corfe, B. M. (1996) Alanine germination receptors of *Bacillus subtilis*. *Lett. Appl. Microbiol.* **23**, 290–294.
20. Liang, L., Gai, Y., Hu, K., and Liu, G. (2008) The gerA operon is required for spore germination in *Bacillus thuringiensis*. *Wei Sheng Wu Xue Bao*. **48**, 281–286. (Article in Chinese)
21. Powell, J. F. (1950) Factors affecting the germination of thick suspensions of *Bacillus subtilis* spores in L-alanine solution. *J. Gen. Microbiol.* **4**, 330–338.
22. Pulvertaft, R. J. V., and Haynes, J. A. (1951) Adenosine and spore germination; phasecontrast studies. *J. Gen. Microbiol.* **5**, 657–663.
23. Powell, J. F., and Strange, R. E. (1953) Biochemical changes occurring during the germination of bacterial spores. *Biochem. J.* **54**, 205–209.
24. Murrell, W. G., and Scott W. J. (1958) The permeability of bacterial spores to water. *Proc. 7th Int. Congr. Microbiol.* Stockholm, p. 26.
25. Powell, J. F. (1957) Biochemical changes occurring during spore germination in bacillus species. *J. Appl. Bacteriol.* **20**, 349–358.
26. Bhattacharya, S., and Sarkar, N. (1981) Study of deoxyribonucleic acid replication in permeable cells of *Bacillus subtilis* using mercurated nucleotide substrates. *Biochemistry* **20**, 3029–3034.
27. Woese, C., and Morowitz, H. J. (1958) Kinetics of the release of dipicolinic acid from spores of *Bacillus subtilis*. *J. Bacteriol.* **76**, 81–83.

# Chapter 12

# Synchronization of Yeast


## Arkadi Manukyan, Lesley Abraham, Huzefa Dungrawala, and Brandt L. Schneider



## Abstract

The budding yeast *Saccharomyces cerevisiae* and fission yeast *Schizosaccharomyces pombe* are amongst the simplest and most powerful model systems for studying the genetics of cell cycle control. Because yeast grows very rapidly in simple and economical media, large numbers of cells can easily be obtained for genetic, molecular, and biochemical studies of the cell cycle. The use of synchronized cultures greatly aids in the ease and interpretation of cell cycle studies. In principle, there are two general methods for obtaining synchronized yeast populations. Block and release methods can be used to *induce* cell cycle synchrony. Alternatively, centrifugal elutriation can be used to *select* synchronous populations. Because each method has innate advantages and disadvantages, the use of multiple approaches helps in generalizing results. An overview of the most commonly used methods to generate synchronized yeast cultures is presented along with working *Notes*, a section that includes practical comments, experimental considerations and observations, and hints regarding the pros and cons innate to each approach.



**Key words:** Yeast, cell cycle, synchronization, block and release, centrifugal elutriation.


## 1. Introduction

The budding yeast, *Saccharomyces cerevisiae,* and the fission yeast, *Schizosaccharomyces pombe,* are the two most frequently studied yeasts (1–7). While they share a number of basic characteristics, the *S. cerevisiae* and *S. pombe* genomes evolutionarily diverged more than a billion years ago. Both yeasts have relatively small and compact genomes, on the order of only three to four times larger than the *Escherichia coli* genome (1–6). The fission yeast genome is slightly smaller and more unique because unlike budding yeast, it lacks large segmental genome duplications. Nonetheless, despite a small genome, the genetic,


G. Banfalvi (ed.), *Cell Cycle Synchronization*, Methods in Molecular Biology 761,
DOI 10.1007/978-1-61779-182-6_12, © Springer Science+Business Media, LLC 2011

biochemical, and molecular mechanisms of many common cellular processes (e.g., cell cycle control) are highly conserved between yeasts and higher eukaryotes. Moreover, like bacteria, the culturing of yeast is simple and inexpensive. Extremely rapid growth and short cell cycle times (1.5–2 h) are easily achieved in rich medium allowing for the production of enormously large numbers of cells in very short periods of time. Given adequate nutrients, both yeasts can be mitotically propagated *ad infinitum*, but deprivation of key nutrients (e.g., nitrogen and glucose) induces meiosis. Moreover, unlike most microorganisms, yeasts can be easily propagated as haploids. This improves the ease with which recessive mutations can be isolated and studied. These characteristics coupled with protocols that allow for highly efficient transformation of DNA molecules make yeast an amazingly powerful genetic system and one of the best and most tractable experimental model organisms.

Both budding and fission yeast grow and divide rapidly in rich medium containing glucose. However, excellent growth can be obtained in a wide range of minimal synthetic media allowing for the selection and propagation of strains with specific auxotrophies. Haploid fission yeast has a cylindrical shape that averages 3–4 μm in diameter and 7–15 μm long while diploids range from 4 to 5 μm in diameter and 15 to 25 μm long at division. In contrast, haploid budding yeast is ovoid with an average diameter of 3–8 μm. Diploid budding yeast has a size range from 4 to 12 μm in diameter depending upon the strain. However, cell size is not a static phenotype (8, 9). Rather, size is strongly modulated by environmental factors and nutrient quality (8, 9). In general, rapidly proliferating cells tend to be large while slowly dividing cells are considerably smaller. While the cell cycle times of both yeasts are highly sensitive to incubation temperatures, they can be successfully propagated over a very wide range of temperatures (e.g., from 12 to 38°C for *S. cerevisiae*). In contrast to the fission yeast, the budding yeast can also be cultured in the presence of a wide range of carbon sources (e.g., glucose, galactose, ethanol, and glycerol) (6, 10, 11). Thus, cell cycle times, growth rates, and cell size can be easily manipulated by altering the amount or quality of the carbon source provided in the growth medium. These properties are often useful in synchronization protocols.

Like higher eukaryotes, the cell cycle of yeast is divided into four independent phases: G1, S, G2, and M. In the budding yeast, cell cycle position can be easily determined microscopically (**Fig. 12.1**). G1 phase cells are unbudded and often smaller than average (**Fig. 12.1a**). Consequently, cell cycle progression and commitment past the yeast equivalent of the restriction point (START) is dependent upon growth to a critical cell size (**Fig. 12.1b, c**) (8, 9). The emergence of a small bud signals entry into S phase (**Fig. 12.1c**). Buds grow dramatically with cell cycle

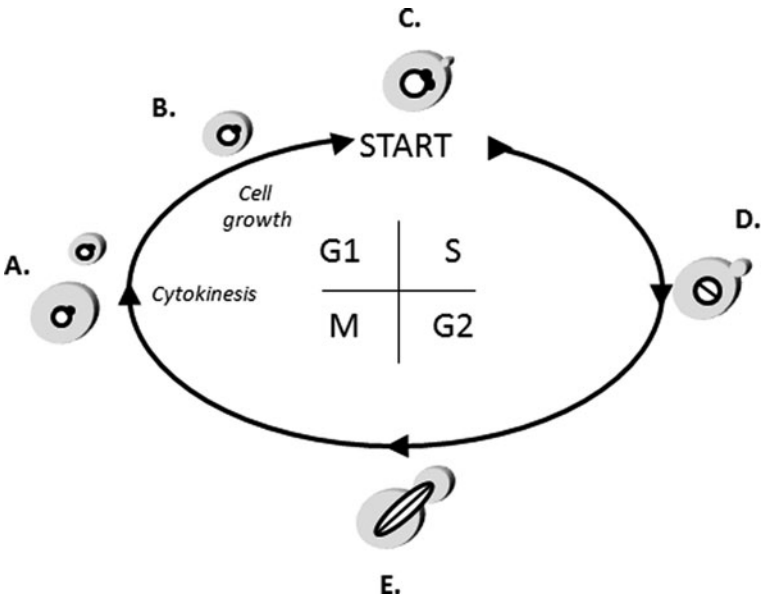


Fig. 12.1. *S. cerevisiae* cell cycle. In the budding yeast, cell cycle position can be determined microscopically. Yeast cells are shown in *gray*, nuclei in *white*, and spindles in *black*. Nuclei and spindles can only be visualized by fluorescence or electron microscopy. (**a**) Following cytokinesis, separated mother and daughter cells are in G1 phase with a round nucleus and a single spindle pole body. Because budding yeast divide asymmetrically, mother cells are nearly always larger than daughter cells. (**b**) However, both cells must grow in size in order to progress past START. Typically, this growth requirement is smaller in mother cells. (**c**) The emergence of a small bud signals progression past START. (**d**) Subsequently, the bud enlarges in S phase and a short spindle is formed. (**e**) In G2/M phase, buds are even larger. Nuclei and spindles become elongated. In *S. pombe*, cell cycle progression is less distinct. However, since fission yeast grow steadily in length with cell cycle progression, cell cycle position can be inferred from cell size measurements.

progression. Subsequently, cell cycle position can be inferred by comparing the size of the bud to the mother cell (**Fig. 12.1d–e**). Thus, analysis of the budding profile of a culture (Protocol 10) is a good means of assessing cell synchrony.

In contrast to the budding yeast, in the fission yeast there are no obvious morphological features that can be used to microscopically determine cell cycle position. However, like the budding yeast, cell cycle progression is size dependent. Thus, small cells tend to be in G1 phase. Moreover, because fission yeast only grows in length during the cell cycle, size measurements can be used to estimate cell cycle position. Most of the protocols and techniques described herein are specifically relevant to the synchronization of budding yeast; however, where possible relevant approaches for the synchronization of fission yeast are noted. Detailed below are 13 specific protocols complete with a detailed *Notes* section for the growth (Protocol 1) and synchronization of yeast. The synchronization section is sub-divided into

methods for monitoring cell synchrony (Protocols 2–4), methods for inducing synchrony (Protocols 5–10), and methods for selecting synchronous cells (Protocols 11–13).

## 2. Materials

1. Rich medium (*see* **Note 1**).
2. Synthetic medium (*see* **Note 2**).
3. Drop-out medium (*see* **Note 3**).
4. Rotating incubator.
5. Glass culture tubes and flasks.
6. Microcentrifuge tubes.
7. Spectrophotometer and cuvettes.
8. Sonicator.
9. Handheld counters.
10. 95% ethanol (*see* **Note 8**).
11. 20 mg/ml Proteinase K (*see* **Note 9**).
12. PI solution: 16 mg/ml propidium iodide (*see* **Note 10**).
13. 10 mg/ml RNase A (DNase free) (*see* **Note 11**).
14. 50 mM sodium citrate pH 7.0.
15. Cytometer.
16. Formaldehyde solution.
17. DAPI mounting medium (*see* **Note 12**).
18. Teflon-coated slides.
19. Poly-L-lysine solution (*see* **Note 12**).
20. Alpha factor (*see* **Note 13**).
21. Hydroxyurea (*see* **Note 14**).
22. Nocodazole (*see* **Note 15**).
23. Centrifugal elutriator (*see* **Note 16**).

## 3. Methods

### 3.1. Growth and Propagation of Yeast

Liquid log phase cultures are used for most synchronization protocols (*see* **Note 17**). Because yeast grows best when highly aerated, the use of baffled Erlenmeyer flasks is recommended (*see* **Note 18**). Log phase is frequently subdivided into early log ($<1 \times 10^7$ cells/ml), mid log ($1–4 \times 10^7$ cells/ml), and late log

phase (>4 × $10^7$ cells/ml) based predominantly on cell number. As cell density increases and cultures become saturated, yeast cells collect in G1 phase and tend to be more round and refractile. Depending on the protocol used, either log phase or saturated cultures might be needed. Therefore, the determination of cell density (Protocol 1) is frequently a prerequisite to begin a synchronization protocol.

#### *3.1.1. Protocol 1: Determination of Cell Density*

1. Starting with ~1 × $10^6$ cells/ml in the appropriate medium propagate cells until the approximate cell density is achieved (*see* **Note 19**). Determining the optical density (OD) of a yeast culture is the easiest method for estimating cell density (*see* **Note 20**).
2. Place 1 ml of culture medium in spectrophotometer cuvette and read $OD_{600}$. Zero the absorbance and use this sample as a blank control. Remove 1 ml of culture and place in a cuvette. Read $OD_{600}$ absorbance. If necessary for better accuracy, dilute initial culture such that $OD_{600}$ readings are <1.
3. In this range, an $OD_{600}$ reading of 0.1 is equivalent to ~3 × $10^6$ cells/ml (*see* **Note 21**).

### *3.2. Monitoring Cell Cycle Synchrony*

Before beginning any cell cycle synchronization experiment, it is vital to both determine the cell cycle position of individual cells and monitor the rate of cell cycle progression. These observations are essential in order to accurately assess the degree of synchronization. The simplest method of monitoring cell cycle position in *S. cerevisiae* involves observing the number and size of buds (**Fig. 12.1**). G1 phase cells are unbudded and have a 1 N DNA content (**Fig. 12.2a**). S phase cells have small buds (**Fig. 12.2b**). In G2/M phase cells, buds are larger and nearly approach the size of the mother cell (**Fig. 12.2c**). Thus, by counting the number of cells that are budded (also known as the budding index), the percentage of cells in G1 phase or S/G2/M phases can be easily determined (Protocol 2). In addition, flow cytometry can also be readily used for determining cell cycle position (**Fig. 12.2**) by measuring the DNA content of individual cells stained with propidium iodide (Protocol 3). Immunofluorescent staining of DNA (Protocol 4) and/or microtubules are the best methods for microscopically determining cell cycle position in single cells (4, 6, 10–16). Finally, excellent microarray studies have identified stage-specific gene transcripts that are very useful in confirming mitotic or meiotic cell cycle position (*see* **Note 22**) (17, 18).

#### *3.2.1. Protocol 2: Determining the Percentage of Budded Cells*

1. Add 500 µl of the culture into a labeled ice-cold microcentrifuge tube (*see* **Note 23**).
2. Sonicate each tube to disperse cells that have completed cytokinesis (*see* **Note 24**).

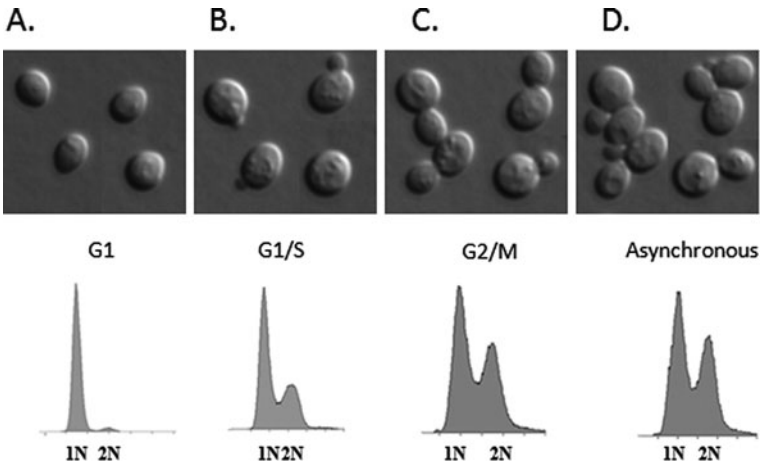


Fig. 12.2. Differential interference contrast microscopy of budding yeast and corresponding flow cytometry analyses. (**a**) In a culture of synchronized unbudded G1 phase cells, a single peak of cells with 1 N DNA content is observed. (**b**) As cells progress past START, larger cells with small buds become apparent. A second peak of cells with 2 N DNA content is observed, and cells in the "saddle" between the 1 N and 2 N peaks are in S phase. (**c**) In G2/M phase cells, buds are larger and the 2 N DNA peak higher. (**d**) An asynchronous culture is shown for reference.

3. To ensure precise and accurate measurements, count the number of budded cells amongst a total of at least 200 cells.
4. Determine the percentage of budded and unbudded cells by dividing by the total number of cells counted (*see* **Note 25**).

*3.2.2. Protocol 3: Analyses of Cell Cycle Distributions by Flow Cytometry* (*See* **Note 26**)

1. Place 0.5 ml of log phase culture in a 2 ml microcentrifuge tube (*see* **Note 27**).
2. Fix cells by adding 1.5 ml 95% ethanol.
3. Sonicate briefly.
4. Centrifuge in a microcentrifuge for 5 min at max speed.
5. Pour off supernatant and resuspend pellet in 2 ml of 50 mM sodium citrate. Repeat.
6. Add 25 μl of 10 mg/ml RNase A and incubate at 50°C for 1 h.
7. Add 25 μl of 20 mg/ml Proteinase K and incubate at 50°C for 1 h.
8. Add 1 ml of PI solution.
9. Analyze samples with a cytometer or save tubes in a light-protected box at 4°C.

*3.2.3. Protocol 4: Analyses of Cell Cycle Position by DAPI Staining of Nuclear DNA* (*See* **Note 28**)

1. Place 0.5 ml of log-phase culture in a 2 ml microcentrifuge tube (*see* **Note 27**).
2. Fix cells by adding 1.5 ml 95% ethanol or formaldehyde (*see* **Note 29**).

3. Sonicate briefly.
4. Centrifuge in a microcentrifuge for 5 min at max speed.
5. Resuspend cells in 50 μl DAPI mounting medium.
6. Coat Teflon slide wells with poly-L-lysine solution.
7. Place 3–5 μl of cells on a slide, cover, and observe with UV fluorescence (*see* **Note 30**).

### *3.3. Synchronization of Yeast*

There are two methods that are commonly used for yeast cell synchronization. In the first case, an agent or a condition is used that blocks cell cycle progression. By removing the block, synchronized cells progress into the next stages of the cell cycle. There are several advantages to block and release methods. First, block and release protocols can be carried out faster and yield a large number of synchronized cells. In addition, these protocols can be used successfully with small cultures. Finally, block and release protocols do not require special and expensive equipment. However, inducing synchrony using blocking agents has several distinct disadvantages. A major disadvantage is the disruption of the normal coordination between cell growth and cell division or the induction of cell stress responses. Drug-induced cell cycle arrests are unnatural and can have potentially toxic effects on the cells. Using temperature-sensitive mutants to block the cell can cause heat shock effects. Below, common protocols for block and release synchronization are provided.

### *3.4. Induced Synchronization: Block and Release Methods*

Block and release protocols prevent cell cycle progression but not cell growth. Cells can be blocked at various points in the cell cycle using pheromones, different drugs, or temperature-sensitive mutants. The basic protocol involves blocking cell cycle progression for a short time. Synchrony is achieved by releasing cells into fresh medium. Numerous block and release protocols can be used to obtain a synchronized cell culture. For example, alpha factor (Protocol 5), nutrient starvation (Protocol 6), depletion of essential cell cycle regulators (Protocol 7), or temperature-sensitive mutants (e.g., *cdc28*) (Protocol 10) can be used to arrest the cells in G1 phase. Hydroxyurea can be used to arrest the cells in S phase (Protocol 8). Finally, cells can be arrested in G2/M phase by nocodazole (Protocol 9) or by using a variety of temperature-sensitive *cdc* mutants (e.g., *cdc15*) (Protocol 10).

#### *3.4.1. Protocol 5: Synchronization of S. cerevisiae in G1 Phase with Alpha Factor* (*See* **Note 31**)

Alpha factor is a mating pheromone that is produced by MATα cells and arrests MATa cells at the G1/S transition point (**Fig. 12.1**) with 1 N DNA content by inhibiting Cdc28 kinase activity. Arrested cells become enlarged and display a distinct comma-shaped "schmoo" morphology (**Fig. 12.3a**). Pheromone-mediated arrests are useful because cells recover rapidly after release due to the Bar1p protease (*see* **Note 32**) and progress synchronously through two or three cell cycles.

1. Grow yeast cultures in YPD at 30°C to early log phase ($0.2–0.5 \times 10^7$ cells/ml) (*see* **Note 33**).
2. Centrifuge cells and wash 2X in sterile YPD pH 3.5 (*see* **Note 34**).
3. Resuspend cells at a density of $1 \times 10^6$ cells/ml and add α-factor to 5–10 μg/ml.
4. To arrest cells in G1 phase, incubate cultures at 30°C for 3 h (*see* **Note 35**).
5. Centrifuge cultures (4,000×*g* for 3–5 min) and wash twice by resuspending cell pellets in large volumes of pre-warmed YPD.
6. Resuspend cultures ($1 \times 10^7$ cells/ml) in pre-warmed YPD to release from arrest (*see* **Note 36**).
7. Remove a time zero aliquot (*see* **Note 37**).
8. Collect samples every 15 min to monitor cell cycle progression (*see* **Note 38**).

*3.4.2. Protocol 6: Synchronization by Nutrient Depletion* (*See* **Note 39**)

When yeast exhaust nutrients in the culture medium or grow to saturating densities, they arrest as highly retractile unbudded G1 phase cells.

1. Grow yeast cultures in YPD or YEP Raffinose at 30°C to saturation (*see* **Note 40**).
2. Centrifuge 1–2 min at 1,800–2,000×*g* in swing-out rotor.
3. Discard the supernatant containing debris and small cells. Repeat (*see* **Note 41**).
4. Resuspend the pellet in sterile YEP and incubate at 30°C for 6 h (*see* **Note 42**).
5. Centrifuge 1–2 min at 1,800–2,000×*g* in swing-out rotor.
6. Discard the supernatant containing debris and small cells. Repeat.
7. Resuspend ($1 \times 10^7$ cells/ml) in pre-warmed YPD to initiate a synchronously dividing culture.
8. Remove a time zero aliquot (*see* **Note 37**).
9. Collect samples every 15 min to monitor cell cycle progression (*see* **Note 38**).

*3.4.3. Protocol 7: Synchronization of Cultures by G1 Phase Cyclin Depletion* (*See* **Note 43**)

1. Grow yeast cultures (*see* **Note 44**) in YEP Raffinose–Galactose at 30°C to early log phase (*see* **Note 45**).
2. Centrifuge cells and wash twice in sterile YEP Raffinose (*see* **Note 46**).
3. Resuspend cells ($1 \times 10^7$ cells/ml) in sterile YEP 2% Raffinose.
4. Incubate at 30°C for 3 h (*see* **Note 47**).

5. Add galactose to 1% to initiate a synchronously dividing culture.
6. Remove a time zero aliquot (*see* **Note 37**).
7. Collect samples every 15 min to monitor cell cycle progression (*see* **Note 38**).

*3.4.4. Protocol 8: Synchronization in S Phase with Hydroxyurea* (*See* **Note 48**)

Hydroxyurea blocks cells in S phase by inhibiting ribonucleotide reductase. Subsequently, cells accumulate with medium-sized buds (**Fig. 12.3b**) and DNA content between 1 N and 2 N.

1. Grow yeast cultures in YPD at 30°C to early log phase ($0.2–0.5 \times 10^7$ cells/ml).
2. To arrest cells, add hydroxyurea as a powder to final concentration of 0.2 M.
3. Incubate cultures at 30°C for 3 h (*see* **Note 49**).
4. Centrifuge cultures ($4{,}000\times g$ for 3–5 min) and wash twice by resuspending cell pellets in large volumes of pre-warmed YPD.
5. Resuspend cultures ($1 \times 10^7$ cells/ml) in pre-warmed YPD to release from arrest.
6. Remove a time zero aliquot (*see* **Note 37**).

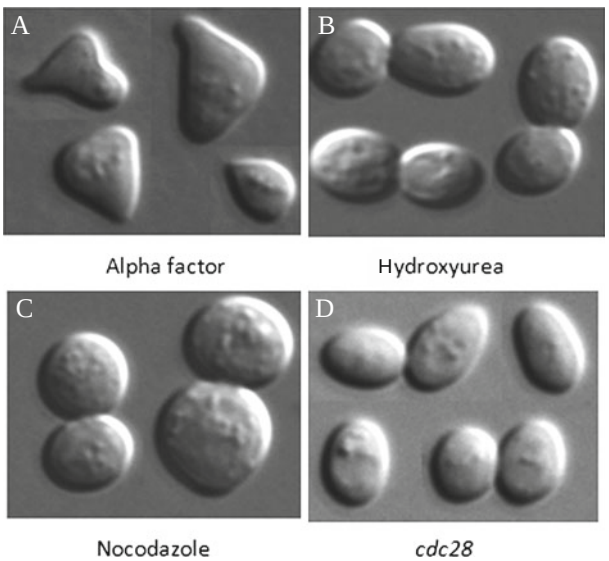


Fig. 12.3. Synchronized cultures of *S. cerevisiae*. (**a**) Cells treated with alpha factor arrest as enlarged unbudded cells. The "schmoo" morphology shown here is typical of arrested cells. (**b**) Hydroxyurea arrests cells in S phase as large budded doublets. (**c**) Nocodazole arrests cells in G2/M phase also as large budded doublets that frequently resemble "dumbbells." (**d**) A *cdc28* mutant arrested at the restricted temperature collects as large unbudded cells. Note other *cdc* mutants have terminal phenotypes like that seen in hydroxyurea or nocodazole arrests.

7. Collect samples every 15 min to monitor cell cycle progression (*see* **Note 38**).

*3.4.5. Protocol 9: Synchronization in G2/M Phase with Nocodazole (See* **Note 48**)

Nocodazole inhibits microtubule polymerization and blocks cells in G2/M phase. Subsequently, cells accumulate as large budded cells (**Fig. 12.3c**) with 2 N DNA content.

1. Grow yeast cultures in YPD at 30°C to early log phase ($0.2–0.5 \times 10^7$ cells/ml).
2. Add nocodazole to a final concentration of 15 μg/ml.
3. Incubate cultures at 30°C for 3 h (*see* **Note 50**).
4. Centrifuge cultures (4,000×*g* for 3–5 min) and wash twice by resuspending cell pellets in large volumes of pre-warmed YPD.
5. Resuspend cultures ($1 \times 10^7$ cells/ml) in pre-warmed YPD to release from arrest.
6. Remove a time zero aliquot (*see* **Note 37**).
7. Collect samples every 15 min to monitor cell cycle progression (*see* **Note 38**).

*3.4.6. Protocol 10: Synchronization of Cultures Using cdc$^{ts}$ Mutants*

Temperature-sensitive *c*ell *d*ivision *c*ycle (*cdc*) mutants are widely used to synchronize cell cultures. With these mutations, specific and essential cell cycle control proteins are rapidly inactivated at elevated temperature. The result is a stage-specific cell cycle arrest. Subsequently, by lowering the culture temperature, synchronous cell cycle progression is initiated. In *S. cerevisiae*, *cdc28* (arrests in G1 phase), *cdc7* (arrests in S phase), *cdc14*, *cdc15*, and *cdc20* (arrests in G2/M phase) are most commonly used (*see* **Note 51**).

1. Grow the appropriate strain (e.g., *cdc15*) in YPD at 23°C to early log phase ($0.2–0.5 \times 10^7$ cells/ml).
2. Transfer the culture to a 37°C incubator.
3. Incubate cultures at 37°C for 3.0–3.5 h to arrest the cells (*see* **Note 52**).
4. Transfer cultures to a 23°C incubator to release from arrest.
5. Remove a time zero aliquot (*see* **Note 37**).
6. Collect samples every 15 min to monitor cell cycle progression (*see* **Note 38**).

### *3.5. Synchronization Through Cell Selection*

The use of centrifugal elutriation is another method for yeast cell synchronization (10, 11, 18–23). Unlike block and release protocols, this method does not induce synchrony but rather directly selects for synchronized cells. Specifically, centrifugal elutriation separates cells on the basis of size, mass, and shape. Centrifugal elutriation uses a counterflow to oppose centrifugal force (**Fig. 12.4**). In so doing, this creates two opposing forces that

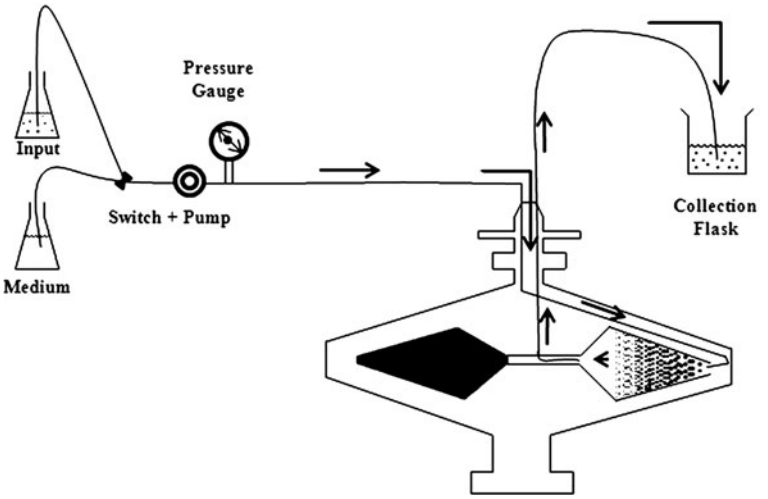


Fig. 12.4. Basic centrifugal elutriation setup. *Arrows* indicate direction of cell movement. Larger cells collect at the outer edge of the rotor (**Fig. 12.5**) while smaller cells can easily be elutriated and enriched in a collection flask.

act on cells (**Fig. 12.5**). The centrifugal force sediments cells toward the bottom of the chamber, while the fluid flow washes cells toward the top of the chamber (**Fig. 12.5**). The balance of the two forces causes large budded or irregularly shaped cells to move slower than small unbudded cells. Consequently, large cells collect at the bottom of the rotor (**Fig. 12.5b, c**). In contrast, the large surface-area-to-volume ratio typical of small cells causes little cells to be pushed toward the top of the elutriation chamber (**Fig. 12.5b, c**). Subsequently, by increasing the fluid

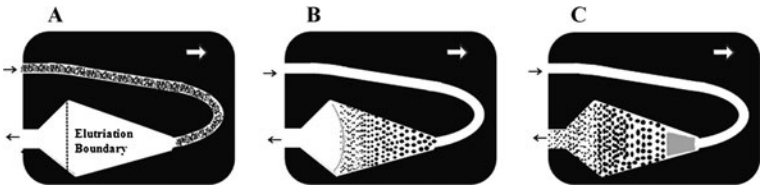


Fig. 12.5. Elutriation rotor. Using a strobe light and a viewing port, the elutriation process can be visualized throughout the experiment. *Small arrows* indicate the direction of fluid flow, and the *white arrow* indicates the direction of centrifugal force. (**a**) The appearance of cloudy and opaque medium at the outer edge of the rotor signifies the entrance of small and large cells into the elutriation chamber. The *dotted line* indicates the elutriation boundary. The chamber should not be filled past this point or poor size separation will occur. (**b**) Centrifugal elutriation generates a size gradient with smaller cells toward the top and larger cells toward the bottom of the elutriation chamber. Note that when the chamber is filled to capacity the elutriation boundary (*gray line*) will appear as concave opaque line. (**c**) After the chamber is filled to capacity, gradually increasing pump speed results in a higher rate of counterflow which in turn begins to elute the smallest cells out of the elutriation chamber and into a collection flask.

flow rate through the elutriation chamber while maintaining the centrifuge at a constant speed, cells are forced out of the rotor in a size-dependent manner. In this way, a log phase culture can be easily size-fractionated. Since progression past START is size dependent (**Fig. 12.1**), the selection of similarly sized cells allows for the synchronous outgrowth of yeast cultures.

Centrifugal elutriation is probably the best method for obtaining a pure population of synchronously dividing cells. Compared to block and release methods, this technique has three main advantages. First, it generates synchrony in the most physiologically relevant manner. Since this is a size selection technique, it does not perturb the normal coordination between cell growth and cell division. Second, it is a widely used, adaptable protocol and virtually any yeast strain can be used for this technique. Finally, elutriation is the only method which provides the opportunity of studying the earliest events in cell cycle regulation. The major disadvantage to elutriation is the requirement for large and expensive centrifugation equipment. Moreover, the manipulation and centrifugation has the potential to induce stress responses in the yeast cells. Therefore, it is suggested to compare the results from the elutriation protocols with other cell synchronization protocols. Two different methods of elutriation are detailed here: synchronized outgrowth of size-fractionated cells and chilled incremental fractionation.

*3.5.1. Protocol 11: Centrifugal Elutriation I: Synchronized Outgrowth of Size-Fractioned Cells*

In the first protocol, log phase cultures are loaded onto the rotor at 30°C and elutriated off in warm clarified medium. If done properly, this allows for the rapid and synchronous outgrowth of size-selected cells (*see* **Note 53**).

1. Grow 2–4 l of the appropriate strain to mid log phase ($2–3 \times 10^7$ cells/ml).
2. Assemble the elutriator and set the centrifuge to the corresponding culture temperature. Ensure that a pressure gauge or bubble trap is installed in the input line as large air bubbles can disrupt the sensitivity of separation (**Fig. 12.4**).
3. To help reduce the risk of contamination, flush all tubing and the rotor with 70% ethanol. Subsequently, rinse the elutriator with sterile water.
4. Measure cell density and pellet the cells by centrifugation at the proper growth temperature. Pour off supernatant and resuspend the pellet in 100–200 ml of fresh medium. Best results can be achieved by minimizing the time that cells spend in Steps 5–12 as timely efficiency increases synchrony and decreases artifacts.

5. Sonicate the cells at a medium setting twice for 30 s. Continuously swirl cells for even sonication and dispersion of heat (*see* **Note 54**).
6. Fill the elutriator chamber, tubing, and pressure gauge with clarified medium. Invert the pressure gauge to ensure it is filled completely. Tap the pressure gauge to remove any bubbles. Make sure that there are no air bubbles in the tubing or elutriation chamber and begin collecting the flow-through in a sterile flask (**Fig. 12.4**).
7. Set the centrifuge to 2,400 rpm (*see* **Note 55**), place the centrifuge timer on "hold," and start the centrifuge. Begin pumping the cells into the centrifuge at a rate of approximately 20 ml/min. Cells can be visualized while being loaded into the chamber using the strobe lamp and observation port (**Fig. 12.5**). At first the cell front will appear cloudy and turbulent, but as the remainder of cells load into the elutriation chamber, they will appear as a compact, sharp crescent front (**Fig. 12.5b**).
8. After cells have been loaded into the elutriation chamber, begin pumping in a clarified medium (**Fig. 12.5c**) (*see* **Note 56**). Gradually increase pump speed every 1–2 min until the cell front reaches the top of the elutriation chamber. Depending on the number and size of cells, this should take between 10 and 20 min at a pump rate of approx 30–40 ml/min (*see* **Note 57**).
9. As the cell front reaches the top of the elutriation chamber, the smallest cells, debris, and cell ghosts (cells broken by sonication) will begin to elute off the centrifuge (**Fig. 12.5c**).
10. When cells begin to elute, the flow-through medium will become slightly cloudy. At this point examine 3 μl of flow with a phase contrast microscope with a 40X objective. Begin collecting 200–300 ml fractions. Increase the pump speed in small increments between fractions. Check 3 μl of the flow-through after every 100 ml with a phase contrast microscope to determine the morphology and density of the cells that are eluting in each fraction. Roughly assess the number of budded cells. The goal is to collect a high-density fraction of cells that are <5% budded. It is very useful at this time to measure the cell number and size with a Z2 Coulter Counter/Channelyzer (*see* **Note 58**). Continue collecting fractions until the percentage of budded cells approaches 10%.
11. Depending on the experimental design and the number of cells needed, choose either the best fraction (e.g., the highest concentration of cells with a budding percentage (<5%))

or pool fractions. The final cell concentration should be $\sim 1 \times 10^7$ cells/ml (*see* **Note 59**).

12. Remove time zero samples as a control to assess synchrony. Return the synchronized population to the original incubator. Begin taking time points every 15–30 min. Monitor synchrony and cell cycle progression (*see* **Note 60**).

*3.5.2. Protocol 12: Synchronization by Centrifugal Elutriation: Chilled Incremental Fractionation*

Outgrowth of a size-selected log phase culture is an excellent method for initiating synchronous yeast cultures. Alternatively, centrifugal elutriation can be used to size fractionate a chilled log phase culture. In this case, each elutriation fraction represents a single "synchronized snapshot" of the entire yeast cell cycle. Using this approach, early small unbudded fractions will be enriched for G1 phase cells (**Fig. 12.6**). Subsequent fractions will contain larger cells, with a higher budding index as cells are enriched in S phase and G2/M phase (**Fig. 12.6**). While the

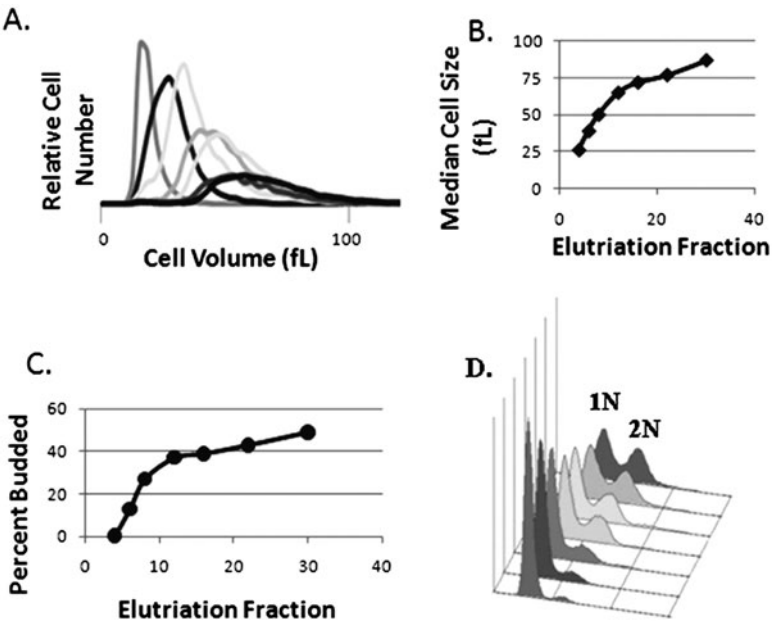


Fig. 12.6. Typical centrifugal elutriation results. (**a**) Z2 Coulter counter/Channelyzer analyses of seven elutriation fractions reveals a homogenous and sharp initial peak (*left most curve*) which enlarges and gradually flattens out in subsequent fractions. The first peak is typically used in an outgrowth experiment, and other fractions typify results obtained in an incremental elutriation. (**b**) Plotting of median cell size as a function of fraction number indicates that size increases rapidly in the first ~15 fractions and then more slowly. (**c**) Plotting of the budding index of cells as a function of fraction number demonstrates cell cycle progression. The appearance of >50% budded cells is suggestive of progression past START. Note the initial fraction has <5% budded cells suggestive of a high degree of homogeneity. (**d**) Flow cytometry analyses of individual fractions can be used to assign cell cycle position. Note that the initial fraction consists of >95% G1 phase cells, whereas the last fraction has >50% S/G2/M phase cells.

synchrony achieved using this approach is not as high as the previous approach (*see* **Note 61**), it is technically much easier (*see* **Note 62**) and considerably larger numbers of cells can be obtained. Alternatively, centrifugal elutriation of saturated cultures can be used to age-fractionate cells (*see* **Note 63**) or to induce meiotic synchrony (*see* **Note 64**).

1. Grow 2–4 l of the appropriate strain to mid log phase ($2–3 \times 10^7$ cells/ml) (*see* **Note 65**).
2. Assemble the elutriator and set the centrifuge to the corresponding culture temperature. Ensure that a pressure gauge or bubble trap is installed in the input line as large air bubbles can disrupt the sensitivity of separation (**Fig. 12.4**).
3. Set the elutriator centrifuge to 4°C and chill a mid-speed centrifuge and centrifuge bottles to 4°C.
4. Mid log phase grown culture (e.g., $2–3 \times 10^7$ cells/ml) should be immediately chilled by placing the flask on ice and adding an equal volume of ice into it. Once chilled at 0–4°C, centrifuge the cells.
5. Pour off supernatant and resuspend pellet in 100–200 ml of ice-cold water.
6. Sonicate cells (setting 7) twice for 30 s while swirling cells continuously on ice.
7. Set the centrifuge to 2,400 rpm (*see* **Note 55**), place the centrifuge timer on "hold," and start the centrifuge. Begin pumping the cells into the centrifuge at a rate of approx 20 ml/min. Cells can be visualized loading into the chamber using the strobe lamp and observation port (**Fig. 12.5**). At first the cell front will appear cloudy and turbulent, but as the remainder of cells load into the elutriation chamber, they will appear as a compact, sharp crescent front (**Fig. 12.5b**).
8. After cells have been loaded into the elutriation chamber, begin pumping in a clarified medium (**Fig. 12.5c**) (*see* **Note 56**). Gradually increase pump speed every 1–2 min until the cell front reaches the top of the elutriation chamber. Depending on the number and size of cells, this should take between 10 and 20 min at a pump rate of approx 30–40 ml/min (*see* **Note 57**).
9. As the cell front reaches the top of the elutriation chamber, the smallest cells, debris, and cell ghosts (cells broken by sonication) will begin to elute off the centrifuge (**Fig. 12.5c**).
10. When cells begin to elute, the flow-through medium will become slightly cloudy. At this point examine 3 µl of flow with a phase contrast microscope with a 40X objective.

Begin collecting 200–300 ml fractions. Increase the pump speed in small increments between fractions. Check 3 μl of the flow-through after every 100 ml with a phase contrast microscope to determine the morphology and density of the cells that are eluting in each fraction. Roughly assess the number of budded cells. The goal is to collect high-density fractions of cells that range from 0 to 95% budded.

11. Making sure to keep cells chilled, remove samples for cell cycle analyses (*see* **Note 66**).
12. Centrifuge the remaining fractions and pellet cells. Pour off supernatant and resuspend cells in 1 ml of ice-cold water. Transfer cells to prechilled 1.5–2.0 ml microcentrifuge tubes. Centrifuge for 30 s to pellet cells. Pour off the supernatant and freeze cells at –80°C for future studies (*see* **Note 67**).

*3.5.3. Protocol 13: Centrifugal Elutriation of Nutrient Depleted Cultures* (*See* **Note 39**)

When yeast exhaust nutrients in the culture medium or grow to saturating densities, they arrest as highly retractile unbudded G1 phase cells. Depending upon growth conditions, arrested G1 phase cells will be found in a wide range of sizes. Centrifugal elutriation can be used to collect different sized fractions which, in turn, will have distinct cell cycle kinetics (*see* **Note 68**).

1. Grow yeast cultures in YPD or YEP Raffinose at 30°C to saturation (*see* **Note 40**).
2. Centrifuge 1–2 min at 1,800–2,000×*g* in swing-out rotor.
3. Discard the supernatant containing debris and small cells. Repeat (*see* **Note 41**).
4. Resuspend the pellet in sterile YEP and incubate at 30°C for 6 h (*see* **Note 42**).
5. Centrifuge 1–2 min at 1,800–2,000×*g* in swing-out rotor.
6. Assemble and load elutriator as in Protocol 11.
7. When cells begin to elute, the flow-through medium will become slightly cloudy. At this point examine 3 μl of flow with a phase contrast microscope with a 40X objective. Begin collecting 200–300 ml fractions. Increase the pump speed in small increments between fractions. Check 3 μl of the flow-through after every 100 ml with a phase contrast microscope to determine the morphology and density of the cells that are eluting in each fraction. Roughly assess the number of budded cells. The goal is to collect a high-density fraction of cells that are <5% budded. It is very useful at this time to measure the cell number and size with a Z2 Coulter Counter/Channelyzer (*see* **Note 58**).
8. Depending on the experimental design and the number of cells needed, collect either small, medium, or large cells. For best synchrony, ensure that the budding percentage is <5%.

For best results, the final cell concentration should be ~1 × $10^7$ cells/ml (*see* **Note 59**).

9. Remove time zero samples as a control to assess synchrony. Return the synchronized population to the original incubator. Begin taking time points every 15–30 min. Monitor synchrony and cell cycle progression (*see* **Note 60**).

### 3.6. Conclusions

Synchronization of yeast cultures is essential for many different types of studies. There are two general methods for obtaining synchronized yeast populations: block and release methods and centrifugal elutriation. Several variations of each type of protocol are detailed here. In addition, basic approaches for monitoring yeast cell cycle are provided. Finally, an extensive *Notes* section is appended. Herein basic materials are listed and brief discussion of appropriate steps is available including practical comments, experimental considerations and observations, and hints regarding the pros and cons innate to each approach. In summary, this chapter provides a place to start for beginners and detailed specifics for investigators ready to synchronize yeast.

## 4. Notes

1. Yeast extract peptone (YEP) is a rich, complex medium without a carbon source. YEP is made by 1% yeast extract and 2% peptone in 1 l distilled water, sterilized by autoclaving. YPD is YEP supplemented with 2% filter-sterilized D-glucose (U.S. Biological cat. no. G1030). Because autoclaving can break down complex carbon sources into simple sugars like glucose, it is highly recommended that all carbon sources be filter-sterilized and added after autoclaved media has cooled. Detailed alternative recipes for yeast-rich and synthetic media are also available (6, 24).
2. Synthetic dextrose medium (SD) is a synthetic minimal medium containing yeast nitrogen base (YNB), vitamins, trace elements, salts, and glucose. SD is made by adding 1.7 g YNB (without amino acids and without ammonium sulfate) (Fisher/Difco cat. no. DF0335159), 5 g ammonium sulfate (U.S. Biological A1450), and 20 g glucose in 1 l distilled water. Synthetic complete medium (SC) is made by supplementing SD with 0.65 g primary amino acid mix (**Note 6**), 0.35 g secondary amino acid mix (**Note 7**), 0.2 g "drop-out" amino acid mix (**Note 8**), 0.45 g $Na_2HPO_4$ (Fisher cat. no. BP 332-1), and 20 g glucose in 1 l distilled water.

3. "Drop-out" medium is basic SC medium where one or more supplemented amino acids have been omitted ("dropped out"). Most frequently these are histidine, leucine, tryptophan, or uracil but could include any amino acid in the primary or secondary mixes. For the sake of simplicity, individual "drop-out" powders can be made for each medium (**Note 9**).
4. Primary amino acid mix contains 6 g each of the following amino acids from Sigma (cat. #): alanine (A7627), aspartic acid (A9256), asparagine (A0884), cysteine (C7755), glutamic acid (G1626), glutamine (G3126), isoleucine (I2752), valine (V0500), phenylalanine (P2126), proline (P0380), serine (S4500), threonine (T8625), and glycine (G7126) and 0.6 g of PABA (A9878) (21).
5. Secondary amino acid mix: This mix contains 6 g of each of the following amino acids from Sigma (cat. #): arginine (A5131), lysine (L5626), methionine (M6039), tyrosine (T3754), and adenine (A9126) (21).
6. "Drop-out" amino acid mix: This mix contains 1 g of each of the following amino acids from Sigma (cat. #): histidine (H8125), leucine (L8000), tryptophan (T0254), and uracil (U0750).
7. As an example, the recipe for –URA "drop-out" medium is given. It contains 1.7 g YNB without amino acids and with ammonium sulfate, 5 g ammonium sulfate, 0.65 g primary amino acid mix, 0.35 g secondary amino acid mix, 0.05 g leucine, 0.05 g histidine, 0.05 g tryptophan, 0.45 g $Na_2HPO_4$, and 20 g glucose in 1 l distilled water.
8. Ethanol can be industrial grade.
9. Proteinase K (Fisher BP1700-500) is made up by adding 5 ml of sterile water to one 100 mg bottle.
10. Propidium iodide (PI) solution is stored as a 100X stock (1.6 mg/ml in 50 mM sodium citrate (Fisher BP327-1)) in a light protected bottle at 4°C.
11. To prepare DNase-free RNase A, add 2.5 ml of water to one 5 mg bottle. Boil for 30 min. Aliquot into 1 ml tubes and store at –20°C.
12. DAPI (4′,6-diamidino-2-phenylindole dihydrochloride) is made up by adding 5 ml of sterile water to one 5 mg bottle. DAPI mounting medium is prepared by adding DAPI (final concentration 0.05–1 μg/ml determined empirically) in mounting medium: add 10 ml PBS, pH 8.0, to 100 mg *p*-phenylenediamine (Sigma 7842). Store at –20°C and discard if it turns brown. Adding 0.1% Triton X-100

can improve staining. Poly-L-lysine solution is from Sigma (P4832). Alternative protocols are also available.

13. Alpha factor is a 13 amino acid peptide (TRP-HIS-TRP-LEU-GLN-LEU-LYS-PRO-GLY-GLN-PRO-MET-TYR, MW 1684). Stocks are made up at 1–50 mg/ml in ethanol and stored at –20°C. Alpha factor is available from a variety of sources, but it is much more economical to have it synthesized and purified.
14. Hydroxyurea stock solution.
15. Nocodazole stock solutions (1.5 mg/ml) are made by adding 6.7 ml of dimethyl sulfoxide (DMSO) directly to a 10 mg bottle. Aliquots are stored at –20°C. The addition of DMSO (final concentration of 1%) to the culture medium prevents nocodazole from precipitating and improves the kinetics of arrest.
16. Complete elutriation systems are available from Beckman Instruments (Fullerton, CA, USA) (**Fig. 12.4**). The JE-5.0 rotor is recommended and can be used in Beckman J6 series or Avanti J-20 series centrifuges. Three sizes of elutriation chambers are available: a large 40 ml chamber, a standard 4 ml chamber, and a Sanderson 5.5 ml chamber. Researchers are encouraged to examine the Beckman manual for detailed equipment specifications, references, and instructions on use. The complete elutriator system includes a mid-speed centrifuge, rotor, one or two elutriation chambers, pressure gauge, stroboscope, control unit, tubing, injection ports, and spare parts. In addition, a variable-speed peristaltic pump (Cole-Parmer Masterflex drive 7520-20 and pump head 7016-20) and appropriate tubing are required.
17. Standard yeast culture requires prior knowledge of general yeast manipulation techniques. In addition, access to the following typical yeast culture equipment and supplies is necessary (3, 5, 7): variable temperature incubators, shaking water baths, standard culture flasks, tubes, glassware, microcentrifuges, mid-speed centrifuges, spectrophotometer, centrifuge tubes and bottles, filter apparatus, and standard and fluorescent microscopes. Although not required, access to a Z2 Coulter Counter/Channelyzer (for monitoring cell size and cell number) and a bench top flow cytometer is highly recommended. All other equipments and/or reagents are specifically stated. It is highly recommended that beginning researchers read *Methods in Yeast Genetics* (24), *Guide to Yeast and Molecular Biology* (6), and *Getting Started with Yeast* (3). Other excellent resources are also available (1, 2, 4, 5, 11, 25) and

the Saccharomyces Genome Database web site (http://www.yeastgenome.org/) is an invaluable resource. Additional excellent protocols can also be found online at CSHL protocols (http://cshprotocols.cshlp.org/).

18. The use of flasks with narrow necks (OD 38 mm) and foam stoppers (Fisher cat. no. 14-127-40E) helps limit bacterial contamination. In general, the possibility of contamination can be easily assessed microscopically, and a visual examination of all working cultures is always highly recommended prior to beginning synchronization experiments. This also helps ensure that the yeast culture is growing and proliferating with a normal and healthy morphology. Because rapidly proliferating yeast cultures seem to preclude bacterial growth, contamination should rarely be an issue except in cultures that propagate very slowly. In such cases, the addition of standard antibiotics (e.g., ampicillin) at bacteriostatic levels can be useful, but is not recommended under standard culture conditions.
19. In rich medium (e.g., YPD), cell number doubles approximately every 1.5 h. Given 1–2 h to exit lag phase, a starting culture is expected to reach early log phase in 5–8 h. For cells propagated in synthetic media (e.g., SC, SD, or "drop-outs") or with poorer carbon sources (e.g., raffinose, ethanol, or glycerol) this time increases due to longer cell cycle times. Empirically determining cell cycle times is essential in accurately predicting the time it will take any given culture to reach log phase. An excellent example for mathematically determining cell cycle times and preparing cultures for log phase growth can be found online at CSHL protocols (http://cshprotocols.cshlp.org/).
20. Alternatively, the use of a Z2 Coulter Counter/Channelyzer, while considerably more expensive, is a more precise method for determining cell number. Count 100 μl diluted in 10 ml of sheath fluid for cultures $<2 \times 10^7$ and 10 μl for more concentrated cultures. Additionally, this method also allows for cell size measurements and distributions.
21. OD readings are dependent upon both cell number and cell size. Therefore, it is advisable to calibrate the spectrophotometer using either a hemacytometer or through plating cells and counting the number of colonies. Keep in mind that the latter method measures the number of viable cells.
22. The expression of specific genes can be used for staging cells in both the mitotic and meiotic cell cycles. For the mitotic cell cycle, *CLN2, H2A, CLB4, CLB2*, and *EGT2* can be used to stage cells in G1/S-, S-, G2-, M-, and M/G1 phases, respectively (17, 26). For the meiotic cell

cycle, *DMC1, SPS1, DIT1*, and *SPS100* are useful for staging cells in early, middle, late middle, and late sporulation (27, 28). However, meiotic gene expression patterns are more strain-specific than are mitotic gene expression patterns (27, 28).

23. Coding the tubes or having two lab members independently count buds helps eliminate investigator bias. Cells can be stored on ice for 4–6 h or fixed with formaldehyde (3% final concentration) and stored at 4°C indefinitely.
24. Place sonicator (Fisher cat. no. 15-338-53) on a low setting for only 1–3 s. Wipe sonicator tip between tubes to avoid cross-contamination.
25. It is easiest to use two handheld counters using one to count the number of budded and the other to count the number of unbudded cells observed.
26. Excellent alternative protocols also exist (10, 21, 27, 29–31).
27. Because too many cells distort the results, use 50 μl for stationary or late log phase cultures.
28. Microscopic immunofluorescent analysis of the mitotic spindle by staining for tubulin is also an excellent method for ascertaining cell cycle position (4, 6, 10–15, 24, 31). G1 phase cells have a small number of microtubules associated with the spindle pole body (**Fig. 12.1a–c**) which expands to become a short spindle spanning the nucleus in S phase (**Fig. 12.1d**). Later in the cycle, the nucleus and the spindle become elongated and thinner (**Fig. 12.1e**).
29. Cells may also be fixed by adding 37% formaldehyde to a final concentration of 3%.
30. DAPI excitation wavelengths are 340–365 nm and emission wavelengths are 450–488 nm.
31. Synchronization of *S. cerevisiae* with alpha factor is straightforward and easy (10, 18, 21, 23, 32). In addition, large cultures can be arrested. Release from arrest is rapid and synchronous. Moreover, partial synchrony can last for several cycles. However, the fact that alpha factor arrest produces abnormally large cells can lead to significant artifacts. For example, the absence of a G1 phase leads to cell cycle times that are shorter than normal. Moreover, alpha arrest disrupts the normal coordination between growth and cell division and since some molecular pathways are size dependent, they are likely to be disrupted. In addition, MATα, diploid cells, and some mutants cannot be arrested with alpha factor. Finally, some mutant strains (e.g., *swi4*)

will not synchronously release from alpha factor arrests (10, 19, 20).

32. *MATa* cells produce the Bar1p protease that degrades alpha factor (10, 18, 21, 23, 32). For this reason, some investigators use *bar1*-strains because they can be efficiently arrested with 100- to 1,000-fold less alpha factor. However, while these strains arrest at lower concentrations of alpha factor, they release less synchronously. The effects of the Bar1p protease can be counteracted by thoroughly washing cells prior to the addition of alpha factor. In addition, low cell densities and low medium pH improve the kinetics of arrest.
33. Cultures grown in YPD arrest better than any other medium.
34. YPD buffered to pH 3.5 with 50 mM sodium succinate helps inactivate the Bar1p protease.
35. Examine 3 μl of the culture under the microscope. In addition, count and size 100 μl with a Z2 Coulter Counter/Channelyzer. Cells will arrest at the G1/S phase boundary, adopt "schmoo" morphology, and continue to get larger. Cell number should not increase after 2 h. Cultures are fully arrested when 5% less cells are budded.
36. The addition of the filter-sterilized pronase E final concentration of 0.1 mg/ml increases the rate at which cells recover from the alpha factor arrests.
37. Time zero samples are an essential control. At this point, cultures should display the highest degree of cell cycle synchrony.
38. When monitoring cell cycle progression, small aliquots (1–2 ml) can be stored on ice for 4–6 h before processing. Immediately chilling samples stops cell cycle progression and prevents inappropriate degradation of unstable RNAs and proteins. Subsequently, these samples can be fixed or stored at 4°C. However, if the purpose of the experiment is to collect large aliquots for RNA or protein extraction, it is most effective to collect samples in pre-chilled 50 ml centrifuge tubes. For these experiments, add 25 ml of culture to a chilled 50 ml tube already containing ~25 ml of ice. Centrifuge and transfer pelleted cells to a prechilled microcentrifuge tube by resuspending the pellet with ice-cold water. Microcentrifuge, remove supernatant, and store cell pellets at –80°C before extracting RNA or proteins. Yeast cell pellets kept at –80°C are stable for years, and RNA and protein can easily and efficiently be isolated from frozen cell pellets.

39. Limitless numbers of cells can be synchronized using this method. However, because starved cells are less metabolically active, release from starvation arrests is slow and less synchronous than with other protocols. Moreover, nutrient starvation reduces cell size and induces stress response pathways which may adversely affect cell cycle synchrony and progression.
40. Cultures should be grown in large baffled flasks with constant aeration in a rotary shaker at 300 rpm. Culture volumes should not exceed 25% of the flask volume. Cultures should be incubated for 1–3 days or until the budding index is less than 5%. Cultures grown in poorer mediums reach saturation later.
41. Because small cells must grow in order to bud, they disrupt culture synchrony. However, because they sediment less well, they are easily washed out.
42. Incubating cultures in YEP without a carbon source primes cultures for cell cycle release. However, this step can be skipped.
43. G1 phase cyclins (Clns) are required for progression past START (33). Because these cyclins are extremely unstable with a half-life less than 10 min (34), Cln depletion leads to a rapid G1 phase arrest. Because growth is not blocked, arrested cells rapidly become large, unbudded refractile cells. Unlike alpha factor arrested cells, Cln depletion results in round cells. Strains lacking both *CLN2* and *CLN3* and kept viable by a *CLN1* gene under the control of the *GAL* promoter are the best for this approach (9). This approach suffers from the same disadvantages that result from the generation of abnormally large cells due to extensive unbalanced growth.
44. While strains engineered for Cln depletion are the most commonly used, in principle the depletion of any unstable *CDC* gene should also induce cell cycle arrest (23).
45. In YEP Raffinose/Galactose, each carbon source is added to a final concentration of 1% from sterile-filtered 20% stocks.
46. In order to ensure a rapid G1 phase cell cycle arrest, it is important to remove all galactose. Alternatively, glucose can be added to a final concentration of 2%. However, in this case, cultures must be washed 2X in YEP after Step 4, before resuspending in fresh pre-warmed YEP Raffinose/Galactose in Step 5.
47. Cultures should arrest as large unbudded spherical cells. When culture is >95% unbudded, the G1 phase arrest is complete.

48. The use of drugs (e.g., hydroxyurea or nocodazole) or *cdc* mutations to induce cell cycle arrest is simple and large cultures can be arrested. Release from arrest is rapid and very synchronous. Partial synchrony can last for several cycles. However, like all block and release protocols, they produce abnormally large cells that can lead to significant artifacts due to a disruption of the normal coordination between cell growth and proliferation. Thus, care must be taken in interpreting results.
49. Examine 3 μl of the culture under the microscope. In addition, count and size 100 μl with a Z2 Coulter Counter/Channelyzer. Cells will arrest as budded cells in S phase boundary, and the buds will continue to get larger (**Fig. 12.3b**). Cell number should not increase after 2 h. Cultures are fully arrested when greater than 95% cells are budded.
50. Examine 3 μl of the culture under the microscope. In addition, count and size 100 μl with Z2 Coulter Counter/Channelyzer. Cells will arrest as budded cells in G2/M phase. Most cells should be doublets with buds similar in size to mother cells (**Fig. 12.3c**). Cell number should not increase after 2 h. Cultures are fully arrested when greater than 95% cells are budded.
51. Similar protocols are also available for *S. pombe* that routinely use alleles of *cdc2* and *cdc25* (4, 10–12, 16, 23, 31). Note that the genetic nomenclature is not consistent between *S. pombe* and *S. cerevisiae* such that *cdc25* represents a different gene in each organism (7).
52. Examine 3 μl of the culture under the microscope. In addition, count and size 100 μl with Z2 Coulter Counter/Channelyzer. Cell number should not increase after 2 h. Cultures are fully arrested when greater than 95% cells are budded. **Figures 12.2** and **12.3** illustrate the phenotypes of appropriate arrests.
53. Centrifugal elutriation is a challenging technique that demands practice and patience to become adept (10, 11, 18–23). Because a number of tasks need to be performed in rapid succession, it is suggested that investigators work in pairs. The first consideration is the determination of the appropriate growth conditions. Culture conditions that support rapid cell division (e.g., YPD) generate buds that are close in size to mother cells, particularly in haploid cells. In this case G1 phase is so short that it is nearly impossible to isolate a homogenous population of small unbudded cells (>95% unbudded). As a result, synchrony is poor. Thus, the use of YPD cultures for haploid elutriations is not recommended. Substitution of raffinose for

glucose or the use of synthetic medium alleviates these difficulties. In contrast, it is much easier to successfully elutriate diploid YPD cultures. Care must also be taken to ensure that cultures are in mid log phase. Cultures in early log phase yield too few cells, and cultures in late log phase proliferate less synchronously upon release. A single 40 ml elutriation chamber can hold 4–6 $\times$ $10^{10}$ cells. Too many cells reduce the resolution of size fractionation, and too few reduces yield and lengthens elutriation time.

54. Sonication helps ensure the separation of daughters from the mother cells and disperses clumps that are caused by centrifugation.
55. Observe and listen to the centrifuge carefully. An unbalanced rotor can be easily visualized through the viewing port (unstable image), heard (unusual rattles or sounds), or felt (strong vibrations). Any loose tubing or leaking fittings can lead to an unbalanced rotor, and this condition usually presents itself early in the experiment. If the rotor becomes seriously unbalanced, it is necessary to stop the centrifuge to avoid damage to the elutriation equipment.
56. This is achieved by switching the stopcock from input cells to clarified medium (**Fig. 12.4**). Ensure that no air bubbles enter the tubing and that the clarified medium flask is not allowed to run dry.
57. Because the length of the tubing, pump strength, cell number, cell size, and the density of the medium all affect the rate of elutriation, the time and pump rate necessary to elute cells must be empirically determined.
58. Uniformity of cell size is an excellent measure of the homogeneity of a given elutriation fraction (**Fig. 12.6a**). Fractions that display sharp cell size peaks tend to display a high degree of synchrony upon release.
59. While cells can be released in clarified medium, best results are obtained by centrifuging fractions and resuspending pelleted cells in prewarmed fresh medium.
60. Save at least four different aliquots for each time point. For example, a 100 μl sample is used for determining cell number and size, a 200 μl for the percentage of budded cells, a 500 μl for flow cytometry, and the remainder 25–50 ml for protein and/or RNA isolation. In addition, samples from the log phase culture prior to elutriation should be kept and analyzed as controls.
61. The types of data that can be obtained using this approach are illustrated in **Fig. 12.6**. Using an *S. cerevisiae* log phase culture, fractions can be obtained that range from a median size of 25–85 fl (**Fig. 12.6a, b**). Analysis of budding

(**Fig. 12.6c**) or flow cytometry data (**Fig. 12.6d**) demonstrates cell cycle progression from G1 phase to G2/M phase. However, because later elutriation fractions also contain large G1 phase cells synchrony is not as good as when a single homogenous G1 phase fraction is released into fresh medium.

62. Elutriations of chilled cultures are much simpler because speed is not of essence. As long as cells are kept cold, the procedure may be completed slowly and methodically.
63. As older cells tend to be larger than younger cells, a number of protocols have been developed to use elutriation to age-fractionate cells (35, 36).
64. Like mitosis, meiotic cell cycle progression is also size dependent. Therefore, size fractionation by elutriation helps initiate synchronous entry into meiosis (37, 38).
65. Centrifugal elutriation can also be used in combination with a nutrient starvation (*see* Protocol 13) because size selection improves synchrony. Thus, when using saturated cultures ($\sim 1 \times 10^8$ cells/ml) smaller input cultures (0.5–1 l) can be used. This is also applicable when synchronizing meiotic cell cultures. In both cases, selection of large unbudded fractions for subsequent release works best.
66. Save at least three different aliquots for each time point. For example, a 100 μl sample for determining cell number and size, a 200 μl sample for determining the percentage of budded cells, and a 500 μl for determining flow cytometry. In addition, samples from the log phase culture prior to elutriation should be kept and analyzed as controls.
67. Yeast cell pellets kept at –80°C are stable for years, and RNA and protein can easily and efficiently be isolated from frozen cell pellets.
68. Since small cells have a larger growth requirement in order to progress past START, small cells will spend a considerably longer amount of time in G1 phase as compared to larger cells. As a result, cell cycle times are significantly longer.

## Acknowledgements

B. L. S. has been supported by grants from NIH R01GM077874 and R01GM077874-04S1 and the Ted Nash Long Life Foundation.

## References


1. Forsburg, S. L. (2003) Overview of Schizosaccharomyces pombe, *Curr Protoc Mol Biol* Chapter 13, Unit 13 14.
2. Forsburg, S. L. (2005) The yeasts Saccharomyces cerevisiae and Schizosaccharomyces pombe: models for cell biology research, *Gravit Space Biol Bull 18*, 3–9.
3. Sherman, F. (2002) Getting started with yeast, *Methods Enzymol 350*, 3–41.
4. Forsburg, S. L., and Rhind, N. (2006) Basic methods for fission yeast, *Yeast (Chichester, England) 23*, 173–183.
5. Broach, J. R., Pringle, J. R., and Jones, E. W. (1991) *The Molecular and Cellular Biology of the Yeast Saccharomyces*, Cole Spring Harbor Laboratory Press, Cold Spring Harbor, NY.
6. Guthrie, C., and Fink, G. R. (1991) *Guide to Yeast Genetics and Molecular Biology*, Vol. 194, Academic, Pasadena, CA.
7. Murray, A. W., and Hunt, T. (1993) *The Cell Cycle: An Introduction*, W.H. Freeman, New York, NY.
8. Jorgensen, P., and Tyers, M. (2004) How cells coordinate growth and division, *Curr Biol 14*, R1014–R1027.
9. Schneider, B. L., Zhang, J., Markwardt, J., Tokiwa, G., Volpe, T., Honey, S., and Futcher, B. (2004) Growth rate and cell size modulate the synthesis of, and requirement for, G1 phase cyclins at start, *Mol Cell Biol 24*, 10802–10813.
10. Fantes, P., and Brooks, R. (1993) *The Cell Cycle: A Practical Approach*, IRL Press; Oxford University Press, Oxford; New York.
11. Johnston, J. R. (1994) *Molecular Genetics of Yeast: A Practical Approach*, IRL Press; Oxford University Press, Oxford; New York.
12. Gomez, E. B., and Forsburg, S. L. (2004) Analysis of the fission yeast Schizosaccharomyces pombe cell cycle, *Methods Mol Biol (Clifton, NJ) 241*, 93–111.
13. Green, M. D., Sabatinos, S. A., and Forsburg, S. L. (2009) Microscopy techniques to examine DNA replication in fission yeast, *Methods Mol Biol (Clifton, NJ) 521*, 463–482.
14. Humphrey, T., and Brooks, G. (2005) *Cell Cycle Control: Mechanisms and Protocols*, Humana, Totowa, NJ.
15. Lieberman, H. B. (2004) *Cell Cycle Checkpoint Control Protocols*, Humana, Totowa, NJ.
16. Luche, D. D., and Forsburg, S. L. (2009) Cell-cycle synchrony for analysis of S. pombe DNA replication, *Methods Mol Biol (Clifton, NJ) 521*, 437–448.
17. Spellman, P. T., Sherlock, G., Zhang, M. Q., Iyer, V. R., Anders, K., Eisen, M. B., Brown, P. O., Botstein, D., and Futcher, B. (1998) Comprehensive identification of cell cycle-regulated genes of the yeast Saccharomyces cerevisiae by microarray hybridization, *Mol Biol Cell 9*, 3273–3297.
18. Futcher, B. (1999) Cell cycle synchronization, *Methods Cell Sci 21*, 79–86.
19. Walker, G. M. (1999) Synchronization of yeast cell populations, *Methods Cell Sci 21*, 87–93.
20. Johnston, L. H., and Johnson, A. L. (1997) Elutriation of budding yeast, *Methods Enzymol 283*, 342–350.
21. Day, A., Schneider, C., and Schneider, B. L. (2004) Yeast cell synchronization, *Methods Mol Biol (Clifton, NJ) 241*, 55–76.
22. Sonoda, E. (2006) Synchronization of cells, *Subcell Biochem 40*, 415–418.
23. Amon, A. (2002) Synchronization procedures, *Methods Enzymol 351*, 457–467.
24. Amberg, D. C., Burke, D., Strathern, J. N., and Cold Spring Harbor Laboratory. (2005) *Methods in Yeast Genetics: A Cold Spring Harbor Laboratory Course Manual*, 2005 ed., Cold Spring Harbor Laboratory Press, Cold Spring Harbor, NY.
25. Ausubel, F. M. (1987) *Current Protocols in Molecular Biology*, Greene Publishing Associates, Brooklyn, NY; Media, PA.
26. Futcher, B. (2002) Transcriptional regulatory networks and the yeast cell cycle, *Curr Opin Cell Biol 14*, 676–683.
27. Chu, S., DeRisi, J., Eisen, M., Mulholland, J., Botstein, D., Brown, P. O., and Herskowitz, I. (1998) The transcriptional program of sporulation in budding yeast, *Science (New York, NY) 282*, 699–705.
28. Primig, M., Williams, R. M., Winzeler, E. A., Tevzadze, G. G., Conway, A. R., Hwang, S. Y., Davis, R. W., and Esposito, R. E. (2000) The core meiotic transcriptome in budding yeasts, *Nat Genet 26*, 415–423.
29. Haase, S. B., and Reed, S. I. (2002) Improved flow cytometric analysis of the budding yeast cell cycle, *Cell Cycle (Georgetown, TX) 1*, 132–136.
30. Sabatinos, S. A., and Forsburg, S. L. (2009) Measuring DNA content by flow cytometry in fission yeast, *Methods Mol Biol (Clifton, NJ) 521*, 449–461.
31. Zhang, H., and Siede, W. (2004) Analysis of the budding yeast Saccharomyces cerevisiae cell cycle by morphological criteria and flow cytometry, *Methods Mol Biol (Clifton, NJ) 241*, 77–91.

32. Breeden, L. L. (1997) Alpha-factor synchronization of budding yeast, *Methods Enzymol 283*, 332–341.
33. Richardson, H. E., Wittenberg, C., Cross, F., and Reed, S. I. (1989) An essential G1 function for cyclin-like proteins in yeast, *Cell 59*, 1127–1133.
34. Schneider, B. L., Patton, E. E., Lanker, S., Mendenhall, M. D., Wittenberg, C., Futcher, B., and Tyers, M. (1998) Yeast G1 cyclins are unstable in G1 phase, *Nature 395*, 86–89.
35. Woldringh, C. L., Fluiter, K., and Huls, P. G. (1995) Production of senescent cells of *Saccharomyces cerevisiae* by centrifugal elutriation, *Yeast (Chichester, England) 11*, 361–369.
36. Egilmez, N. K., Chen, J. B., and Jazwinski, S. M. (1990) Preparation and partial characterization of old yeast cells, *J Gerontol 45*, B9–B17.
37. Day, A., Markwardt, J., Delaguila, R., Zhang, J., Purnapatre, K., Honigberg, S. M., and Schneider, B. L. (2004) Cell size and Cln-Cdc28 complexes mediate entry into meiosis by modulating cell growth, *Cell Cycle (Georgetown, TX) 3*, 1433–1439.
38. Nachman, I., Regev, A., and Ramanathan, S. (2007) Dissecting timing variability in yeast meiosis, *Cell 131*, 544–556.

# Chapter 13

# Synchronization of Pathogenic Protozoans

**Staffan Svärd and Karin Troell**

## Abstract

Protozoans are single-cell eukaryotes and many of the best studied protozoans are parasitic to humans (e.g., *Plasmodium falciparum* causing malaria and *Trypanosoma brucei* causing sleeping sickness). These organisms are distantly related to humans but with retained eukaryotic type of cellular processes, making them good model systems for studies of the evolution of basic processes like the cell cycle. *Giardia intestinalis* causes 250 million cases of diarrhea yearly and is one of the earliest diverging protozoans. It has recently been possible to synchronize its cell cycle using compounds that inhibit different steps of the cell cycle and the detailed protocol is described here.

**Key words:** Cell cycle, malaria, parasite, aphidicolin, *Giardia*.

## 1. Introduction

Pathogenesis of infectious diseases is often the result of uncontrolled expansion of the infectious microbes, resulting in tissue destruction and inflammation. Protozoan parasites are not an exception to this but surprisingly little is known about the regulation of cell growth and the cell cycle in these organisms. Protozoans are single-cell eukaryotic microbes and most are free living. However, several are parasitic to humans and other mammals and they cause significant morbidity and mortality worldwide. Our understanding of cell cycle regulation in protozoans has been lagging behind, mainly due to the lack of good synchronization protocols. Genomic analyses performed during the last 10 years have shown that parasitic protozoans have typical eukaryotic setups for cell cycle regulation (1, 2). The number of regulatory components (e.g., cyclins and cyclin-dependent kinases) is reduced and

G. Banfalvi (ed.), *Cell Cycle Synchronization*, Methods in Molecular Biology 761,
DOI 10.1007/978-1-61779-182-6_13, 

this makes these organisms interesting model systems to understand the evolution of cell cycle regulation in higher eukaryotes. Here we will first summarize what is currently known about synchronization of medically important human protozoan parasites and then we will focus on protocols for synchronization of the most diverged protozoan parasite, *Giardia intestinalis*.

Malaria, one of the most important infectious diseases, is caused by *Plasmodium* parasites. Patients with severe disease show higher parasite burdens (high parasitemia), and virulent strains isolated from these patients have a more rapid multiplication rate *in vitro* (3). The erythrocytic cycle of *P. falciparum* has been best studied due to its relevance to disease and treatment. The merozoite, a haploid invasive form of the parasite, invades an erythrocyte and after approximately 48 h up to 32 new merozoites leave the erythrocyte. This process is called schizogony and the first recognizable cell cycle event is initiation of DNA replication 30 h after invasion of the erythrocyte (4). This DNA replication continues for at least 8–10 h and the first M phase occurs 36 h after invasion. However, the understanding of the regulation of these processes is still very fragmented. Several protocols for synchronization of the erythrocytic cycle of *P. falciparum* have been developed using density gradients (5), temperature shifts (6), osmotic lysis (7), magnets (8), and inhibitors of the cell cycle (9). The main problem with these methods is that the synchrony and yield are not good enough for detailed molecular studies of the cell cycle. One recent publication describes a method for preparing cultures with very high parasitemia, synchronized at any erythrocytic stage (10). This type of protocol will in the future allow detailed cell cycle studies in *P. falciparum*.

*Toxoplasma gondii* is a relative of the *Plasmodium* parasite in the Apicomplexa group and it is a leading cause of death due to food-borne disease (11). Rates of proliferation play a critical role in the disease pathogenesis and certain types of the parasite with high multiplication rate are much more virulent in mice (12). Two main protocols have been developed for synchronization of the cell cycle. Parasites have been engineered to express the herpes simplex virus thymidine kinase (13). Treatment of these recombinant parasites with exogenous thymidine arrests parasites in late G1/early S phase and this can be released by addition of fresh medium, resulting in synchronized cultures (13). A novel method uses the antioxidant and metal chelating compound pyrrolidine dithiocarbamate (PDTC, 14). This can be used on all types of *T. gondii* parasites and it synchronizes parasites in the G1 stage.

*Leishmania* and *Trypanosoma* parasites belong to the order Kinteoplastida. *Leishmania* parasites are transmitted by sandflies and depending on species they cause cutaneous, mucocutaneous,

and systemic (visceral) infections. *Trypanosoma cruzi* is transmitted by bugs and cause Chagas disease in South America. *Trypanosoma brucei* is transmitted by the tse-tse fly and it causes sleeping sickness in Africa. Hydroxyurea has been used to synchronize *L. tarentolae* and *T. cruzi* parasites (15, 16) and partial synchronization of *T. brucei* can be obtained by re-feeding stationary phase cells (17). Re-feeding of stationary phase cells has also been used to get semi-synchronized cultures of *Acanthamoeba castellanii* (18). *Acanthamoeba* can cause keratitis and it is also known to transmit pathogenic bacteria like *Legionella* and *Campylobacter*. *Acanthamoeba* is transmitted as resistant cysts and cyst formation is optimal in the end of the G2 stage of the cell cycle, close to the stationary phase exit point (19).

Another cyst-forming parasitic protozoan is *G. intestinalis*. *Giardia* is a eukaryotic microbe that forms one of the earliest diverging lineages within the eukaryotic part of the universal tree of life. The basal position in the phylogenetic tree makes *Giardia* an excellent model system for identification and investigation of fundamental eukaryotic processes like cell cycle regulation (19). The organism is unusual in containing two, apparently identical, diploid nuclei. Moreover, it is able to leave the vegetative cell cycle and enter into a differentiation pathway (encystation), triggered by intestinal stimuli (bile stress or cholesterol starvation). During encystation, a trophozoite undergoes two rounds of DNA replication with a single karyokinesis, to form a quadrinucleate 16 N cyst (19). Although presumed to be asexual, *Giardia* has low levels of allelic heterozygosity (1), indicating that the two nuclear genomes may exchange genetic material. Recent data demonstrate fusion between nuclei during encystations (20). When a cyst awakens from dormancy, in response to signals from the host, it undergoes two rounds of cytokinesis, with a single round of nuclear division, to form four binucleate trophozoites, which only then reenter the cell cycle. Thus, the giardial cell cycle displays unusual features and DNA replication is tightly coupled to vegetative growth and differentiation of the parasite. Furthermore, *Giardia* is also a medically important diarrhea-causing parasite and an effective replication of trophozoites is essential for the induction of symptoms (21). We have for the first time been able to synchronize *Giardia* cultures by arresting the cells at the G1/S transition point with aphidicolin (22) and cell cycle-regulated genes were identified. The cell cycle can also be synchronized using aphidicolin in combination with nocodazole treatment (23). Nocodazole affects the microtubuli system, which results in arrest in the junction between G2 and M but the use of nocodazole treatment in synchronization has been questioned (24).

## 2. Materials

### 2.1. Cell Culture

1. Diamond's TYI-S-33 (Tryptone-Yeast extract-Iron-Serum): 30 g/l BBL Biosate peptone (tryptone and yeast extract mixture) (BD Biosciences 211862), 55.6 mM glucose, 34.2 mM NaCl, 1.14 mM L-ascorbic acid, 5.74 mM $K_2HPO_4 \cdot 3H_2O$, 4.41 mM $KH_2PO4$, 11.4 mM L-cysteine, and 0.038 mM ferric ammonium citrate. The pH is set to 7.0. Sterile-filter through a 0.45 μm filter. Add sterile-filtered bovine bile (Sigma B3883) to a final concentration of 0.5 mg/ml and 10% v/v heat-inactivated bovine serum.
2. 10 ml Nunclon delta flat side tubes.

### 2.2. Whole Culture Synchronization

1. Diamond's TYI-S-33 medium.
2. 50 ml Falcon tubes (*see* **Note 1**).
3. Aphidicolin is dissolved in dimethyl sulfoxide (DMSO) to a final concentration of 10 mg/ml and is stored at –20°C.
4. Cell scrapers.
5. Phosphate-buffered saline (PBS): 137 mM NaCl, 2.7 mM KCl, 10 mM $Na_2HPO_4$, 1.76 mM $KH_2PO_4$ (adjust to pH 7.4 with HCl if necessary).

### 2.3. Flow Cytometry

#### 2.3.1. Fixing Cells

1. Cell fixative: 1% Triton X-100, 40 mM citric acid, 20 mM dibasic sodium phosphate, 0.2 M sucrose, adjust pH to 3.0.
2. Diluent buffer: 125 mM $MgCl_2$ in PBS.
3. Phosphate-buffered saline (PBS): as above.

#### 2.3.2. Wash and DNA Labeling

1. Phosphate-buffered saline (PBS): as above.
2. Dissolve RNase A in $ddH_2O$ to a concentration of 10 mg/ml.
3. Flow buffer: 10 mM Tris (pH 7.5), 10 mM $MgCl_2$. Filter through 0.2 μm pore size filter to remove particles to avoid light scatter background noise. Store at 4°C.
4. Dissolve ethidium bromide in $ddH_2O$ to a concentration of 4 mg/ml.
5. Dissolve mithramycin A in $ddH_2O$ to a concentration of 2.5 mg/ml.
6. DNA staining solution: Prepare fresh each time a staining solution for the number of samples you have. For each

sample use 0.75 μl ethidium bromide (4 mg/ml), 6 μl mithramycin A (2.5 mg/ml), and 68.25 μl Flow buffer.

## 3. Methods

### 3.1. Cell Culture

1. Trophozoites from *Giardia* is axenically maintained in 10 ml flat side tubes in TYI-S-33 medium at 37°C.
2. The cells are sub-cultured twice per week. Before re-inoculation the cells are kept on ice for 10 min to let cells detach from the tube surface. The sample is homogenized and 5–10 μl of confluent trophozoite culture is transferred to a new tube with pre-warmed TYI-S-33 medium.

### 3.2. Measuring Generation Time

Since the generation time for *Giardia* isolates all differ depending on the isolate, this protocol is based on number of generation cycles rather than hours. A simple way to determine the generation time of your cells is described below. The knowledge of generation time together with FLOW data can also be used to estimate the length of the different stages during the cell cycle.

1. The generation time of exponentially growing trophozoites is determined by continuous counting of a culture.
2. Fresh cultures with $5 \times 10^4$ cells/ml are set up into three separate 10 ml tubes in 37°C TYI-S-33 medium.
3. Every 90 min, for up to 12 h, the cells are detached by chilling the tube on ice for 10 min and then swirled to obtain a homogenized culture.
4. The total cell count is determined in a Bürker chamber. 10 μl from each tube is administered to the chamber and the average of counts from the three tubes per time point is used to determine the generation time.

### 3.3. Whole Culture Synchronization

1. TYI-S-33 enough for all cultures for both aphidicolin treatment and re-feeding to release the cells from the drug is prepared and filtered. The medium is kept refrigerated. However, appropriate amount should be prewarmed to 37°C at all steps to avoid cold stress on the cells.
2. Grow cells to ~80% confluence.
3. Chill cells on ice for 10 min and dilute cells 1:10 with fresh medium (*see* **Note 2**). Make sure to swirl the bottle regularly and keep it on ice while preparing your cultures for synchronization. This is important to make sure all cultures are equal from the start.
4. For synchronization with release from the drug the number of samples plus two DMSO controls is set up. Use one tube

or flask per time point as *Giardia* trophozoites attach to the surface and need to be kept on ice or scraped to detach. This will influence the cells too much in case cells would be harvested from the same sample.

5. Let the cultures grow for three generation cycles or to approximately 70% confluence before adding the drug.
6. Add aphidicolin, 0.5 μl/ml culture to each tube (except the controls), and 0.5 μl/ml culture DMSO to the controls.
7. Let the cultures grow for one generation cycle before release to allow all cells to reach the synchronization point in the cell cycle.
8. To release the cells from aphidicolin arrest, pour of the drug containing medium and add fresh prewarmed medium. The release is instant, so to allow a sample with all cells arrested in G1 that sample should not be released but collect cells with aphidicolin-containing medium.
9. Use a small cell scraper to harvest the cells (*see* **Note 3**). If the cells are to be analyzed with flow cytometry as well make sure to save approximately 7 ml of culture for that analysis (*see* fixing cells). Spin cells at 900 × *g* for 5 min at 4°C and snap freeze in liquid nitrogen and then move to freezer to preserve the sample for further analysis of RNA, DNA, or proteins.

### 3.4. Flow Cytometry

In flow cytometry cells are individually analyzed. In this case, when cells are stained with DNA-specific dye the strength of fluorescence signal is proportional to the intracellular DNA content in each cell. The method is one way to visualize the success of the cell cycle synchronization as the flowgrams illustrate the number of cells with the different number of genome copies (in the case of *Giardia* 4 N for GI cells and 8 N for G2 cells) (**Figs. 13.1** and **13.2**).

### 3.5. Fixing Cells

1. The scraped cell culture is spun at 900 × *g* for 5 min at 4°C.
2. As much of the medium as possible is removed. Some liquid (~50 μl) needs to be kept to avoid destroying the oftentimes loose pellet.
3. Immediately add 150 μl cell fixative. Mix carefully by pipetting the sample twice. Incubate for 5 min in room temperature.
4. After incubation 350 μl Diluent buffer is added to the sample. Mix by pipetting carefully. Do not vortex the sample (*see* **Note 4**).

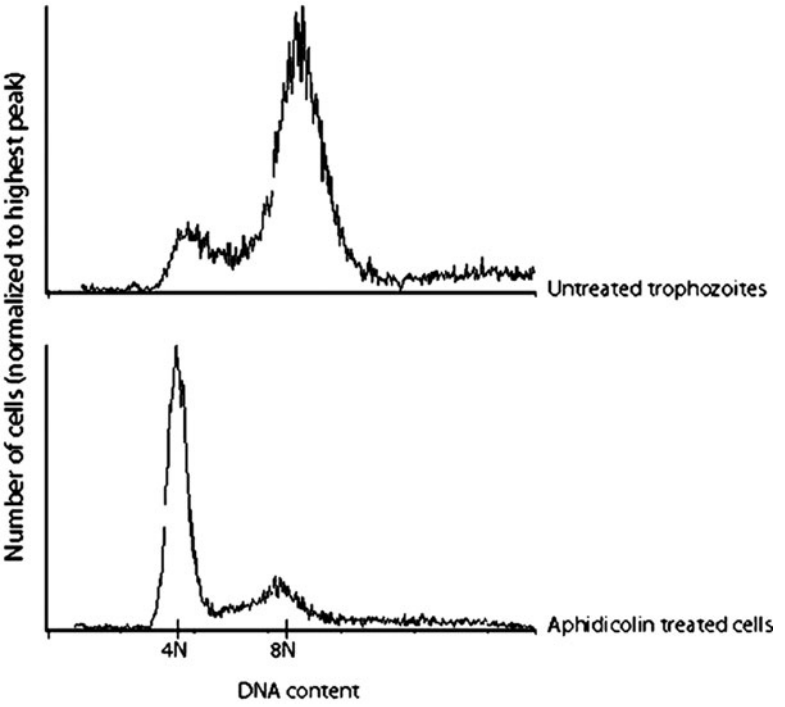


Fig. 13.1. Flow cytometry analysis of treated and untreated *Giardia* trophozoites. Cells were treated with aphidicolin according to the protocol described here.

5. The cells could either be kept in 4°C until the day after or continue the protocol immediately.

### 3.6. Wash and DNA Labeling

1. Transfer the sample to a 1.5 ml tube. Spin for 3 min at 900 × *g*.
2. Remove the supernatant carefully to avoid losing cells and add 100 µl PBS. Mix sample very gentle until pellet is dissolved. Spin again for 3 min at 900 × *g*.
3. Remove the supernatant carefully and add 500 µl PBS and 2.5 µl RNase A (10 mg/ml). Mix sample very gently until pellet is dissolved.
4. Incubate samples for 30 min at 37°C.
5. Spin sample for 3 min at 900 × *g*. Remove supernatant and add 75 µl of DNA-staining solution. Mix carefully not to destroy the cells. When the cell pellet is dissolved add 75 µl Flow buffer and mix carefully. Incubate samples on ice for 20 min and keep covered from light until analysis.
6. Read samples at 405 nm in a flow cytometry analyzer (*see* **Note 5**).

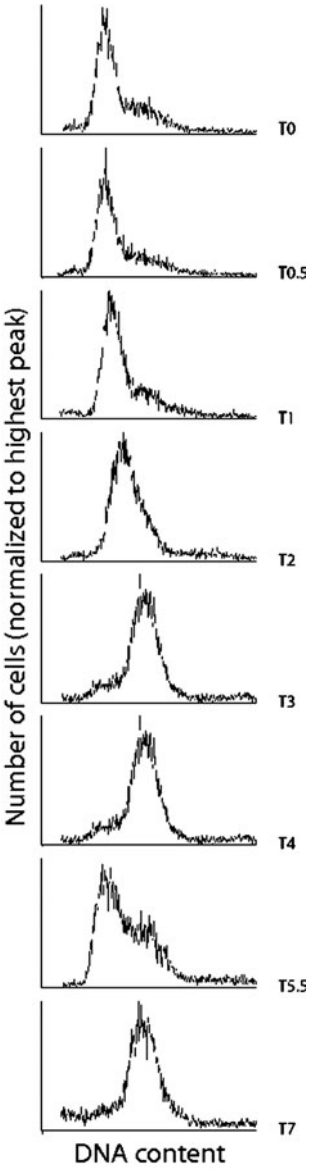


Fig. 13.2. Flow cytometry analysis of synchronized *Giardia* trophozoites. The cells were arrested in GI/S with aphidicolin and released from the drug after 6 h (i.e., one generation cycle. The WB strain C6 has a generation time of 6 h).

## 4. Notes

1. Depending on further analysis of the synchronized cells less or more cells might be needed. However, synchronizing cells in tubes instead of flasks results in more cells per volume and therefore saves aphidicolin. If it is important to easily view

the cells during the progression through the cell cycle flask or flat side tubes should be used.

2. Depending on what the cultures are grown in (10 ml tube, 50 ml tube, or flask), the number of cells/ml needed for 100% confluence differs. This is important to take into consideration if cells or the type of container is changed (tube for flask or vice versa) for synchronization. If using different containers there is a great risk of having too many or too few cells in the final culture, which will affect the result of the synchronization.
3. Cells could also be put on ice to de-attach from the tube. However, to minimize the time from harvest to fixation use of cell scraper is recommended.
4. The cells are very fragile after the acid cell fixative and it is crucial to be careful when mixing the sample with diluent buffer. If the cells are handled too rough they break and the Flow will not be satisfactory.
5. The cells are fixed in acid but the diluent buffer should neutralize the pH to protect the cells and the DNA. However, best results are reached if the flow analysis is performed within the next 2 days.

## References


1. Morrison, H. G., McArthur, A. G., Gillin, F. D., Aley, S. B., Adam, R. D., Olsen, G. J., et al. (2007) Genomic minimalism in the early diverging intestinal parasite *Giardia lamblia*. *Science* **317**, 1921–1926.
2. Gardner, M. J., Hall, N., Fung, E., White, O., Berriman, M., Hyman, R. W., et al. (2002) Genome sequence of the human malaria parasite *Plasmodium falciparum*. *Nature* **419**, 498–511.
3. Reilly, H. B., Wang, H., Steuter, J. A., Marx, A. M., and Ferdig, M. T. (2007) Quantitative dissection of clone-specific growth rates in cultured malaria parasites. *Int. J. Parasitol.* **37**, 1599–1607.
4. Inselburg, J., and Banyal, H. S. (1984) Synthesis of DNA during the asexual cycle of *Plasmodium falciparum* in culture. *Mol. Biochem. Parasitol.* **10**, 79–87.
5. Kutner, S., Breuer, W. V., Ginsburg, H., Aley, S. B., and Cabantchik, Z. I. (1985) Characterization of permeation pathways in the plasma membrane of human erythrocytes infected with early stages of *Plasmodium falciparum*: association with parasite development. *J. Cell Physiol.* **125**, 521–527.
6. Rojas, M. O., and Wasserman, M. (1993) Effect of low temperature on the in vitro growth of *Plasmodium falciparum*. *J. Eukaryot. Microbiol.* **40**, 149–152.
7. Lambros, C., and Vanderberg, J. P. (1979) Synchronization of *Plasmodium falciparum* erythrocytic stages in culture. *J. Parasitol.* **65**, 418–420.
8. Bhakdi, S. C., Ottinger, A., Somsri, S., Sratongno, P., Pannadaporn, P., Chimma, P., et al. (2010) Optimized high gradient magnetic separation for isolation of *Plasmodium*-infected red blood cells. *Malar. J.* **9**, 38.
9. Naughton, J. A., and Bell, A. (2007) Studies on cell-cycle synchronization in the asexual erythrocytic stages of *Plasmodium falciparum*. *Parasitology* **134**, 331–337.
10. Radfar, A., Mendez, D., Moneriz, C., Linares, M., Marín-García, P., Puyet, A., et al. (2009) Synchronous culture of *Plasmodium falciparum* at high parasitemia levels. *Nat. Protoc.* **4**, 1828–1844.
11. Mead, P. S., Slutsker, L., Griffin, P. M., and Tauxe, R. V. (1999) Food-related illness and death in the United States reply to Dr. Hedberg. *Emerg. Infect. Dis.* **5**, 841–842.
12. Taylor, S., Barragan, A., Su, C., Fux, B., Fentress, S. J., Tang, K., et al. (2006) A secreted serine-threonine kinase determines

virulence in the eukaryotic pathogen *Toxoplasma gondii*. *Science* **314**, 1776–1780.
13. Radke, J. R., and White, M. W. (1998) A cell cycle model for the tachyzoite of Toxoplasma gondii using the *Herpes simplex* virus thymidine kinase. *Mol. Biochem. Parasitol.* **94**, 237–247.
14. Conde de Felipe, M. M., Lehmann, M. M., Jerome, M. E., and White, M. W. (2008) Inhibition of *Toxoplasma gondii* growth by pyrrolidine dithiocarbamate is cell cycle specific and leads to population synchronization. *Mol. Biochem. Parasitol.* **157**, 22–31.
15. Simpson, L., and Braly, P. (1970) Synchronization of Leishmania tarentolae by hydroxyurea. *J. Protozool.* **17**, 511–517.
16. Galanti, N., Dvorak, J. A., Grenet, J., and McDaniel, J. P. (1994) Hydroxyurea-induced synchrony of DNA replication in the Kinetoplastida. *Exp. Cell Res.* **214**, 225–230.
17. Gale, M., Jr., Carter, V., and Parsons, M. (1994) Cell cycle-specific induction of an 89 kDa serine/threonine protein kinase activity in *Trypanosoma brucei*. *J. Cell Sci.* **107**, 1825–1832.
18. Jantzen, H., Schulze, I., and Stohr, M. (1988) Relationship between the timing of DNA replication and the developmental competence in *Acanthamoeba castellanii*. *J. Cell Sci.* **91**, 389–399.
19. Svard, S. G., Hagblom, P., and Palm, J. E. (2003) *Giardia lamblia* – a model organism for eukaryotic cell differentiation. *FEMS Microbiol. Lett.* **218**, 3–7.
20. Poxleitner, M. K., Carpenter, M. L., Mancuso, J. J., Wang, C. J., Dawson, S. C., and Cande, W. Z. (2008) Evidence for karyogamy and exchange of genetic material in the binucleate intestinal parasite *Giardia intestinalis*. *Science* **319**, 1530–1533.
21. Roxstrom-Lindquist, K., Palm, D., Reiner, D., Ringqvist, E., and Svard, S. G. (2006) Giardia immunity – an update. *Trends Parasitol.* **22**, 26–31.
22. Reiner, D. S., Ankarklev, J., Troell, K., Palm, D., Bernander, R., Gillin, F. D., et al. (2008) Synchronisation of *Giardia lamblia*: identification of cell cycle stage-specific genes and a differentiation restriction point. *Int. J. Parasitol.* **38**, 935–944.
23. Poxleitner, M. K., Dawson, S. C., and Cande, W. Z. (2008) Cell cycle synchrony in Giardia intestinalis cultures achieved by using nocodazole and aphidicolin. *Eukaryot. Cell* **7**, 569–574.
24. Cooper, S., Iyer, G., Tarquini, M., and Bissett, P. (2006) Nocodazole does not synchronize cells: implications for cell-cycle control and whole-culture synchronization. *Cell Tissue Res.* **324**, 237–242.

# Chapter 14

# Synchronization of *In Vitro* Maturation in Porcine Oocytes

**Tamas Somfai and Yuji Hirao**

## Abstract

When removed from the follicles, during the 44 h process of *in vitro* maturation (IVM) fully grown porcine oocytes resume meiosis spontaneously from the late diplotene stage of the first meiotic prophase and proceed to the metaphase-II (MII) stage at which they remain arrested until fertilization. However, the resumption may start at various times causing heterogeneity in the nuclear stage and also in cytoplasmic characteristics (i.e., the activity of certain protein kinases) within a population. Those oocytes that reach the MII stage earlier than others undergo an ageing process which is detrimental for further embryo development. The synchronization of nuclear progression is possible by a transient inhibition of meiotic resumption during the first 20–22 h of IVM either by (1) the elevation of intracellular levels of cyclic adenosine monophosphate (cAMP) or (2) suppressing the activity of the metaphase promoting factor (MPF). A protocol for each approach is described.

**Key words:** Porcine, oocyte, *in vitro* maturation, cAMP, MPF.

## 1. Introduction

Recent progress in the *in vitro* embryo production (IVP) technology in farm animals allows us to produce large numbers of embryos at relatively low cost. The IVP technology includes three major consecutive steps: *in vitro* maturation (IVM) of immature oocytes, *in vitro* fertilization (IVF), and *in vitro* culture (IVC) of the fertilized oocytes. The first step, IVM, mostly determines the scale in number of embryo production, as it provides the base material (i.e., fertilizable oocytes) for further steps of IVP or for other applications represented by nuclear transfer (1).

In porcine IVP systems, immature oocytes are usually obtained from ovaries collected at commercial slaughterhouses. More specifically, antral follicles present abundantly in ovaries

G. Banfalvi (ed.), *Cell Cycle Synchronization*, Methods in Molecular Biology 761,
DOI 10.1007/978-1-61779-182-6_14, 

are the source of immature oocytes, most of which – under *in vivo* conditions – would eventually degrade through atresia (2). Among the healthy antral follicles, those that are 3–6 mm in diameter are optimal for IVP, since they contain a fully grown oocyte with an adequate developmental competence (3).

Technically, however, collecting oocytes from 3 to 6 mm follicles does not sufficiently ensure a population of oocytes at exactly the same developmental stage. It is true that the oocytes in such follicles are all in the late diplotene of the first meiotic prophase (also known as germinal vesicle or GV stage), but many of them are at various stages toward the end of diplotene (4). In short, the population of fully grown porcine oocytes from 3 to 6 mm follicles is still somewhat "heterogeneous," which actually impairs the efficiency of IVM as discussed in detail below. We herewith describe methods to synchronize those "heterogeneous" oocytes by controlling the meiotic maturation.

As it is well known, making immature oocytes only progress to metaphase-II (MII, nuclear maturation) *in vitro* is not difficult. The early experiments of Pincus and Enzmann (5) showed that immature mammalian oocytes removed from the follicle into culture conditions resume meiosis spontaneously, demonstrating the meiosis-suppressing effect of the follicle. Essentially using the same principle, but under more sophisticated *in vitro* conditions today, immature porcine oocytes undergo germinal vesicle breakdown (GVBD) in 16–20 h and reach MII by 40 h, at which stage meiosis is arrested again until oocyte activation by sperm penetration (3, 6).

The mass production of MII oocytes by IVM may have generated a paradoxical problem in that there may be oocytes forced to resume meiosis while unprepared to start it properly. Specifically, there is a large variation in nuclear morphology of GV-stage porcine oocytes in the follicles (7, 8). This morphological heterogeneity persists after a certain period of culture (7). It seems possible that the heterogeneity may affect the timing of overall meiotic progression (9). In fact, previous studies have shown that porcine oocytes allowed to mature "freely" *in vitro* reached the MII stage at various time points of culture (10, 11). From that aspect alone, synchronization of the meiotic progress by temporary prevention will have a great advantage, since it enables us to manipulate a large number of oocytes at the same time (12).

In porcine oocytes the transient inhibition of GVBD can be achieved either by elevating intercellular levels of cyclic adenosine monophosphate (cAMP) (**Note 1**) or by the suppression of activity of *m*etaphase (or *m*aturation) *p*romoting *f*actor (MPF) (**Note 2**). Intracellular cAMP levels in porcine oocytes can be effectively elevated by 1 mM dibutyryl cyclic AMP (dbcAMP), a membrane-permeable cAMP analogue (10, 13). MPF, consisting of a regulator subunit (cyclin B1) and a catalytic subunit ($p34^{cdc2}$), plays a key role in the meiotic progression to the

consecutive two metaphases (14). MPF activity can be effectively suppressed by butyrolactone-I (BL-I) or roscovitine (Ros), specific reversible inhibitors of $p34^{cdc2}$ protein kinase, and also by protein synthesis inhibitors (**Note 3**). During the temporary arrest at the GV stage the nuclear progression does not stop immediately and completely; the chromatin exhibits a very slow but progressive condensation (15, 16), reaching a certain stage, the so-called GV II stage in the pig (4, 10). Owing to this phenomenon the progression of meiotic maturation becomes synchronous (10) and accelerated (17) after the release from the meiosis blocking agent. Besides the convenience of optimizing the timing, oocytes of various species showed improved developmental competence after blocking at the GV stage (10, 18, 19). In the pig, a transient blocking for the first 20–22 h of oocyte culture was effective to prevent precocious nuclear maturation (10) and to reduce the frequency of polyspermic fertilization (20, 21), which is significant since the high incidence of polyspermic fertilization has always been a major problem that impairs the efficiency of IVP in the pig (22). Probably, when allowed to mature without blocking, some oocytes may reach MII earlier than others and undergo ageing which manifests its detrimental effects in an elevated incidence of polyspermic fertilization (20, 23). While ageing *in vitro* various changes occur in MII oocytes, such as altered $Ca^{2+}$ regulation and mitochondrial activities and premature exocytosis of cortical granules, which greatly reduce the developmental competence (24). In the following paragraphs two optional protocols are discussed which are (1) *transient elevation of intracellular cAMP with dbcAMP (Protocol A)* and (2) *transient suppression of MPF activity using BL-I (Protocol B)*. The preference of these protocols may depend on the species (**Note 4**), although both ways are highly effective in pigs. Furthermore, the possible positive (**Note 5**) and negative side effects (**Note 6**) of the protocols should also be considered.

## 2. Materials

### 2.1. Reagents

Specific reagents or media necessary for *Protocol A* are denoted by one asterisk (*) whereas specific reagents/media of *Protocol B* are denoted by two asterisks (**). Reagents and media applied by both protocols are without denotations.

Trivial reagents such as inorganic components of media are not listed.

### 2.2. Stock Solutions

1. NCSU-37 Stock A*: 136 mM NaCl, 5.98 mM KCl, 2.13 mM $CaCl_2$, 1.49 mM $KH_2PO_4$, 1.49 mM $MgSO_4$, and 1.25 mM glutamine. It can be supplemented with

phenol red (optional). The osmolarity is adjusted to 273 ± 3 mOsm/l, the pH is 7.1. After sterilization with a 0.22 μm filter the solution can be stored for several months at 4°C.

2. NCSU-37 Stock B* solution: 125 mM $NaHCO_3$. Phenol red is optional. Adjust osmolality to 229 ± 3 mOsm/l, sterilize it with a 0.22 μm filter, and store it at 4°C for several months.
3. Porcine follicular fluid (pFF): pFF is aspirated with a 20 G needle and 10 ml syringe from the 3–6 mm follicles of ovaries derived from prepubertal gilts at slaughterhouse. The aspirated fluid is centrifuged at 1,800 × *g* for 90 min at 4°C. The supernatant solution is collected to make 10–15 ml aliquots in polystyrene tubes and stored at –20°C until the amount of collected pFF reaches approximately 1 l. The pFF aliquots are then thawed and mixed as a single lot. The lot is filtered with 0.45 μm Millipore filters, divided in tubes (10 ml/tube), and stored at –20°C until use.
4. Cysteine* (100×): L-cysteine is dissolved in the base IVM medium at 60 mM. 1 ml aliquots are stored at –20°C.
5. Cysteamine** (100×): Cysteamine is dissolved in the base IVM medium at 15 mM. Store 200 μl aliquots at –20°C.
6. Hormones (100×): Dissolve pregnant mare's serum gonadotropin (PMSG; Serotropin 1000 IU/tube) and human chorionic gonadotropin (hCG; Pubergen 1500 IU/tube) together at a concentration of 1,000 IU/ml each in the base IVM medium. Store the stock at –20°C in 200 μl aliquots.
7. Antibiotics (1,000×): Dissolve streptomycin sulfate (0.1 g/ml) and Penicillin G potassium ($1\times10^5$ U/ml) in water. The stock is stored at –20°C in 200 μl aliquots.
8. β-Mercaptoethanol (2-ME) (1,000×): 2-ME (4.3 M) is diluted to 50 mM with the base IVM medium. The stock is stored at –20°C in 200 μl aliquots.
9. dbcAMP* (100×): dbcAMP is dissolved in pFF free base IVM medium at 100 mM. The solution is stored in 200 μl aliquots in cryotubes at –20°C until use.
10. Butyrolactone-I** (BL-I): BL-I is dissolved in DMSO; the optimal concentration of the stock should be determined by the final concentration of BL-I in order to avoid an unnecessarily high dose of DMSO in the medium. The stock concentration can be up to 25 mg/ml (58.9 mM), according to the manufacturer's information. To use 20 μM BL-I in medium to prevent porcine oocyte maturation (17), a stock solution at 10 mM is prepared, which keeps

the final DMSO concentration at 0.2%. The effective concentration of BL-I, however, may depend on the purpose of use, e.g., induction of artificial activation (25), and even on the composition of the medium (26, 27). When BL-I is used at 100 μM or higher a stock denser than 10 mM is recommended. The stock solution is stored at –20°C as 5 μl aliquots. Care should be taken to avoid repeated freezing and thawing of the stock solution.

11. Roscovitine is another specific inhibitor of $p34^{cdc2}$, which can be dissolved in DMSO and used in the same manner as BL-I, except that the (*R*)-enantiomer of Ros has slightly lower specificity than the (*S*)-enantiomer of Ros and BL-I, according to the manufacturer's information.

### 2.3. Reagent Setup

#### 2.3.1. Oocyte Collection Medium

TCM-199 (with Hanks salt) supplemented with 10% (v/v) fetal bovine serum, 20 mM HEPES, 100 U/ml penicillin G potassium, and 0.1 mg/ml streptomycin sulfate, pH 7.3 (hereafter referred to as "TCM-199 Air") (**Note 7**).

#### 2.3.2. Media for cAMP Elevation (Protocol A)

1. IVM medium (NCSU-37 base): Our current protocol applies an NCSU-37-based medium (28) modified by Kikuchi et al. (29) (**Note 8**). Briefly, for 100 ml medium mix NCSU-37 stock A (72 ml), NCSU-37 stock B (18 ml), pFF (10 ml), glucose (90 mg), sorbitol (196.7 mg), 2-ME stock (100 μl), L-cysteine stock (1 ml), and antibiotics stock (100 μl). A two-step filtration of the medium (first with a 0.45 μm filter and then with a 0.22 μm filter) is recommended. The filtered IVM medium can be stored for up to 3 weeks at 4°C.
2. IVM-Arrest medium (NCSU-37 base): For 10 ml medium add 100 μl dbcAMP stock and 100 μl hormone stock to 9.8 ml of IVM medium. Clear the solution with a 0.22 μm filter. This solution should be prepared fresh before use. To elevate intracellular cAMP levels dbcAMP can be substituted with other drugs (**Note 9**).

#### 2.3.3. Media for MPF Suppression (Protocol B)

1. IVM medium (TCM-199 Base): Our experiments of suppressing MPF activity using BL-I (17) were conducted with a TCM-199 (with Earl's salts and 25 mM HEPES, pH 7.4) with modifications similar to that made on NCSU-37 as described in **Section 2.2**. In brief, the medium was supplemented with sodium pyruvate, gonadotropins, antibiotics, and 150 μM cysteamine. We also added 20 ng/ml epidermal growth factor (EGF, Sigma). In addition, as a source of macromolecules, either 0.1% polyvinyl alcohol (PVA) or 10% pFF was supplemented (**Note 10**). These modified media are hereafter referred to as modified TCM-199/PVA and modified TCM-199/pFF, respectively.

2. IVM-Arrest medium (TCM-199 Base): For 2.5 ml medium add 5 μl BL-I stock to the modified TCM-199/PVA. This solution should be prepared fresh before use. For the culture following the BL-I treatment, however, the modified TCM-199/pFF is recommended, since the rate of oocytes progressing to MII was higher in the medium than in the modified TCM-199/PVA (unpublished observations).

## 3. Methods

In general meiosis synchronization of oocytes during *in vitro* maturation consists of three technological steps: (1) oocyte collection; (2) meiosis suppression; and (3) meiosis resumption (**Fig. 14.1**). These steps are performed similarly when either cAMP elevators (*Protocol A*) or MPF blockers (*Protocol B*) are used to synchronize meiosis. In brief, after collection cumulus-enclosed oocytes are cultured in an IVM-Arrest medium containing a blocking substrate (either an elevator of intracellular cAMP or the suppressor of MPF) to block meiotic resumption temporarily for 22–24 h. After treatment with IVM-Arrest medium the oocytes are subsequently cultured in IVM medium which allows the resumption of meiosis in a synchronized manner.

### 3.1. Oocyte Collection

1. The ovaries are placed in Petri dishes (60 × 15 mm) on a 37°C warm plate and follicles of 3–6 mm in diameter are dissected with a lance (**Note 11**). Alternatively the oocytes can be aspirated from the follicles using a syringe and needle (size 19–20).
2. The pFF is collected in 15 ml centrifuge tubes and left at a vertical position in a water bath for 10 min at 37°C. During this time the oocytes and other follicle cells are deposited on the bottom forming a pale sediment.

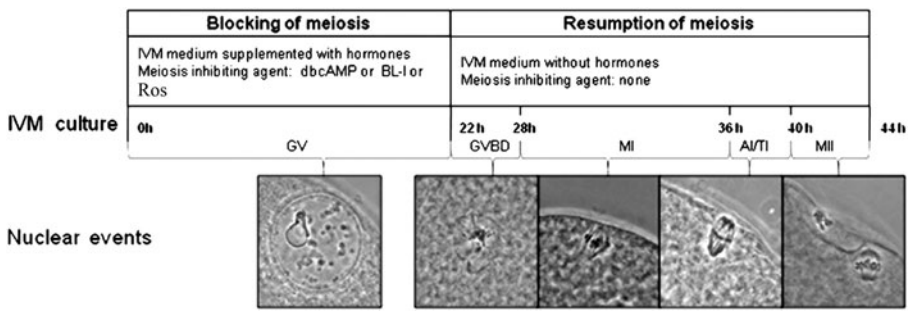


Fig. 14.1. Treatment regimen and the approximate timing of nuclear events with and without meiosis blocking during the first 22 h of IVM culture. Nuclear stages in oocytes were evaluated by phase contrast microscopy (400×) after staining the chromatin with 1% orcein. Abbreviations: GV = germinal vesicle stage (prophase, late diplotene); GVBD = germinal vesicle breakdown; MI = metaphase-I; AI = anaphase-I; TI = telophase-I; MII = metaphase-II.

3. Remove the upper (clear) layer of pFF and dilute the sediment by dropping it in 5 ml of the collection medium in a 60 × 15 mm Petri dish. Approximately 6–10 drops (0.3–0.5 ml) sediment can be diluted in one Petri dish.
4. The oocytes can be then selected under a stereo microscope with a warm stage. Collect only fully grown oocytes with a homogenous cytoplasm surrounded by several layers of cumulus cells. The presence of morphologically normal cumulus cells completely surrounding the oocytes is indispensable, since the cumulus cells play a basic role in the regulation of both nuclear (30, 31) and cytoplasmic processes (32) which are elemental for gaining developmental competence of porcine oocytes. Cumulus (COCs) oocyte complexes attached with a part of the granulosa layer of the follicle wall can also be used (**Note 12**).
5. Wash the selected oocytes three times in the collection medium. The entire collection procedure should not be longer than 2 h.

### 3.2. Meiosis Suppression

This step refers to the preparatory period of oocyte maturation (also called as "prematuration") in the presence of one of the meiosis blocking agents.

1. The washing and culture dishes should be prepared and preincubated for at least 2 h before use at culture conditions.
2. The oocytes are washed three times in 2 ml aliquots of IVM-Arrest medium in Petri dishes (35 × 10 mm) covered by paraffin oil under a stereo microscope with a warm stage.
3. Then the oocytes are placed in 500 μl aliquots of IVM-Arrest medium in four well dishes (Nunclon Multidishes, Nalge Nunc International, Roskilde, Denmark) in groups of 30–50 per well without oil covering.
4. The COCs are cultured in an atmosphere of 5% $CO_2$, 20% $O_2$, and 75% $N_2$. Optionally maturation culture can be performed under 5% $CO_2$, 5% $O_2$, and 90% $N_2$ tensions (**Note 13**).
5. The optimal length of the suppression stage is approximately 20–24 h. During this stage the oocytes remain at the GV-II stage whereas over 40% of the oocytes cultured without a meiosis blocking agent would resume meiosis and undergo GVBD (10, 20) (**Fig. 14.2**).

### 3.3. Meiosis Resumption

During this phase the COCs are transferred to the *IVM medium* that allows the nuclear progression of oocytes.

1. The oocytes are removed from the IVM-Arrest medium and washed consecutively three times in 2 ml aliquots of IVM medium under a stereo microscope with a warm stage.

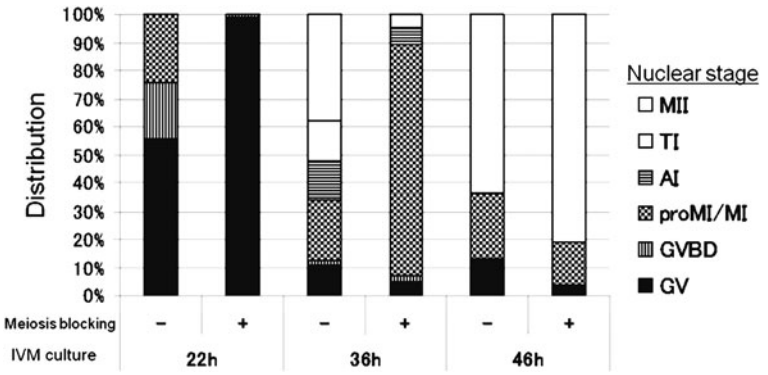


Fig. 14.2. The distribution of oocytes at different nuclear stages at 22, 36, and 46 h after IVM with or without meiosis blocking by 1 mM dbcAMP during the first 22 h of culture. Abbreviations: GV = germinal vesicle stage (prophase, late diplotene); GVBD = germinal vesicle breakdown; MI = metaphase-I; AI = anaphase-I; TI = telophase-I; MII = metaphase-II.

2. Oocytes are then cultured in 500 μl aliquots of the IVM medium in four well dishes under conditions similar to the previous step of the arrest. The cultured oocytes progress nuclear events in a synchronized manner as follows:
   a. The breakdown of the germinal vesicle occurs shortly after the medium exchange, and the MI stage is reached in about 10 h (at 30–33 h from the beginning of IVM collectively).
   b. The oocytes tend to remain at the MI stage until 36 h of the total period of IVM and then proceed to the A I/T I stages (**Fig. 14.2**).
   c. The oocytes reach the MII stage (**Fig. 14.2**) in a relatively synchronous manner and also develop the ability of activation – to await the penetration by a spermatozoon – by 40 h IVM (20).
3. Oocytes at the MI and MII stages can be harvested at 33 and 44 h IVM, respectively. Since oocytes reach each meiotic stage in the same time en masse confirmation of meiotic stage by nuclear staining (**Note 14**) is not necessary.

## 4. Notes

1. In mammalian oocytes a high level of intercellular cAMP is responsible for activating cAMP-dependent protein kinase (PKA) that controls meiotic arrest at the GV stage within the follicle (33–35). The gonadotropins such as FSH and

LH acting through follicular cells are known to briefly elevate and then reduce the cAMP levels in mammalian oocytes, including those of pigs (30, 36, 37). The drop of intracellular cAMP causes the inactivation of PKA and the activation of mitogen-activated protein (MAP) kinase which lead to the resumption of meiosis (33, 35, 38, 39).

2. Once PKA is inactivated in GV-stage oocytes the progress of meiosis is driven by oscillations in the activity of MPF and by the activation of mitogen-activated protein kinase (MAPK) (40). Selective protein kinase inhibitors such as BL-I and Ros compete for the ATP binding sites of $p34^{cdc2}$ and reversibly block the activity of MPF, which prevents nuclear maturation in bovine (27, 41) and porcine oocytes (42, 43) in a dose-dependent manner without affecting mitochondrial and microfilament dynamics.
3. Inhibition of protein synthesis in a broad manner by puromycin (44) or cycloheximide (45) or the use of protein kinase inhibitors such as 6-dimethylaminopurine (6-DMAP) (46) is also effective in preventing activation of MPF in oocytes. Use of such "broad" inhibitors, however, will increase the risks of side effects that may lead to serious problems in the later stage of oocyte/embryo development (47).
4. Although in denuded bovine oocytes elevated intracellular cAMP level acts as an inhibitor to nuclear maturation this approach is not so effective on cumulus-enclosed oocytes in this species (48), which can be a good reason to use the inhibitors of MPF activity for the purpose of synchronizing oocyte maturation.
5. The meiotic arrest at the GV stage for 20–22 h using 1 mM dbcAMP apparently enhances the ability of oocytes to develop to the blastocyst stage, which seems to be independent from the avoidance of polyspermy (10). Nevertheless such an effect was observed only in the oocytes from follicles smaller than 4 mm in diameter of prepubertal animals (13, 49). A possible reason for this phenomenon might be that oocytes from small follicles of young animals perhaps require additional protein synthesis prior to the meiotic maturation, and the blocking of GVBD allows them time to do so since the protein synthesis persists during the arrest (42). Moreover, cAMP promotes maintenance of gap junctional communications between the cumulus cells and the oocyte and affects gene expression in COCs (50).
6. Although BL-I is a highly specific inhibitor of $p34^{cdc2}$ kinase, the results of the inhibition may affect other events

occurring in the cytoplasm. Some delay in completing cytoplasmic maturation of porcine oocytes (characterized by the ability of oocytes to form female pronucleus after electric stimulus) was observed after the meiotic arrest by BL-I (17). A long-term culture (40 h) of bovine oocytes with 100 μM BL-I resulted in abnormal morphology of the chromatin and cytoplasm and in the loss of the contact between the oocyte and cumulus cells (51). An even longer term of meiotic inhibition (48 h) of porcine oocytes by 50 μM Ros was found to be detrimental to embryo development, which was supposedly explained by the reduced intracellular glutathione levels (52). On the other hand, piglets have been obtained from oocytes after blocking meiosis resumption for 22 h with 50 μM Ros (53). It has also been reported that BL-I and Ros, when combined, were highly effective at low concentrations for preventing bovine oocyte maturation without side effects (54). It should be noted, however, that in the relevant experiments the preparatory arresting culture was conducted in the absence of gonadotropin.

7. Collection and selection of cumulus–oocyte complexes (COCs) from porcine follicular fluid (pFF) sediments are usually performed under atmospheric $O_2$ and $CO_2$ tension (in air). It often takes 1 or 2 h from the collection of the oocytes to the setting up of the cultures. For this purpose use of media containing pH-stabilizing buffer in air is more influential on the oocyte environment than the type of medium. The most commonly used are HEPES-buffered media, such as Tyrode's lactate medium or tissue culture medium 199 (TCM-199 or medium 199).
8. Several different kinds of media are available as a base solution for *in vitro* oocyte maturation in the pig. The most popularly used media in recent years are TCM-199 (55), NCSU-37, NCSU-23 (28), and POM (56). The choice may depend on personal preference and the intention to use undefined supplementations such as pFF and FBS. The supplementation of pFF has been recommended for medium with a simple composition such as NCSU-37 (57). However, media of more complex compositions, such as TCM-199 or POM, apparently need no such undefined factors.
9. The intracellular level of cAMP in mammalian oocytes can be elevated by other alternative reagents such as (1) invasive adenylate cyclase (iAC), a catalytic domain of adenylate cyclase which penetrates into oocytes and directly raises level of cAMP (58); (2) Forskolin, a natural diterpene, which activates adenylate cyclase in oocytes (59); (3) phosphodiesterase inhibitors which, unlike the above

cAMP elevators, prevent the degradation of cAMP in oocytes, e.g., 3-isobutylmethyl-xanthine (IBMX), milrinone, rolipram, or cilostamide (60). Although the intracellular cAMP level might change during the oocyte collection/selection (61) it does not trigger the precocious maturation of porcine oocytes (20).

10. Possible interactions of BL-I with protein supplements should be considered. Bovine serum, follicular fluid, and bovine serum albumin were reported to reduce the meiosis blocking effect of BL-I (27). Therefore, use of media without those factors is recommended for the meiosis blocking with BL-I. Such supplementations can be replaced by PVA (27). Similarly, if the oocytes are cultured in microdrops, BL-I in medium could be partly attenuated by paraffin oil or mineral oil covering the microdrops; however, there have been reports, including ours, on the successful inhibition of oocyte maturation by BL-I achieved in microdrops covered with oil.
11. Use of smaller follicles, 1–2 mm in diameter, should be avoided, because the oocytes within are also small; growing oocytes show a lower chance to undergo the MI to MII transition than fully grown oocytes (62) and, even when fertilized, the resulting embryos show a reduced ability to undergo embryonic development (3). Such small oocytes most likely lack some crucial (amount of) molecules, such as proteins and maternal mRNA, which control the cell cycle and the embryonic development until the genomic transition occurring at the 4-cell stage in the pig (63). Collection of fully grown oocytes is therefore a prerequisite for successful IVP.
12. The presence or absence of granulosa cell mass attached to the COCs is irrelevant for the production of MII oocytes; nevertheless those granulosa cells can exert some positive effect on the quality of oocytes by preventing precocious nuclear progression through the effect on the cumulus cells (11).
13. Although reduced $O_2$ tension during IVM does not affect embryo development to the blastocyst stage it seems to have some merit for the further embryo development by promoting the activation process in oocytes and improving cell numbers in blastocysts during embryo culture (64).
14. The nuclear status of oocytes can be confirmed by vital nuclear stains such as Hoechst 33342 or Sybr14. However, these fluorochromes compromise developmental competence (65); therefore, their application should be avoided when oocytes are used to generate embryos.

## References


1. Betthauser, J., Forsberg, E., Augenstein, M., Childs, L., Eilertsen, K., Enos, J., et al. (2000) Production of cloned pigs from in vitro systems. *Nat. Biotechnol.* **18**, 1055–1059.
2. Manabe, N., Goto, Y., Matsuda-Minehata, F., Inoue, N., Maeda, A., and Manabe, N. (2004) Regulation mechanism of selective atresia in porcine follicles: regulation of granulosa cell apoptosis during *atresia*. *J. Reprod. Dev.* **50**, 493–514.
3. Marchal, R., Vigneron, C., Perreau, C., Bali-Papp, Á., and Mermillod, P. (2002) Effect of follicular size on meiotic and developmental competence of porcine oocytes. *Theriogenology* **57**, 1523–1532.
4. Motlik, J., and Fulka, J. (1976) Breakdown of the germinal vesicle in pig oocytes in vivo and in vitro. *J. Exp. Zool.* **198**, 155–162.
5. Pincus, G., and Enzmann, E. V. (1935) The comparative behavior of mammalian eggs in vivo and in vitro. I. The activation of ovarian eggs. *J. Exp. Med.* **62**, 665–675.
6. Wehrend, A., and Meinecke, B. (2001) Kinetics of meiotic progression, M phase promoting factor (MPF) and mitogen-activated protein kinase (MAP kinase) activities during in vitro maturation of porcine and bovine oocytes: species specific differences in the length of the meiotic stages. *Anim. Reprod. Sci.* **66**, 175–184.
7. Funahashi, H., Cantley, T. C., and Day, B. N. (1997) Preincubation of cumulus–oocyte complexes before exposure to gonadotropins improves the developmental competence of porcine embryos matured and fertilized in vitro. *Theriogenology* **47**, 679–686.
8. Nagai, T., Ebihara, M., Onishi, A., and Kubo, M. (1997) Germinal vesicle stages in pig follicular oocytes collected by different methods. *J. Reprod. Dev.* **43**, 339–343.
9. Mcgaughey, R. W., Montgomery, D. H., and Richter, J. D. (1979) Germinal vesicle configurations and patterns of polypeptide synthesis of porcine oocytes from antral follicles of different size as related to their competence for spontaneous maturation. *J. Exp. Zool.* **209**, 239–254.
10. Funahashi, H., Cantley, T. C., and Day, B. N. (1997) Synchronization of meiosis in porcine oocytes by exposure to dibutyryl cyclic adenosine monophosphate improves developmental competence following in vitro fertilization. *Biol. Reprod.* **57**, 49–53.
11. Somfai, T., Kikuchi, K., Onishi, A., Iwamoto, M., Fuchimoto, D., Papp, A. B., et al. (2004) Relationship between the morphological changes of somatic compartment and the kinetics of nuclear and cytoplasmic maturation of oocytes during in vitro maturation of porcine follicular oocytes. *Mol. Reprod. Dev.* **68**, 484–491.
12. Alfonso, J., García-Rosello, E., García-Mengual, E., Salvador, I., and Silvestre, M. A. (2009) The use of roscovitine to fit the 'time frame' on in vitro porcine embryo production by intracytoplasmic sperm injection. *Zygote* **17**, 63–70.
13. Bagg, M. A., Nottle, M. B., Grupen, C. G., and Armstrong, D. T. (2006) Effect of dibutyryl cAMP on the cAMP content, meiotic progression, and developmental potential of in vitro matured pre-pubertal and adult pig oocytes. *Mol. Reprod. Dev.* **73**, 1326–1332.
14. Hashimoto, N., and Kishimoto, T. (1988) Regulation of meiotic metaphase by a cytoplasmic maturation promoting factor during mouse oocyte maturation. *Dev. Biol.* **126**, 242–252.
15. Kubelka, M., Rimkevičová, Z., Guerrier, P., and Motlík, J. (1995) Inhibition of protein synthesis affects histone H1 kinase, but not chromosome condensation activity, during the first meiotic division of pig oocytes. *Mol. Reprod. Dev.* **41**, 63–69.
16. Kubelka, M., Anger, M., Kalous, J., Schultz, R. M., and Motlík, J. (2002) Chromosome condensation in pig oocytes: lack of a requirement for either cdc2 kinase or MAP kinase activity. *Mol. Reprod. Dev.* **63**, 110–118.
17. Hirao, Y., Nishimoto, N., Kure-bayashi, S., Takenouchi, N., Yamauchi, N., Masuda, H., et al. (2003) Influence of meiotic inhibition by butyrolactone-I during germinal vesicle stage on the ability of porcine oocytes to be activated by electric stimulation after nuclear maturation. *Zygote* **11**, 191–197.
18. Downs, S. M., Schroeder, A. C., and Eppig J. J. (1986) Developmental capacity of mouse oocytes following maintenance of meiotic arrest in vitro. *Gamete Res.* **15**, 305–316.
19. Hashimoto, S., Minami, N., Takakura, R., and Imai, H. (2002) Bovine immature oocytes acquire developmental competence during meiotic arrest in vitro. *Biol. Reprod.* **66**, 1696–1701.
20. Somfai, T., Kikuchi, K., Onishi, A., Iwamoto, M., Fuchimoto, D., Papp, A. B., et al. (2003) Meiotic arrest maintained by cAMP during the initiation of maturation enhances meiotic potential and developmental competence and

reduces polyspermy of IVM/IVF porcine oocytes. *Zygote* **11**, 199–206.
21. Kim, J. S., Cho, Y. S., Song, B. S., Weec, G., Park, J. S., Choo, Y. K., et al. (2008) Exogenous dibutyryl cAMP affects meiotic maturation via protein kinase A activation; it stimulates further embryonic development including blastocyst quality in pigs. *Theriogenology* **69**, 290–301.
22. Nagai, T., Funahashi, H., Yoshioka, K., and Kikuchi, K. (2006) Update of in vitro production of porcine embryos. *Front. Biosci.* **11**, 2565–2573.
23. Grupen, C. G., Nagashima, H., and Nottle, M. B. (1997) Asynchronous meiotic progression in porcine oocytes matured in vitro: a cause of polyspermic fertilization? *Reprod. Fertil. Dev.* **9**, 187–191.
24. Miao, Y. L., Kikuchi, K., Sun, Q. Y., and Schatten, H. (2009) Oocyte aging: cellular and molecular changes, developmental potential and reversal possibility. *Hum. Reprod. Update* **15**, 573–585.
25. Dinnyés, A., Hirao, Y., and Nagai, T. (2000) Parthenogenetic activation of porcine oocytes by electric pulse and/or butyrolactone I treatment. *Cloning* **1**, 209–216.
26. Motlik, J., Pavlok, A., Kubelka, M., Kalous, J., and Kalab, P. (1998) Interplay between CDC2 kinase and MAP kinase pathway during maturation of mammalian oocytes. *Theriogenology* **49**, 461–469.
27. Kubelka, M., Motlík, J., Schultz, R. M., and Pavlok, A. (2000) Butyrolactone I reversibly inhibits meiotic maturation of bovine oocytes, without influencing chromosome condensation activity. *Biol. Reprod.* **62**, 292–302.
28. Petters, R. M., and Wells, K. D. (1995) Culture of pig embryos. *J. Reprod. Fertil. Suppl.* **48**, 61–73.
29. Kikuchi, K., Onishi, A., Kashiwazaki, N., Iwamoto, M., Noguchi, J., Kaneko, H., et al. (2002) Successful piglet production after transfer of blastocysts produced by a modified in vitro system. *Biol. Reprod.* **66**, 1033–1041.
30. Shimada, M., Nishibori, M., Isobe, N., Kawano, N., and Terada, T. (2003) Luteinizing hormone receptor formation in cumulus cells surrounding porcine oocytes, and its role during meiotic maturation of porcine oocytes. *Biol. Reprod.* **68**, 1149–1159.
31. Shimada, M., Ito, J., Yamashita, Y., Okazaki, T., and Isobe, N. (2003) Phosphatidylinositol 3-kinase in cumulus cells is responsible for both suppression of spontaneous maturation and induction of gonadotropin-stimulated maturation of porcine oocytes. *J. Endocrinol.* **179**, 25–34.
32. Maedomari, N., Kikuchi, K., Ozawa, M., Noguchi, J., Kaneko, H., Ohnuma, K., et al. (2007) Cytoplasmic glutathione regulated by cumulus cells during porcine oocyte maturation affects fertilization and embryonic development in vitro. *Theriogenology* **67**, 983–993.
33. Bornslaeger, E. A., Mattei, P., and Schultz, R. M. (1986) Involvement of cAMP-dependent protein kinase and protein phosphorylation in regulation of mouse oocyte maturation. *Dev. Biol.* **114**, 453–462.
34. Cameron, I. L. (1987) Maintenance of oocyte meiotic arrest by follicular fluid factors. In: Schlegel, R. A., Halleck, M. S., Rao, P. N. (Eds.) Molecular Regulation of Nuclear Events in Mitosis and Meiosis, Academic, New York, NY.
35. Sun, Q. Y., Miao, Y. L., and Schatten, H. (2008) Towards a new understanding on the regulation of mammalian oocyte meiosis resumption. *Cell Cycle* **8**, 2741–2747.
36. Bornslaeger, E. A., and Schultz, R. M. (1985) Regulation of mouse oocyte maturation: Effect of elevating cumulus cell cAMP on oocyte cAMP levels. *Biol. Reprod.* **33**, 698–704.
37. Mattioli, M., Galeati, G., Barboni, B., and Seren, E. (1994) Concentration of cyclic AMP during the maturation of pig oocytes in vivo and in vitro. *J. Reprod. Fertil.* **100**, 403–409.
38. Schultz, R. M., Montgomery, R. R., and Belanoff, J. R. (1983) Regulation of mouse oocyte meiotic maturation: implication of a decrease in oocyte cAMP and protein dephosphorylation in commitment to resume meiosis. *Dev. Biol.* **97**, 264–273.
39. Sun, Q. Y., Lu, Q., Breitbart, H., and Chen, D. Y. (1999) cAMP inhibits mitogen-activated protein (MAP) kinase activation and resumption of meiosis, but exerts no effects after spontaneous germinal vesicle breakdown (GVBD) in mouse oocytes. *Reprod. Fertil. Dev.* **11**, 81–86.
40. Sun, Q. Y., and Nagai, T. (2003) Molecular mechanisms underlying pig oocyte maturation and fertilization. *J. Reprod. Dev.* **49**, 347–359.
41. Mermillod, P., Tomanek, M., Marchal, R., and Meijer, L. (2000) High developmental competence of cattle oocytes maintained at the germinal vesicle stage for 24 hours in culture by specific inhibition of MPF kinase activity. *Mol. Reprod. Dev.* **55**, 89–95.
42. Marchal, R., Tomanek, M., Terqui, M., and Mermillod, P. (2001) Effects of cell cycle

dependent kinases inhibitor on nuclear and cytoplasmic maturation of porcine oocytes. *Mol. Reprod. Dev.* **60**, 65–73.
43. Wu, G. M., Sun, Q. Y., Mao, J., Lai, L., McCauley, T. C., Park, K. W., et al. (2002) High developmental competence of pig oocytes after meiotic inhibition with a specific M phase promoting factor kinase inhibitor, butyrolactone I. *Biol. Reprod.* **67**, 170–177.
44. Motlik, J., Nagai, T., and Kikuchi, K. (1991) Resumption of meiosis in pig oocytes cultured with cumulus and parietal granulosa cells: the effect of protein synthesis inhibition. *J. Exp. Zool.* **259**, 386–391.
45. Kubelka, M., Motík, J., Fulka, J., Jr., Procházka, R., Rimkevicová, Z., and Fulka, J. (1988) Time sequence of germinal vesicle breakdown in pig oocytes after cycloheximide and P-aminobenzamidine block. *Gamete Res.* **19**, 423–431.
46. Avery, B., Hay-Schmidt, A., Hyttel, P., and Greve, T. (1998) Embryo development, oocyte morphology, and kinetics of meiotic maturation in bovine oocytes exposed to 6-dimethylaminopurine prior to in vitro maturation. *Mol. Reprod. Dev.* **50**, 334–344.
47. Lonergan, P., Fair, T., Khatir, H., Cesaroni, G., and Mermillod, P. (1998) Effect of protein synthesis inhibition before or during in vitro maturation on subsequent development of bovine oocytes. *Theriogenology* **50**, 417–431.
48. Bilodeau, S., Fortier, M. A., and Sirard, M. A. (1993) Effect of adenylate cyclase stimulation on meiotic resumption and cyclic AMP content of zona-free and cumulus-enclosed bovine oocytes in vitro. *J. Reprod. Fertil.* **97**, 5–11.
49. Bagg, M. A., Nottle, M. B., Armstrong, D. T., and Grupen, C. G. (2007) Relationship between follicle size and oocyte developmental competence in prepubertal and adult pigs. *Reprod. Fertil. Dev.* **19**, 797–803.
50. Ozawa, M., Nagai, T., Somfai, T., Nakai, M., Maedomari, N., Fahrudin, M., et al. (2008) Comparison between effects of 3-isobutyl-1-methylxanthine and FSH on gap junctional communication, LH-receptor expression, and meiotic maturation of cumulus-oocyte complexes in pigs. *Mol. Reprod. Dev.* **75**, 857–866.
51. Fair, T., Hyttel, P., Motlik, J., Boland, M., and Lonergan, P. (2002). Maintenance of meiotic arrest in bovine oocytes in vitro using butyrolactone I: effects on oocyte ultrastructure and nucleolus function. *Mol. Reprod. Dev.* **62**, 375–386.
52. Romar, R., and Funahashi, H. (2006) In vitro maturation and fertilization of porcine oocytes after a 48 h culture in roscovitine, an inhibitor of p34cdc2/cyclin B kinase. *Anim. Reprod. Sci.* **92**, 321–333.
53. Coy, P., Romar, R., Ruiz, S., Cánovas, S., Gadea, J., García Vázquez, F., et al. (2005) Birth of piglets after transferring of in vitro-produced embryos pre-matured with R-roscovitine. *Reproduction* **129**, 747–755.
54. Ponderato, N., Lagutina, I., Crotti, G., Turini, P., Galli, C., and Lazzari, G. (2001) Bovine oocytes treated prior to in vitro maturation with a combination of butyrolactone I and roscovitine at low doses maintain a normal developmental capacity. *Mol. Reprod. Dev.* **60**, 579–585.
55. Mattioli, M., Bacci, M. L., Galeati, G., and Seren, E. (1989) Developmental competence of pig oocytes matured and fertilized in vitro. *Theriogenology* **31**, 1201–1207.
56. Yoshioka, K., Suzuki, C., and Onishi, A. (2008) Defined system for in vitro production of porcine embryos using a single basic medium. *J. Reprod. Dev.* **54**, 208–213.
57. Abeydeera, L. R., Wang, W. H., Prather, R. S., and Day, B. N. (1998) Maturation in vitro of pig oocytes in protein-free culture media: fertilization and subsequent embryo development in vitro. *Biol. Reprod.* **58**, 1316–1320.
58. Aktas, H., Wheeler, M. B., First, N. L., and Leibfried-Rutledge, M. L. (1995) Maintenance of meiotic arrest by increasing [cAMP]i may have physiological relevance in bovine oocytes. *J. Reprod. Fertil.* **105**, 237–245.
59. Racowsky, C. (1985) Effect of forskolin on maintenance of meiotic arrest and stimulation of cumulus expansion, progesterone and cyclic AMP production by pig oocyte-cumulus complexes. *J. Reprod. Fertil.* **74**, 9–21.
60. Tsafriri, A., Chun, S. Y., Zhang, R., Hsueh, A. J., and Conti, M. (1996) Oocyte maturation involves compartmentalization and opposing changes of cAMP levels in follicular somatic and germ cells: studies using selective phosphodiesterase inhibitors. *Dev. Biol.* **178**, 393–402.
61. Luciano, A. M., Pocar, P., Milanesi, E., Modina, S., Rieger, D., Lauria, A., et al. (1999) Effect of different levels of intracellular cAMP on the in vitro maturation of cattle oocytes and their subsequent development following in vitro fertilization. *Mol. Reprod. Dev.* **54**, 86–91.
62. Hirao, Y., Tsuji, Y., Miyano, T., Okano, A., Miyake, M., Kato, S., et al. (1995) Association between p34cdc2 levels and meiotic

arrest in pig oocytes during early growth. *Zygote* **3**, 325–332.
63. Kopecny, V. (1989) High-resolution autoradiographic studies of comparative nucleogenesis and genome reactivation during early embryogenesis in pig, man, and cattle. *Reprod. Nutr. Dev.* **29**, 589–600.
64. Iwamoto, M., Onishi, A., Fuchimoto, D., Somfai, T., Takeda, K., Tagami, T., et al. (2005) Low oxygen tension during in vitro maturation of porcine follicular oocytes improves parthenogenetic activation and subsequent development to the blastocyst stage. *Theriogenology* **63**, 1277–1289.
65. Dominko, T., Chan, A., Simerly, C., Luetjens, C. M., Hewitson, L., Martinovich, C., et al. (2000) Dynamic imaging of the metaphase II spindle and maternal chromosomesin bovine oocytes: implications for enucleation efficiency verification, avoidance of parthenogenesis, and successful embryogenesis. *Biol. Reprod.* **62**, 150–154.

# Chapter 15

# Synchronization of *Medicago sativa* Cell Suspension Culture

**Ferhan Ayaydin, Edit Kotogány, Edit Ábrahám, and Gábor V. Horváth**

## Abstract

Deepening our knowledge on the regulation of the plant cell division cycle depends on techniques that allow for the enrichment of cell populations in defined cell cycle phases. Synchronization of cell division can be achieved using different plant tissues; however, well-established cell suspension cultures provide the largest amount of biological sample for further analysis. Here we describe the methodology of the establishment, propagation, and analysis of a *Medicago sativa* suspension culture that can be used for efficient synchronization of the cell division and also the application and removal of hydroxyurea blocking agent. A novel method is used for the estimation of cell portion that enters S phase during the assay. The protocol can be used in the case of other species as well.

**Key words:** *Medicago sativa* suspension culture, cell cycle synchronization, hydroxyurea, 5-ethynyl-2′-deoxyuridine staining, fluorescence microscopy.

## 1. Introduction

Understanding the changes in the metabolic processes and in the structure of plant cells during cell division requires a detailed analysis of the cell cycle. This can be complicated because the cell cycle progression in most somatic tissues is asynchronous and only a minor fraction of the cells are cycling. Therefore, different methods have been developed for the enrichment of cells in a single stage of the cell cycle to synchronize cells artificially. Different plant tissues and cell cultures can be used to obtain synchronously dividing cell populations.

Leaf mesophyll protoplasts from *Petunia hybrida* were shown to reenter the mitotic cell cycle from G1 phase after incubation in

G. Banfalvi (ed.), *Cell Cycle Synchronization*, Methods in Molecular Biology 761,
DOI 10.1007/978-1-61779-182-6_15, 

a medium supplemented with growth regulators (1). This system has been used for other species (2, 3); however, its application may be limited by the lack of protoplast isolation and culture procedures.

Root meristems can be a material of choice for a variety of studies, since root tips are very rich in rapidly cycling cells. In *Vicia faba* more than 90% of the cells in the root meristems are cycling (4). Seedlings with actively growing roots can be obtained from most plant species and it is easy to expose the root tips to a great variety of nutritional, hormonal, and other chemical treatments. Reliable root meristem synchronization protocol is available (5) and this can be modified for different species.

Rapidly growing suspension cultures are a suitable system to follow cell cycle-associated changes in most biochemical or cytological parameters because large number of cells are grown in an aqueous environment under well-defined conditions and they can be exposed uniformly to synchronizing treatments. High degree of synchrony could be achieved in cultured cells of *Arabidopsis* (6), carrot (7), tomato (8), and wheat (9). One of the most popular systems is the tobacco BY-2 cell line which has an improved, efficient synchronization protocol (10).

Chemical methods of the synchronization of suspension cultures are reproducible and effective; these are based either on the deprivation of an essential growth compound (6) or on the action of chemical agents that blocks cell cycle progression. Hydroxyurea is frequently used for root meristem and suspension culture synchronization; this compound reversibly inhibits the ribonucleotide reductase enzyme and hence the production of deoxyribonucleotides (11). A treatment of suspension cells for 24–36 h at a concentration of 10–20 mM will lead to the accumulation of cells in G1 and early S phase. Aphidicolin, a fungal toxin derived from *Cephalosporium aphidicola*, is a specific inhibitor of the eukaryotic DNA polymerase and the plant α-like DNA polymerase arrests cycling cells also in G1/S phase, giving similar or slightly better results on suspension cultures than hydroxyurea (7). Besides hydroxyurea and aphidicolin, a plant amino acid mimosine can be used to block cell cycle traverse near the G1/S phase boundary by suppressing the formation of the rare amino acid hypusine in the eukaryotic translation factor 4D (12). This compound can be also efficiently used in plant suspension cultures; in carrot cells it was found to be superior to aphidicolin or to hydroxyurea (7).

The detailed analysis of mitotic events may require a highly synchronous population of the cells from M to the second S through G1 phase. In such a case a two-step protocol can be followed (10), in which the cells released from aphidicolin are subsequently treated with propyzamide, a microtubule assembly

inhibitor. However, the two-step protocol in this setup would not be appropriate for analyzing metaphase-specific changes.

In the present protocol we give a detailed description for the establishment of *Medicago sativa* cell suspension culture, the synchronization procedure using hydroxyurea, and a novel *in vivo* method for the determination of the fraction of cells entering S phase using ethynyl-deoxyuridine (EdU)-based fluorescent staining (13).

## 2. Materials

### 2.1. Cell Culturing

1. Murashige and Skoog Basal Salt Mixture (MS) – Plant tissue culture tested.
2. *M. sativa* cell culture medium: 4.3 g/l MS basal salt, 3% (w/v) sucrose, 100 mg/l myoinositol, 10 mg/l thiamine hydrochloride, 1 mg/l nicotinic acid, 1 mg/l pyridoxine HCl with 1 mg/l 2,4-D. Adjust the pH of the solution to 5.8 with 1 M KOH and for plates the medium is solidified with 0.8% Plant Agar.
3. Sucrose.
4. Myoinositol: Prepare a 10 g/l stock solution (100× stock, final concentration 100 mg/l) and store at 4°C.
5. Thiamine hydrochloride: Prepare a 100× stock solution at 1 g/l (final 10 mg/l) and store at 4°C.
6. Nicotinic acid (Free Acid): Prepare a 100× stock solution at 100 mg/l (final 1 mg/l) and store at 4°C.
7. Pyridoxine HCl: Prepare a 100× stock solution at 100 mg/l (final 1 mg/l) and store at 4°C.
8. 2,4-Dichlorophenoxyacetic acid (2,4-D): Prepare 1,000× stock solution (1 g/l, final 1 mg/l) and store at 4°C.
9. Kinetin (6-Furfuryladenine): Prepare 1,000× stock solution (0.2 g/l, final 0.2 mg/l), store at 4°C.
10. Plant Agar (Duchefa Biochemie).
11. Sterile tissue culture equipment.
12. Glass pipettes.
13. Erlenmeyer flasks.
14. Gyratory shaker and laminar flow hood.

### 2.2. Synchronization

1. Hydroxyurea: Prepare 1 M stock solution (final 10 mM, 100× stock) and store at 4°C (*see* **Note 1**).
2. Miracloth (or glass filter funnel with G3 pore size).

### 2.3. Flow Cytometry

1. 5-Ethynyl-2′-deoxyuridine (EdU) stock solution: 10 mM EdU is prepared in dimethyl sulfoxide (DMSO) as a 1,000× concentrated stock solution.
2. Nuclei isolation buffer: 45 mM $MgCl_2$, 20 mM MOPS, 30 mM sodium citrate, 0.1% Triton X-100, pH 7.0.
3. Sharp razor blades.
4. Plastic dishes (6 cm in diameter).
5. Nylon sieve (20 μm).
6. Desktop centrifuge with swing-out rotor.
7. Formaldehyde stock solution: Prepare 8% (w/v) stock solution by dissolving 8 g paraformaldehyde powder in 100 ml water by heating to 60–70°C in a fume hood (*see* **Note 2**). Add a drop of 5 M KOH to the solution to depolymerize paraformaldehyde by heating at alkaline pH. After cooling to room temperature, adjust pH between 6.5 and 7.5 with 5% (v/v) $H_2SO_4$. Aliquots of this stock solution can be stored at –20°C for 6 months.
8. EdU detection cocktail: For each sample prepare 0.5 ml detection cocktail freshly (*see* **Section 2.4**).
9. Propidium iodide (PI) solution: Prepare 10 mg/ml PI stock solution in water (*see* **Note 3**).
10. FACSCalibur flow cytometer (Becton, Dickinson and Company, NJ, USA) with the standard 488 nm laser for detection of PI and AlexaFluor 488.
11. CellQuest software.

### 2.4. In Vivo EdU Staining, Mitotic Index Determination, and Fluorescence Microscopy

1. Formaldehyde stock solution (8% w/v): *See* **Section 2.3**.
2. Fixation solution (4% formaldehyde in PBS with Triton X-100): Mix 8% formaldehyde stock solution with equal volume of 2× PBS (2× PBS: 5.4 mM KCl, 2.94 mM $NaH_2PO_4$, 274 mM NaCl, and 16 mM $Na_2HPO_4$, pH 7.4) and add Triton X-100 to a final concentration of 0.1% (*see* **Note 4**).
3. DNA staining (DAPI) solution: Prepare 1 mg/ml DAPI (4′,6-diamidino-2-phenylindole) solution in DMSO (10,000× stock) and dilute to 100 ng/ml in 1× PBS (2.7 mM KCl, 1.47 mM $NaH_2PO_4$, 137 mM NaCl, and 8 mM $Na_2HPO_4$, pH 7.4) for staining nuclei (*see* **Note 5**).
4. EdU detection cocktail (Invitrogen, Click-iT EdU-Alexa Fluor 488 HCS assay): For one sample reaction (167 μl), mix the following volumes of the kit components with 144 μl distilled water: 1.6 μl buffer additive (Component F, kept frozen at –20°C in small aliquots), 14 μl reaction buffer

(Component D), 6.7 μl copper (II) sulfate solution (Component E, 100 mM $CuSO_4$), and 0.07 μl Alexa Fluor 488 azide (Component B, in 70 μl DMSO). Alternatively, a substitute of the cocktail can be prepared by mixing the following components: 4 mM $CuSO_4$, 40 mM sodium ascorbate, and 2.5–10 μM Alexa Fluor 488 azide (Invitrogen) in 1× PBS (for intact cells) or in nuclei isolation buffer (for nuclei). To prevent oxidation of the formed Cu (I) to non-catalytic Cu (II) species, prepare the detection cocktail freshly and use within an hour.

5. Mounting solution: For short-term mounting of samples use 1× PBS which prevents cell shrinkage. For long-term preservation of samples use Fluoromount-G anti-fade mounting solution (Southern Biotech).
6. Fluorescence microscope or confocal laser scanning fluorescence microscope with appropriate filter sets.

## 3. Methods

### *3.1. Establishment and Maintenance of M. sativa Cell Suspension Culture for Synchronization*

1. Initiate *M. sativa* ssp. varia (genotype A2) callus cultures from the hypocotyl explants of 7-day-old seedlings on *M. sativa* cell culture medium.
2. Subculture proliferative friable calli to 20 ml of the above-mentioned medium lacking Plant Agar and supplemented with 0.2 mg/l kinetin.
3. After 2 and 4 weeks add 10–10 ml of fresh medium to the culture.
4. After this pour off 20 ml of the supernatant culture medium and replace with 20 ml fresh medium weekly (no cells should be wasted!).
5. Following four rounds of such subculturing increase the culture volume stepwise: first dilute 25 ml of non-sedimented culture to 50 ml with fresh culture medium in a 100 ml Erlenmeyer flask.
6. Finally (after 3 months from the beginning of the suspension culture) establish 100 and 200 ml cultures by weekly subculturing: dilute 50 ml non-sedimented culture to 100 ml (2× dilution) or 200 ml (4× dilution) by adding 50 or 150 ml fresh culture medium in a 300 or 500 ml Erlenmeyer flask, respectively (*see* **Note 6**). Only well-established, rapidly dividing suspension culture can be used for a reproducible, efficient synchronization.

7. Monitor the status of the suspension culture continuously as follows: pour 50 ml non-sedimented culture to a sterile graduated tube (for example, 50 ml CELLSTAR tube from Greiner Bio-One) and measure sedimented cell volume. Indicate this value (12–15 ml for 4× diluted and 18–22 ml for 2× diluted culture) on the flask; thus variation in the sedimented volume of the culture (that should not exceed ± 10%) can be recognized (*see* **Note 6**).

Different dilution ratios will result in suspension cultures of distinct proliferative activity. Rapid cycling can be assayed by the detection of the levels of cell cycle regulators in the protein extracts of the cultures. The proteins examined can be cyclin-dependent kinases (particularly CDKB2;1-type plant-specific kinases that show G2/M phase-specific accumulation (14), cyclins, or other cell division regulators). Plant retinoblastoma-related proteins are also good choice for this purpose, since, for example, *Arabidopsis thaliana* RBR1 protein shows proliferative activity-dependent accumulation in sucrose-starved suspension cultures (15). We used the α-AtRBR1 C-terminal polyclonal antibody to detect changes in the level of MsRBR1 protein in alfalfa cell suspension cultures. Such approach can help to optimize not only the subculturing regime of the cell suspension but also the correct timing of blocking agent treatment. G1/early S phase blockers like hydroxyurea should be added to the culture that is determined to undergo cell division but does not contain high portion of cells in S phase, since hydroxyurea has an irreversible toxic effect on these cells (16). According to our results, the 4× diluted culture should be blocked after 3 days of subculture (*see* **Note 6**).

### *3.2. Synchronization of M. sativa Cell Culture with Hydroxyurea Treatment*

1. Add 2 ml 1 M hydroxyurea solution to 200 ml of an early exponential phase *M. sativa* ssp. varia (genotype A2) suspension culture (4× dilution regime, 3 days after subculture) under sterile conditions. Efficient blocking of the cells needs 36 h long treatment (26°C, 130 r.p.m. shaking on a rotary shaker in the dark).
2. Remove the blocking agent from the culture by excessive washing. Use preconditioned medium for this purpose (*see* **Note 7**). Filter the suspension culture on Miracloth placed in a glass funnel of appropriate size or on glass filter. Use only gravitational flow of the culture medium and never allow the suspension cells to dry completely. After the first filtration, resuspend the cells gently but thoroughly (no clumps should remain in the suspension) in 200 ml preconditioned culture medium and filter them again. Repeat this washing step two more times. Finally resuspend the cells in the original (200 ml) volume of the preconditioned medium.

3. Take samples for flow cytometry (**Section 3.3**), *in vivo* EdU staining, mitotic index determination, fluorescence microscopy (**Section 3.4**), and RNA and protein analysis. For the last two purposes take 10 ml of the suspension, filter the cells on Miracloth, and dry them by pressing the cells wrapped in Miracloth gently to two–three layers of filter paper. Divide the cells into microfuge tubes in 2:1 ratio; the bigger samples are for RNA isolation (give several hundred micrograms total RNA) and the smaller ones for protein analysis (at least 100 μg protein can be isolated from such samples).

A typical flow cytometric histogram of the cell cycle progression of hydroxyurea-blocked alfalfa cell suspension is presented in **Fig. 15.1a**. The data demonstrate that most of the cells enter G2/M phase between 12 and 14 h after the removal of the blocking agent and after 24–26 h the cells are ready to start a new round of cell division. A sharp increase in EdU-stained cells following hydroxyurea removal (**Figs. 15.1b** and **15.2**) clearly shows that the chemical block is reversible and the cells start DNA synthesis simultaneously (*see* **Note 8**). The efficient staining and the sharp change in the number of the fluorescent cells during cell cycle progression also demonstrate the usability of the presented method for the calculation of cells entering S phase.

### *3.3. Analysis of Cell Cycle Parameters with Flow Cytometry*

1. Incubate 5 ml of alfalfa culture with 10 μM EdU for 1 h in 6 cm Petri dishes by gentle rotation at 25°C in the dark.
2. Centrifuge (5 min, 400×*g*) EdU-labeled and 0.1% DMSO-treated control cultures.
3. Chop the pellet with a sharp razor blade in 2 ml nuclei isolation buffer in 6 cm Petri dishes on ice.
4. Filter nuclei into 15 ml conical bottom tubes through 20 μm nylon sieves and fix on ice for 30 min by the addition of 8% formaldehyde solution to a final concentration of 1%.
5. Wash the fixed nuclei twice with 2 ml 1× PBS containing 0.01% Triton X-100 (resuspension and centrifugation at 4°C, 10 min, 400×*g*) using a desktop centrifuge with swing-out rotor.
6. Incubate nuclei in 500 μl EdU detection cocktail for 30 min at room temperature in the dark.
7. Wash nuclei (4°C, 10 min, 400×*g*) with 1× PBS containing 0.01% Triton X-100 and counterstain either with 100 ng/ml (final concentration) DAPI (for microscopy check) or with 5 μg/ml (final concentration) PI.
8. Analyze on a FACSCalibur flow cytometer with CellQuest software. Use two fluorescence detectors with the standard 488 nm laser. For Alexa Fluor 488-EdU intensity, use

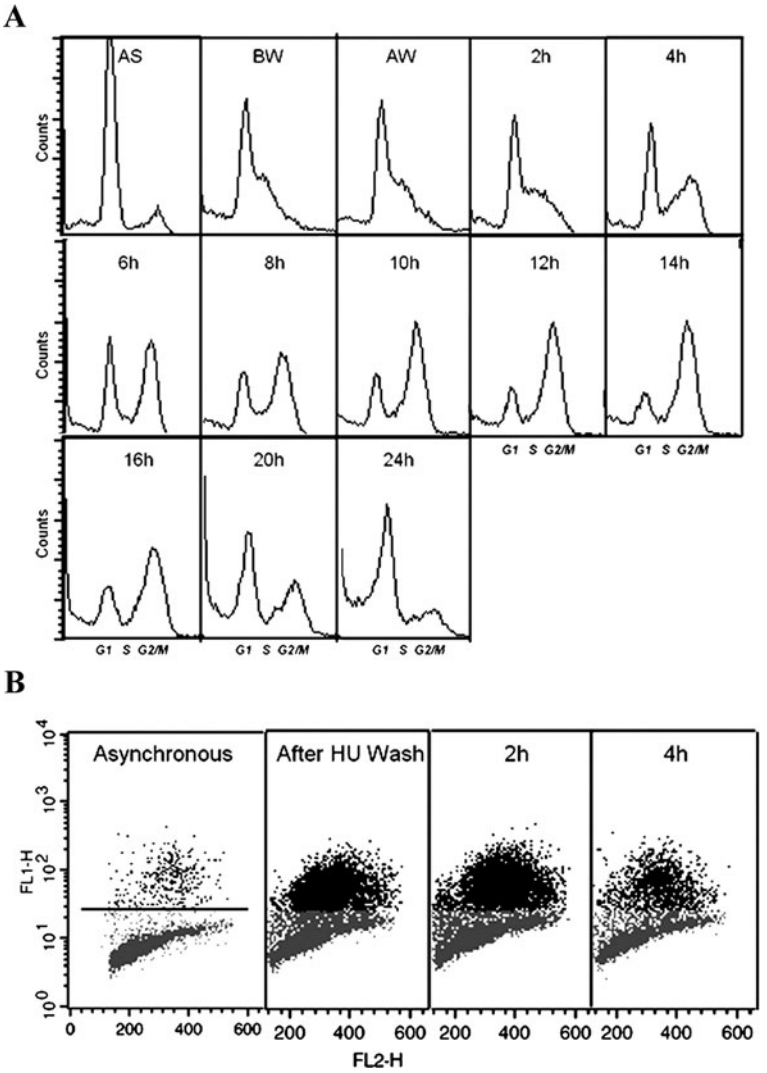


Fig. 15.1. Flow cytometric histogram analysis. (**a**) Cell cycle progression of cells synchronized at the G1/S boundary. AS: Asynchronous culture; BW: Before wash; AW: After wash. (**b**) Flow cytometric dual parameter analysis of the *in vivo* ethynyl-deoxyuridine-labeled cells (cells in S phase) synchronized at the G1/S boundary. *Horizontal line* at the *leftmost panel* indicates the EdU labeling threshold.

515–545 nm emission range (FL1 channel). For detection of PI intensity (DNA content), use 564–606 nm emission range (FL2 channel). Locate and gate nuclear populations by particle size using side scatter versus forward scatter diagrams. To exclude particles which are not fluorescent with PI staining, use dot-plot diagram of "total PI fluorescence of a particle at FL2 channel" (FL2-A) versus "transit time of a particle at FL2 channel" (FL2-W) as secondary gating. To locate the boundary of EdU-Alexa Fluor

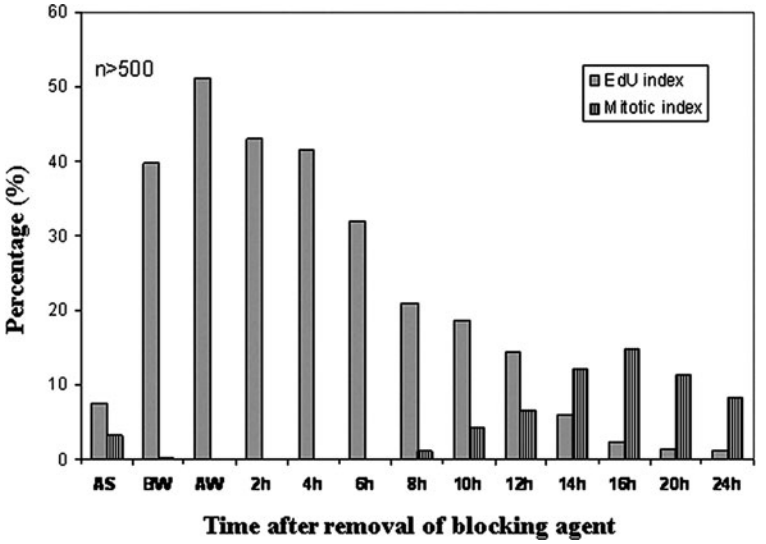


Fig. 15.2. The EdU index (cells in S phase) and mitotic index of hydroxyurea-synchronized alfalfa cultures (*see* **Note 3**).

488-labeled nuclei in biparametric plots (EdU threshold value), use counts versus FL1-H (Alexa488-EdU channel, log scale) histograms. The left (major) peak of this histogram (with low green channel intensity) represents EdU-unlabeled G1 and G2 populations while the higher green intensity second peak represents EdU-labeled nuclei. To determine the EdU threshold value, use the right border of the leftmost major peak (where the unlabeled G1/G2 counts reach zero value).

### *3.4. In Vivo EdU Staining, Mitotic Index Determination, and Fluorescence Microscopy*

1. Incubate 1 ml of alfalfa culture in a 2 ml microfuge tube on a roller with 10 μM final concentration of EdU for 1 h in its own culture medium.
2. Settle cells by centrifugation (5 min, 400×*g*) and resuspend the pellet in 2 ml 1× PBS and re-centrifuge. Discard the supernatant.
3. Fix the cell pellet 15 min in 2 ml fixation solution on a roller. Replace the fixer with the same volume of 1× PBS by centrifugation. At this stage the cells can be kept in the refrigerator for several weeks until further processing.
4. Following 3 × 5 min washes with 1× PBS (2 ml each), incubate 20–30 μl packed cell volume of cells in 167 μl EdU detection cocktail by rotating for 30 min at room temperature in a 0.2 ml microfuge tube (*see* **Note 9**).
5. After 2 × 5 min washes with 1× PBS (2 ml each) containing 100 ng/ml (final concentration) DAPI, mount 20 μl aliquot

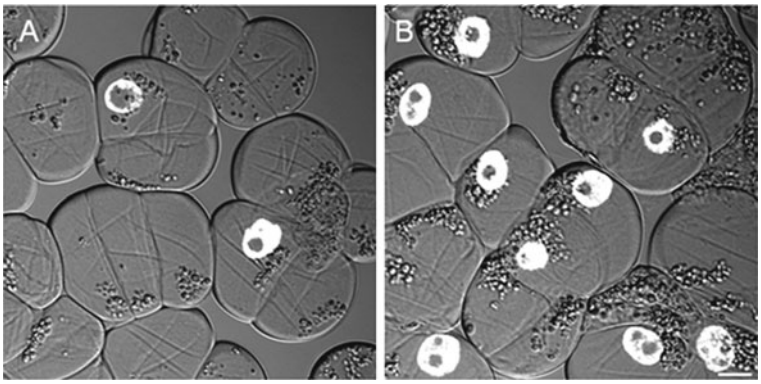


Fig. 15.3. EdU-based replication assay on (**a**) asynchronous and (**b**) hydroxyurea-synchronized (after wash sample) alfalfa cells. Transmission images (*grayscale*) are overlaid onto AlexaFluor488-labeled (pseudocolored *white*) nuclei. Bar 10 μm.

of cells onto microscope slide with a coverslip and gently press with a tissue paper to flatten the clusters. The rest of the labeled cells can be kept at 0–4°C in a dark container for several weeks (*see* **Note 10**).

6. Set the confocal microscope configuration as follows: objective lenses: UPLSAPO 20× (dry, NA 0.75) and UPLFLN 40× (oil, NA 1.3); sampling speed: 4 μs/pixel; line averaging: 2×; scanning mode: sequential unidirectional; excitation: 405 nm (DAPI) and 488 nm (Alexa Fluor 488); laser transmissivity: less than 1% for DAPI and 5% for Alexa Fluor 488, respectively; main dichroic beamsplitter: DM405/488; intermediate dichroic beamsplitter: SDM 490; DAPI fluorescence detection: 425–475 nm; Alexa Fluor 488 detection: 500–600 nm. For transmitted light imaging (**Fig. 15.3**) differential interference contrast (DIC) mode can be used. Count more than 500 cells for mitotic index and EdU labeling index determinations.

## 4. Notes

1. Caution: Hydroxyurea is toxic and carcinogenic; use appropriate precautions.
2. Paraformaldehyde is very hazardous in case of skin contact, eye contact, or inhalation (irritant/corrosive). Work in a fume hood and wear protective equipment.
3. Caution: Propidium iodide is a known mutagen; use appropriate precautions.
4. The addition of Triton X-100 to the fixation solution provides uniform fixation with reduced cell shrinkage.

5. Caution: DAPI is a known mutagen; use appropriate precautions.
6. Careful propagation of the cell culture is an absolute prerequisite of efficient synchronization. Since the establishment of a culture may exceed the described time demand this should be started well before the planned synchronization. For scientific purposes established cultures of *M. sativa* ssp. varia (genotype A2) can be obtained from Dr. Gábor V. Horváth (Institute of Plant Biology, Biological Research Center HAS, Szeged, Hungary, e-mail: hvg@brc.hu).
7. Use of preconditioned medium in the washing steps and for the final resuspension will greatly increase the success of synchronization. To obtain this, the same *M. sativa* suspension culture should be grown under the same subculture regime, and just prior to the beginning of hydroxyurea removal, four times 200 ml of this culture should be filtered through sterile glass filter. Cells can be collected and used as unblocked control; the resulting preconditioned medium is used to remove hydroxyurea from blocked suspension.
8. Relatively high labeling efficiency can be detected in "Before Wash" samples, although the labeling intensity is very low compared to the other samples. Since EdU is a thymidine analog, cells with depleted nucleotide pools (due to the action of hydroxyurea) start to incorporate EdU; however, the DNA synthesis cannot proceed due to the lack of other nucleotides.
9. Fluorochrome-containing solutions should not be exposed to strong light; therefore, labeling reaction should be performed at dark or under dim light. The simplest solution is to wrap the centrifuge tubes in aluminum foil for the time of the labeling.
10. Glycerol-based (or high osmolarity) mounting media may cause cell shrinkage but they better suit imaging with oil immersion objectives. Mounting the samples in PBS prevents cell shrinkage; however, care must be taken not to dry out the sample. Occasional PBS loading may be necessary for prolonged observations to prevent sample drying.

## Acknowledgment

The authors are grateful to Katalin Török for excellent technical assistance. This work was funded by OTKA grant no. NK 69227. Edit Ábrahám was supported by the János Bolyai Fellowship of the Hungarian Academy of Sciences.

## References


1. Bergounioux, C., Perennes, C., Brown, S. C., and Gadal, P. (1988) Cytometric analysis of growth regulator-dependent transcription and cell cycle progression in *P. hybrida* protoplast cultures. *Planta* 175, 500–505.
2. Kapros, T., Bögre, L., Németh, K., Bakó, L., Györgyey, J., Wu, S. C., and Dudits, D. (1992) Differential expression of histone H3 gene variants during cell cycle and somatic embryogenesis in alfalfa. *Plant Physiol.* 98, 621–625.
3. Carle, S. A., Bates, G. W., and Shannon, T. A. (1998) Hormonal control of gene expression during reactivation of the cell cycle in tobacco mesophyll protoplasts. *J. Plant Growth Regul.* 17, 221–230.
4. Doležel, J., Číhalíková, J., and Lucretti, S. (1992) A high yield procedure for isolation of metaphase chromosomes from root tips of *Vicia faba*. *Planta* 188, 93–98.
5. Doležel, J., Číhalíková, J., Weiserová, J., and Lucretti, S. (1999) Cell cycle synchronization in plant root meristems. *Methods Cell Sci.* 21, 95–107.
6. Menges, M., and Murray, J. A. H. (2002) Synchronous *Arabidopsis* suspension cultures for analysis of cell-cycle gene activity. *Plant J.* 30, 203–212.
7. Ghosh, S., Sen, J., Kalia, S., and Guha-Mukherjee, S. (1999) Establishment of synchronization in carrot cell suspension culture and studies on stage specific activation of glyoxalase I. *Methods Cell Sci.* 21, 141–148.
8. Arumuganathan, K., Slattery, J. P., Tanksley, S. D., and Earle, E. D. (1991) Preparation and flow cytometric analysis of metaphase chromosomes of tomato. *Theor. Appl. Genet.* 82, 101–111.
9. Wang, M. L., Leitch, A. R., Schwarzacher, T., Heslop-Harrison, J. S., and Moore, G. (1992) Construction of a chromosome-enriched *HpaII* library from flow-sorted wheat chromosomes. *Nucleic Acids Res.* 20, 1897–1901.
10. Kumagai-Sano, F., Hayashi, T., Sano, T., and Hasezawa, S. (2006) Cell cycle synchronization of tobacco BY-2 cells. *Nat. Protoc.* 1, 2621–2627.
11. Young, C. W., and Hodas, S. (1964) Hydroxyurea: inhibitory effect on DNA metabolism. *Science* 146, 1172.
12. Watson, P. A., Hanauske-Abel, H. H., Flint, A., and Lalande, M. (1991) Mimosine reversibly arrests cell cycle progression at the $G_1$-S phase border. *Cytometry* 12, 242–246.
13. Kotogány, E., Dudits, D., Horváth, V. G., and Ayaydin, F. (2010) A rapid and robust assay for detection of S phase cell cycle progression in plant cells and tissues by using ethynyl deoxyuridine. *Plant Methods* 6, 1–15.
14. Mészáros, T., Miskolczi, P., Ayaydin, F., Pettkó-Szandtner, A., Peres, A., Magyar, Z., Horváth, V. G., Bakó, L., Fehér, A., and Dudits, D. (2000) Multiple cyclin-dependent kinase complexes and phosphatases control G2/M progression in alfalfa cells. *Plant Mol. Biol.* 43, 595–605.
15. Hirano, H., Harashima, H., Shinmyo, A., and Sekine M. (2008) *Arabidopsis* retinoblastoma-related protein 1 is involved in G1 phase cell cycle arrest caused by sucrose starvation. *Plant Mol. Biol.* 66, 259–275.
16. Nias, A. H. W., and Fox, M. (1971) Synchronization of mammalian cells with respect to the mitotic cycle. *Cell Tissue Kinet.* 4, 375–398.

# Chapter 16

# Cell Cycle Synchronization for the Purpose of Somatic Cell Nuclear Transfer (SCNT)

**Yoel Shufaro and Benjamin E. Reubinoff**

## Abstract

Somatic cell nuclear transfer (SCNT) is a technically and biologically challenging procedure during which a differentiated committed nucleus undergoes rapid reprogramming into the totipotent state in a few hours. SCNT can be utilized to generate patient- and disease-specific embryonic stem cell (ESC) lines, which carry great promise in improving our understanding of major disease conditions and hope for better therapies. In this section, we will describe how mouse SCNT is performed and survey the importance of donor cell cycle synchronization and the methods to perform it.

**Key words:** Somatic cell nuclear transfer, reprogramming, cell cycle synchronization.

## 1. Introduction

Mammalian somatic cells can be reprogrammed back to a totipotent embryo capable of regenerating a complete organism from the same genetic material found in the original differentiated donor cells (1, 2). This procedure is performed by injecting a somatic nucleus into an enucleated oocyte – Somatic Cell Nuclear Transfer (SCNT). The injected ova are activated into a zygote-like state and allowed to further develop into embryos. This conceptual idea was initially based on experiments in amphibians in which cell differentiation was fully reversed after injection of somatic nuclei into growing oocytes by changes in nuclear gene expression but not in gene content (3). The next major advance in this field came with the emergence of mammalian SCNT. The first normal adult animal generated by SCNT was the sheep Dolly, which originated from reprogrammed cultured mammary gland cells (4). In the years afterward, SCNT was successfully performed

G. Banfalvi (ed.), *Cell Cycle Synchronization*, Methods in Molecular Biology 761,
DOI 10.1007/978-1-61779-182-6_16, 

in a variety of animal models including mice, cattle, goat, pigs, dog, and primates (5, 6). Human SCNT was performed with very limited success resulting in poor quality *in vitro* cultured embryos (7).

SCNT for reproductive purposes is ethically accepted only in animals. This procedure is very inefficient, with many of the resulting embryos showing an increased rate of miscarriages, malformations, and perinatal deaths (8). However, SCNT is efficient enough to create *in vitro* cultured blastocysts, from which embryonic stem cell (ESCs) lines can be derived. ESCs derived from reprogrammed somatic cells are phenotypically and functionally identical to native ESCs (9). SCNT-derived ESC lines are genetically identical to the donor of the nucleus. Once transplanted into the donor, the SCNT ES cells and all their differentiated progenitors are expected not to be rejected by the immune system of the (nuclei) donor, even without immune suppression (10). The mitochondrial DNA of the enucleated oocyte, which is not replaced during SCNT, probably does not contribute immunogenicity. In animal models, progenitors derived from SCNT ESC lines were not rejected following transplantation into the immune intact nucleus donor host (10). In humans, such cells might substantially improve the treatment of neurodegenerative diseases, blood disorders, or diabetes, since therapy for these diseases is currently limited by the availability or immunocompatibility of tissue transplants. Moreover, embryonic stem cells provide a renewable source of replacement tissue, allowing therapy to be repeated whenever needed. An additional equally important application of SCNT ESC lines is the generation of highly reliable *in vitro* human disease models. Nuclei from an endless variety of diseased patients can potentially be reprogrammed by SCNT into embryos. The derived ESC lines have the possibility of being the best platform for investigating disease pathogenesis and in the development of new drugs and therapeutic approaches. In recent years, direct reprogramming of somatic cells into induced pluripotent stem cell-like cells (iPS) has emerged (11). This type of reprogramming is performed by hyperexpression of several transcription factors (TFs) associated with pluripotency. Initially, transgenic copies of these TFs were introduced for reprogramming. Later on, other and safer methods to activate the endogenic TFs have emerged. Although these oocyte-independent technologies are very appealing in their simplicity, reprogramming in the oocytic environment is presently still the gold standard despite its disadvantages.

There are two contributors to successful reprogramming: (i) the ooplasmic environment and (ii) the injected nucleus. In most mammalian species, optimal reprogramming occurs in the

mature (metaphase II) oocyte. The cytoplasmic activity termed maturation/meiosis/mitosis-promoting factor (MPF) is a key factor in this process (12). Metaphase II oocytes have high MPF activity which declines rapidly after fertilization and is therefore the best reprogramming vehicle. High oocytic quality and viability ensure its survival after enucleation and are a mandatory requirement for successful reprogramming by SCNT.

The success rate of nuclear reprogramming decreases as donor cells become more differentiated. The less differentiated cells bear a greater epigenetic resemblance to the totipotent state and are therefore more readily reprogrammed. However, such undifferentiated cells are epigenetically less stable than cells with a committed fate. Therefore, when terminally differentiated (contrary to undifferentiated) nuclei are used for SCNT, the primary success rate is quantitatively lower, but the resulting cells bear a greater resemblance to their normal native parallels.

As donor nuclei progress in the cell cycle, the extent of the development of reconstituted embryos is reduced (13). All nuclei transferred when MPF activity is high undergo nuclear envelope breakdown, which is followed by premature chromosome condensation (12). The nuclear envelope is then reformed and DNA synthesis starts. Therefore, unless the nucleus is in the $G_0/G_1$ phase at the time of transfer, re-replication of previously replicated DNA will occur, resulting in incorrect DNA content and possible chromosomal damage. As a result, mammalian somatic nuclei are reprogrammed without altering their DNA content only if injected at the $G_0$ or $G_1$ stages. In addition, the chromatin is stable at $G_0/G_1$ and its exposure to the oocytic environment is steady for the hours needed to induce its reprogramming. This process is less successful once the chromatin is open for DNA replication or packed in chromosomes for mitosis. In naturally fertilized oocytes, the S phase starts only after the organization of two pronuclei (12). In SCNT reconstructed oocytes, two pseudopronuclei appear only after completion of oocyte activation, well after the injection of the somatic nucleus (14). It is therefore necessary for the transplanted nucleus to be at $G_0$ or $G_1$ in order to be molecularly and morphologically "in phase" with the ooplasm it was transplanted into.

In most published mammalian SCNT systems, the injected nuclei are from quiescent differentiated cells which do not require special treatment to be maintained in this state. However, it is possible to inject and reprogram nuclei isolated from cells growing in culture if treated properly prior to their injection. We will describe the method used in our center for mouse SCNT and survey the published methods for cell cycle synchronization of the donor nuclei.

## 2. Materials

1. Pregnant mare serum gonadotropin (PMSG).
2. Human chorionic gonadotropin (hCG).
3. Self-prepared HEPES–CZB medium (15) with the following modifications: 5.56 mM glucose, 20 mM HEPES, and 5 mM sodium bicarbonate. Prepared daily to twice-weekly from X10 stocks (prepared biweekly and stored at 4°C). Polyvinylpyrrolidone (PVP MW 40,000) added from a 10% stock.
4. Modified Ca-free, 10 mM $SrCl_2$ M16 medium supplemented with bovine serum albumin (0.4% w/v), vitamins (1X, Sigma-Aldrich), and cytochalasin B (CB) 5 μg/ml. The M16 medium is self-prepared daily from biweekly prepared stocks. The $SrCl_2$ powder is to be weighed and dissolved daily in water prior to its addition. CB is stored as frozen aliquots dissolved in DMSO 1 mg/ml. The vitamins solution is stored as that in frozen aliquots.

   All self-prepared media are filtered on a 0.22 μm cellulose acetate membrane.
5. Bovine testicular hyaluronidase.
6. Protease inhibitor (PI).
7. Quinn's Advantage Cleavage Medium (Sage Media, CT, USA).
8. Embryo-tested mineral oil for incubator culture. DMPSV silicon oil for micromanipulation stages.
9. Holding pipette (small 25°) and Piezodrill enucleation (12 μm 25°) and injection (6 μm 25°) pipettes (Humagen, VA, USA).
10. Electronics-grade mercury (>99% purity).
11. Nunclon 35 and 100 mm culture dishes.
12. Handling pipettes. Pasteur pipettes heated and pulled. Broken edge diameter is approx. 150–200 μm.
13. Mercury disposal container.

## 3. Methods

### 3.1. SCNT

1. 8- to 12-week-old $B_6C_3F_1$ or $B_6D_2F_1$ female mice are stimulated with an *i.p.* injection of PMSG (10 IU) followed by an *i.p.* hCG injection (10 IU) 48 h afterward (*see* **Note 1**).

Oocytes are retrieved 13 h after hCG administration. Following scarification, the oviducts are excised by laparotomy and opened and incubated in HEPES–CZB–PVP 0.1% containing hyaluronidase (50 IU/ml) and PI (0.2%) at 28°C for 10–12 min (100 μl drop on a 35 mm dish). At the end of this period, the mature oocytes are self-denuded from the surrounding cumulus cells and are transferred for incubator culture in Quinn's Advantage Cleavage Medium (seven 30 μl drops on a 35 mm dish covered with oil) at 37°C 5% $CO_2$ (*see* **Note 2**).

2. The cumulus cells are left inside the HEPES–CZB–PVP 0.1% Hyaluronidase PI drop. An equal volume of Quinn's Advantage Cleavage Medium is added and the entire drop is gently pipetted. It is afterward covered with mineral oil and maintained at 4°C until nuclear injection. The purpose of this step is to maintain cellular quiescence and prevent surface adhesion.
3. Micromanipulation is performed on the stage of an inverted microscope equipped with either a Nomarski (DIC) or a Hoffman (HMC) optical system. A temperature-controlled heated stage is beneficial but not mandatory. Top quality micromanipulators and microinjectors of a leading brand are used on each side. It is especially important that the microinjector controlling enucleation and injection of the transferred nucleus is very sensitive. A piezomicromanipulator (PMM 150 FU, PrimeTech, Japan) is essential for mouse SCNT, but is not mandatory in other species. If this device is used, its pulses are conducted via mercury which is introduced inside the enucleation and injection micropipettes. Each such micromanipulation system is individually calibrated for its users.
4. Enucleation is performed in HEPES–CZB–PVP 0.1% supplemented with 2 μg/ml CB at room temperature (or 27°C if a temperature-controlled stage is available). A 100 mm plate is used. A central 30 μl drop in which the PVP concentration is raised to 1% is placed first (*see* **Note 3**). Additional 2–3 enucleation drops are placed equally across the diameter line from each side prior to covering the entire plate with silicone oil. The meiotic spindle is visible to the naked, but skilled, eye as a lucent ball which is aspirated gently from the oocyte after the *zona pellucida* (ZP) is penetrated with the PMM. The presence of CB permits the aspiration of the spindle without tearing the oocyte. The volume of the ooplasm accompanying the spindle should be minimal.
5. After the rapid (<10 min) completion of the enucleation, the ooplasts are returned for recovery in the incubator in

Quinn's Advantage Cleavage Medium (different dish of the same type) at 37°C 5% $CO_2$ for at least 1 h.

6. The (nuclei donor) cumulus cells are then taken out of refrigeration and placed on a new 100 mm stage plate, inside drops containing injection medium. This medium is hypertonic (110%) CZB medium 1% PVP. The plate contains a central 50 μl clean drop for maintenance of the piezo-driven injection micropipette and injection drops along the diameter line (*see* **Note 3**). The oocytes are placed and injected with the assistance of the PMM in the same drop containing the somatic cells. Prior to injection, the nuclei are stripped from the cell membrane and cytoplasm by repeated trituration through the injection micropipette with the PMM emitting pulses. Care should be taken to prevent stickiness inside the pipette and not to destroy the nucleus during this process.
7. After the injection, the reconstructed oocytes are allowed to recover for 1 h at room temperature in a 1:1 mixture of HEPES–CZB–0.1% PVP and Quinn's Advantage Cleavage Medium. In the next step, they are transferred for incubator culture in Quinn's Advantage Cleavage Medium for an additional 1–2 h (same type of drops and dish).
8. The reconstructed oocytes are then activated for 6 h in calcium-free M16 supplemented with 10 mM $SrCl_2$ CB (5 μg/ml) and vitamins and then transferred to Quinn's Advantage Cleavage Medium at 37°C 5% $CO_2$. At the end of this activation stage, two pronuclei-like structures can be identified in almost all SCNT reconstructed oocytes. This point parallels the two pronuclei zygote stage observed after normal fertilization. Embryonic development occurs *in vitro* up to the blastocyst stage.

### *3.2. Donor Nuclei Cell Cycle Synchronization*

1. The somatic nuclei are successfully reprogrammed by the ooplasm only when in the diploid $G_0$ or $G_1$ states (16). If DNA synthesis ensues or completes in the donor nucleus prior to its injection, aneuploidy and chromosome damage will occur.
2. In most published SCNT experiments, the injected nuclei are from quiescent differentiated cells which do not require special treatment to be maintained in this state. However, it is possible to inject and reprogram nuclei isolated from cells growing in culture. The principal approaches for cellular arrest are serum starvation, culture confluence, and $G_1$ arrest by inhibition of DNA synthesis.
3. The most prevalent method to arrest growing cells in the $G_0$ stage is serum starvation. For example, Baguisi et al., pioneer

in goat SCNT, used nuclei from a fetal cell line cultured in a very low (0.5%) FBS concentration for 1 week prior to SCNT (17). Kues et al. quantified the impact of serum deprivation on porcine fibroblasts and found that 48 h of such serum starvation was sufficient to halt the growth of 98% of the cells, without causing DNA damage and nuclear fragmentation (which appeared 24 h later under these conditions) (18).

4. Dalman et al. demonstrated that full culture confluence was as good as serum starvation for preventing entry into the S phase with a lower rate of apoptosis than the latter (19) (*see* **Note 4**).
   Serum starvation and culture confluence are simple to perform, but require familiarity with the specific conditions that the cultured cells require in order not to cause DNA damage or induce apoptosis.
5. $G_1$ arrest was reported by Collas et al. (13). The purpose of this earlier work was to investigate the impact of cell cycle stage on nuclear morphology and chromosome constitution in blastomeres. The method used was mitotic arrest by adding colcemid 0.5 μg/ml for 10 h, thorough washing with PBS, followed by the addition of aphidicolin 0.1 μg/ml in order to inhibit DNA synthesis. Using this method, the cells are arrested very accurately at the end of $G_1$.
6. Kues et al. (18) have shown that cell culture with aphidicolin (6 μM for 14 h) or butyrolactone (118 μM for 5 h) is efficient in preventing DNA synthesis and cell division in the presence of standard (10% FBS) conditions. Both drugs were used to maintain cell cycle synchronization once FBS was returned to the depleted cultures after 48 h (in order to prevent DNA fragmentation).
7. Kurosaka et al. have compared serum starvation (FBS 0.2% 20 h) ($G_0$ arrest) to DNA synthesis inhibition by aphidicolin (2 μg/ml 20 h, 10% FBS) ($G_1$ arrest). Both methods were efficient in achieving cell cycle arrest. However, when $G_1$-arrested nuclei were used, the first round of DNA synthesis occurred earlier and SCNT was more efficient (20).

Serum starvation, culture in confluence, and $G_1$ chemical arrest are all suitable for donor cell cycle synchronization prior to SCNT. However, it seems that the chemical arrest methods at the transition $G_1$–S are slightly superior. The explanations might be the following: (i) a greater homogeneity of the cell population when chemical methods are used; (ii) the $G_1$–S transition point is more suitable for reprogramming and initiation of DNA synthesis in synchrony with the ooplasmic program.

## 4. Notes

1. PMSG is dissolved in normal saline (NS) and aliquots for injection are stored at –20°C. hCG is dissolved in double distilled water (DDW), divided into aliquots for injection, and then dried in a vacuum centrifuge. Each dried aliquot is resuspended in NS prior to injection.
2. It is important to confirm at this stage that all the collected oocytes are actually at metaphase II and contain a polar body. Undenuded immature oocytes should be discarded.
3. This central drop is used for the clean maintenance of the piezo-driven enucleation pipette. Cautious spillage of mercury micro-drops inside this drop is acceptable as long as they do not contaminate the other drops.
4. Goat fibroblasts were grown on 60 mm plates in DMEM supplemented with 15% FBS. They were arrested once the culture was confluent and did not lose this property even after several transfers.

### References


1. Jaenisch, R., Hochedlinger, K., Blelloch, R., Yamada, Y., Baldwin, K., and Eggan, K. (2004) Nuclear cloning, epigenetic reprogramming, and cellular differentiation, *Cold Spring Harb. Symp. Quant. Biol.* **69**, 19–27.
2. Markoulaki, S., Meissner, A., and Jaenisch, R. (2008) Somatic cell nuclear transfer and derivation of embryonic stem cells in the mouse, *Methods* **45**, 101–114.
3. Shufaro, Y., Lacham-Kaplan, O., Tzuberi, B. Z., McLaughlin, J., Trounson, A., Cedar, H., and Reubinoff, B. E. (2010) Reprogramming of DNA replication timing, *Stem Cells* **28**, 443–449.
4. Wilmut, I., Schnieke, A. E., McWhir, J., Kind, A. J., and Campbell, K. H. (1997) Viable offspring derived from fetal and adult mammalian cells, *Nature* **385**, 810–813.
5. Wilmut, I., and Paterson, L. (2003) Somatic cell nuclear transfer, *Oncol. Res.* **13**, 303–307.
6. Mitalipov, S. M., Zhou, Q., Byrne, J. A., Ji, W. Z., Norgren, R. B., and Wolf, D. P. (2007) Reprogramming following somatic cell nuclear transfer in primates is dependent upon nuclear remodeling, *Hum. Reprod.* **22**, 2232–2242.
7. Cibelli, J. B., Lanza, R. P., West, M. D., and Ezzell, C. (2002) The first human cloned embryo. *Sci. Am.* **286**, 44–51.
8. Solter, D. (2000) Mammalian cloning: advances and limitations. *Nat. Rev. Genet.* **1**, 199–207.
9. Brambrink, T., Hochedlinger, K., Bell, G., and Jaenisch, R. (2006) ES cells derived from cloned and fertilized blastocysts are transcriptionally and functionally indistinguishable. *Proc. Natl. Acad. Sci. USA* **103**, 933–938.
10. Shufaro, Y., and Reubinoff, B. E. (2004) Therapeutic applications of embryonic stem cells. *Best Pract. Res. Clin. Obstet. Gynaecol.* **18**, 909–927.
11. Okita, K., Ichisaka, T., and Yamanaka, S. (2007) Generation of germline-competent induced pluripotent stem cells. *Nature* **448**, 313–317.
12. Campbell, K. H., Loi, P., Otaegui, P. J., and Wilmut, I. (1996) Cell cycle co-ordination in embryo cloning by nuclear transfer. *Rev. Reprod.* **1**, 40–46.
13. Collas, P., Pinto-Correia, C., Ponce de Leon, F. A., and Robl, J. M. (1992) Effect of donor cell cycle stage on chromatin and spindle morphology in nuclear transplant rabbit embryos. *Biol. Reprod.* **46**, 501–511.
14. Wakayama, T., Perry, A. C., Zuccotti, M., Johnson, K. R., and Yanagimachi, R. (1998) Full-term development of mice from enucleated oocytes injected with cumulus cell nuclei. *Nature* **394**, 369–374.

15. Chatot, C. L., Ziomek, C. A., Bavister, B. D., Lewis, J. L., and Torres, I. (1989) An improved culture medium supports development of random-bred 1-cell mouse embryos in vitro. *J. Reprod. Fertil.* **86**, 679–688.
16. Wells, D. N., Laible, G., Tucker, F. C., Miller, A. L., Oliver, J. E., Xiang, T., Forsyth, J. T., Berg, M. C., Cockrem, K., L'Huillier, P. J., Tervit, H. R., and Oback, B. (2003) Coordination between donor cell type and cell cycle stage improves nuclear cloning efficiency in cattle. *Theriogenology* **59**, 45–59.
17. Baguisi, A., Behboodi, E., Melican, D. T., Pollock, J. S., Destrempes, M. M., Cammuso, C., Williams, J. L., Nims, S. D., Porter, C. A., Midura, P., Palacios, M. J., Ayres, S. L., Denniston, R. S., Hayes, M. L., Ziomek, C. A., Meade, H. M., Godke, R. A., Gavin, W. G., Overstrom, E. W., and Echelard, Y. (1999) Production of goats by somatic cell nuclear transfer. *Nat. Biotechnol.* **17**, 456–461.
18. Kues, W. A., Anger, M., Carnwath, J. W., Paul, D., Motlik, J., and Niemann, H. (2000) Cell cycle synchronization of porcine fetal fibroblasts: effects of serum deprivation and reversible cell cycle inhibitors. *Biol. Reprod.* **62**, 412–419.
19. Dalman, A., Eftekhari-Yazdi, P., Valojerdi, M. R., Shahverdi, A., Gourabi, H., Janzamin, E., Fakheri, R., Sadeghian, F., and Hasani, F. (2010) Synchronizing cell cycle of goat fibroblasts by serum starvation causes apoptosis. *Reprod. Domest. Anim.*, 45: e46–e53. doi: 10.1111/j.1439-0531.2009.01520x
20. Kurosaka, S., Nagao, Y., Minami, N., Yamada, M., and Imai, H. (2002) Dependence of DNA synthesis and in vitro development of bovine nuclear transfer embryos on the stage of the cell cycle of donor cells and recipient cytoplasts. *Biol. Reprod.* **67**, 643–647.

# Chapter 17

# *Ex Vivo* Expansion of Haematopoietic Stem Cells to Improve Engraftment in Stem Cell Transplantation

**Kap-Hyoun Ko, Robert Nordon, Tracey A. O'Brien, Geoff Symonds, and Alla Dolnikov**

## Abstract

The efficient use of haematopoietic stem cells (HSC) for transplantation is often limited by the relatively low numbers of HSC collected. The *ex vivo* expansion of HSC for clinical use is a potentially valuable and safe approach to increase HSC numbers thereby increasing engraftment and reducing the risk of morbidity from infection. Here we describe a protocol for the robust *ex vivo* expansion of human CD34(+) HSC isolated from umbilical cord blood. The protocol described can efficiently generate large numbers of HSC. We also describe a flow cytometry-based method using high resolution division tracking to characterise the kinetics of HSC growth and differentiation. Utilising the guidelines discussed, it is possible for investigators to use this protocol as presented or to modify it for their specific needs.

**Key words:** Haematopoietic stem cell, expansion, cell division.

## 1. Introduction

The use of haematopoietic stem cells (HSC) for effective transplantation can be limited by the relatively low numbers of HSC collected from the patient (1–5). A potential solution to this is to develop a strategy to expand HSC prior to transplantation (5, 6). Fast haematopoietic recovery after transplantation of HSC has been demonstrated in clinical trials performed with *ex vivo* expanded HSC and there has been evidence of improved engraftment (5–7).

Once considered a biological waste, UCB has emerged as a viable source of stem cells for transplantation. Because cord units are pre-tested for HLA (human leukocyte antigens)

G. Banfalvi (ed.), *Cell Cycle Synchronization*, Methods in Molecular Biology 761,
DOI 10.1007/978-1-61779-182-6_17, 

compatibility and then cryogenically stored, umbilical cord blood (UCB) is a stem cell source readily on hand that can reduce the delay in transplantation for patients with high-risk malignancies. The major drawback of cord blood as an alternate source of HSC is the slower haematopoietic recovery and higher incidence of graft failure. This finding has been repeatedly demonstrated to relate to the infused cell dose with higher cell doses resulting in improved engraftment. The minimum accepted cell dose to achieve engraftment is variably reported to range between 2 and $3 \times 10^7$/kg total nucleated cells per recipient weight. The average cell yield in a single cord unit collection therefore provides sufficient cells for recipients less than 40 kg (personal communication, Prof Marcus Vowels, Director Australian Cord Blood Bank, Sydney Children's Hospital) and is the major reason for limitation of this stem cell source in adult patients. Thus, the strategy of providing sufficient increased numbers of cord blood stem cells may shorten the time to engraftment and improve survival in adult UCB recipients.

Two main methods to expand HSC have been explored to date: static liquid and stromal co-culture systems (8–11). The majority of static liquid and some stromal co-culture expansion systems require the isolation of CD34(+) cells from fresh or frozen haematopoietic tissue (11–12). Stem cell transplantation studies indicate that a CD34(+) subpopulation in UCB can provide durable long-term donor-derived lymphohaematopoietic reconstitution. Therefore, the CD34 antigen has been routinely used to identify and enrich HSC. CD34(+) cells contain both primitive HSC with long-term regenerative ability and more mature haematopoietic progenitor cells (HPC) shown to mediate short-term haematopoiesis.

Positively selected CD34(+) cells enriched with HSC can be incubated in culture medium supplemented with different combinations of cytokines (13). Cytokines promote quiescent HSC to enter the cell cycle. Different cytokine combinations and varying doses of the cytokines have previously been shown to drive HSC expansion (14). Although, this strategy is effective in increasing total cell numbers, it is generally the case that these procedures drive HSC differentiation to progeny cells at the expense of HSC self-renewal (15). The *ex vivo* expansion of short-term reconstituting HPC at the expense of long-term reconstituting higher quality HSC has been shown to negatively impact on haematopoietic reconstitution (15, 16).

Here we describe (i) a protocol for the efficient *ex vivo* expansion of human CD34(+) HSC isolated from UCB and (ii) a flow cytometry-based method using high-resolution division tracking to characterise the kinetics of HSC expansion (17). The stem cell expansion protocol describes the robust *ex vivo* proliferation of human CD34(+) cells isolated from umbilical cord blood using a combination of cytokines previously optimised by our group (17).

The division tracking method identifies consecutive cell generations by monitoring the serial halving of carboxyfluorescein diacetate succinimidyl ester (CFDA-SE) fluorescence with each cell division and thus provides a powerful tool to monitor and quantify cell division (17). The protocol outlines the steps used to analyze CFDA-SE-labelled cells and its utility has been demonstrated by our group in a number of CD34(+) cell culture systems (17). This method is highly useful for the analysis of the specific parameters of, and critical modulating conditions for, HSC expansion. By combining CFDA-SE staining with the analysis of CD34 antigen, division tracking analysis provides insight into how the fundamental processes of cell division, differentiation, and apoptosis contribute to haematopoietic growth dynamics.

## 2. Materials

### 2.1. Cell Sources

1. UCB was collected by the Sydney Cord Blood Bank (Sydney Children's Hospital, Sydney, Australia). Informed consent was obtained from mothers, and both University of New South Wales and Eastern Sydney Area Health Service Human Ethics Committees approved the use of UCB for this research project (**Note 1**).
2. The acute myelogenous leukaemia cell line, KG1a (18), was used to optimise CFDA-SE staining.

### 2.2. Cell Culture Reagents

1. Serum-free medium.
2. Stemline II Haematopoietic stem cell expansion medium (Sigma-Aldrich) was used for expansion of UCB derived CD34(+) cells.
3. Iscove's Modified Dulbecco's Media (IMDM) was used for KG1a cells.
4. Stem cell factor (SCF).
5. Granulocyte colony stimulation factor (G-CSF).
6. Thrombopoietin (TPO) (R&D systems).
7. Flt-3 ligand (FL) (R&D systems).
8. Growth factors were dissolved in Dulbecco's Phosphate Buffered Saline (DPBS) containing 1% Bovine Serum Albumin (BSA) to concentration of 100 μg/ml. Dissolved growth factors were aliquoted into microtubes and stored at –20°C.
9. 9.55 g of DPBS was dissolved in 1,000 ml of water for irrigation (Baxter) and a pH was adjusted to 7.2 using sodium

hydroxide (NaOH) or hydrochloric acid (HCl) since pH may rise during filtration. Media was sterilized by membrane filtration (0.22 μm). The solution was stored for up to 3 months at 4°C.

10. BSA was made as a stock solution at concentration of 200 mg/ml. 20 g of BSA was dissolved in 100 ml of DPBS and pH was adjusted to 7.2 using NaOH or HCl. BSA concentrate was sterilized by membrane filtration (0.22 μm). BSA was stored for up to 6 months at 4°C.

### 2.3. CD34(+) Cell Isolation

The following materials were used for CD34(+) cell isolation:

1. Histopaque (Sigma-Aldrich) was used for density gradient isolation of mononuclear cells from UCB;
2. Magnetic-activated cell sorting (MACS) FCR blocking reagent (Miltenyi Biotech) and CD34 multisort microbeads (Miltenyi Biotech) were added to the mononuclear cells (100 μl per $10^8$ cells).
3. Cells were separated using MACS columns (Miltenyi Biotech) according to manufacturer's recommendations. A pre-separation filter (Miltenyi Biotech) was used to prevent blockage of columns by cell aggregates.
4. A ten times stock solution of ammonium chloride ($NH_4Cl$) was made to lyse red blood cells. 80.2 g of $NH_4Cl$, 8.4 g of $NaHCO_3$, and 3.7 g of disodium ethylenediaminetetraacetic acid (EDTA) were dissolved in 900 ml of water (Baxter). The pH was adjusted to 7.2 using NaOH or HCl and water (Baxter) was added to a final volume of 1,000 ml. The solution was sterilized by membrane filtration (0.22 μm) and stored for up to 6 months at 4°C. The ten times stock of $NH_4Cl$ was diluted in cold water (Baxter) before use.

### 2.4. Cell Labelling and Staining

1. CFDA-SE (Bioscientific) was dissolved in dimethylsulphoxide (DMSO) at 2.8 mg/ml. 50 μl of CFDA-SE stock was stored in a sterile microtube at –20°C overnight and then transferred to –70°C. CFDA-SE working stock was made up just before staining cells.
2. CD34 PE antibody (Becton Dickinson Bioscience; BD) was used for CD34(+) cell expression.

### 2.5. Cell Counting Using Flow Cytometry

Beads for calibration representing non-fluorescent polystyrene uniform microspheres (9.62 μm diameter, Bangs Laboratories, Fishers, IN) were added into cultures or into flow cytometry tubes (BD) before analysis. The bead count was determined by gating on their distinctive low forward vs. high side-light-scatter (FSC vs. SSC) properties (**Fig. 17.1**).

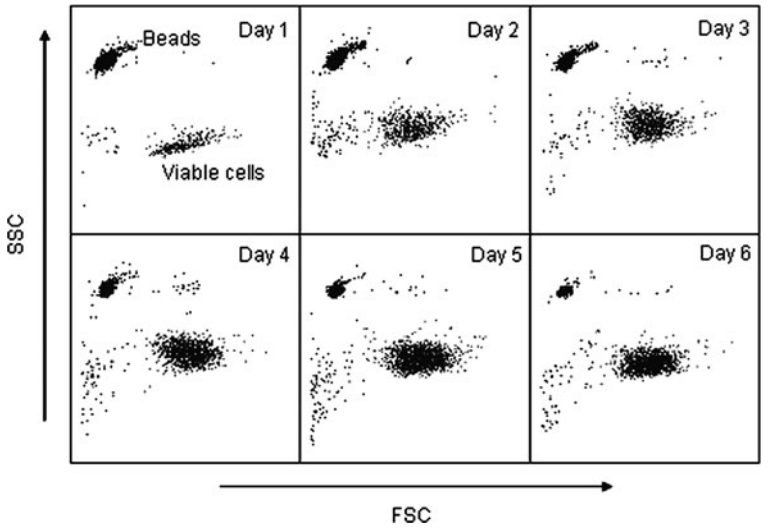


Fig. 17.1. Cell number measurement using flow cytometry. CFDA-SE stained and sorted CD34+ cells were grown for 6 days in serum-free media containing SCF, TPO, G-CSF, and FL, each at 100 ng/ml. Cell counting was performed on each consecutive day. Cell number is calculated as the ratio of live cells to beads events multiplied by the number of beads added to the sample.

## 3. Methods

### *3.1. Ex Vivo HSC Expansion*

*3.1.1. Isolation of CD34(+) Cells from UCB*

1. Transfer 10 ml of blood from the collection bag into 50 ml Falcon tubes, add 20 ml of DPBS and underlay with 15 ml of Histopaque.
2. Centrifuge at 400×*g* for 35 min.
3. Collect the buffy coat layer consisting of mononuclear cells. Red cells contaminating buffy coat layer should be lysed by addition of 50 ml of $NH_4Cl$ followed by 15 min incubation in the dark at 4°C.
4. Wash the cells twice with 50 ml of MACS washing buffer (DPBS containing 2 mM EDTA). Resuspend washed cells in 300 µl of MACS buffer (PBS containing 2 mM EDTA and 0.5% BSA) at a concentration of $10^8$ mononuclear cells.
5. Label cells using MACS CD34 multisort microbeads and FCR blocking reagent with 100 µl per $10^8$ cells. Incubate labelled cells for 30 min at 4°C followed by two washes with MACS buffer.
6. Separate CD34(+) and CD34(−) cells using MACS column according to manufacturer's instructions. CD34(+) cell yield depends on the volume of UCB collection and may comprise 0.01–0.05% of total nucleated cells (our unpublished data).

*3.1.2. Analysis of CD34(+) Cell Purity*

1. Transfer cells (up to $10^6$ cells) to flow cytometry tube and centrifuge at $180 \times g$ for 5 min.
2. Remove the supernatant with care not to disturb the cell pellet. Add 5–20 μl of anti-CD34 antibody into the tube (20 μl per $10^6$ cells).
3. Incubate cells on ice for a 30 min after mixing the suspension by gentle vortexing.
4. Wash the cell suspension with DPBS containing 10% FBS and analyze by flow cytometry (**Fig. 17.2**).

*3.1.3. Freezing and Thawing Cells*

Freshly isolated CD34(+) cells can be cultured immediately after isolation. Alternatively, CD34(+) cells can be frozen and then thawed prior to expansion. The procedure for cryopreservation and thawing of cells is as follows:

1. Wash cells with DPBS containing 10% FBS.
2. Resuspend cells in 700 μl of cold media, transfer to a cryovial followed by addition of 200 μl cold FBS and 100 μl DMSO.
3. Keep cells in a –70°C freezer overnight and then transfer into liquid nitrogen.
4. Thaw cells in a 37°C water bath before expansion. Transfer cells into a sterile centrifuge tube. Add appropriate media containing 50% FBS slowly up to 10 ml to dilute DMSO from the cells without lysing the cell pellet.

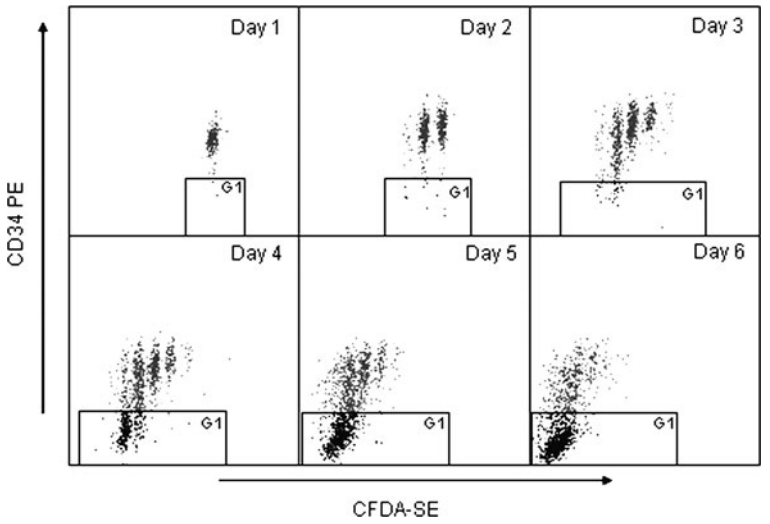


Fig. 17.2. The bivariate histograms of CFDA-SE/CD34/ expression in *ex vivo* expanded UCB CD34+ cells. CFDA-SE stained and sorted CD34+ cells were grown for 6 days in serum-free media containing SCF, TPO, G-CSF, and FL, each at 100 ng/ml. CFDA-SE/CD34 staining was performed daily. Isotype control (G1 gate) was used to define the CD34+ cell region.

5. Wash cells by centrifugation at 180×*g* and resuspend in appropriate media for culture.

*3.1.4. CD34(+) Cell Expansion*

1. Resuspend CD34(+) cells at concentration of $2 \times 10^4$ cells/ml in serum-free medium, containing SCF, G-CSF, TPO, and FL at 100 ng/ml (**Note 2**).
2. Cells should be always maintained at cell density lower than $10^6$ cells/ml. Fresh media containing cytokines should be added when cells reach higher cell density.
3. Harvest cells on day 5–7 and count using haemocytometer. Cells can be expanded in serum-free medium for 5–7 days with some loss of CD34 expression associated with cell differentiation occurs (17).
4. Perform CD34 staining as described above.
5. Calculate the expansion of total nucleated and CD34(+) viable cells by multiplying the proportion of viable CD34(+) cells by total cell numbers.

### 3.2. Cell Division Tracking

Here we present the detailed protocol for the combined analysis of CFDA-SE and CD34 expression to quantify cell division and phenotype of *ex vivo* expanded CD34(+) cells.

*3.2.1. CFDA-SE Staining and Sorting*

1. To monitor cell divisions CFDA-SE staining of CD34(+) cells should be performed prior to cell culture.
2. Resuspend cells in 1 ml of DPBS containing 0.1% BSA after and incubate at 37°C in a water bath for 10 min (**Note 3**).
3. Add 5 μM CFDA-SE solution to an equal volume of cells to give final concentration of 2.5 μM CFDA-SE (**Notes 3** and **4**). Vortex and then incubate at 37°C for 10 min in a water bath.
4. Quench staining by adding cold FBS at three times of the original volume of the cell suspension. Centrifuge cells at 180×*g*, 5 min followed by two further washes with PBS containing 10% FBS.
5. Resuspend cells in serum-free medium containing cytokines. Incubate cells at 37°C overnight to remove residual CFDA-SE.
6. Centrifuge cells at 180×*g*, 5 min, and resuspend in culture medium. Pass cells through a 40 μm cell mesh strainer (BD) to remove cell aggregates. Cells must be kept on ice until sorting is performed.
7. Prepare sterilized flow cytometry tubes (BD) for collecting cells by adding 1 ml of culture media with 1% of penicillin–streptomycin and keep them on ice. Our group routinely uses a FACSVantage (BD) for cell sorting.

8. Establish a viable sort gate using FSC vs. SSC bivariate histogram. Establish gates for CFDA-SE fluorescence by bisecting the CFDA-SE peak at the mode. Uniform labelling with CFDA-SE is essential to obtain clearly defined peaks following division. Therefore it is useful to sort for CFSE labelling in narrow gate (19).
9. Resuspend sorted cells in culture medium. Culture cells in serum-free medium containing SCF, G-CSF, TPO, and FL at 100 ng/ml in 37°C incubator for 6 days.

*3.2.2. CFDA-SE and CD34 Expression Analysis*

Combined CFDA-SE /CD34 analysis should be performed on the day of sorting (day 1) and for the next five consecutive days in culture (**Notes 5** and **6**).

1. Harvest cells and wash once in 3 ml DPBS. Centrifuge cells at 180×*g* for 5 min.
2. Perform CD34 antibody staining.
3. Analyze CFDA-SE/CD34 by multi-parameter flow cytometry. Compensate the spectral overlap between CFDA-SE (FL1) and anti-CD34 conjugated monoclonal antibody (HPCA2-PE) (FL2) using the hardware. It is important to have appropriate unstained and single-stained cell controls to apply the appropriate compensation. Use the same instrument settings for all of the analyses.
   a. Perform cell counts by adding known number beads to the culture or to the sample prior to collection on the flow cytometer to allow subsequent enumeration of cells in individual CFDA-SE peaks.
   b. When analysing the data, apply appropriate electronic gates to individually view live cells, apoptotic cells, and counting beads. The ratio of bead number to cell number gives the actual cell concentration in the sample (**Fig. 17.1**). For acquisition on the flow cytometer, the logarithmic mode for the side-scatter (granularity) parameter must be used with counting beads. Collect all events, so that the dataset includes beads, apoptotic cells, and live cells. Collect a sufficient number of events, so that the proportion of cells in each peak can be accurately determined.
   c. The proportion of cells in the individual CFDA-SE peaks can be determined on histogram.
   d. Obtain the bivariate histograms showing CFDA-SE vs. CD34 antigen expression. The typical bivariate histogram series obtained on each consecutive day following sort is shown in **Fig. 17.2**.
   e. Use corresponding isotype controls to define the CD34(+) cell region (**Fig. 17.2**).

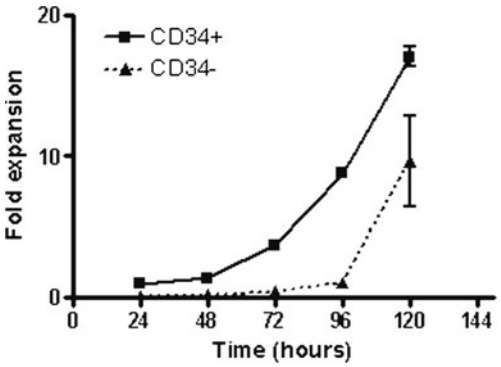


Fig. 17.3. Growth kinetics of UCB-derived CD34+ and CD34– cells. Cells were grown for 5 days with a cytokine cocktail containing SCF, TPO, FL, and G-CSF each at 100 ng/ml. Cells were counted and analysed for CD34 expression daily. Fold increase in cell number (*y*-axis) is the number of CD34+ or CD34– cells divided by the input cell number at the start of culture. The *x*-axis is time in hours.

f. Calculate the cell expansion at time *t* by dividing the cell number at time *t* by the number of cells that were inoculated (**Figs. 17.1** and **17.3**).

## 4. Notes

1. UCB can only be kept for 24 h at room temperature before use following blood collection.
2. There are no ideal phenotypic markers that allow *in vitro* isolation of a pure and homogenous human HSC population, and there is no ultimate cytokine cocktail that allows expansion of HSC in prolonged *ex vivo* liquid culture. Here we used a combination of four cytokines (SCF, FLT3L, TPO, and G-CSF) at relatively high concentration (100 ng/ml) to cultivate CD34(+) cells for up to 6 days. *Ex vivo* expansion of UCB-derived CD34(+) cells using this cytokine combination can be prolonged for as long as 2 weeks (group's unpublished data).
3. The cell number is one of the major considerations for CFDA-SE staining protocols; at low cell numbers the adsorption of dye per cell is higher. Commercial protocols suggest that $1 \times 10^7$ cells/ml should be used for CFDA-SE staining. However, when working with rare cells such as CD34(+) HSC, cell number is a significant consideration. **Figure 17.4a** shows that CFDA-SE and cell concentration at the time of CFDA-SE staining affects KG1a cell expansion. Higher cell numbers at the time of staining were

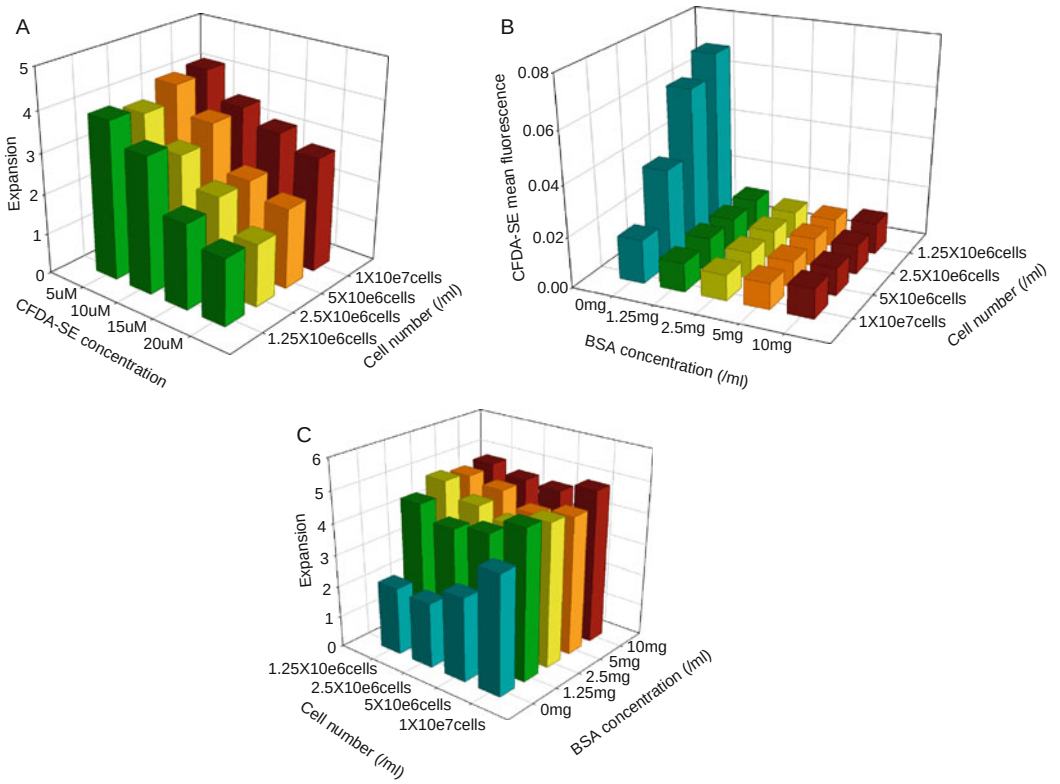


Fig. 17.4. Optimisation of CFDA-SE and cell dose. (**a**) CFDA-SE-stained KG1a cells were cultured in IMDM with 10% FBS. Cell numbers were counted at day 3. CFDA-SE dose vs. cell number vs. expansion is shown in three-dimensional bar graph. (**b**) Addition of BSA minimises variations in mean CFDA-SE fluorescence in KG1a cells cultured at low cell density. Cells were stained with 5 μM of CFDA-SE on day 0. Mean CFDA-SE fluorescence is the ratio of mean fluorescence intensity measured from day 1 to day 3 in KG1a cells. (**c**) Addition of BSA protects KG1a cells cultured at low cell density from CFDA-SE-mediated cytotoxicity. Three-day expansion is shown in *y*-axis.

less influenced by increase in CFDA-SE concentration compared to low cell numbers. BSA appears to act to 'buffer' CFDA-SE cell adsorption, making cell number at the time of staining less of a critical parameter. When cells were stained with CFDA-SE in the absence of BSA, there were significant variations in CFDA-SE mean fluorescence. 1 mg/ml BSA was used to perform CD34(+) cell staining with CFDA-SE (**Fig. 17.4b, c**).

The number of successive divisions that can be tracked depends on the CFDA-SE fluorescence intensity. Fluorescent tracking dyes produce cytotoxicity and thus delay cell growth. The titration of the CFDA-SE is required to optimise the dose of the dye. When CD34(+) cells were stained with 2.5 μM of CFDA-SE their level of expansion was close to that seen in unstained cells (data not shown). Therefore, 2.5 μM of CFDA-SE was further used for CD34(+) cell staining.

4. Labelling with CFDA-SE occurs rapidly and it is essential that CFDA-SE be dispersed as evenly and quickly as possible, so that cells are uniformly labelled.
5. Interpretation of data from time series division tracking is important to estimate specific parameters of cell growth and differentiation. Time series division tracking analysis provides accurate measurement of the distribution of cells across all generations in a relatively short time.
6. Although the assay is easy to perform, the flow cytometry read-out requires acquisition and analysis of multiple samples at regular time intervals. This makes it laborious compared with some other cell proliferation assays such as DNA analysis and BrdU incorporation. Therefore, application of division tracking should be reserved for applications where a high level of sensitivity and specificity is required to detect subtle effects on cell cycle and differentiation.

## Acknowledgements

The authors thank the Australian Cord Blood Bank for providing cord blood.

### References

1. Copelan, E. A. (2006). Hematopoietic stem-cell transplantation. *N. Engl. J. Med.* **354**, 1813–1826.
2. Gluckman, E., Rocha, V., and Chastang, C. L. (1999). Umbilical cord blood hematopoietic stem cell transplantation. *Cancer Treat. Res.* **101**, 79–96.
3. Scheding, S., Meister, B., Buhring, H. J., Baum, C., McKearn, J. P., Bock, T., et al. (2000). Effective *ex vivo* generation of granulopoietic postprogenitor cells from mobilized peripheral blood CD34(+) cells. *Exp. Hematol.* **28**, 460–470.
4. Wingard, J. R., Vogelsang, G. B., and Deeg, H. J. (2002). Stem cell transplantation supportive care and long-term complications. *Hematology (Am. Soc. Hematol. Educ. Program)* **1**, 422–444.
5. Haylock, D. N., and Nilsson, S. K. (2007). Expansion of umbilical cord blood for clinical transplantation. *Curr. Stem Cell Res. Ther.* **2**, 324–335.
6. Brunstein, C. G., and Laughlin, M. J. (2010). Extending cord blood transplant to adults: dealing with problems and results overall. *Semin. Hematol.* **47**, 86–96.
7. McNiece, I., Jones, R., Cagnoni, P., Bearman, S., Nieto, Y., and Shpall, E. (1999). *Ex-vivo* expansion of hematopoietic progenitor cells: preliminary results in breast cancer. *Hematol. Cell Ther.* **41**, 82–86.
8. Takagi, M. (2005). Cell processing engineering for *ex-vivo* expansion of hematopoietic cells. *J. Biosci. Bioeng.* **99**, 189–196.
9. Madkaikar, M., Ghosh, K., Gupta, M., Swaminathan, S., and Mohanty, D. (2007). *Ex vivo* expansion of umbilical cord blood stem cells using different combinations of cytokines and stromal cells. *Acta Haematol.* **118**, 153–159.
10. Kelly, S. S., Sola, C. B., de Lima, M., and Shpall, E. (2009). *Ex vivo* expansion of cord blood. *Bone Marrow Transplant.* **44**, 673–681.
11. Yao, C. L., Feng, Y. H., Lin, X. Z., Chu, I. M., Hsieh, T. B., and Hwang, S. M. (2006). Characterization of serum-free *ex vivo*-expanded hematopoietic stem cells

derived from human umbilical cord blood CD133(+) cells. *Stem Cells Dev.* **15**, 70–78.
12. Mobest, D., Mertelsmann, R., and Henschler, R. (1998). Serum-free *ex vivo* expansion of CD34(+) hematopoietic progenitor cells. *Biotechnol. Bioeng.* **60**, 341–347.
13. Heike, T., and Nakahata, T. (2002). *Ex vivo* expansion of hematopoietic stem cells by cytokines. *Biochim. Biophys. Acta* **1592**, 313–321.
14. Rose-John, S. (2006). Designer cytokines for human haematopoietic progenitor cell expansion: impact for tissue regeneration. *Handb. Exp. Pharmacol.* **174**, 229–247.
15. McNiece, I. K., Almeida-Porada, G., Shpall, E. J., and Zanjani, E. (2002). *Ex vivo* expanded cord blood cells provide rapid engraftment in fetal sheep but lack long-term engrafting potential. *Exp. Hematol.* **30**, 612–616.
16. Peters, S. O., Kittler, E. L., Ramshaw, H. S., and Quesenberry, P. J. (1995). Murine marrow cells expanded in culture with IL-3, IL-6, IL-11, and SCF acquire an engraftment defect in normal hosts. *Exp. Hematol.* **23**, 461–469.
17. Ko, K. H., Odell, R., and Nordon, R. E. (2007). Analysis of cell differentiation by division tracking cytometry. *Cytometry A* **71**, 773–782.
18. Koeffler, H. P., Billing, R., Lusis, A. J., Sparkes, R., and Golde, D. W. (1980). An undifferentiated variant derived from the human acute myelogenous leukemia cell line (KG-1). *Blood* **56**, 265–273.
19. Nordon, R. E., Nakamura, M., Ramirez, C., and Odell, R. (1999). Analysis of growth kinetics by division tracking. *Immunol. Cell Biol.* 77, 523–529.

# Chapter 18

# Flow Cytometry Developments and Perspectives in Clinical Studies: Examples in ICU Patients

**Fabienne Venet, Caroline Guignant, and Guillaume Monneret**

## Abstract

Septic syndromes represent a major, although largely under-recognized, healthcare problem worldwide accounting for thousands of deaths every year. Although flow cytometry (FCM) remains a relatively confidential diagnostic tool, it is useful at every step of intensive care unit (ICU) patients' management. This review will focus on biomarkers measurable by FCM on a routine standardized basis and usable for the diagnosis of sepsis and for prediction of adverse outcome, occurrence of secondary nosocomial infections or guidance of putative immunotherapy relative to innate and adaptive immune dysfunctions in ICU patients. Regarding early diagnosis of infection, neutrophil CD64 has been shown to be a highly sensitive and specific marker for systemic infection and sepsis in adults, neonates, and children. A diminished monocyte HLA-DR expression is a reliable marker for the development of monocyte anergy, secondary nosocomial infection, and death in critically ill patients. Finally, the measurement of an increased $CD4^+CD25^+CD127^{low}$ regulatory T cell percentage may represent a reliable marker for the diagnosis of lymphocyte dysfunctions in these patients. These stainings can be performed using lyse-no-wash methods and results are available within 1 h. Ideally, these biomarkers should be part of a panel helping to define ICU patients' immune status. In the specific clinical context of ICU patients' monitoring, the increasing potential of FCM is further illustrated by the use of the biomarkers listed above as stratification tools in preliminary clinical studies. The next critical step is to use these standardized FCM protocols in large multicentric clinical trials testing individualized immunotherapy. Importantly, many other markers of immune dysfunction are currently under development that could further enable the administration of targeted individualized therapy in ICU patients.

**Key words:** Sepsis, flow cytometry, CD64, HLA-DR, regulatory T lymphocytes.

## 1. Introduction

### *1.1. Monitoring ICU Patients by Flow Cytometry*

Despite marked improvements over the last decades, flow cytometry (FCM) remains a relatively confidential diagnostic tool. Indeed, clinical situations in which FCM is used on a routine

G. Banfalvi (ed.), *Cell Cycle Synchronization*, Methods in Molecular Biology 761,
DOI 10.1007/978-1-61779-182-6_18, © Springer Science+Business Media, LLC 2011

basis are still limited (e.g., lymphoma and leukaemia phenotyping, $CD4^+$ T cell counting in HIV-infected patients, basophil testing in allergy, paroxysmal nocturnal hemoglobinuria). However, we strongly believe that under standardized conditions, FCM is ready from prime time and vulgarization. In particular, a promising new domain of application for FCM is intensive care unit (ICU) with potential use at every step of patients' management: from the diagnostic to the definition of targeted and individualized therapy and finally, and most importantly, for the control of drug efficacy.

### *1.2. Sepsis Pathophysiology*

Septic syndromes represent a major, although largely under-recognized, healthcare problem worldwide accounting for thousands of deaths every year. Mortality remains high ranging from 20% for sepsis to over 50% for septic shock despite almost 20 years of anti-inflammatory clinical trials (1, 2). Several recent lines of evidence now establish that death from septic shock is probably due to the effects of distinct mechanisms over time (1, 2). Early in the course of the disease, a massive release of inflammatory mediators (normally designated to trigger immune response against pathogens) is occurring that may be responsible for organ dysfunctions and hypoperfusion. Concomitantly, the body develops compensatory mechanisms to prevent overwhelming inflammation and dampen an overzealous anti-infectious response. These negative feedback mechanisms, although having protective effects during the first initial hours, may paradoxically become deleterious as they persist over time leading to immune paralysis (**Fig. 18.1**) (1, 2). Indeed, considerable clinical and experimental evidences indicate that patients rapidly present with numerous compromised immune functions (1, 2).

As our capacity to treat patients during the very first hours of shock has improved (early and aggressive initial supportive therapy) (1), many patients now survive this critical step but eventually die later in a state of immunosuppression that is illustrated by patients' difficulty to fight the primary bacterial

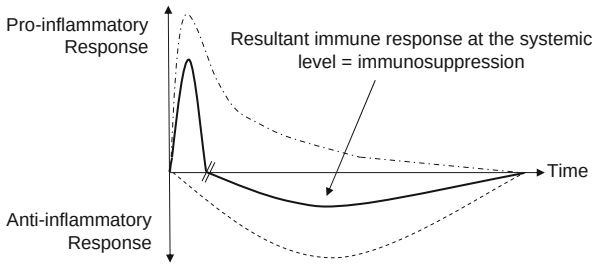


Fig. 18.1. Simplified description of systemic pro- and anti-inflammatory immune responses over time after septic shock. The *dashed lines* represent pro- or anti-inflammatory responses; the *bold line* represents the resultant at the systemic level. The shift from a pro-inflammatory to an anti-inflammatory immune response predominant at the systemic level likely occurs before 24 h after diagnosis of shock.

infection and their decreased resistance to secondary nosocomial infections (1, 2). Consequently, immunostimulatory therapies are now considered as an innovative strategy for the treatment of sepsis. However, the first critical step is to beforehand identify patients who would actually benefit from these therapies. Indeed, in the absence of specific clinical signs of their immune response, it is therefore critical to determine the best biological tools for patients' stratification according to their immune status, a missing step in most of previous clinical trials (1, 2). This would define the right action (i.e., stimulating innate immunity and/or adaptive immunity, blocking apoptosis, restoring other altered functions) at the right time (early or delayed treatment) in the right patient (individualized/tailored therapy). This chapter will focus on biomarkers measurable by FCM on a routine standardized basis and usable for the diagnosis of sepsis (CD64 expression on neutrophil) and for prediction of adverse outcome, occurrence of secondary nosocomial infections, or guidance of putative immunotherapy relative to innate, Human Leukocyte Antigen-DR (HLA-DR) expression on monocytes, and adaptive (percentage of circulating $CD4^+CD25^+$ regulatory T cells) immune dysfunctions.

### *1.3. Diagnosis of Severe Infections: CD64 Expression on Neutrophils*

Infection remains a major healthcare problem in hospitals and especially in the ICU where seriously ill patients with impaired immunity are readily exposed to pathogenic micro-organisms. Antibiotherapy, if appropriate and given early during the course of the infection, has been shown to reduce five times mortality in patients with septic shock (3). It is thus of vital importance for clinicians to detect severe infections at an early stage, when effective treatment and complete recovery are still possible. Usual biomarkers of infection such as procalcitonin (PCT) or C-reactive protein lack specificity (4). In particular, PCT has been shown to be a poor diagnosis marker of infection, although reliable for the monitoring of antibiotic efficacy (5, 6).

Recently, neutrophil CD64 has been shown to be a highly sensitive and specific marker for systemic infection and sepsis (4). The membrane molecule defined by monoclonal antibody CD64 is a high-affinity receptor (FcγRI) found on normal monocytes and only expressed at low levels by normal neutrophils. Neutrophil CD64 expression is regulated in a graded fashion in parallel with the degree of inflammatory response to a significant clinical process of infection or tissue injury (7). Neutrophil CD64 has been shown to be a highly sensitive and specific marker for systemic infection and sepsis in adults, neonates, and children. CD64 measurement has, for example, been shown to allow clinicians to discontinue antimicrobial treatment if negative within 24 h of suspected infection, without waiting for the definitive microbiological results (8).

Earlier studies on neutrophil CD64 were performed using cells isolated from whole blood using sedimentation or density gradient centrifugation. Neutrophil CD64 is now determined in whole blood without prior manipulation, using direct immunofluorescence and lyse-no-wash methods (9, 10).

Since CD64 expression is stable in EDTA-anticoagulated blood at least 24 h at room temperature, it is well suited for application in any clinical lab having access to a flow cytometer. This test is almost fully automated, the results are available rapidly (<20 min) and the assay can be performed on a 24/7 basis without specific expertise in flow cytometry (11).

### 1.4. Diagnosis of Monocyte Dysfunctions: HLA-DR Expression on Monocytes

Monocytes from septic patients are mainly characterized by a decreased capacity to mount a pro-inflammatory reaction upon a secondary bacterial challenge and by impairment in antigen presentation capacity most likely due to the lowered expression of major histocompatibility class II molecules (MHC class II). Regarding molecules expressed on monocytes, which are readily measured by standardized flow cytometry protocols, numerous studies have been performed regarding the measurement of HLA-DR expression.

Under normal conditions, monocytes strongly express HLA-DR on their surfaces. This molecule can thus easily be detected by flow cytometry. Monocytes with diminished or missing HLA-DR expression are markedly inhibited in their antigen-presenting function and in their ability to produce inflammatory mediators in response to a stimulus (2, 12). In septic patients, a decreased cell-surface expression of HLA-DR has regularly been observed on circulating monocytes (mHLA-DR) and there is now a general consensus that a diminished mHLA-DR expression is a reliable marker for the development of immunosuppression in critically ill patients (2). Indeed, a decreased mHLA-DR expression has been assessed as a predictor of septic complications after trauma, surgery, pancreatitis, burn patients, and after septic shock. In these studies, low levels of mHLA-DR (<40% of positive monocytes, normal values >90%) were observed in patients who subsequently developed nosocomial infections (2, 13–15). In contrast, in injured patients with uneventful recovery, mHLA-DR rapidly returned to normal values (in general in less than 1 week). Finally, decreased mHLA-DR has been shown to be predictive of adverse outcome in different groups of critically ill patients, including burn and septic shock patients (2, 13).

### 1.5. Diagnosis of T Lymphocyte Dysfunctions: Percentage of Circulating Regulatory T Cells

Due to their ability to interact not only with cells of the innate immune system but also with other cells of the adaptive response, T lymphocytes play a central role in anti-infectious immune response both as effectors and as regulators of this response. A growing body of evidence has now confirmed that lymphocyte-mediated immune response may be dysfunctional after severe

sepsis and may play a major role in the development of a state of immunosuppression in patients (16, 17).

T lymphocyte dysfunctions after severe sepsis include the occurrence of a state of anergy with a decreased proliferation to mitogen stimulation, a shift toward a Th2 profile of cytokine secretion, an increased apoptosis, and an increased percentage of $CD4^+CD25^+$ regulatory T lymphocytes (Treg) (1, 2, 16, 18).

Treg have recently been reported as a potent regulatory T cell lineage playing an essential role in the control of both adaptive and innate immune responses (19). An increased Treg percentage has been described in septic shock patients (16, 20). A similar increase in Treg percentage has been observed in trauma patients and in mice after polymicrobial septic challenge and stroke (16). We recently observed a strong correlation between the increased Treg/effector ratio measured in whole blood after septic shock and the decreased proliferative response of patients' lymphocytes after mitogenic stimulation (21). This suggests not only that the measurement of Treg's percentage may represent a reliable marker for the diagnosis of lymphocyte dysfunctions in patients but also that these cells may play a central role in the development of immunoparalysis after sepsis.

In mice, although activated murine $CD4^+$ T cells express CD25, the $CD4^+CD25^+$ phenotype identifies a largely homogenous regulatory population. However, in humans, complications arise because of the presence of a sizeable population of activated $CD4^+$ T cells that express CD25 (22). The $CD4^+CD25^+$ phenotype is therefore not Treg cell specific, and this lack of specificity is also exhibited by other surface markers, including glucocorticoid-induced tumor necrosis factor receptor family-related protein (GITR), CTLA-4, CD45RB, CD62L, neuropilin-1, CD103, and lymphocyte activation gene (LAG)-3, that have been shown to be overexpressed in Treg cell populations (22).

A more specific marker is the forkhead box (FOX)P3 transcription factor. However, this marker can only be used to isolate cells that are permeabilized and fixed and the staining procedure is long (around 3 h for completion) (23).

Two groups have recently addressed these issues by identifying the utility of CD127 expression for discriminating between $CD25^+$ regulatory and $CD25^+$-activated T cells (22, 24, 25). Sorted cells with the surface phenotype $CD4^+CD25^+CD127^{low}$ had higher levels of intracellular FOXP3 and CTLA-4 and, as determined by functional assays, were suppressive, hypoproliferative, and poorly responsive to T cell receptor signaling (23).

Thus, a combination of $CD25^+$ and $CD127^{low}$ identified a regulatory population comprising approximately 6–8% of the $CD4^+$ T cells in adults (22). The accuracy of this three-color staining for the monitoring of Treg in human blood is also further illustrated by the small variation in the percentage of Treg

measured in healthy individuals in different studies [6.35% of $CD4^+$ T cells for Seddiki et al. (24), 7–8% for Liu et al. (25), 6% for Ndhlovu et al. (26), 8.34% for Hoffmann et al. (27), and 6.8% in our study (21)]. In this study, we verified that the combined expressions of CD4 and CD25 and the low expression of CD127 appeared adequate for the characterization of circulating Treg in whole blood of either healthy volunteers or septic shock patients (21). A significant increase in the percentage of circulating $CD4^+CD25^+CD127^{low}$ Treg in septic shock patients was measured in comparison with healthy individuals (21). This study showed the validity of the three-color flow cytometry staining (CD4/CD25/CD127) for the standardized routine monitoring of Treg in patients.

### 1.6. Targeted Individualized Therapy Based on Beforehand FCM-Measured Biomarkers

In the specific clinical context of ICU patients' monitoring, the increasing potential of FCM is further demonstrated by the use of the biomarkers listed above as stratification tools in preliminary clinical studies testing immunomodulating therapies. In particular, several clinical trials have recently used the measurement of mHLA-DR expression to stratify the administration of IFN-γ or GM-CSF in small cohorts of ICU patients (28–31). These studies showed promising results and such strategy should now be tested in clinical trials including a large number of patients.

Moreover, several other innovative immunotherapies may be proposed for the treatment of immune dysfunctions in ICU patients based on the beforehand measurement by FCM of biomarkers (**Table 18.1**). In particular, interleukin 7 (IL-7) represents an interesting candidate. This molecule is an essential cytokine for T lymphocyte development, survival, expansion, and maturation in humans (32).

Finally, beside markers listed in this chapter, other markers of immune dysfunctions measurable by FCM have been proposed. These include markers of apoptosis, increased co-signaling receptor expression such as PD-1, measurement of intracellular co-signaling pathways or circulating cytokine dosages using beads (**Table 18.1**). Again, under standardized protocols, these aspects have to be investigated in multicentric clinical trials.

## 2. Materials

### 2.1. Solutions

1. PBS: dissolve 8.0 g of NaCl, 0.2 g of KCl, 1.15 g of $Na_2HPO_4$, and 0.2 g of $KH_2PO_4$ in 1 l of distilled water (with adjusted pH at 7.4). This solution may be stored at 4°C up to 1 month.
2. Lysing solution with ammonium chloride: dissolve 41.45 g of $NH_4Cl$, 5.0 g of $KHCO_3$, and 185 mg of EDTA in

**Table 18.1**
**Immune dysfunctions in septic patients: potential biomarkers and therapies**

| | | Biomarker | Technique | Targeted therapy |
|---|---|---|---|---|
| Innate immune response | Functional testing | ↓ *Ex vivo* cytokine production after TLR agonist stimuli | ELISA or CBA | GM-CSF<br>G-CSF<br>IFN-γ |
| | Cytokines | ↑ Plasma IL-10 | ELISA or CBA | AS101 |
| | Cell surface marker expression | ↓ mHLA-DR<br>↓ CD14, CD86, GM-CSF, CX3CR1 … | FCM | GM-CSF<br>G-CSF<br>IFN-γ |
| | Apoptosis | Depolarized mitochondria<br>↓ CD14 | FCM | GM-CSF<br>G-CSF<br>IFN-γ |
| Adaptive immune response | Functional testing | ↓ Proliferation after antigenic or non-specific stimulation | $^{3}$H-thymidine uptake or CFSE probes | IL-7<br>Ig IV |
| | Cell surface marker expression | ↑ Inhibitory receptors: PD1, CTLA4, CD47 …<br>↓ Co-activator receptors: CD28, CD3<br>↑ % Treg | FCM | Anti-GITR agonistic Abs<br><br>Ig IV |
| | Apoptosis | ↓ T cell count<br>↑ Annexin V staining<br>↓ Bcl2 expression protein/gene<br>Bax/Bcl-xl or Bax/Bcl2 ratios | FCM<br>RT-PCR/FCM<br>RT-PCR/FCM | IL-7<br>Caspase-inhibitors<br>Ritonavir |

TLR: toll-like receptor, ELISA: enzyme-linked immunosorbent assay, CBA: cytometric bead array, HLA-DR: human leukocyte antigen-DR, FCM: flow cytometry, CFSE: carboxyfluorescein succinimidyl ester, Ig: immunoglobulin, IV: intravenous, GITR: glucocorticoid-induced tumor necrosis factor receptor, RT-PCR: real-time polymerase chain reaction.

500 ml of distilled water (with adjusted pH at 7.3). Store solution at 4°C, in an aluminium-coverted bottle, up to 6 months. Before use, dilute the solution 1/10 in distilled water.

3. FACS lysing solution (BD Biosciences, San Jose, CA): dilute the solution 1/10 in distilled water. This solution may be stored at 4°C for up to 2 weeks.
4. Immunoprep reagent system (Beckman Coulter, Miami, FL) is composed of three reagents: Immunoprep A (erythrocyte lytic agent), Immunoprep B (leukocyte stabilizer), and Immunoprep C (cell membrane fixative).
5. Fixative solution: prepare 4% (v/v) solution of paraformaldehyde in PBS. This solution may be stored at 4°C for up to 2 weeks.

### 2.2. Antibodies

1. Fluorescein isothiocyanate (FITC)-labeled anti-CD64 antibody.
2. FITC-labeled anti-CD14 antibody.
3. Phycoerythrin (PE)-labeled anti-HLA-DR antibody (clone L243) (BD Biosciences, San Jose, CA).
4. PE-labeled isotype controls (IgG2a – BD Biosciences, San Jose, CA).
5. FITC-labeled anti-CD25 antibody.
6. PE-labeled anti-CD127 antibody.
7. PE-Texas Red (ECD)-labeled anti-CD4 antibody.

### 2.3. Calibration/ Standardization Beads

PE fluorescence quantitation kit (Quantibrite PE – BD Biosciences, San Jose, CA). Reconstitute with 500 µl of buffer such as phosphate-buffered saline with azide plus 5 g/l bovine serum albumin and vortex-mix.

## 3. Methods

### 3.1. CD64 Expression

1. Collect samples of peripheral blood in EDTA anticoagulant tubes.
2. Mix 100 µl whole blood with 5–10 µl FITC-labeled anti-CD64 antibody (according to manufacture recommendations for whole blood staining).
3. Incubate at room temperature for 15 min in the dark.
4. Lyse red blood cells by adding 1 ml of ammonium chloride lysing solution.

5. Vortex and incubate at room temperature for 15 min in the dark.
6. Add 3 ml of PBS, vortex, and centrifuge for 6 min at 300×*g* at 10°C.
7. Discard the supernatant and resuspend the pellet in 500 µl of fixative solution.
8. Flow cytometry gating strategy: neutrophils are readily gated out from other cells on a SSC/FSC bi-parametric dot-plot, and CD64 expression is then measured on their surface. Results are expressed as mean of fluorescence intensity (MFI) related to the entire neutrophil population.

### *3.2. Monocyte Major Histocompatibility Complex (mHLA-DR, MHC Class II-DR) Expression*

1. Collect samples of peripheral blood in EDTA anticoagulant tubes.
2. Mix 100 µl whole blood with 10 µl FITC-labeled anti-CD14 antibody and 20 µl PE-labeled anti-HLA-DR antibody or respective isotype controls.
3. Incubate at room temperature for 30 min in the dark.
4. Lyse red blood cells by adding 1 ml of diluted FACS lysing solution.
5. Vortex and incubate at room temperature for 15 min in the dark.
6. Add 3 ml of PBS, vortex, and centrifuge for 6 min at 300×*g* at 10°C.
7. Discard the supernatant and resuspend the pellet in 500 µl of fixative solution.
8. Flow cytometry gating strategy. Monocytes are first gated out from other cells on the basis of labeling with FITC-CD14 (**Fig. 18.2a**) and mHLA-DR expression is then measured on their surface. All results are expressed either as percentages of HLA-DR-positive monocytes among the total monocyte population (a threshold is defined with the isotype control – **Fig. 18.2b**) or as MFI related to the entire monocyte population (12, 33). This method is fast and results are available within 1 h.
9. Regarding calibration beads, the singlet bead populations are gated on a FSC vs SSC plot (**Fig. 18.2c**) and are analyzed with the histogram plot of FL2 (**Fig. 18.2d**). The number of HLA-DR molecule per monocyte can then be calculated either automatically (e.g., for Becton Dickinson flow cytometers, with BD CellQuest 3.1 and later versions) or manually by entering the geometric means of the four bead populations and the lot-specific values for the PE molecules per bead population on a statistics spreadsheet. The known ratio of PE to anti-HLA-DR antibody (the anti-HLA-DR antibody, clone L243, reacts with a non-polymorphic

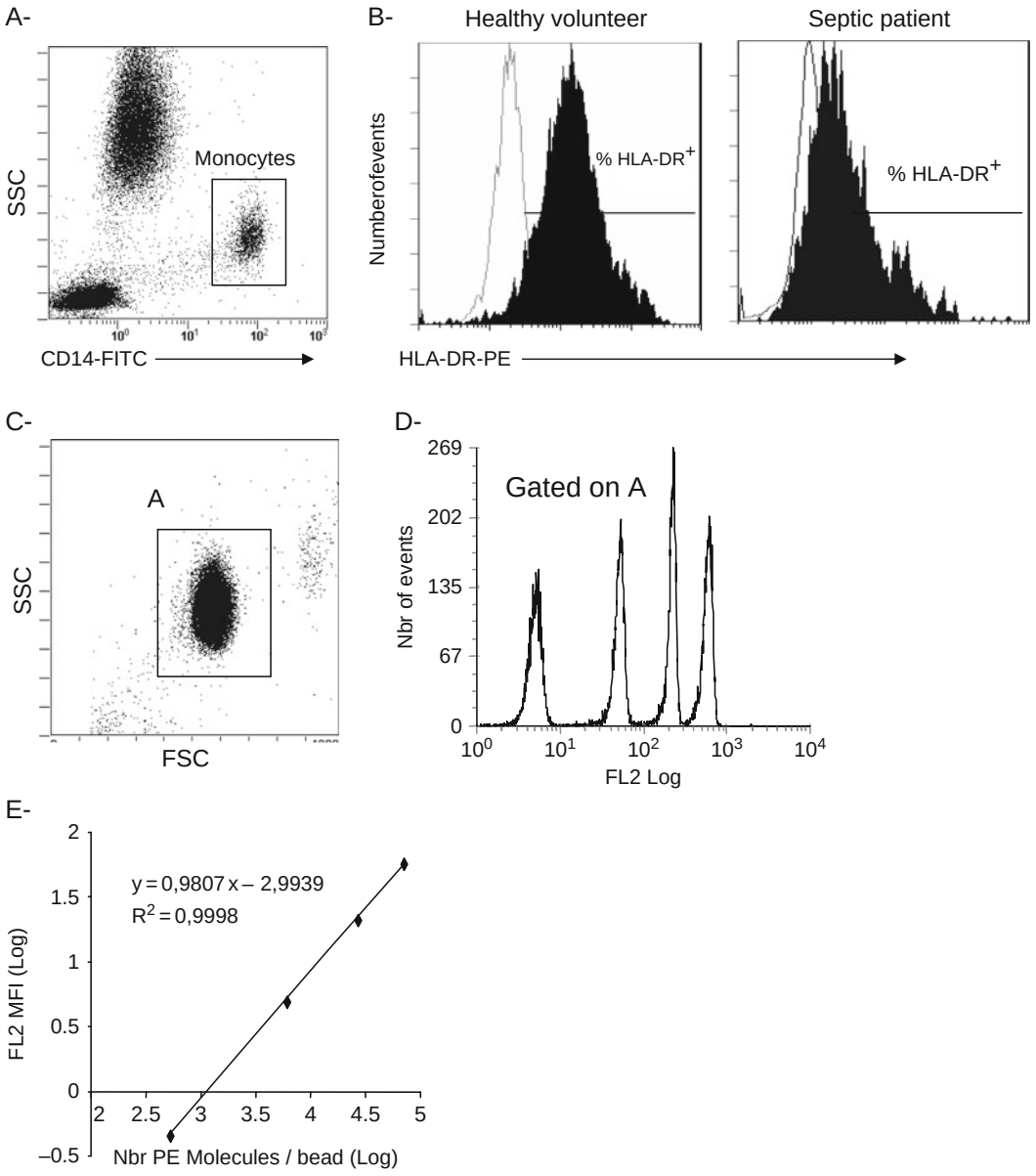


Fig. 18.2. Monocyte HLA-DR expression measurement by flow cytometry. **a** One representative CD14 vs SSC dot plot. **b** Representative HLA-DR linear histograms gated on monocytes in one healthy volunteer and septic patient (White histogram = isotype control). **c** A representative SSC vs FSC dot plot for the gating of singlet beads (Gate A). **d** Gated on A, a representative FL2 linear histogram. **e** Based on means of fluorescence intensity (MFI) measured on each bead subpopulation and on the number of PE molecule per bead given by the manufacturer, one representative calibration curve for the calculation of numbers of antibody bound per cells.

HLA-DR epitope and is conjugated with PE molecules in a 1:1 ratio) is used to convert the PE molecules per cell into antibodies per cell (AB/c) thanks to the generation of a calibration curve (**Fig. 18.2e**) (12).

### 3.3. Regulatory T Cells

1. Collect samples of peripheral blood in EDTA anticoagulant tubes.
2. Mix 100 µl EDTA-anticoagulated whole blood with 5 µl ECD-labeled anti-CD4, 10 µl FITC-labeled anti-CD25, and 10 µl PE-labeled anti-CD127 antibodies.
3. Incubate at room temperature for 15 min in the dark.
4. Red blood cells are then lysed using an automated technique (TQprep, Beckman Coulter) delivering Immunoprep® solution (when antibodies purchased from Beckman Coulter; if not, use ammonium chloride lysing solution as described in **Section 3.1 – Step 4**).
5. Flow cytometry gating strategy. $CD4^+$ T cells are first gated on a SSC/CD4 bi-parametric dot-plot (**Fig. 18.3a**). The $CD25^+CD127^{low}$ gate is then set to encompass an obviously distinct population among $CD4^+$ cells, as shown in **Fig. 18.3b**.

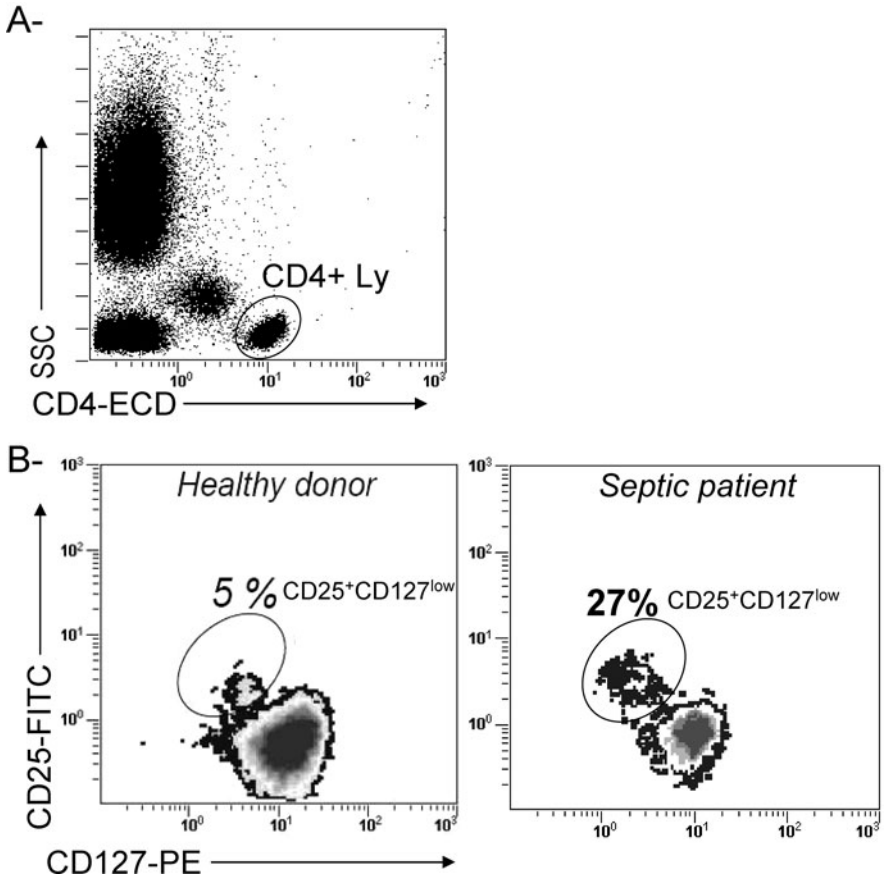


Fig. 18.3. $CD4^+CD25^+CD127^{low}$ regulatory T cell measurement by flow cytometry. **a** One representative CD4 vs SSC dot plot that allows the gating of $CD4^+$ lymphocytes (Ly). **b** Gated on $CD4^+$ Ly, representative CD25 vs CD127 dot plots in one healthy volunteer and a septic patient. The $CD25^+CD127^{low}$ population is easily identified and its percentage is increased in septic patients.

### 3.4. Conclusions

Patients with sepsis present with features consistent with immunosuppression and stimulating their immune system may thus represent a promising therapeutic strategy. However, an absolute prerequisite for the next clinical trials is to systematically beforehand assess patients' immune functions to be able to define individualized immunotherapy. For that purpose, the measurement of biomarkers using standardized FCM protocols appears to be the appropriate tool for the forthcoming years. Eventually, FCM will provide a panel of biomarkers giving clinicians an overview of patients' immune status and thus indicate the best immunostimulating therapy to be initiated.

## 4. Notes

1. Regarding CD64 result expression, two methods have been primarily used: percentage of $CD64^+$ cells and MFI, with or without calculating the number of molecules per cell. However, it is known that in infection and sepsis, the entire neutrophil population uniformly shifts to higher fluorescence (9). The only circumstances in which myeloid cells in blood show a skewed or bimodal distribution of the fluorescence histogram is in patients with immature granulocytes and with eosinophilia (9). Moreover, it has been demonstrated that the MFI distinguishes more reliably between different patients' groups than percent $CD64^+$ cells (8). Therefore, the use of percent $CD64^+$ neutrophils is not recommended as a measure of FcγRI expression. Moreover, in order to compare results between laboratories, it is desirable to standardize the assay using certified calibration beads (34). This renders the assay essentially independent of technique and antibodies and it enables laboratories to express CD64 in a quantitative manner as number of molecules per neutrophil.
2. A kit is available for CD64 measurement (and also CD163): Leuko64, Trillium Diagnostics, Brewer, ME, USA.
3. Because HLA-DR is a marker that is rapidly regulated, the storage temperature and the delay before staining are important issues. We compared results from fresh whole blood and those obtained after storage for 24 h at 4°C (33). In healthy donors, storage significantly increased MFI results. In septic patients, both the percentage values and the MFI were increased after storage. We also stored blood from five healthy donors at 37°C for 1 h and found a dramatic increase in the HLA-DR values measured for each sample, which supports a rapid nonspecific *in vitro* modulation of

this expression. Finally, we investigated the stability of HLA-DR expression at room temperature in five healthy patients. Our results indicated that samples should be stained within 1 h after sampling (33). Similarly, Döcke et al. observed that HLA-DR expression increased significantly after pre-analytical storage of blood for 2 h at room temperature, particularly in heparin- and citrate-anticoagulated blood. In contrast, the mean increase in HLA-DR values in EDTA blood stored on ice for 4 h was very low (12). However, our precision results illustrate that despite critical steps in the measurement, accurate determination of HLA-DR on monocytes allows day-to-day comparisons. In conclusion, use of EDTA blood, storage of unprocessed blood on ice as soon as possible before staining, and staining within 4 h after blood drawing were the conditions that produced the lowest variance between *ex vivo* values (12).

4. In mHLA-DR protocol, antibodies must be used at saturating concentrations to provide results as AB/c (33). If cells are fixed after staining, acquisition on FCM can be delayed by 24 h (35).
5. In mHLA-DR protocol, when MFI and calibrated beads for fluorescence quantification are used, results become comparable between different laboratories independent of the flow cytometer and the instrument settings (12).
6. In mHLA-DR protocol, a commercial kit using a similar staining procedure has been developed by BD Biosciences (QuantiBRITE$^{TM}$ Anti-HLA-DR PE/Anti-Monocyte PerCP-Cy5.5). This kit was used by Döcke et al. in an international multicentric feasibility study and showed good results especially when results were expressed as AB/c (12). Using this technique, reference values were defined: 13,200–42,500 AB/c for females and 15,300–40,100 AB/c for males (2.5th–97.5th percentiles, respectively) with median values of 26,200 AB/c for females and 25,300 AB/c for males (12).
7. As conventional CD4+ T cells tend to downregulate CD127 expression after TCR activation (36), Treg gating can be hindered in some cases.

## Acknowledgments

The authors would like to thank the Hospices Civils de LYON for their constant support over years.

## References


1. Hotchkiss, R. S. and Karl, I. E. (2003) The pathophysiology and treatment of sepsis. *N. Engl. J. Med.* **348**, 138–150.
2. Monneret, G., Venet, F., Pachot, A. and Lepape, A. (2008) Monitoring immune dysfunctions in the septic patient: a new skin for the old ceremony. *Mol. Med.* **14**, 64–78.
3. Kumar, A., Ellis, P., Arabi, Y., Roberts, D., Light, B., Parrillo, J. E., et al. (2009) Initiation of inappropriate antimicrobial therapy results in a fivefold reduction of survival in human septic shock. *Chest.* **136**, 1237–1248.
4. Groselj-Grenc, M., Ihan, A., Pavcnik-Arnol, M., Kopitar, A. N., Gmeiner-Stopar, T. and Derganc, M. (2009) Neutrophil and monocyte CD64 indexes, lipopolysaccharide-binding protein, procalcitonin and C-reactive protein in sepsis of critically ill neonates and children. *Intensive Care Med.* **35**, 1950–1958.
5. Nobre, V., Harbarth, S., Graf, J. D., Rohner, P. and Pugin, J. (2008) Use of procalcitonin to shorten antibiotic treatment duration in septic patients: a randomized trial. *Am. J. Respir. Crit. Care Med.* **177**, 498–505.
6. Tang, H., Huang, T., Jing, J., Shen, H. and Cui, W. (2009) Effect of procalcitonin-guided treatment in patients with infections: a systematic review and meta-analysis. *Infection* **37**, 497–507.
7. Davis, B. H., Olsen, S. H., Ahmad, E. and Bigelow, N. C. (2006) Neutrophil CD64 is an improved indicator of infection or sepsis in emergency department patients. *Arch. Pathol. Lab. Med.* **130**, 654–661.
8. Hoffmann, J. J. (2009) Neutrophil CD64: a diagnostic marker for infection and sepsis. *Clin. Chem. Lab. Med.* **47**, 903–916.
9. Davis, B. H. and Bigelow, N. C. (2005) Comparison of neutrophil CD64 expression, manual myeloid immaturity counts, and automated hematology analyzer flags as indicators of infection or sepsis. *Lab. Hematol.* **11**, 137–147.
10. Groselj-Grenc, M., Ihan, A. and Derganc, M. (2008) Neutrophil and monocyte CD64 and CD163 expression in critically ill neonates and children with sepsis: comparison of fluorescence intensities and calculated indexes. *Mediators Inflamm.* **2008**, 202646.
11. van der Meer, W., van Dun, L., Gunnewiek, J. K., Roemer, B. and Scott, C. S. (2006) Simultaneous determination of membrane CD64 and HLA-DR expression by blood neutrophils and monocytes using the monoclonal antibody fluorescence capability of a routine haematology analyser. *J. Immunol. Methods* **311**, 207–219.
12. Docke, W. D., Hoflich, C., Davis, K. A., Rottgers, K., Meisel, C., Kiefer, P., et al. (2005) Monitoring temporary immunodepression by flow cytometric measurement of monocytic HLA-DR expression: a multicenter standardized study. *Clin. Chem.* **51**, 2341–2347.
13. Venet, F., Tissot, S., Debard, A. L., Faudot, C., Crampe, C., Pachot, A., et al. (2007) Decreased monocyte human leukocyte antigen-DR expression after severe burn injury: correlation with severity and secondary septic shock. *Crit. Care. Med.* **35**, 1910–1917.
14. Landelle, C., Lepape, A., Voirin, N., Tognet, E., Venet, F., Bohe, J., et al. (2010) Low monocyte human leukocyte antigen-DR is independently associated with nosocomial infections after septic shock. *Intensive Care Med.* **36**, 1859–1966.
15. Lukaszewicz, A. C., Grienay, M., Resche-Rigon, M., Pirracchio, R., Faivre, V., Boval, B., et al. (2009) Monocytic HLA-DR expression in intensive care patients: interest for prognosis and secondary infection prediction. *Crit. Care. Med.* **37**, 2746–2752.
16. Venet, F., Chung, C. S., Monneret, G., Huang, X., Horner, B., Garber, M., et al. (2008) Regulatory T cell populations in sepsis and trauma. *J. Leukoc. Biol.* **83**, 523–535.
17. Lederer, J. A., Rodrick, M. L. and Mannick, J. A. (1999) The effects of injury on the adaptive immune response. *Shock.* **11**, 153–159.
18. Remick, D. G. (2007) Pathophysiology of sepsis. *Am. J. Pathol.* **170**, 1435–1444.
19. Belkaid, Y. (2007) Regulatory T cells and infection: a dangerous necessity. *Nat. Rev. Immunol.* **7**, 875–888.
20. Monneret, G., Debard, A. L., Venet, F., Bohe, J., Hequet, O., Bienvenu, J., et al. (2003) Marked elevation of human circulating CD4+CD25+ regulatory T cells in sepsis-induced immunoparalysis. *Crit. Care. Med.* **31,** 2068–2071.
21. Venet, F., Chung, C. S., Kherouf, H., Geeraert, A., Malcus, C., Poitevin, F., et al. (2009) Increased circulating regulatory T cells (CD4(+)CD25 (+)CD127 (−)) contribute to lymphocyte anergy in septic shock patients. *Intensive Care Med.* **35**, 678–686.
22. Banham, A. H. (2006) Cell-surface IL-7 receptor expression facilitates the purification of FOXP3(+) regulatory T cells. *Trends Immunol.* **27**, 541–544.

23. Hartigan-O'Connor, D. J., Poon, C., Sinclair, E. and McCune, J. M. (2007) Human CD4+ regulatory T cells express lower levels of the IL-7 receptor alpha chain (CD127), allowing consistent identification and sorting of live cells. *J. Immunol. Methods* **319,** 41–52.
24. Seddiki, N., Santner-Nanan, B., Martinson, J., Zaunders, J., Sasson, S., Landay, A., et al. (2006) Expression of interleukin (IL)-2 and IL-7 receptors discriminates between human regulatory and activated T cells. *J. Exp. Med.* **203**, 1693–1700.
25. Liu, W., Putnam, A. L., Xu-Yu, Z., Szot, G. L., Lee, M. R., Zhu, S., et al. (2006) CD127 expression inversely correlates with FoxP3 and suppressive function of human CD4+ T reg cells. *J. Exp. Med.* **203**, 1701–1711.
26. Ndhlovu, L. C., Loo, C. P., Spotts, G., Nixon, D. F. and Hecht, F. M. (2008) FOXP3 expressing CD127lo CD4+ T cells inversely correlate with CD38+ CD8+ T cell activation levels in primary HIV-1 infection. *J. Leukoc. Biol.* **83**, 254–262.
27. Hoffmann, H. J., Malling, T. M., Topcu, A., Ryder, L. P., Nielsen, K. R., Varming, K., et al. (2007) CD4dimCD25bright Treg cell frequencies above a standardized gating threshold are similar in asthmatics and controls. *Cytometry A.* **71**, 371–378.
28. Docke, W. D., Randow, F., Syrbe, U., Krausch, D., Asadullah, K., Reinke, P., et al. (1997) Monocyte deactivation in septic patients: restoration by IFN-gamma treatment. *Nat. Med.* **3**, 678–681.
29. Kox, W. J., Bone, R. C., Krausch, D., Docke, W. D., Kox, S. N., Wauer, H., et al. (1997) Interferon gamma-1b in the treatment of compensatory anti-inflammatory response syndrome. A new approach: proof of principle. *Arch. Intern. Med.* **157**, 389–393.
30. Meisel, C., Schefold, J. C., Pschowski, R., Baumann, T., Hetzger, K., Gregor, J., et al. (2009) Granulocyte-macrophage colony-stimulating factor to reverse sepsis-associated immunosuppression: a double-blind, randomized, placebo-controlled multicenter trial. *Am. J. Respir. Crit. Care Med.* **180**, 640–648.
31. Drossou-Agakidou, V., Kanakoudi-Tsakalidou, F., Sarafidis, K., Tzimouli, V., Taparkou, A., Kremenopoulos, G., et al. (2002) In vivo effect of rhGM-CSF And rhG-CSF on monocyte HLA-DR expression of septic neonates. *Cytokine* **18**, 260–265.
32. Sportes, C. and Gress, R. E. (2007) Interleukin-7 immunotherapy. *Adv. Exp. Med. Biol.* **601**, 321–333.
33. Monneret, G., Elmenkouri, N., Bohe, J., Debard, A. L., Gutowski, M. C., Bienvenu, J., et al. (2002) Analytical requirements for measuring monocytic human lymphocyte antigen DR by flow cytometry: application to the monitoring of patients with septic shock. *Clin. Chem.* **48**, 1589–1592.
34. Nuutila, J., Hohenthal, U., Laitinen, I., Kotilainen, P., Rajamaki, A., Nikoskelainen, J., et al. (2007) Simultaneous quantitative analysis of FcgammaRI (CD64) expression on neutrophils and monocytes: a new, improved way to detect infections. *J. Immunol. Methods* **328**, 189–200.
35. Finck, M. E., Elmenkouri, N., Debard, A. L., Bohe, J., Lepape, A., Bienvenu, J., et al. (2003) Preliminary results in standardization of flow cytometry protocols for monocytic HLA-DR measurement and their application in the follow up of septic shock. *Ann. Biol. Clin. (Paris).* **61**, 441–448.
36. Mazzucchelli, R. and Durum, S. K. (2007) Interleukin-7 receptor expression: intelligent design. *Nat. Rev. Immunol.* **7**, 144–154.

# Chapter 19

# Molecular Network Dynamics of Cell Cycle Control: Transitions to *Start* and *Finish*

**Attila Csikász-Nagy, Alida Palmisano, and Judit Zámborszky**

## Abstract

The cell cycle is controlled by complex regulatory network to ensure that the phases of the cell cycle happen in the right order and transitions between phases happen only if the earlier phase is properly finished. This regulatory network receives signals from the environment, monitors the state of the DNA, and decides when the cell can proceed in its cycle. The transcriptional and post-translational regulatory interactions in this network can lead to complex dynamical responses. The cell cycle dependent oscillations in protein activities are driven by these interactions as the regulatory system moves between steady states that correspond to different phases of the cell cycle. The analysis of such complex molecular network behavior can be investigated with the tools of computational systems biology. Here we review the basic physiological and molecular transitions in the cell cycle and present how the system-level emergent properties were found by the help of mathematical/computational modeling.

**Key words:** Systems biology, bistability, oscillation, computational modeling, checkpoints, budding yeast, hysteresis.

## 1. Introduction

Cell theory (1) states that the cell is the functional unit of life as it is able to perform self-reproduction individually. In addition, cells are also the structural pieces of systematically organized living organisms. All cells arise from pre-existing cells through their division. During a coordinated sequence of phases (referred to as cell cycle) the cell replicates all its internal components (e.g., DNA, ribosomes, RNAs, phospholipid bilayers, carbohydrates, metabolic machinery, proteins) and separates them into two nearly identical daughter cells. This crucial biological process is governed by a complex molecular machinery of macromolecules which need to act in synchrony to avoid all the

G. Banfalvi (ed.), *Cell Cycle Synchronization*, Methods in Molecular Biology 761,
DOI 10.1007/978-1-61779-182-6_19, 

potential errors leading to cell's malfunction or even death. In addition to the control of the alternation of DNA replication and cell division, cells need to grow to an accurate size. In order to ensure that, each step of cell cycle has to occur at the right time. A sophistically intertwined interaction network of the regulatory elements gives rise to fundamental physiological properties, such as oscillations, bistability, or hysteresis (2).

It becomes clear that to understand biology at the system level, researchers need to step over the boundaries of disciplines. Biology is far too complex to comprehend it piece by piece. Despite the enormous amount of biological data that are available, we are still far from a detailed understanding about how cells function. Mathematical and computational models can help biologists to understand a system's structure and dynamics. A multidisciplinary field called systems biology emerged from molecular biology and genetics in the early 2000s (3, 4). The systems biology approach has its root in the use of modeling and simulation, combined with experiment, to explore the dynamic behavior of biological systems. The interactions of the components defining the system under study need to be formalized by a computational model in order to arrive at testable quantitative predictions despite the complexity of these networks.

Cell cycle regulation was always a particular interest of mathematical biology leading to several success stories on the field. Mathematical modeling of the cell cycle goes back to the middle of the last century when scientists were making hypotheses about the underlying mechanism without knowing the molecules controlling cell division. From the 1960s, we can find fascinating discoveries of some of the rules that determine the observed physiology of cells (5). Research on chemical oscillations by theoretical physical chemists led to some methods and tools that were later used for the investigations of biological oscillators – such as the cell cycle. With time other computational frameworks were born to serve systems biological research and help to understand cell cycle regulation (6).

In this chapter, we introduce the readers to the basic principles of the physiology of cell cycle control and its underlying regulatory mechanisms. We will focus our attention on the classical model organism budding yeast, *Saccharomyces cerevisiae* (7), since the regulatory network and most of its dynamical features are well conserved among all eukaryotes (8, 9).

## 2. Physiology of the Cell Cycle

Cells run cycles of coordinated events resulting in self-reproduction. All eukaryotic cells share the major processes of the cell cycle. The underlying steps of the cell division cycle have to

occur in the right order (10). As the first step of the process, a cell must replicate its DNA in the S phase and later separate the two copies into two daughter nuclei in mitosis (M phase) and finally induce the separation of the two daughter cells (cytokinesis). DNA replication, chromatin condensation, and chromosome segregation should alternate to ensure that all cells have the same DNA content. If a cell commits another run of mitosis before finishing the previous DNA replication, the daughter cells would inherit incomplete chromosomes that would be lethal to cells. In multicellular systems, it can be a fatal mistake for the whole organism if these types of errors remain unrecognized (11).

Keeping the homeostasis of a population of cells is crucial for both single cell and multicellular organisms. Temporal gaps are inserted in the process in order to keep growth balanced (12). G1 and G2 phases provide the sufficient time for cells to double all their components. Although, there are exceptions to this rule when cells grow to a very large size (huge eggs) or when early embryos go over several rapid divisions without growth (10). The typical cyclic alternation of the four phases in normal somatic cells is depicted in **Fig. 19.1**.

Newborn cells start cell cycle in the G1 phase where they have one copy of the unreplicated chromosomes. They commit to start the cell cycle only if both internal and external conditions are suitable for cell proliferation. This transition is called *Start* in

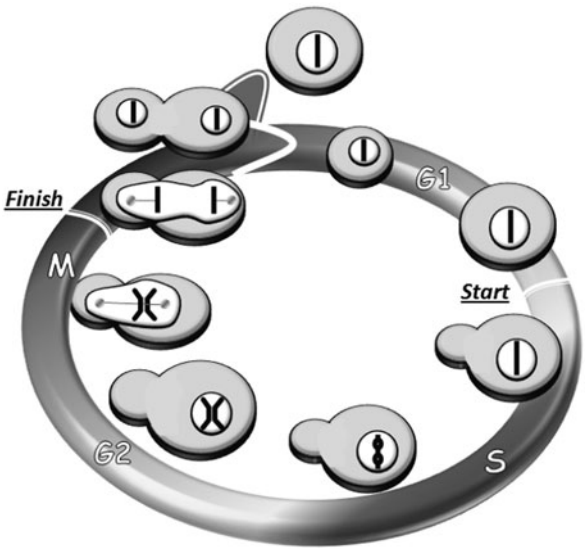


Fig. 19.1. Phases and transitions of the cell cycle. In G1 phase a newborn cell has a single copy of DNA. At the *Start* transition it commits itself toward the initiation of the cycle and starts budding and DNA replication (S phase). In budding yeast cells the S, G2, and M phases overlap, since the three chromosomes do not need to fully condense for mitosis. When the chromosomes are aligned to the middle of the nucleus the *Finish* transition induces the separation of the chromosomes which eventually leads to the separation of the bud. Thus cell division is asymmetric in these cells.

lower eukaryotes and *restriction point* in mammals (13, 14). The decision is irreversible: once the cell starts the cycle, eventually it goes to completion even if the internal or external conditions become worse, they will stop only in the upcoming cycle in G1 phase at the *Start* point.

In the S phase each DNA molecule is replicated. Accuracy of this event is crucial for producing healthy and viable daughter cells, thus the synthesis is permanently checked. Checkpoint mechanisms monitor if the replication complex proceeds an error or DNA is damaged. In case of a recognized damage the cell cycle process halts and repair mechanisms are initiated to correct defective DNA. Once the correction is done, the cells can continue their cell cycle. Budding yeast cells also start budding after the *Start* transition and in the remaining of the cell cycle only this bud will grow (**Fig. 19.1**). Generally the G2 phase is used to ensure the DNA replication is properly finished before initiation of mitosis, but in budding yeast the few chromosomes do not need to be tightly packed for mitosis, thus S, G2, and M phases somewhat overlap (7, 15).

The mitotic process has several subphases: first of all, replicated chromosomes condense into compact structures (prophase); then they become aligned on the center of the cell with the help of mitotic spindles (metaphase). By the time of the metaphase to anaphase transition of mitosis the chromosomes need to be properly replicated and their kinetochores need to be captured by the mitotic spindles. If there is a problem with the replication or the separation machinery then the cell cycle is stopped before it can be finished (16). With proper mitotic chromosomes the cells can pass the *Finish* transition (or meta–ana transition), the proteins (cohesins) that "glue" the two sister chromatids together are destroyed allowing the chromosomes to be pulled to the opposite poles of the cell (anaphase). After distributing the DNA content in telophase, the daughter nuclei form and eventually the two daughter cells separate during cytokinesis (17).

## 3. Checkpoints of the Cell Cycle

The major events of the cell cycle described in **Section 2** must be tightly regulated, checked and corrected for errors. If problems arise during cell cycle, "checkpoint" mechanisms block cycle progression until the problems are solved (18). Cells monitor the state of the cell cycle, the state of the DNA and environmental conditions as well. Surveillance mechanisms are present in every phase of the cell cycle. Spindle poles, anaphase progression, and the size of the cell are checked at specific time of the cycle, while

DNA damage is monitored continuously and checkpoint mechanisms arrest cell cycle progression either at the *Start* transition, anytime during S phase, or at the entry or *Finish* of mitosis. If DNA damage occurs, a signaling pathway is switched on and triggers several molecular events (repair mechanisms, cell cycle block, and probably even apoptosis). Sophisticated feedback regulations induce immediate stops of the process in case of a failure (19, 20). As we described above, cells go over transitions that are triggered by transient signals that emerge when the checkpoint conditions are all satisfied. The regulation of these state-changes is crucial for checkpoint mechanisms as it provides an opportunity to give an immediate response upon arising problems (21, 22).

If a checkpoint is activated for a longer time than the mass doubling time of the cell population then all cells will end up at the same checkpoint. Release of this checkpoint can induce population level synchronization of cells, which synchrony could last for a few cycles. In case of budding yeast cells such synchronization lasts only for one cell cycle due to the asymmetric divisions of mother and daughter cells. Some most recent genetic tricks allowed researchers to keep synchronized divisions in a budding yeast colony for several cell cycles. One method is to halt cells during DNA synthesis or at the *Finish* transition by inhibitory drugs that inhibit the DNA replication of chromosome segregation machinery (e.g., thymidine, aminopterin, hydroxyurea, taxol). At *Start* the cells can be collected by nutrition or growth factor deprivation leading to unfavorable external conditions when cells decide not to start their cycle. Sexual hormones can also induce block at *Start* transition and lead to mating of budding yeast cells (23). Temperature-sensitive mutants in genes of *Start* and *Finish* regulation can be also used to stop the cells at these checkpoints (24). Cell cycle synchronization can emerge naturally by the daily cycles through connections between circadian rhythms or temperature cycles and the cell division cycle (25).

In the next section we focus on the description of the interactions of the genes that regulate these crucial cell cycle transitions.

## 4. Molecular Mechanism of Cell Cycle Control

The proper order of cell cycle events is controlled by a complex regulatory network of interacting macromolecules that control the cell cycle transitions. Systematic analysis of cell cycle mutants in the 1970s by Lee Hartwell (24), Paul Nurse (26), and others led to the discovery of the key regulator of the cell cycle (CDK – cyclin-dependent kinase) that works in a complex with a cyclically appearing molecule (cyclin), what was discovered

by Tim Hunt (27). These three researchers received the Nobel Prize in 2001 for their breakthrough results in understanding cell cycle regulation (28). Hartwell identified the cell division cycle (Cdc) genes in the budding yeast *S. cerevisiae* through a genetic screen of temperature-sensitive mutants that were viable at 23°C but stopped proliferating at 36°C. He found that the differences between them were due to checkpoint events stopping cells at different points of their cycle. He proposed that Cdc28 might encode the key regulator of the cell cycle. Following these, Paul Nurse isolated temperature-sensitive mutants of the rod-shaped fission yeast, *Schizosaccharomyces pombe*. He found cell cycle blocked long cells, but also noticed unusually small cells that seemed to be able to proliferate normally. He named this mutant Wee (small in Scottish) and realized that the related genes must have an important role in controlling proper cell cycle control. Later, Nurse noticed that one of the genes with Wee phenotype can be mutated in another point to produce cell cycle-blocked elongated cells and soon he discovered that this gene (Cdc2) is homologue to Hartwell's Cdc28 in budding yeast as well as he found the human version of the gene. Tim Hunt contributed to the previous work of Hartwell and Nurse when he studied the control of mRNA translation and found proteins whose level oscillated. He gave the name "cyclins" to these periodically degraded molecules. Later discoveries showed that the complex of cyclin and Cdc2 (generally called CDK – cyclin-dependent kinase) is responsible for the initiation of mitosis in eukaryotic cells. After these breakthrough discoveries, several cell cycle regulators and their functions have been identified that helped us to better understand the crucial regulatory steps of the cell cycle (6, 10). The basic mechanisms behind the cell cycle steps are well conserved among eukaryotes, thus we can introduce the key regulatory loops on the budding yeast system without loosing much generality. For a "conversion table" that converts the budding yeast nomenclature to other organisms we refer the readers to earlier works (8).

### 4.1. Cell Cycle Control in Budding Yeast

After 70 years of genetic and molecular biology research now we know that CDK proteins work as effective kinases only if they are bound by a regulatory cyclin partner that helps substrate recognition . The budding yeast cell cycle is controlled by only one Cdk (Cdc28) and its nine cyclin partners (Cln1-3, Clb1-6). Cdc28/Cln1-3 complexes control the *Start* transition and bud initiation, Cdc28/Clb5,6 complexes initiate DNA replication by phosphorylating proteins bound to chromosomes at "origins of replication" (specific nucleotide sequences, where DNA replication can start) and Cdc28/Clb3-4 has early mitotic roles, and Cdc28/Clb1-2 complexes are the most important for different steps of mitosis (29). The separation of chromosomes at the

*Finish* transition happens together with the destruction of cyclins and the resulting drop in CDK activity induces cell division.

The activity of Cdc28/cyclin complexes can be regulated in several ways, one of which is the controlled degradation of their cyclin subunits. The anaphase promoting complex (APC), with the help of the regulatory protein Cdc20, labels Clb1-6 for degradation. APC can also work with another regulator Cdh1, which can recognize only Clb1,2 molecules and induce their degradation at the end of the cell cycle (30). Interestingly, the Cdc28/Clb2 complex can phosphorylate and inactivate Cdh1 proteins, what leads to an antagonistic relation between Cdc28/Clb2 and Cdh1/APC. This antagonism creates two, alternative stable steady states of the control system: (1) a G1 state, with high Cdh1/APC activity and low Cdc28/Clb2 activity, (2) and an S-G2-M state, with high Cdc28/Clb2 activity and low Cdh1/APC activity. The transition between G1 and S–G2–M phases is facilitated by Cdc28/Cln1-3 molecules that cannot be destroyed by Cdh1/APC, while the opposite phase change is initiated by the Cdc14 phosphatase that reverts the Cdc28-induced phosphorylation on target molecules. Cdh1/APC is also helped by the CDK inhibitor Sic1 that can bind to Cdc28/Clb complexes and inhibit their activity. Importantly Sic1 is also in an antagonistic relation with Cdc28/Clb complexes that can induce Sic1 degradation by phosphorylating it. Thus G1 phase is stabilized by the concerted action of Cdh1/APC and Sic1 and at the *Start* transition the Cdc28/Clb complexes take over and are active until the *Finish* transition when the system reverts to the initial state (7, 19, 21).

In order to better explain how the progression between the different phases is driven by these antagonistic relationships, let us consider the simple mechanical metaphor of the seesaw in **Fig. 19.2**. The lever represents the strong connection between the two antagonist partners. The height of the left part of the lever represents the activity of the Cdh1/APC complex and the abundance of the stoichiometric inhibitor Sic1. The height of the right part of the lever illustrates the amount of the Cdc28/Clb complexes (Clb's, for short in **Fig. 19.2**). The two buckets represent the helper molecules that induce the two transitions (Cln1-3, Cdc14).

After cell division the newborn cells are in G1 phase, with high Sic1 and Cdh1 activity, and no Cdc28/Clb complexes are present. As the cell grows (the "Growth" signal in **Fig. 19.2**) it starts to produce Cln1,2,3 cyclins that bind to Cdc28 and these complexes phosphorylate – thus inactivate – Cdh1 and Sic1. As the lever turns Cdk/Clb level increases that further helps Cdh1 and Sic1 inactivation. When the lever turned high Cdc28 activity induces bud emergence, DNA replication, and spindle pole body duplication. Further molecular intricacies of the *Start* transition

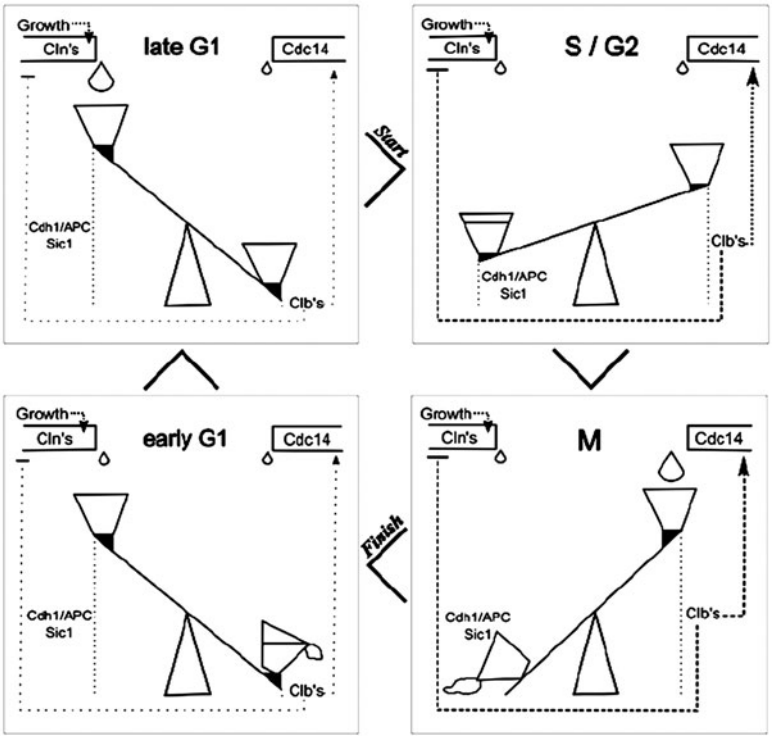


Fig. 19.2. A seesaw metaphor for the antagonism between Cdc28/Clb2 and its G1 enemies (Cdh1/APC and Sic1). See text for description.

include the activation of the transcription factors (SBF/MBF) of the G1 cyclins (Cln1 and Cln2). SBF is kept inactive by the Whi5 inhibitor that could be phosphorylated and exported from the nucleus by Cdc28/Cln3 complexes. The transcription factors induce the expression of Cln1,2 and Clb5,6. These cyclins bind to Cdc28 and phosphorylate Cdh1 and Sic1 to flip the lever of **Fig. 19.2**. Later the high Cdc28/Clb activity induces the inactivation of the transcription factors of the starter kinases Cln1,2,3 (see dashed line on **Fig. 19.2**), thus turns off Cln synthesis, what empties the left side bucket after the *Start* transition happened.

The *Finish* transition is facilitated by Cdc20 and Cdc14. Cdc20 in complex with the APC degrades the Clb kinases and separates the sister chromatids (16, 30). Cdc20, together with Cdc28/Clb2, helps the activation of the Cdc14 phosphatase (see the dashed arrow on **Fig. 19.2**). The active Cdc14 reactivates Cdh1 and Sic1 helping these proteins to flip the lever back to the G1 state and to *Finish* the cell cycle. When conditions are favorable, the whole process may start again.

This antagonism (or double negative = positive feedback) is responsible for the irreversibility of these transitions as the cell is not running as a free oscillator rather jumps between stable steady

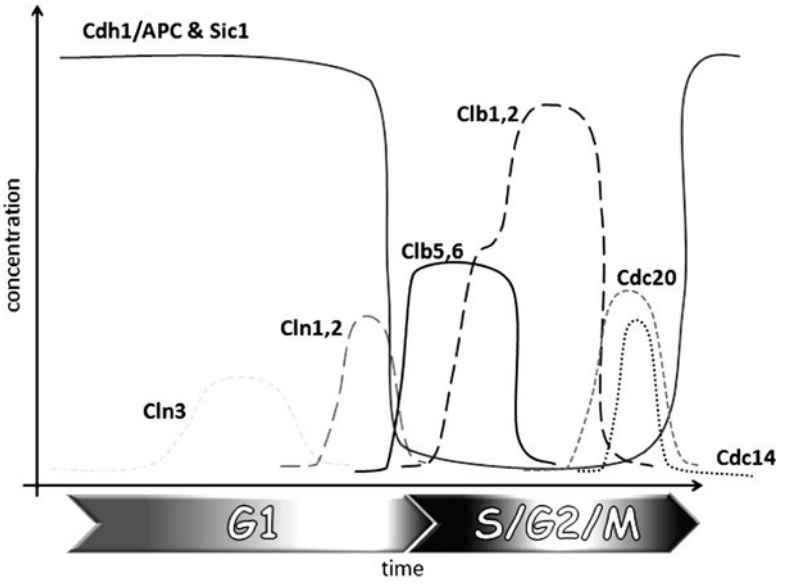


Fig. 19.3. Fluctuations in the activities of key cell cycle regulators during the cell cycle. Idealized time course of protein activity waves during the cell cycle. Cdc28 is always present in excess so only the levels of cyclin partners are noted.

states at the critical cell cycle transitions closing a hysteresis loop (19). Still the result of the hysteric interaction of Cdc28/Clb's and the Cdh1/APC, Sic1 pair together with the transition regulator proteins shows relaxation oscillatory behavior with long phases in near steady states and quick jumps between these states (**Fig. 19.3**).

### *4.2. Models of Cell Cycle Regulation*

As some data on the key regulator of cell cycle (CDK) were found by Nurse and others (see above), theoreticians started to create models to understand how CDK can regulate cell cycle events (31, 32). Some of these works laid down crucial details and basic properties of cell cycle regulation. Further experiments on yeasts and frog eggs produced a molecular description of the protein interaction network of these systems, inspiring further mathematical analysis. This success story created a great interest for modelers to answer questions of cell biology with the help of an interdisciplinary work of mathematicians, physicists, and other scientists (6).

The dynamical properties of a cell are implicit in the topology of the protein networks that underlie cell physiology. A detailed characterization of such a complex system can be achieved only by mathematical and computational approaches that model the temporal and spatial evolution of the system (33). In general, to determine whether a hypothetic regulatory network like the one in **Fig. 19.4** is correct, the classical approach is to convert

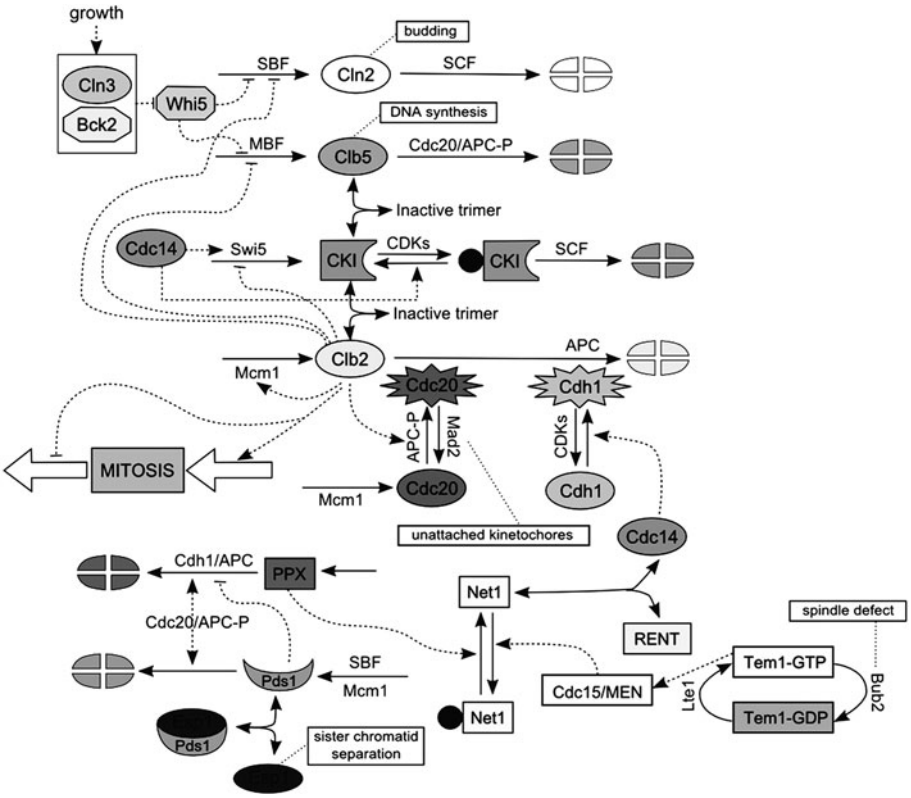


Fig. 19.4. Regulatory network of the budding yeast cell cycle. Adapted from Chen et al. (21). In the diagram, Cln2 stands for Cln1 and 2, Clb5 for Clb5 and 6, and Clb2 for Clb1 and 2. Moreover the kinase protein Cdc28 is not shown explicitly because there is an excess of Cdc28 and it combines rapidly with the different cyclin partners as soon as they are synthesized. Newborn daughter cells must grow to a critical size to have enough Cln3 and Bck2 to activate the transcription factors SBF and MBF, which induce synthesis of Cln2 and Clb5, respectively. Cln2 is primarily responsible for bud emergence, and Clb5 for initiating DNA synthesis. Clb5-dependent kinase activity is not immediately evident because in G1 phase cyclin-dependent kinase inhibitors (CKI; namely, Sic1 and Cdc6) are prevalent. After the CKIs are phosphorylated by Cln2 and other active cyclin-dependent kinase complexes (collectively denoted by CDKs), they are rapidly degraded by SCF, releasing Clb5 to do its job. A fourth class of cyclins, denoted Clb2, is not involved in G1 because their transcription factor Mcm1 is inactive, their degradation pathway Cdh1/APC is active, and their stoichiometric inhibitors CKI are abundant. CDKs active complexes remove CKI and inactivate Cdh1, allowing Clb2 to accumulate after some delay, as it activates its own transcription factor, Mcm1. Clb2 turns off SBF and MBF. As Clb2 drives the cell into mitosis, it also sets the stage for exit from mitosis by stimulating the synthesis of Cdc20 and by phosphorylating components of the APC. Meanwhile, Cdc20/APC is kept inactive by the Mad2-dependent checkpoint signal responsive to unattached chromosomes. When the replicated chromosomes are attached, active Cdc20/APC initiates mitotic exit. First, it degrades Pds1, releasing Esp1, a protease involved in sister chromatid separation. It also degrades Clb5 and partially Clb2, lowering their strength on Cdh1 inactivation. In this model, Cdc20/APC promotes degradation of a phosphatase (PPX) that has been keeping Net1 in its unphosphorylated form, which binds with Cdc14. As the attached chromosomes are properly aligned on the metaphase spindle, Tem1 is activated, which in turn activates Cdc15 – the endpoint of the MEN signal transduction pathway in the model). When Net1 gets phosphorylated by Cdc15, it releases its hold on Cdc14. Cdc14 phosphatase then works against the cyclin-dependent kinases: activating Cdh1, stabilizing CKIs, and activating Swi5 (the transcription factor for CKIs). In this manner, Cdc14 returns the cell to G1 phase (no cyclins, abundant CKIs, and active Cdh1).

the mechanism informally described by the wiring diagram into a formal mathematical/computational model and to compare the results of these models to the observed behavior of the cells. Classically mostly physiological observations could be fitted (lethality of deletion mutants, cell size differences, lengths of the different phases) but recent experiments also provide data on molecular level fluctuations to fit. If a model is found to be fitting most of the collected observations but inconsistent with a few of them, then it might highlight the aspects of the mechanism that require revision and further testing (21).

The type of approach to be used depends on the biological question in which the user is interested in. For instance, genetic regulatory circuits of the cell cycle can be modeled by differential equations or by Boolean networks (34). Spatial signaling of cell cycle-related pathways might be modeled by partial differential equations (35) or by cellular automata, and when the regulation of transcription is investigated, thus small numbers of molecules are involved, stochastic models should be used (36, 37).

The groups of Bela Novak and John J. Tyson published several models built on the hypothesis that is presented above on the "two state model" of the budding yeast cell cycle regulation. The two landmark papers by Katherine C. Chen and colleagues from the Tyson lab stand as the most influential and comprehensive mathematical models of cell cycle regulation (15, 21). These models are based on an extensive literature data collection on more than 100 budding yeast cell cycle mutants and the final model can simulate the findings of almost all of these experiments. In their first paper, Chen et al. (15) particularly examined the molecular events regulating the *Start* transition of the cell cycle. It accounts for many details of the cells' physiology (viability–lethality, cell size, lengths of different cell cycle phases) in wild type and about 50 mutant cells. The authors proposed here the above-presented idea, that G1 and S/G2/M phases are alternative states and cells switch between them during the *Start* transition, when CDK activity abruptly increases. The bistability of the system is given by the antagonism between Cdc28/Clb complexes and their inhibitors Sic1 and Cdh1. The authors also proposed an experiment which could verify the existence of this bistability. In 2002 Fredrick R. Cross and his group performed experiments following these suggestions and confirmed the prediction (38). In this groundbreaking paper Cross went much further and made an extensive experimental test of various properties of the model while also performing some crucial measurements to help further model development. This milestone paper was the first one that was fully devoted to test a mathematical model, giving one of the earliest steps toward systems biology (4, 6). Two years later the measurements and corrections by Cross were implemented into a new version of the Chen model (21),

furthermore it was also extended with the detailed regulation of the *Finish* transition. The resulting model was tested against the behavior of 131 mutants and failed only on 11 of them. These failures highlighted the parts of the network that need more experimental observations, since the current knowledge that is built in the model cannot capture the behavior of some related mutants. This extended model also predicted the existence of a phosphatase that removes phosphates from Net1 (PPX on **Fig. 19.4**). This hypothetical phosphatase was experimentally identified in 2006 (39).

As our knowledge about the regulatory network of the cell cycle and its interactions with other cellular pathways increases, complexity of mathematical models is growing with it. Detailed analysis and parameterization of such large systems can be difficult with huge number of ordinary differential equations (ODEs). Simplification by logical modeling has been proposed to overcome this problem (40). Logical modeling has a long tradition in biology (41) and recently some applications to cell cycle research also appeared (34, 42). These models are based on Boolean algebra, where the activity of each component is represented by two states: ON and OFF, providing a method which is computationally less expensive. Behaviors that originate from the topology of the system can be nicely investigated in this way. An advantage of logical models that they reduce the size of the possible state space, thus they permit the use of some analysis methods that work only for smaller systems. One of the emerging methods is called model checking (43, 44) and it could be used to test if a model matches some specific conditions. It is emerged from studies of logic in computer science and it is widely used for testing safety requirements in hardware or software systems. This approach uses some temporal logic formulae and gives an opportunity to verify if a system can reach a given state or not. This method has already approached cell cycle models as well (45).

Noise can notably affect biological systems. While fluctuations in the average behavior of a cell population can be described by deterministic ODE models, the answer changes a lot on single cell level. Stochastic modeling approaches are getting more and more popular because they provide opportunity to analyze single cells and find relevant results in cooperation with novel experimental techniques such as quantitative flow cytometry (46) and fluorescence microscopy (47). As a result of these experiments, recently some much more detailed stochastic models of cell cycle regulation appeared, that take into account measured molecular levels, protein, and mRNA half-lives, and several other details. Mura and Csikasz-Nagy (37) showed that the stochastic fluctuations could be relevant for certain mutant phenotypes that show partial viability, what could not been identified by deterministic models on the population level. Barik et al. (48) studied the effect

of molecular fluctuations on cell cycle progression in a model of budding yeast in which feedback loops involving CDK complexes are realized through multisite phosphorylation mechanisms.

Some other modeling concepts also expanded from computer science toward biological systems. Rule-based modeling (49, 50) and especially various process algebras were built to handle the problem of combinatorial complexity caused by complex formation and various protein modifications. These allow an easier handling of multisite phosphorylation and multi-component complex formations, which are both relevant issues for cell cycle models. They also provide tools for performing stochastic simulations of the modeled system. Such simulation results of a model of budding yeast cell cycle regulation (51) are plotted in **Fig. 19.5**. We can notice the noise in molecular level fluctuations in both plots

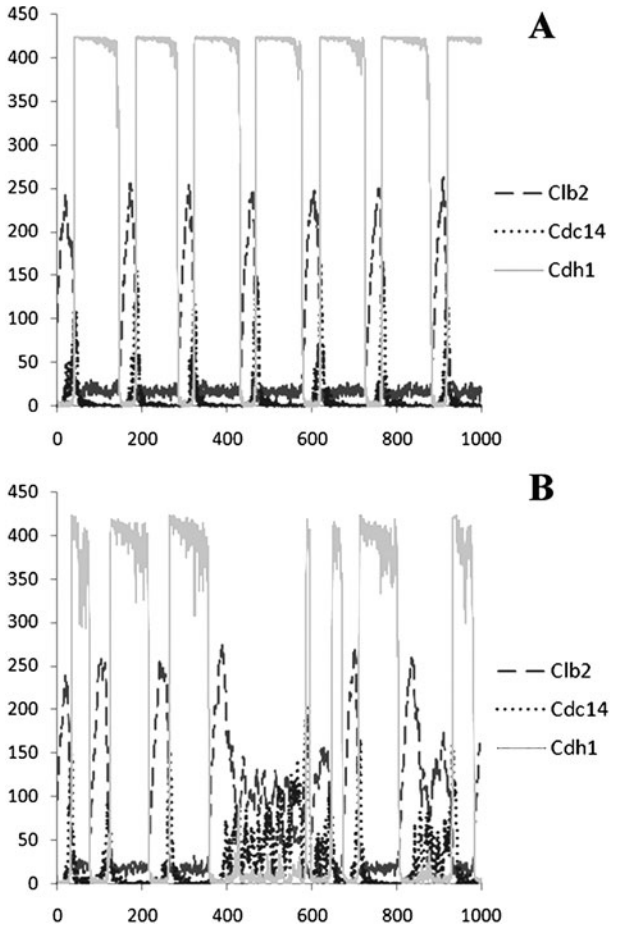


Fig. 19.5. Time series of simulation runs of a stochastic model of budding yeast cell cycle. Stochastic fluctuations in the key regulatory components of the wild type (*upper*) and *sic1Δ* mutant (*lower*) budding yeast cell cycles following the behavior of daughter cells after each cell division.

and the elevated noise in *sic1Δ* mutant that is missing one of the G1 regulators of Cdc28/Clb complexes.

## 5. Conclusions

As discussed above, the critical transitions of the cell cycle are understood thanks to some help from mathematical/computational biology. The expanding field of systems biology investigates the cells in large scale and tries to understand not only the major driving forces but all the intricacies of biological systems. We can hope that soon we will have a more complete understanding of cell cycle regulation not only in simple yeast cells but also in higher eukaryotes. This could be a great step also in cancer research since understanding how cell cycles loose control during tumor formation could help to cure this disease.

### References


1. Mazzarello, P. (1999) A unifying concept: the history of cell theory. *Nat. Cell Biol.* **1**, E13–E15.
2. Tyson, J. J., Chen, K. C., and Novak, B. (2003) Sniffers, buzzers, toggles and blinkers: dynamics of regulatory and signaling pathways in the cell. *Curr. Opin. Cell Biol.* **15**, 221–231.
3. Kirschner, M. W. (2005) The meaning of systems biology. *Cell* **121**, 503.
4. Kitano, H. (2002) Systems biology: a brief overview. *Science* **295**, 1662–1664.
5. Koch, A. L., and Schaechter, M. (1962) A model for statistics of the cell division process. *J. Gen. Microbiol.* **29**, 435–454.
6. Csikasz-Nagy, A. (2009) Computational systems biology of the cell cycle. *Brief Bioinform.* **10**, 424–434.
7. Nasmyth, K. (1996) At the heart of the budding yeast cell cycle. *Trends Genet.* **12**, 405–412.
8. Csikasz-Nagy, A., Battogtokh, D., Chen, K. C., Novak, B., and Tyson, J. J. (2006) Analysis of a generic model of eukaryotic cell-cycle regulation. *Biophys. J.* **90**, 4361–4379.
9. Nurse, P. (1990) Universal control mechanism regulating onset of M phase. *Nature* **344**, 503–508.
10. Morgan, D. O. (2006) *The Cell Cycle: Principles of Control*. New Science Press, London.
11. Kastan, M. B., and Bartek, J. (2004) Cell-cycle checkpoints and cancer. *Nature* **432**, 316–323.
12. Sveiczer, A., Novak, B., and Mitchison, J. M. (2004) Size control in growing yeast and mammalian cells. *Theor. Biol. Med. Model.* **1**, 12.
13. Bartek, J., Bartkova, J., and Lukas, J. (1996) The retinoblastoma protein pathway and the restriction point. *Curr. Opin. Cell Biol.* **8**, 805–814.
14. Nasmyth, K. (1996) Viewpoint: putting the cell cycle in order. *Science* **274**, 1643–1645.
15. Chen, K. C., Csikasz-Nagy, A., Gyorffy, B., Val, J., Novak, B., and Tyson, J. J. (2000) Kinetic analysis of a molecular model of the budding yeast cell cycle. *Mol. Biol. Cell* **11**, 369–391.
16. Ciliberto, A., and Shah, J. V. (2009) A quantitative systems view of the spindle assembly checkpoint. *EMBO J* **28**, 2162–2173.
17. Guertin, D. A., Trautmann, S., and McCollum, D. (2002) Cytokinesis in Eukaryotes. *Microbiol. Mol. Biol. Rev.* **66**, 155.
18. Hartwell, L. H., and Weinert, T. A. (1989) Checkpoints: controls that ensure the order of cell cycle events. *Science* **246**, 629–634.
19. Novak, B., Tyson, J. J., Gyorffy, B., and Csikasz-Nagy, A. (2007) Irreversible cell-cycle transitions are due to systems-level feedback. *Nat. Cell Biol.* **9**, 724–728.
20. Tyson, J. J., Csikasz-Nagy, A., and Novak, B. (2002) The dynamics of cell cycle regulation. *Bioessays* **24**, 1095–1109.
21. Chen, K. C., Calzone, L., Csikasz-Nagy, A., Cross, F. R., Novak, B., and Tyson, J. J.

(2004) Integrative analysis of cell cycle control in budding yeast. *Mol. Biol. Cell* **15**, 3841–3862.
22. Cross, F. R. (2003) Two redundant oscillatory mechanisms in the yeast cell cycle. *Dev. Cell* **4**, 741–752.
23. Marsh, L., Neiman, A. M., and Herskowitz, I. (1991) Signal transduction during pheromone response in yeast. *Ann. Rev. Cell Biol.* **7**, 699–728.
24. Hartwell, L. H., Mortimer, R. K., Culotti, J., and Culotti, M. (1973) Genetic control of the cell division cycle in yeast: V. genetic analysis of cdc mutants. *Genetics* **74**, 267–286.
25. Hunt, T., and Sassone-Corsi, P. (2007) Riding tandem: circadian clocks and the cell cycle. *Cell* **129**, 461.
26. Nurse, P. (1975) Genetic control of cell size at cell division in yeast. *Nature* **256**, 547–551.
27. Evans, T., Rosenthal, E. T., Youngblom, J., Distel, D., and Hunt, T. (1983) Cyclin: a protein specified by maternal mRNA in sea urchin eggs that is destroyed at each cleavage division. *Cell* **33**, 389–396.
28. Nasmyth, K. (2001) A prize for proliferation. *Cell* **107**, 689–701.
29. Bloom, J., and Cross, F. R. (2007) Multiple levels of cyclin specificity in cell-cycle control. *Nat. Rev. Mol. Cell Biol.* **8**, 149–160.
30. Zachariae, W., and Nasmyth, K. (1999) Whose end is destruction: cell division and the anaphase-promoting complex. *Genes Dev.* **13**, 2039–2058.
31. Goldbeter, A. (1991) A minimal cascade model for the mitotic oscillator involving cyclin and cdc2 kinase. *Proc. Natl. Acad. Sci. USA* **88**, 9107–9111.
32. Tyson, J. J. (1991) Modeling the cell division cycle: cdc2 and cyclin interactions. *Proc. Natl. Acad. Sci. USA* **88**, 7328–7332.
33. Tyson, J. J. (2007) Bringing cartoons to life. *Nature* **445**, 823.
34. Faure, A., and Thieffry, D. (2009) Logical modelling of cell cycle control in eukaryotes: a comparative study. *Mol. Biosyst.* **5**, 1569–1581.
35. Csikasz-Nagy, A., Gyorffy, B., Alt, W., Tyson, J. J., and Novak, B. (2008) Spatial controls for growth zone formation during the fission yeast cell cycle. *Yeast* **25**, 59–69.
36. Kar, S., Baumann, W. T., Paul, M. R., and Tyson, J. J. (2009) Exploring the roles of noise in the eukaryotic cell cycle. *Proc. Natl. Acad. Sci. USA* **106**, 6471–6476.
37. Mura, I., and Csikasz-Nagy, A. (2008) Stochastic Petri Net extension of a yeast cell cycle model. *J. Theor. Biol.* **254**, 850–860.
38. Cross, F. R., Archambault, V., Miller, M., and Klovstad, M. (2002) Testing a mathematical model for the yeast cell cycle. *Mol. Biol. Cell* **13**, 52–70.
39. Queralt, E., Lehane, C., Novak, B., and Uhlmann, F. (2006) Downregulation of PP2A(Cdc55) phosphatase by separase initiates mitotic exit in budding yeast. *Cell* **125**, 719–732.
40. Thieffry, D. (2007) Dynamical roles of biological regulatory circuits. *Brief Bioinform* **8**, 220–225.
41. Thomas, R. (1973) Boolean formalization of genetic control circuits. *J. Theor. Biol.* **42**, 563–585.
42. Davidich, M. I., and Bornholdt, S. (2008) Boolean network model predicts cell cycle sequence of fission yeast. *PLoS One* **3**, e1672.
43. Heath, J., Kwiatkowska, M., Norman, G., Parker, D., and Tymchyshyn, O. (2008) Probabilistic model checking of complex biological pathways. *Theor. Comput. Sci.* **391**, 239–257.
44. Monteiro, P. T., Ropers, D., Mateescu, R., Freitas, A. T., and de Jong, H. (2008) Temporal logic patterns for querying dynamic models of cellular interaction networks. *Bioinformatics* **24**, i227–i233.
45. Ballarini, P., Mazza, T., Palmisano, A., and Csikasz Nagy, A. (2009) Studying irreversible transitions in a model of cell cycle regulation. *Electron Notes Theor. Comput. Sci.* **232**, 39–53
46. Pozarowski, P., and Darzynkiewicz, Z. (2004) Analysis of cell cycle by flow cytometry, In *Checkpoint Controls and Cancer*, Humana Press, Totowa, NJ, pp. 301–311.
47. Di Talia, S., Skotheim, J. M., Bean, J. M., Siggia, E. D., and Cross, F. R. (2007) The effects of molecular noise and size control on variability in the budding yeast cell cycle. *Nature* **448**, 947–951.
48. Barik, D., Baumann, W. T., Paul, M. R., Novak, B., and Tyson, J. J. (2010) A model of yeast cell-cycle regulation based on multisite phosphorylation. *Mol. Syst. Biol.* **6**, 405.
49. Hlavacek, W. S., Faeder, J. R., Blinov, M. L., Posner, R. G., Hucka, M., and Fontana, W. (2006) Rules for modeling signal-transduction systems. *Sci STKE* **2006**, re6.
50. Regev, A., and Shapiro, E. (2002) Cells as computation. *Nature* **419**, 343.
51. Palmisano, A. (2010) Coding biological systems in a stochastic framework: the case study of budding yeast cell cycle. In *Proceedings of 1st International Conference on Bioinformatics*, Valencia, Spain.

# SUBJECT INDEX




G. Banfalvi (ed.), *Cell Cycle Synchronization*, Methods in Molecular Biology 761,
DOI 10.1007/978-1-61779-182-6, © Springer Science+Business Media, LLC 2011

## T



## U



## V



## W



## Z